Modeling the psychopathology in schizophrenia: symptom dimensions, subtypes, brain connectivity patterns, and molecular architecture

Inaugural dissertation

for the attainment of the title of doctor
in the Faculty of Mathematics and Natural Sciences
at the Heinrich Heine University Düsseldorf

presented by

Ji Chen
from Zhejiang

Düsseldorf, July 2020

from the institute for Psychology
at the Heinrich Heine University Düsseldorf

Published by permission of the
Faculty of Mathematics and Natural Sciences at
Heinrich Heine University Düsseldorf

Supervisor: Univ.-Prof. Dr. Simon Eickhoff
Co-supervisor: Univ.-Prof. Dr. Christian Bellebaum

Date of the oral examination: 07/10/2020

Author Declaration

According to the PO § 5 section 1b and the § 6 section 5, I hereby declare under oath that I have produced my thesis independently and without any undue assistance by third parties under consideration of the „Principles for the Safeguarding of Good Scientific Practice at Heinrich Heine University Düsseldorf". With the agreement of the supervisor, experimental work is conducted at Institute of Neuroscience and Medicine, Brain & Behaviour (INM-7), Research Centre Jülich, Jülich, Germany.

Date:_____ Signature:_____

Summary

Schizophrenia is a severe, debilitating, and heterogeneous mental disorder. Disentangling the psychopathological heterogeneity in schizophrenia from its underlying dimensions and the related neurobiology remains a challenge. Although ample efforts have been devoted to their study, symptom dimensions and subtypes, as well as neurobiological substrates and differentiations in schizophrenia remain unclear. In my project, I implemented machine-learning frameworks aiming to develop a new method to robustly and reliably conceptualize the psychopathology of schizophrenia at both symptom and brain levels in a data-driven fashion.

First, an orthonormal and projective variant of non-negative matrix factorization (OPNMF) was employed to identify the latent dimensions of the well-established Positive and Negative Syndrome Scale (PANSS). This method is capable of learning compact and homogeneous factors which can be readily generalized to novel patients. By evaluating OPNMF-derived factor models within a large, homogeneous schizophrenia dataset and then cross-validating the yielded models with an independent multi-site sample recruited from Europe, Asia, and the United States, a structure with four dimensions representing negative, positive, affective and cognitive symptoms was identified as the most stable and generalizable. This four-dimensional structure showed higher internal consistency than the original PANSS subscales and previously proposed factor models. Based on the identified dimensions, fuzzy-clustering was employed to derive symptomatically well-separated schizophrenia subtypes. Two core subtypes of schizophrenia patients were identified, with one featuring prominent negative and affective symptoms while the other featuring positive symptomatology. This positive-negative dichotomy was longitudinally stable in about 80% of the repeatedly assessed patients.

Neurobiological divergence of the identified subtypes was assessed using classification analysis of resting-state functional MRI measurement with cross-validation in a subset of the multi-site sample. Individual subtypes could be well-discriminated using resting-state functional connectivity (rsFC) profiles of the ventromedial frontal cortex, temporoparietal junction, and precuneus, with the highest classification accuracy of 70%. Individual expression of the four symptom dimensions were predicted using relevance vector machine based on rsFC within 17 meta-analytically defined task-activation networks. A strict validation procedure including 10-fold cross-validation, leave-one-site-out experiments, and generalization to independent samples was conducted to derive robust symptom-network associations. Finally, the significant and robust symptom-predictive networks were spatially correlated with whole-brain density maps of nine receptors and transporters from prior molecular imaging in healthy populations to reveal the molecular architecture related to these networks. The theory-of-mind and the extended socio-affective default networks, which are implicated in social cognition and affective processes, were identified as significantly and robustly predictive of the cognitive symptom dimension. Moreover, node importance of these two networks showed a spatial pattern positively co-varying with D_1 dopamine receptor and serotonin reuptake transporter densities as well as presynaptic dopamine capacity.

The current work provides a systematic modeling framework of schizophrenia from symptomatology to neurobiology. Together the proposed hybrid dimensional-categorical conceptualization of symptomatology and the revealed intrinsic neurobiological processes and molecular architecture further disentangle the heterogeneity in schizophrenia, possibly allowing for the development of more specifically targeted treatments.

TABLE OF CONTENTS

1. General background on Schizophrenia

Patients with schizophrenia are prominently characterized by paranoid delusions, hallucinations, negative symptoms, and cognitive deficits. However, individual patients can present marked variability in psychopathology and their symptomatic expressions are often difficult to explain. Consequently, considerable effort has been devoted to disentangling the psychopathological heterogeneity in schizophrenia through identifying factor models (i.e., latent dimensions) of schizophrenia symptomatology and clustering patients into psychopathological subtypes based on the well-established and validated 30-item Positive and Negative Syndrome Scale (PANSS). Schizophrenia is an intractable syndrome. Anti-psychotics, which mainly regulate the D_2 dopamine receptor systems, are the mainstay of pharmacological treatment strategy for alleviating the symptoms of schizophrenia patients; however, they are only effective for positive symptoms while producing significant side effects. Therefore, clarifying the neural pathophysiological underpinnings of schizophrenia different symptom dimensions remains an urgent goal. As a seemingly human-specific mental disorder, non-invasive invivo neuroimaging techniques offer a unique avenue to investigate brain structure, function, and molecular substrates of schizophrenia.

In the following subheadings, I provided a detailed introduction to prior factor models of PANSS, clinical subtypes, and the neurobiological findings in schizophrenia patients.

1.1 Prior factor models of PANSS

The PANSS is originally divided into three subscales (positive, negative, and general psychopathology) based on theoretical and heuristic considerations (Kay et al., 1987). However, these original three subscales of PANSS were found to be neither optimal nor adequate to capture the symptom variation across individual schizophrenia patients (Peralta and Cuesta, 1994). The PANSS developers later introduced a four-component structure as the pyramidical model comprising negative, positive, excited, and depressive symptom dimensions (Kay and Sevy, 1990). However, items reflecting cognitive disturbances were distributed across all dimensions or discarded in the final pyramidical model. This might contradict with the fact that cognitive deficits are a core feature of schizophrenia. Other factorial studies have identified inconsistent factor models with number of factors varying from five to seven (Kim et al., 2012; Levine et al., 2007; Wallwork et al., 2012; van der Gaag et al., 2006a; Emsley et al., 2003; Van den Oord et al., 2006; White et al., 1997; Jiang et al., 2013). A five-factor structure was most frequently proposed (Kim et al., 2012; Levine et al., 2007; Wallwork et al., 2012; van der Gaag et al., 2006a; Jiang et al., 2013) which commonly represents positive, negative, disorganized (or cognitive), depressed, and excited symptom dimensions. Only a few studies identified six- or seven-factor model as the more-superior representation. For example, a model with six latent factors provided five factors similar to that in previous five-factor models while a sixth withdrawn factor was additionally identified. The author argued that the six PANSS scales measure meaningful aspects of schizophrenia (Van den Oord et al., 2006). Another study applying equamax factor analysis to a multicenter, 11 country drug trial with 535 schizophrenia patients revealed that a seven-factor solution is more-superior with depression and anxiety symptoms separating and a motor component emerging as compared to prior five-factor

models. The author suggested that, in addition to a structure with five factors, scales for catatonia, depressive and anxiety syndromes might also be included in future studies (Emsley et al., 2003).

Although most of previous factorial studies have identified a model with five factors, five-factor models continuously failed to be confirmed in independent samples (White et al., 1997; van der Gaag et al., 2006b; Jiang et al., 2013) and hence the identification of a stable and well-generalizable factor model remains challenging. Specifically, White and colleagues re-visited prior 20 factor models in their confirmatory study and found that none of these models met criteria for an adequate fit to the empirical data with 1233 schizophrenia patients. Then they put forward a new pentagonal model which only used 25 of the 30 PANSS items to represent the positive, the negative, the dysphoric mood, the activation, and the autistic preoccupation symptom dimensions. However, this model, together with 24 others, were failed to be confirmed in *van der Gaag's* study which assessed a large, homogeneous international sample (van der Gaag et al., 2006a). In the same study (van der Gaag et al., 2006b) the authors developed an improved five-factor model using 10-fold cross-validation. This improved five-factor model did achieve a satisfactory goodness-of-fit in their sample. However, along with other 31 five-factor models proposed in the literature, this improved five-factor model showed inadequate fit to both of the two large Chinese schizophrenia samples recruited in Singapore (Jiang et al., 2012). Basically, the authors found, or replicated, that there are five factors underlying the multi-dimensional symptomatology of schizophrenia. However, with regard to specific five-factor models, none of the previously proposed 32 models but the one derived from their own sample was confirmed in their data sets. They ascribed the inadequate fit of previous five-factor models to cultural difference and the difference in the interpretation of PANSS items across countries. Collectively, these studies contradict to each other, and the fundamental instability of five factor models still presented.

On the other hand, as in the aforementioned pentagonal model, some studies have derived their final factor models after excluding several PANSS items which demonstrated ambiguous or unstable factor-assignment in literature. For example, *Wallwork et al.* (2012) reviewed each PANSS item loaded on each factor in 29 published PANSS factor-models, and excluded 10 items with inconsistent factor-assignment from their final five-factor model. The inconsistent item-to-factor assignment presented in the literature can possibly be attributed to methodological factors that both the PCA with Equamax or Varimax rotation and the EFA method used in prior studies suffer from the downside of non-sparse factorization where the substantial cross-loadings of some PANSS items may play an important role in the observed instability. To conclude, reproducibility, external validity, and generalizability remain a concern for previous factor models of PANSS (Lykouras et al., 2000), and hence future studies on large, multi-site samples with systematic cross-validation and out-of-sample generalization assessments are needed.

1.2 Previously proposed clinical subtypes

Apart from identifying dimensions of symptomatology, subtyping also serves as one of the most promising attempts to reduce the heterogeneous psychopathology within schizophrenia. The classic classification of schizophrenia including hebephrenic, paranoid, catatonic and undifferentiated, which was used for several decades to approach the heterogeneity, however, has been dropped in DSM-5 owing to the fact that this taxonomy showed poor diagnostic stability over time with also limited prognostic value (Braff et al., 2013; Tandon et al., 2013). Other definitions of schizophrenia subtypes have thus been put forward. It is worth noting that the deficit schizophrenia, which characterized by primary (idiopathic, not secondary to other factors) and persistent (trait-like) negative symptoms (Carpenter et al., 1988), has been commonly proposed as a relatively homogeneous subgroup of patients (Kirkpatrick and Galderisi, 2008; Marder and Galderisi, 2017). The deficit subtype was hypothesized to serve as a distinct disease entity within the (broader) schizophrenia syndrome due to its unique etiological, neurobiological and course-related profiles including poor premorbid adjustment, impaired cognitive functioning, and poor functional outcome (Kirkpatrick et al., 2001; Galderisi et al., 2002; Kirkpatrick and Galderisi, 2008; Cohen et al., 2010; Marder and Galderisi, 2017). However, the deficit condition only occurs in roughly 15-30% of individuals diagnosed with schizophrenia (Kirkpatrick et al., 2001; Kirkpatrick et al., 2006), and the remaining others are classified as the non-deficit subgroup. Hence, this set of subtyping (i.e., deficit/non-deficit distinction) may suffer from the limitation of its usefulness as most patients are not well differentiated.

To provide a general definition of schizophrenia subtypes, data-driven approaches of clustering analysis based on symptomatic data were introduced. For example, an earlier study identified a four-subgroup solution with two representative subtypes labeled as the ‗insightful schizophrenia' (featured by good insight, manifested neurotic symptoms, and minimal behavioral aberrance) and the ‗flagrant schizophrenia' (the patients had marked aberrant, agitated, or bizarre behavior, disorganization, restricted affect, but absence of anxiety or depression) (Bartko et al., 1981). A later study identified an optimal solution with six clusters that multiple distinct symptoms (e.g., hallucinations, delusions, social withdrawal) were common in the characterization of these clusters. An alternative two-cluster solution was likewise reported by this study that the first cluster merged the clusters one, two, three, and five of the six-cluster solution while the second cluster was formed by the forth and the sixth clusters (Helmes and Landmark, 2003). Other clustering studies based on the widely used and well-established PANSS scale also revealed inconsistent results. In detail, the earliest study I noticed in the literature was the one applied hierarchical clustering (Ward's method) to 138 schizophrenia patients, which demonstrated that there are at least four subtypes of schizophrenia, representing patients with prominent positive, negative, disorganized symptoms or with a mixed symptomatology. The author further proposed a potential fifth subtype with few symptoms suggesting a simple schizophrenia category (Dollfus et al., 1996). Another study applying a similar hierarchical clustering to 255 DSM-III-R diagnosed schizophrenia patients also revealed an optimal solution with five clusters. Three of the clusters were seemingly in line with the prior study (Dollfus et al., 1996) that the patients within these clusters presented severe positive symptoms, pure negative symptoms, and minimal severity in overall symptomatology, respectively. However, the other two clusters which represented *i)* prominent positive and excitement symptoms and *ii)* high expressions in general psychopathology but lacking the excited symptom dimension (Lykouras et al., 2001) were different from that defined in the prior study with smaller samples (Dollfus et al., 1996).

Data-driven approaches also provided some updates for the clinically-defined deficit subtype. For example, a recent study based on only the negative and the distress dimensions of PANSS proposed a three cluster solution by using a two-step clustering with log-likelihood as the distance measure and Bayesian Information Criterion for deciding how many clusters to retain (Dickinson et al., 2017). In the resulting clusters, patients presented *i)* very severe negative and distress symptoms in cluster one which corresponds to the traditional deficit subgroup, *ii)* prominent high distress symptom level ("distress subgroup") in cluster two, and *iii)* both low levels of these two symptom dimensions in the third cluster ("low-symptom subgroup"). Based on latent class analysis, another study with 706 DSM-IV diagnosed schizophrenia patients identified three subtypes of deficit, persistent, and transit as differentiated by the manifestations of patients in negative symptoms. These subtypes moreover differed in a variety of clinical characterizations (e.g., pattern of positive symptoms and ages of disease onset) and psychosocial functioning (Ahmed et al., 2017).

On the other hand, there is also aprior study attempted to use both categorical and dimensional approaches to characterize the negative symptoms in schizophrenia. Using taxometric and latent variable mixture analyses, the investigator found that, besides a taxometric classification of deficit syndrome, a *hybrid* categorical-dimensional conceptualization of negative symptoms would make sense clinically as being external-validated its predictability of multiple clinical characteristics, neurocognitive performance and social functioning (Ahmed et al., 2015). In light of the proposed hybrid perspective of schizophrenia symptomatology, here I would also tend to provide a categorical-dimensional conceptualization. Hence, following the identification of symptom dimensions, I used fuzzy-clustering approaches, rather than those hard clustering methods (e.g., hierarchical clustering) employed in previous studies, to identify symptomatically well-separated (core) subtypes after filtering out those patients with an ambiguous cluster membership.

1.3 Brain structural, functional, and neurotransmitter implications in schizophrenia

Using machine-learning approaches to classify schizophrenia clinical subtypes from brain imaging data would be substantially helpful to delineate the underlying neurobiological differentiations of the disease. However, studies on the neurobiological divergence of schizophrenia psychopathological subtypes are still scarce. Likewise, a successful prediction of the continuous symptom dimensional scores helps to uncover the neurobiological processes that are robustly linked to specific symptom dimensions. However, prior neuroimaging studies in schizophrenia mostly relied on univariate statistics. That is, between-group comparisons are first used to derive structural and functional brain abnormalities in patients, and then the revealed differences allow for assessment of regional brain parameters for subsequent group-level correlation analysis with symptoms.

1.3.1 Neurobiological differentiations of clinical subtypes and brain regions relate to psychopathological distinction

Here I first summarized the brain regions that have been consistently implicated in schizophrenia pathophysiology and processes relevant to the psychopathological distinction. The temporo-parietal junction (TPJ) subserves auditory-verbal hallucination system due to its critical role in the production of language (Vercammen et al., 2012; Mondino et al., 2016). Also TPJ is a key region involved in the process of social cognition including theory of mind (Döhnel et al., 2012), self-agency (Blanke et al., 2005), and empathy (Derntl et al., 2010). These evidently are themselves core negative symptoms but could also be related to positive symptoms under hypermentalization (Frith, 2004). Structural deficits in ventro-medial prefrontal cortex were only detected in schizophrenia negative subgroup but neither in the positive nor the disorganized subgroups when compared with healthy subjects (Nenadic et al., 2015). Cortical thickness in this region was moreover found to significantly associate with negative symptom severity in schizophrenia patients (Walton et al., 2017). Posterior cingulate cortex and precuneus are hubs of the default mood network and the mirror neuron system. These two network systems were proposed as importantly involved in the neural pathophysiology of negative symptoms in schizophrenia (Azorin et al., 2014). Moreover, grey matter volume deficit (Lee et al., 2011) and neural activation during auditory oddball experiment (Shaffer et al., 2015) in these regions have been related to the severity of negative symptomatology (e.g., anhedonia and apathy) in prior structural and task-based fMRI studies. Besides, the visual cortex, which primarily subserves early-stage visual processing, e.g., visual perception, was found to be dysfunctional with reduced functional connectivity to sensormotor cortex in schizophrenia patients at rest (Chen et al., 2015). Deficits in self-perception and multisensory integration would cause the so called ~~-s~~elf-disorder" in schizophrenia and have been linked to delusional symptoms (Postmes et al., 2014). In a prior task-based fMRI study, an enhanced functional connectivity between the orbitofrontal and the visual cortex in response to tasks targeting delusional ideation was reported and the results implied a link between perceptual instability and the appearance of delusional beliefs (Schmack et al., 2013).

For the deficit/non-deficit subtyping, there are also some neuroimaging studies investigated the neurobiological differentiations between deficit and non-deficit patients. In detail, deficit patients showed

more-severe grey matter loss in right orbito-medial prefrontal cortex, parahippocampal gyrus (Benoit et al., 2012), and superior and middle temporal gyri (Fischer et al., 2012) than non-deficit patients. Another study based on resting-state fMRI reported that, comparing to the non-deficit group, spontaneous neural activity was significantly elevated in visual cortex in the deficit schizophrenia group, while in bilateral insula, anterior cingulate cortex, and the regions extended to the fronto-temporal cortex, the neural activities were decreased (Zhou et al., 2019). By using single-positron emission computed tomography (SPECT), reduced cerebral blood flow was revealed in right orbitrofrontal region in deficit patients when compared with non-deficit patients (Kanahara et al., 2013). Besides, event-related potential (ERP) activations in posterior cingulate and parahippocampal gyri, left superior and middle frontal areas, were aberrant in deficit schizophrenia patients (Mucci et al., 2007).

1.3.2 Functional domains and neurobiological processes implicated in schizophrenia

Since I am not only aimed to investigate the potential neurobiological divergence of the identified psychopathological subtypes, but also devoted to linking functional processes to specific symptom dimensions, I moreover reviewed a broad range of domains reflecting cognitive, socio-affective, and sensory-motor functions that have been implicated in schizophrenia. Details were provided in Table 1.3.2.

Table 1.3.2 Review of the functional domains implicated in schizophrenia

Domain	**General summary**	**References**
Affective		
Emotional scene and face processing	Identifying and discriminating among different facial expressions are impaired in schizophrenia patients. Worse performance and hyper/hypo-activation in frontal and limbic (e.g., amygdala and hippocampus) regions in response to facial emotion recognition, as well as altered functional subnetwork during emotional face processing were reported.	Cao et al (2016) Edwards et al. (2001) Gur et al. (2002) Phillips et al. (1999) Adolphs et al. (1994)
Reward-related decision making	Decision making is disrupted in schizophrenia that the patients are inability to properly estimate reward value, which has been related to severity of negative and cognitive symptoms, and linked to prefrontal GABAergic dysfunction. Increased activations were observed in anterior insula, putamen, and frontal sub-regions in response to reward outcomes.	Piantadosi et al. (2016); Tikàsz et al. (2019); Kim et al. (2016); Collins et al., (2014); Gold et al., (2008, 2013)
Cognitive emotion regulation	Individuals with schizophrenia display emotional regulation abnormalities and cognitive control deficits which tend to increase negative emotion and cause prepotent response of unpleasant scenes via reappraisal.	Strauss et al. (2015); Sullivan et al. (2017)
Social		

Empathy	Empathy deficits are presented in schizophrenia which would lead to social dysfunction. Fronto-temporal functional connectivity was related to cognitive empathy and experiential negative symptoms. Reduced cortical thickness in empathy-related neural regions (e.g., mPFC, aMCC, and insula) was demonstrated. Reduced activation in fusiform gyrus, lingual gyrus, middle and inferior occipital gyrus was found in schizophrenia patients during empathy task and reduced grey and white matter volumes were observed in these same brain areas.	Bonfils et al. (2016) Singh et al. (2015) Abram et al. (2016) Massey et al. (2017)
Mirror neuron system (MNS)	Dysfunctional mirror neuron activity (MNA) has been associated with diverse symptoms (negative, affective) in schizophrenia and abnormal (including both increased and decreased) MNA have been found in the patients	Mehta et al. (2014a, 2014b); Horan et al. (2014); Pridmore et al. (2008)
Theory-of-mind (ToM)	ToM is impaired in schizophrenia, serving as a well-established feature and vulnerability marker of this disorder. The neural basis of ToM deficits has also been indicated previously including findings of abnormal brain activations (TPJ, MPFC middle prefrontal/inferior frontal cortex, PCC and temporal area) in response to tasks targeting ToM and altered brain functional connectivity. Multiple schizophrenia symptoms (e.g., positive, negative and disorganized) have been associated with ToM deficits.	Bora and Pantelis, (2013) Fretland et al. (2015) Benedetti (2009) Shamay-Tsoory (2007) Mothersill (2017) Das et al .(2012)
Task negative		
Extend socio-affective default (eSAD)	Impaired social functioning is associated with cognitive (e.g., working memory) deficits in schizophrenia. Abnormal activation in PCC in response to socio- affective related tasks was co-varied with PCC-vmPFC functional connectivity at rest and correlated with negative symptoms. Abnormal social-affective processing has also been related to disturbed functional cohesion within social-affective affiliation networks.	Ebisch et al. (2018) Hendler et al. (2018) Park et al. (2006)
Default mode network (DMN)	The DMN has been frequently investigated and consistently reported as abnormal in schizophrenia, both structurally and functionally (e.g., reduced grey matter volume, increased and decreased deactivations and functional hyperconnectivity) in e.g., medial prefrontal cortex, anterior/posterior cingulate cortex, and middle temporal gyrus were revealed and have been associated with negative symptoms and cognitive deficits.	Garrity et al. (2017) Hu et al. (2017) Jia et al. (2016) Pomarol-Clotet et al. (2019) Du et al. (2008)
Executive		
Vigilant attention (VigAtt)	Deficits of attention are common in schizophrenia, and abnormal functional brain response to attentional tasks was reported in the frontal cortex, postcentral gyrus, medial temporal lobe and cerebellum. Also, sustained attention was found to correlate with negative symptom severity.	Eyler et al (2004) O'Gráda et al. (2009)
Cognitive action control (CogAC)	Impaired action control was frequently reported in schizophrenia which may influence performance in a wide variety of cognitive domains and are associated with deficits in prefrontal-based control network particularly in (dorsolateral prefrontal cortex as well as premotor, ACC	Reuter et al. (2007) Braver et al. (1999) Barch (2017) Minzenberg et al.

	and thalamus.	(2014)
Extend multi-demand network (eMDN)	The general executive cognition comprises multiple processes that are related but not limited to action/inhibitory control, attention, working memory, and reasoning, which all have been implicated as abnormal in schizophrenia and altered neural activations were consistently found in anterior cingulate cortex, dorsolateral prefrontal and thalamus in the response to executive-related tasks.	Giraldo-Chica et al. (2018) Rubia et al. (2001) Langdon et al. (2010) Ramsey et al. (2002) Minzenberg et al. (2009)
Working memory (WM)	As a cardinal cognitive symptom that may underlie many other cognitive deficits and symptoms, impaired WM is a persistent, disabling feature of schizophrenia, which has been frequently associated with (dorso/ventro lateral) prefrontal dysfunction (e.g., abnormal neural activation and dopamine hypofunction) with also abnormalities in thalamus and basal ganglia reported.	Kaminski et al.(2020); Lee andPark (2005); Manoach et al. (2000); Schlösser (2003); Schneider (2007); Borgan (2019); Eryilmaz (2016)
Long-term memory and language		
Semantic memory (SM)	Semantic memory-based processing is impaired in SCZ, e.g., semantic retrieval, encoding and association, and were found to associate with deficits (e.g., increased connectivity and decreased neural activation) in fronto-parieto-temporal network (e.g., inferior parietal lobule, medial/inferior prefrontal gyrus, and superior/middle temporal gyrus) and relate to negative and positive symptoms and formal thought disorder.	Jamadar et al. (2013a & 2013b) Kubicki et al. (2003) Ragland et al. (2008)
Speech production (SP)	Abnormal speech production in schizophrenia contributes to the symptom of formal thought disorder (FTD). FTD-associated production of disorganized speeches was correlated with activity in fusiform, inferior frontal and superior temporal cortex. Reversed laterality of activation in the lateral temporal cortex was found in schizophrenia patients during speech production, which has been related to glutamatergic imbalance.	Kircher et al. (2012) Nagels et al. (2018) McGuire et al. (1998)
Autobiographic Memory (AM)	AM is impaired (e.g., reduced specificity and retrieval of memories) in schizophrenia and has been found to associate with reduced hippocampal volume and altered neural activations in multiple brain regions (e.g., anterior cingulate cortex, and lateral prefrontal cortex).	Herold et al. (2015) Cuervo-Lombard et al. (2012) Herold et al. (2013)
Sensory-motor		
Motor	Motor cortex and its closely inter-connected brain regions (e.g., prefrontal–motor, cerebello-thalamo-motor, sensory-motor and basal ganglia circuits)showed abnormalities in schizophrenia, and were related to motor behavioral problems observed in the patients including motor learning, sequential movements and postural control, and have also been associated with clinical symptoms.	Walther et al. (2017) Marvel et al. (2007) Berman et al. (2016) Bernard et al. (2014) Du et al., (2018)
Auditory	Auditory processing including automatic, feed forward and pre-attentive functions are impaired in schizophrenia. The auditory oddball tasks revealed multiple regions within the auditory network that were abnormally activated, e.g., the (middle/superior) temporal cortex, insula, prefrontal and inferior parietal cortex, and the abnormalities were associated with negative symptoms and cognitive deficits.	Sweet et al. (2007) Perez et al. (2014) Force et al. (2008) Shin et al (2009) Wolf et al. (2008) Kim et al. (2009) Shim et al. (2014)

1.3.3 Compromised neurotransmitter systems in schizophrenia

For the last part of this section, I would highlight some neurotransmitter systems involved in schizophrenia as a brief introduction for the molecular basis of this disorder and its symptoms. As the final aim of my PhD project, networks identified as robustly predictive of the new OPNMF-derived symptom dimensions will be correlated with whole-brain density maps of relevant receptors and transporters. A plenty of *in-vivo* molecular imaging studies using multi-tracer positron emission tomography (PET) and SPECT have been devoted into the investigation of the potential molecular pathogenesis of schizophrenia. Multiple pathways involving primarily dopaminergic, serotoninergic, and glutamatergic neurotransmitter systems were reported to be abnormal in schizophrenia (Howes and Kapur, 2009; Poels et al., 2014; Selvaraj et al., 2014).

1.3.3.1 Dopaminergic

First and foremost, the dopamine system is evidenced as hyper-responsive in schizophrenia and dopaminergic dysfunction has been commonly hypothesized in the etiopathogenesis of this disorder (i.e., the ~~"~~dopamine hypothesis") (Howes and Kapur, 2009; Gründer and Cumming, 2016). Prior molecular imaging studies indicated potentially an elevated level of endogeneous dopamine release in patients who are experiencing psychosis (Abi-Dargham et al., 1998; Breier et al., 1997; Laruelle et al., 1996; Laruelle et al., 1999; Abi-Dargham et al., 2000). Moreover, presynaptic dopamine synthesis capacity, as assessed by radiolabelled L-DOPA (the precursor molecule for dopamine), is likewise reported as elevated in schizophrenia patients. This elevation is also observed in clinical high-risk patients, and is moreover predictive of clinical high-risk patients in the conversion to full psychosis (reviewed in Cannon et al., 2015).

Dopamine receptors were found to be abnormal in schizophrenia patients. There are five subunits of dopamine receptor in the human brain, including D_1-like (D_1 and D_5) and D_2-like (D_2, D_3, and D_4) receptor groups. Almost all anti-psychotic drugs take anti-psychotic actions by blocking D_2 receptors, and the blockade of D_2 receptor relates to clinical anti-psychotic potencies of anti-psychotics (Mauri et al., 2014). Multiple PET and SPECT studies investigated the *in-vivo* $D_{2/3}$ receptor density using various radiotracers and most of them reported an increased striatal $D_{2/3}$ receptor density in schizophrenia patients when compared with healthy subjects, though the effect size was modest (roughly 10%-20% elevation) (Laruelle et al., 1998; Zakzanis et al., 1998; Kestler et al., 2001). Reduced $D_{2/3}$ receptor density was also detected in extrastriatal areas (e.g., anterior cingulate cortex and thalamus) (Suhara et al., 2002; Mitelman et al., 2019) but an increase of $D_{2/3}$ in thalamus has been reported (Kegeles et al., 2010). The reason for talking the D_2 and the D_3 receptors together is because current radiotracers bind to both of the two receptors and hence it's not readily to interpret which receptor has contributed to the observed alteration. Notwithstanding, a recent PET study using a novel radiotracer has specifically assessed the D_3 receptor density and the preliminary results showed no selective change in the high-affinity state of D_2 and/or D_3 in striatum and thalamic regions in schizophrenia (Graff-Guerrero et al., 2009). Interestingly, however, a down-regulation of D_3 RNA expression has been found in the orbitofrontal cortex of schizophrenia postmortem brains (Meador-Woodruff et al., 1997).

The D_1 receptor has likewise received multiple attentions due to its involvement in schizophrenia cognitive deficits. Dopaminergic transmission in prefrontal area mainly relies on D_1 receptor, and prefrontal dopamine

hypofunction has been commonly proposed as the molecular substrate of the cognitive symptoms presented in schizophrenia patients (Arnsten et al., 2017). Prior PET studies have demonstrated contradictory results regarding the change of D_1 receptor density in schizophrenia. An earlier study showed that D_1 receptor density is decreased in prefrontal cortex in patients with schizophrenia when compared with healthy volunteers (Okubo et al., 1997). However, the radiotracer used in this study might be confounded by dopamine depletion (Guo et al., 2003) and later studies using a more-superior radiotracer have successfully detected an up-regulation of D_1 receptor in schizophrenia as a compensatory (but ineffective) mechanism secondary to the persistent cortical dopamine hypofunctioning (Abi-Dargham et al., 2002). In the same study, D_1 elevation was moreover found to correlate with the cognitive deficits in patients (Abi-Dargham et al., 2002). However, current anti-psychotics which have more or less the affinity for D_1-like receptors showed minimal effects on schizophrenia cognitive symptoms (Vyas et al., 2018). While D_1 receptor antagonists has been hypothesized as novel treatments for schizophrenia (Bourne, 2001), a recent study proposed D_1 agonists to possibly alleviate the cognitive deficits in schizophrenia patients (Arnsten et al., 2017).

1.3.3.2 Serotonergic

Serotonergic dysfunction has been implicated in the pathophysiology of schizophrenia (Eggers, 2013; Malhotra et al., 1998; Stahl, 2018; Selvaraj et al., 2014). There are seven major families of serotonin receptors (5-HT1 to 5-HT7) (Hoyer et al., 2002; Melke et al., 2003). The 5-HT1 and 5-HT2 receptor groups, which acts inhibitory and excitatory functions, respectively, were more frequently reported as abnormal in schizophrenia patients. Plenty of postmortem and in vivo molecular imaging studies have been devoted to investigating the potential alterations in serotonin receptors in schizophrenia patients by contrasting to healthy subjects. Notably, most postmortem studies on schizophrenia brains demonstrated a reduction of 5-HT2 receptor density in cortical areas (Laruelle et al, 1993; Matsumoto et al, 2005; Mita et al, 1986; Pralong et al, 2000). A recent meta-analysis reported that prefrontal 5-HT2a receptors are reduced in schizophrenia patients with a large effect size when compared with healthy controls (Selvaraj et al., 2014). This meta-analytic study also identified an elevation of prefrontal 5-HT1a receptors in schizophrenia. However, in vivo PET experiments did not support the robust finding of 5-HT2a down-regulation in postmortem studies. That is, apart from one voxel-based study which reported a decreased 5-HT2a binding potential in the dorso-lateral prefrontal cortex of neuroleptic-naive schizophrenia patients (Ngan et al., 2000), other regions-of-interest based studies using 5-HT2a selective radiotracers did not demonstrate any between-group difference in cortical 5-HT2a receptor density (Verhoeff et al., 2000; Erritzoe et al., 2008; Lewis et al, 1999; Okubo et al, 2000; Trichard et al, 1998). The authors attributed the contradictions to the different analytic methods used for PET images and the different radioligands employed for assessing the 5-HT2a.

Besides D_2 dopamine receptors, atypical anti-psychotics also exert antagonistic effects on the 5-HT2 receptor group, targeting mainly the 5-HT2a subunit. Interestingly, prior work demonstrated that blocking both of the 5-HT2a and the dopaminergic D_2 receptors by atypical anti-psychotics could slow down whole-brain grey matter loss in schizophrenia patients over time (Lieberman et al., 2005). However, it was proposed that pharmacological treatments will not have any anti-psychotic effect if the agents only modulate the serotonergic pathway without acting on D_2 receptors, (Mauri et al., 2014). Interestingly, anti-psychotic drugs, pimavanserin and SEP-363856,

have just been introduced that preferentially target serotonin and not dopamine receptors (Sahli and Tarazi, 2018; Koblan et al., 2020). Furthermore, different atypical anti-psychotics have been shown to exert differential effects on serotonin receptor subunits (Radhakrishnan et al., 2020). For example, schizophrenia patients treated with olanzapine showed both lower 5-HT6 and 5-HT2a availability, while quetiapine lowers 5-HT6 availability in the putamen and risperidone would lead to prefrontal low 5-HT2a availability. The 5-HTT serotonin reuptake transporter, which is critical for regulating serotonergic concentration and signaling, has also been implicated in schizophrenia (Stahl, 2018; Malhotra et al., 1998; Selvaraj et al., 2014; Kim et al., 2015; Hernandez and Sokolov 1997; Wang et al., 2010). Although atypical anti-psychotics have an effect on the serotonin receptor groups, their effects on 5-HTT remain to be clarified as previous findings were largely inconsistent (Kaiser et al., 2001; Lian et al., 2016; Barkan et al., 2006).

1.3.3.3 Glutamatergic

The involvement of glutamatergic system in schizophrenia pathophysiology is supported by multi-faceted evidence (reviewed in Poels et al., 2014; Uno and Coyle, 2019). First, glutamate elevation was found to correlate with the reduced grey matter volume in schizophrenia patients (Aoyama et al., 2011). The over-expressed glutamate has been proposed to cause neural excitotoxic effect (Schobel et al., 2013), leading to grey matter loss. Second, ketamine and phencyclidine, the noncompetitive antagonists of the Nmethyl-D-aspartate (NMDA) subtype of the glutamate receptor family, have been shown to induce problematic behaviors and thoughts in healthy volunteers which resemble the psychotic, negative, and cognitive symptoms observed in patients with schizophrenia (Krystal et al., 1994; Javitt and Zukin, 1991; Javitt, 1987).

Glutamate serves as the main excitatory neurotransmitter in the human brain and glutamatergic neurotransmission is mediated by two types of receptors (i.e., ionotropic and metabotropic). The NMDA receptors are ionotropic which have drawn the most attentions amongst other glutamate receptor subtypes in schizophrenia studies. The metabotropic glutamate receptor 5 (mGluR5) has also been linked to schizophrenia pathophysiology due to its close interaction with NMDA receptor activation, which could potentiate NMDA receptors. However, mGluR5 mRNA level and protein expression in schizophrenia are found to be unaltered in postmortem studies (Matosin and Newell, 2013).

In vivo glutamate is commonly quantified by proton magnetic resonance spectroscopic (MRS) imaging. Prior meta-analytic studies on proton MRS demonstrated that, comparing with healthy populations, schizophrenia patients present decreased glutamate in medial prefrontal area, increased glutamine in both the medial prefrontal cortex and thalamus (Marsman et al., 2013), and elevated Glx (glutamate+glutamine) in the medial temporal lobe and basal ganglia (Merritt et al., 2018). Since the development of selective glutamatergic radiotracers is difficult, studies assessing the densities of glutamate receptors in vivo were very scarce. Still, I noted that a SPECT study using [^{123}I]CNS-1261, a highly selective tracer that binds the PCP/MK801 intrachannel site of the NMDA receptor, has revealed a reduced NMDA receptor binding in the left hippocampus of unmedicated schizophrenia patients when compared to healthy individuals (Pilowsky et al., 2006). Comparatively, there are multiple postmortem studies that have been conduced to assess mRNA transcript and protein expression of NMDA receptor subunits in schizophrenia brains. A recent meta-analysis demonstrated significant decreases in both mRNA and protein

expressions of the GluN1 subunit, as well as a reduced mRNA transcript of the GluN2c subunit in schizophrenia post-mortem prefrontal cortex relative to healthy controls (Catts et al., 2016). Elevated postsynaptic density of NMDA receptor in dorsolateral prefrontal cortex (Banerjee et al., 2015) and increased NMDA receptor binding in anterior cingulate cortex (Zavitsanou et al., 2002) have also been reported in schizophrenia post-mortem brains, which may serve as a compensatory mechanism secondary to NMDA receptor hypofunction (Coyle et al., 2003) and the impaired glutamatergic transmission (Zavitsanou et al., 2002) in schizophrenia.

Although atypical anti-psychotics which target the dopaminergic system (in particular D_2 receptors) could effectively relieve positive symptoms, their effects on other dimensions of psychopathology including negative and cognitive symptoms are negligible (reviewed in Miyamoto et al., 2005; Fusar-Poli et al., 2015). Hence, dopaminergic hypofunction alone is not sufficient to account for the whole picture of schizophrenia psychopathology. Glutamatergic neurotransmission has been increasingly proposed as a novel target for treating cognitive and negative symptoms in schizophrenia (reviewed in Uno and Coyle, 2019). Indeed, multiple evidences pointed to a relationship between glutamatergic neurotransmission and schizophrenia negative and cognitive symptoms (Thomas et al., 2017). Specifically, a positive correlation between elevated Glx in the hippocampus and poorer performance in executive tasks (Rusch et al., 2008) as well as the neural activation in left dorsolateral prefrontal cortex during working memory tasks was revealed in unmedicated schizophrenia patients (Kaminski et al., 2020). Interestingly, compared to other anti-psychotics, clozapine, a weak D_2 receptor antagonist which targets multiple receptor groups was demonstrated to have an effect on negative symptoms (Girgis et al., 2011) possibly through enhancing the function of NMDA receptors (Javitt et al., 2005; Schwieler et al., 2008; Gray et al., 2009; Veerman et al., 2014). Recent randomized controlled trials presented some promising findings on the improvements of negative and cognitive symptoms in schizophrenia by adding glutamatergic agents onto anti-psychotic drugs (reviewed in Uno and Coyle, 2019). For example, adding N-acetyl-L-cysteine to atypical anti-psychotics including risperidone and clozapine could alleviate both the negative and cognitive symptoms in chronic schizophrenia patients (Rossell et al., 2016; Sepehrmanesh et al., 2018)

2. Motivation and aims

2.1 Dimensions of psychopathology

Rating scales with tens of items, such as the PANSS (Kay et al., 1978) and the Scales for the Assessment of Positive and Negative Symptoms (SAPS and SANS) (Andreasen, 1984; Andreasen, 1989), have been introduced to describe the heterogeneous, multifaceted thought and behavior problems in schizophrenia patients. However, these scales encounter the downside of complexity and raise the question about the dimensional attribute of these item-wise symptoms. A precise definition of the dimensional structure of these scales is important to resolve the complexities in parsing schizophrenia phenomenology (Cichocki et al., 2012; Carpenter and Buchanan, 1989; Lenzenweger et al, 1991) and to shed light on the common neurobiological processes causing co-expressed symptoms as improved disease biomarkers. Principal component analysis (PCA) and exploratory factor analysis (EFA) provide effective ways for deriving the latent dimensional structure of the scales based on the co-expression patterns of symptoms. Although ample factorial studies have been devoted into the investigation of dimensions underlying the well-established 30-item inventory of PANSS (Kay et al., 1987), the factor models yielded by PCA and EFA were largely inconsistent with a varying number of factors (Kay and Sevy, 1990; Emsley et al., 2003; Van den Oord et al., 2006; Wallwork et al., 2012; van der Gaag et al., 2006a).

By definition, the PANSS comprises three subscales, but later studies suggested that these subscales are neither adequate nor optimal for capturing the symptom variation presented across schizophrenia patients. For example, items within a subscale show modest internal consistency (Peralta and Cuesta, 1994), while those across subscales are strongly correlated (Kay and Sevy, 1990; Emsley et al., 2003; Van den Oord et al., 2006). Although a pyramidical model with four components using PCA has been put forward by the PANSS developers (Kay and Sevy, 1990), other studies proposed that a model with five factors would be superior (Kim et al., 2012; Levine et al., 2007; Wallwork et al., 2012; van der Gaag et al., 2006a). A few models with six and seven factors have also been reported (Emsley et al., 2003; Van den Oord et al., 2006). Although a five-factor model is most frequently proposed, its replicability, external validity, and generalizability remain a concern (Lehoux et al., 2009) as prior models continuously failed to be confirmed in independent samples (White et al., 1997; van der Gaag et al., 2006b; Jiang et al., 2013), since systematic cross-validation and generalization analyses have rarely been performed. Also, since PCA loadings and scores contain both positive and negative weights (Devarajan, 2008), factorization methods used in previous studies are limited by the biological interpretability of the yielded factor-structure, while EFA often leads to equally low correlations between an item and multiple factors with ambiguous item-to-factor assignments (Trninić et al., 2013).

Aim 1: *To employ an Orthonormal and Projective variant of an unsupervised learning approach of Non-negative Matrix Factorization (OPNMF) (Yang and Oja, 2010) and a newly developed, sophisticated evaluation framework to identify a robust, stable, and well-generalizable factor-structure (i.e., dimensions) of PANSS to conceptualize the symptomatology of schizophrenia based on over 2000 schizophrenia patients recruited from 13 sites located in Europe, Asia, and the USA.*

OPNMF, compared to previously used PCA and EFA approaches, has several advantages:

1) due to the non-negative constraint on the input and the factorized matrices, NMF, and hence the OPNMF factors demonstrate an improved biological interpretability;
2) due to the projective constraint, the yielded OPNMF factors can be readily applied to out-of-sample data to estimate the factor loadings for novel patients;
3) due to the orthonormal constraint, OPNMF generates a sparse representation of the input data such that the learned factors are more compact and homogeneous than the factors derived from the original NMF method and PCA/EFA factors. Of note, the projective constraint also promotes sparsity in the resulting factors.

2.2 Psychopathological Subtypes

Besides factorizing symptoms into cardinal dimensions, by categorizing patients into subgroups with distinct symptom expression patterns provides an avenue to approach defining schizophrenia phenomenology and the psychopathological heterogeneity within schizophrenia. However, the classic clinical subtypes were eliminated in DSM-5 because of poor diagnostic stability, validity, and utility (Braff et al., 2013). Further, this set of classifications does not exhibit distinctive patterns of treatment response or capture the heterogeneous facets of schizophrenia well. Cumulatively, these downsides challenged a categorical perspective in schizophrenia symptomatology and moreover bring about controversies on whether discontinuously taxonomic components, i.e., subtypes, exist within this heterogeneous disorder. Multiple studies have re-visited the subtyping issue by applying data-driven clustering methods to derive symptomatically distinct subgroups. However, the numbers and definitions of psychopathological subtypes were highly variable across studies (Bartko et al., 1981; Helmes and Landmark, 2003), even when the subgroups were discovered purely based on the PANSS (Dollfus et al., 1996; Lykouras et al., 2001; Dickinson et al., 2017). Also, it is worth noting that a taxometric and latent variable mixture model has recently been introduced to characterize the negative symptoms of schizophrenia (Ahmed et al. 2015), though the model requires verification by future studies with larger sample sizes. The inconsistent clustering results could possibly be attributed to the fact that prior attempts mostly relied on geographically restricted small samples and single clustering strategies, while lacking an evaluation of stability and replicability.

Aim 2: *To investigate whether the newly identified dimensional structure of PANSS by OPNMF could yield new insights into the categorical aspects of schizophrenia. Patients were clustered by an interactive use of two well-established fuzzy-clustering methods based on individual expressions on the OPNMF-derived dimensions. A careful cluster stability assessment was also applied. These analyses would potentially allow for a hybrid dimensional-categorical conceptualization of schizophrenia symptomatology.*

The proposed soft-clustering scheme, compared to previously used hard-clustering methods, could better accommodate cluster-ambiguous patients and capture the expected overlap between subtypes (Insel et al., 2010). Moreover, soft-clustering generates membership degrees for each subject, and those patients with low memberships to any clusters (i.e., cases with an ambiguous cluster attribute) can be filtered out with appropriate cutoffs to symptomatically derive well-separated core psychopathological subtypes for schizophrenia. Also, this

approach would prospectively improve the statistical power to detect potential neurobiological distinctions between the identified subtypes, as cluster-ambiguous patients might obscure otherwise differentiable neurobiological features.

2.3 Neurobiological Substrates

Besides the use of factorization and clustering methods to resolve the symptomatic heterogeneity presented in schizophrenia, exploring the neurobiological basis for psychopathological dimensions and subtypes is critical since pharmacological agents, as the first line of treatment for schizophrenia, act on the central nervous system to presumably alleviate symptoms via regulating neurotransmitter systems. If common neurobiological processes for co-expressed symptoms within a dimension and neurobiological differentiations between subtypes could be clarified, specific and effective treatments targeting individual patients can possibly be developed. This is critical, as current anti-psychotics show limited improvements in functional outcomes for most patients with schizophrenia, and leave residual symptoms and unwanted side effects (Levine et al., 2011). Furthermore, anti-psychotics have minimal effects on negative and cognitive symptoms in schizophrenia patients (Miyamoto et al., 2005; Fusar-Poli et al., 2015). Hence, it is urgent to clarify the neural pathophysiology as well as the molecular substrates of specific dimensions of psychopathology. However, compelling results defining the symptom-neural substrate associations are still lacking. Pioneering efforts based on functional MRI (fMRI) have added valuable insights into the neurobiology of schizophrenia (Silverstein et al., 2016; Mwansisya et al., 2017; Dong et al., 2018) which may reveal an endophenotype underpinning the symptomatic heterogeneity (Gottesman and Gould, 2003). However, using univariate group-level correlation analysis, prior studies have demonstrated largely inconsistent findings when linking different symptom dimensions to functional brain parameters (e.g., reviewed in Giraldo-Chica and Woodward, 2017; Hu et al., 2017; Tregellas et al., 2014; Mehta et al., 2014). This is not unexpected, as the clinical complexity of schizophrenia together with the differences in patient populations, study designs, scanners, and scanning protocols across sites may lead to divergent results. Thus, identifying robust symptom-neural association patterns is challenging. However, pooling data from multiple international sites and applying multivariable machine-learning strategies with cross-validation and generalization analyses might be substantially useful for deriving association patterns that are generally and robustly presented in schizophrenia patients.

Functional brain systems as reflected by connectivity patterns are known to relate with molecular architecture (Zilles et al., 2002; Zilles et al., 2015; Richiardi et al., 2015; Anderson et al., 2020). Specifically, previous studies demonstrated a relationship between network-level resting-state functional connectivity (rsFC) and local neurotransmitter concentration (Stagg et al., 2014; Landek-Salgado et al., 2016; Limongi et al., 2020) and proposed a neuroconnectivity-neurotransmitter coupling framework (Kringelbach et al., 2020). Although resting-state fMRI serves as a powerful tool to inform the intrinsic neurobiological substrates of symptomatology at regional, network connectome or whole-brain level, it cannot directly map neurotransmitter systems, the key towards the development of new anti-psychotic treatments. Prior *invivo* molecular imaging studies, however, mostly relied on regions-of-interest analysis and hence would fall short in the perspective of the whole-brain dysfunctional nature of schizophrenia involving dysconnectivity within and between multiple functional systems

(Pettersson-Yeo et al., 2011; Uhlhaas, 2013). Taken together, identifying functional networks whose intrinsic connectivity patterns are robustly associated with specific symptom dimensions might allow for linking the molecular architecture of the identified networks to schizophrenia symptomatology.

->*Unlike most previous studies which relied on p values as the criteria to derive statistically significant symptom-neural relationships (the downsides of using p-values as the criterion have been commented elsewhere [Amrhein et al., 2019; Kraemer, 2019]), here based on resting-state fMRI data I recruited multiple sites in Europe and the USA, and employed multivariable machine-learning methods with careful cross-validation strategies including 10-fold and leave-one-site-out analyses.*

Aim 3: *Out-of-sample classification of the identified psychopathological subtypes from regional rsFC patterns was assessed using non-linear support vector machine. Regions with higher classification accuracies refer to more differentiated rsFC patterns between subtypes (i.e., higher neurobiological differentiability).*

Aim 4: *Network-based predictive modeling was implemented as leverage to link the identified symptom dimensions to specific neurobiological processes. Specifically, expressions of the four symptom dimensions in individual patients were predicted from rsFC within 17 meta-analytical task-activation networks previously defined using relevance vector machine. Moreover, apart from cross-validations, the model trained within the multi-site main sample of 147 schizophrenia patients tested its generalization performance in an independent sample with 117 schizophrenia patients retrieved from the Bipolar-Schizophrenia Network on Intermediate Phenotypes (B-SNIP) database (Tamminga et al., 2013).*

Aim 5: *A spatial correlation analysis between the symptom-predictive networks and whole-brain density maps of nine receptors and transporters (involving the dopaminergic, the GABAergic, and the serotoninergic systems) from prior molecular imaging in healthy populations was performed to investigate the related molecular architecture of the identified networks.*

A broad range of meta-analytically defined networks relating to social, affective, executive, memory, language, and sensory-motor functions were employed. The use of meta-analytic functional networks is important, as they showed convergent activation associated with specific processes. Hence, this offers an avenue to link the predicted symptom dimensions to specific functional domains, which intrinsic connectivity networks cannot. Also, the use of multivariable predictive modeling with a clean and strict cross-validation procedure could effectively mitigate model overfitting and facilitate the identification of robust network-symptom association patterns.

3. Additional details on the employed methods

3.1 Non-negative matrix factorization and its orthonormal and projectable variant

Non-negative matrix factorization (NMF) produces a factorization that both of the factors (basis vectors) and the factor-loadings contain no negative elements. This parts-based learning approach models data by additive combinations of non-negative basis vectors, making the factorization results can be intuitively interpreted. NMF and its variants have been widely used in recent biomedical studies including metagene discovery, functional characterization of genes, identification of structural brain networks, and cancer subtypes stratification (Kim et al., 2016; Hofree et al., 2013; Sadanandam et al., 2013; Sotiras et al., 2017). The present study is the first practice of applying this promising method to the PANSS data in schizophrenia to explore the latent dimensional structure of psychopathology. NMF is typically achieved by solving the following energy minimization problem:

$$\min \ \|V - WH\|_F$$
$$s.t. W \geq 0;$$

where *W* is the basis matrix (*m* attributes × *r* latent factors) containing the parts information. *H* is the (*r* factors x *n* data instances) matrix containing the loading coefficients, when used together with *W*, approximate the data matrix *V*.

Based on the initial NMF algorithm, plenty of studies have been devoted to developing diversiform extensions of NMF with different constraints to achieve specific practical purposes. One of the principal aspects and what we are most interested in factorizing the PANSS data is to expect a sparse representation of psychopathology. Sparse representation provides almost clustering like structure to facilitate the determination of item-assignment to specific dimensions but also retains the weights information of an item in belonging to each of the dimensions. Moreover, we would expect that the current defined factor-structure can be readily applied to novel samples. In these considerations, we adopted a variant of NMF, namely the orthonormal projective NMF (OPNMF) (Sotiras et al., 2015; Yang and Oja, 2010), to uncover the latent structure of the PANSS. This method differs from the original NMF in that it replaces the loading matrix by the inner product of the basis vectors and the input data matrix, making OPNMF to be projectable [i.e., $H = W^T V$, and thus the dictionary *W* (basis matrix) can be readily generalized to new data]. Due to the projective constraint in OPNMF, the loading coefficients are not free variables any more, which facilitates each factor to focus on specific parts of the data, leading to factors that are sparse, overlap less and are naturally more orthogonal. This is important as we could extract more compact and homogeneous latent factors from the PANSS data. The additional orthonormality constraint promotes the orthogonality between the learned factors. Sparsity is of great importance in signal decomposition and biological interpretation (Daubechies et al., 2009) and has been associated with improved generalizability (Avants et al., 2014). In contrast to other NMF variants to achieve sparsity, OPNMF does not involve any regularization terms or trade-off parameters, but is still able to learn more spatially localized, parts-based representations of the imported data patterns. Importantly, by enforcing the orthonormality constraint, the multiplicative update step becomes simpler which leads to less computational expense. This allows us to converge better to a local minimum and

facilitates the implementation of various cross-validation and out-of-sample generalization evaluations to obtain a stable and robust pattern for the latent factor structure of the PANSS.

The whole optimization process for OPNMF is to minimize the reconstruction error measured by frobenius norm between the input data matrix *V* and its estimate by only updating the basis matrix *W*:

$$\min \ \|V - WW^T V\|_F$$
$$s.t. W \geq 0;\ WW^T = I$$

where matrix *W* conveys factor information in each column with respect to the co-occurrence properties of the PANSS items which has a size of *m (item)* x *r* (*r* is the number of the estimated factors with each of the r columns defining a psychopathological dimension). Entry w_{ij} of *W* is the coefficient of item *i* in factor *j*. WW^T is the projection matrix, on which the matrix *V* can project to yield a subspace so that to approximate itself. In this form, the loading matrix *H* is replaced by W^TV so that the basis matrix *W* can be used to represent new data. The orthonormality constraint of $WW^T=I$ requires *W* to be an orthonormal matrix, and the orthogonality between the vectors in the learned *W* yields sparse factors, i.e., dimensions of psychopathology. *H* then encodes the symptomatology of a given patient along the dimensions spanned by the basis matrix *W* which has a size of *r* x *n* (each of the *n* columns represents the expressed symptom severity for a patient corresponding to the *r* factors defined in *W*) with entry h_{jk} represents the expression level of factor *j* in patient *k* that can be used for further patient-centric analyses, e.g., clustering patients into subtypes.

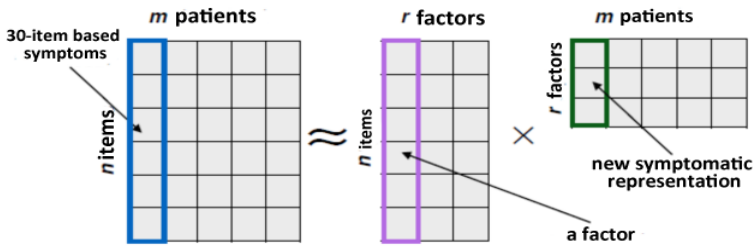

The non-convex problem was approached by iteratively performing the below multiplicative update rule:

$$W_{ij} = W_{ij} \frac{(VV^TW)_{ij}}{(WW^TVV^TW)_{ij}}$$

This update rule guarantees the positivity of the estimated factors, while monotonically decreasing the energy towards attaining a local optimum. Proofs of convergence have been presented in detail in previous literature (Lee and Seung, 2001).

The choice of initialization method is important since a suitable initialization of *W* will facilitate fast convergence. Non-negative singular value decomposition (NNSVD) was employed here as the initialization strategy (Boutsidis and Gallopoulos, 2008), which has the advantages of reduced residual error, faster convergence than using random initialization (Boutsidis and Gallopoulos, 2008), and most critically, renders the final non-negative decomposition to be deterministic.

3.2 Fuzzy-clustering

In the current project, I employed two fuzzy-clustering approaches of fuzzy c-means (Bezdek, 1981) and Gaussian mixture modeling (GMM) (Fraley and Raftery, 2002), and have used them interactively to identify core psychopathological subtypes of schizophrenia. In contrast to hard-clustering methods which impose each data point to be assigned to a certain cluster, fuzzy-clustering techniques allow for an identification of cluster-ambiguous points. The cluster-ambiguous points can be moreover filtered out (if they are reasoned to not attribute to any clusters) with an appropriate cutoff over the generated cluster membership degrees. Specifically, fuzzy c-means clustering provides probabilistic cluster memberships for each patient. The object function for fuzzy c-means contains a fuzzy partition matrix so that each patient is allowed to belong to multiple clusters with varying degrees of membership. The fuzzifier *m* (i.e., the exponent for the fuzzy partition matrix [*U*]; $1 < m < \infty$) controls the amount of fuzzy overlap between clusters (how fuzzy the boundaries between clusters can be) with larger values resulting in fuzzier clusters, i.e. a greater degree of overlap (Ozkan and Turksen, 2007). Squared Euclidean distance is commonly used as the distance metric between subjects. The resulting membership degrees reflect how strong a patient attributes to each cluster, and thus can be used to assign patients to specific clusters according to the maximal membership degree. Optimal cluster number can be determined based on several validity indices, for example, the fuzzy Silhouette index (SI) (Campello and Hruschka, 2006), the Xie and Beni index (XB) (Xie and Beni, 1991), and partition entropy (PE) (Bezdek, 1981). GMM is a model-based clustering approach (Fraley and Raftery, 2002; Scrucca et al., 2016), which employs a probabilistic model and takes moreover the covariance structure of the data into consideration. Clusters are assigned by selecting the component that maximizes the posterior probability. Like that in fuzzy c-means, the generated posterior probabilities by GMM reflect how strong a patient contributes to each Gaussian distribution component and thus can be likewise used to assign each patient to a certain cluster according to the highest posterior probability. The expectation-maximization algorithm is commonly used in practice for fitting the GMM models.

3.3 Brain-based subtype classification and symptom dimension prediction

In my Ph.D project, a supervised support vector machine (SVM) (Soentpiet, 1999) was adopted to approach the classification problem, i.e., to classify psychopathological subtypes from resting-state fMRI features. SVM learns the relationship between a set of input variables or features, and a particular outcome across a set of observations. The goal of SVM is to fit a function which approximates the relation between the features and the outcomes that can be used later to infer the outcomes for a new observation given its features. The non-linear extension of SVM of radial basis function (RBF) kernel SVM can moreover accommodate the potential non-linear relationship between the neural space and psychopathology. A nested 10-fold grid-search is commonly implemented to tune the hyperparameters of C (the error/margin trade-off parameter; in SVM classification case, its target function attempts to find a separating hyperplane based on the feature space that is minimizing a measure of error on the training set while simultaneously maximizing the 'margin' between the two classes) and γ (the kernel parameter) for the RBF kernel (Hsu and Chang, 2003). Class weights can be set when the size of sample is differing across

clusters.

To approach the prediction problem, I employed a Relevance Vector Machine (RVM) (Tipping, 2001) as implemented in the SparseBayes package (http://www.miketipping.com/index.htm) to achieve multivariable regression so that continuous target variables can be predicted based on set of features (i.e., exploratory variables). The RVM refers to a specialization of the general Bayesian framework which has an identical functional form to the support vector machine (SVM) (Soentpiet, 1999). In SVM, a separating hyperplane is computed based on the feature space learned from the training data by maximizing the margin between the two groups. The SV regression (SVR) extends the binary outputs from SVM to achieve an estimation and prediction of continuous variables. Analogous to the margin in SVM classification, the regression line of SVR is surrounded by a tube. Unlike SVM/SVR, RVM is embedded in a probabilistic Bayesian framework which substitutes the margin term in SVM by a prior distribution over the parameters. Specifically, an explicit zero-mean Gaussian prior is imposed to avoid severe overfitting associated with the maximum likelihood estimation of the model weights (Ghosh and Mujumdar, 2008; Zheng et al., 2008). Sparsity can be achieved in RVM without adding any penalty terms to shrink the predictor coefficients since the posterior distributions of many of the estimated weights are already towards zero. By computing the predictive distribution, the target value of a previously unseen input vector can be predicted from the trained model. RVM is free from constraints on the kernel functions (such as the Mercer‘s condition that required by SVM) and utilizes dramatically fewer basis functions. Moreover, the control parameters in RVM can be automatically estimated by the learning procedure itself (i.e., no hyperparameters that need to be tuned), which thus, exerts enhanced efficiency comparing to a classical SVM/SVR.

Ten-fold cross-validation and leave-one-site-out analysis are two common strategies to assess the out-of-sample generalization performance in classification and prediction experiments (Friedman et al. 2001). In 10-fold cross-validation, the available data are randomly split into 10 equal-sized groups, and in turn each one of the 10 groups is treated as the test set (i.e., the sample that is left-out), to which, the model trained based on the remaining 9 groups (training set) is applied, to predict the target for the left-out subjects. Each of the 10 groups will be left out once in the process so that every subject got predicted or classified. Then, classification accuracy can be calculated as how many subjects are correctly assigned to real clusters in proportion to the total number of subjects analyzed. If the sample size is differed across clusters, the balanced accuracy should be used in order to account for sample-imbalance condition which can be calculated using the equation below for a binary classification:

$$Balanced\ accuracy = \frac{1}{2}\left(\frac{TP}{TP + FN} + \frac{TN}{TN + FP}\right)$$

Where *TP* is the number of true positives; *TN* is the number of true negatives; *FP* is the number of false positives; *FN* is the number of false negatives.

For assessing the performance in multivariable prediction, *Pearson’s* linear or *Spearman’s* rank correlation coefficient, mean absolute error (MAE), and normalized root-mean-square-error (nRMSE) are commonly used

metrics. The correlation coefficient denotes the model's ability to predict, where an unseen patient will fall within a previously known distribution (i.e., the relative predictive power). The MAE and the nRMSE denote the absolute predictive accuracy referring to how much predicted values deviate from the corresponding observed values, while nRMSE is moreover expressed as a fraction of the standard deviation of the observed values. Equations for calculating MAE and nRMSE are defined as follows:

$$MAE = 1/N * \sum_n \left| s_n^{'} - s_n \right|$$

with N (1,2,…,n) being the total number of observations (subjects), $s_n^{'}$ the predicted value, and s_n the observed value for the n-th subject**.**

$$nRMSE = \sqrt{\frac{\sum_{i-1}^{N} \left(y_i - \widehat{y_i^{'}} \right)}{\sum_{i-1}^{N} \left(y_i - \overline{y_i^{'}} \right)}}$$

where N is the number of observations (subjects), y is the observed response variable for i-th subject, $\bar{y}$ is its mean, and $\hat{y}$ is the corresponding predicted value.

Leave-one-site-out analysis is particularly useful for evaluating the cross-site generalization performance when the data is pooled from multiple sites. In each leave-one-site-out analysis, researchers leave one site out, training models on the other sites, and then predict the target's values or cluster memberships in the left-out site. The process will be repeated until each site has been left out once, and, then, the classification accuracies or the correlations/MAE/nRMSE between actual values and their out-of-sample predictions for the left-out sites can be averaged to denote the generalization performance. In the prediction of continuous variables, one can also calculate the correlation strength between the actual values and the out-of-sample predictions pooled from the left-out sites.

To assess whether the classification or prediction is significant against chance in 10-fold and leave-one-site-out cross-validations, permutation testing, instead of parametric statistical tests, need to be used. This is because the folds in 10-fold cross-validation and the sites in leave-one-site-out experiments are not completely independent. That means the number of degrees of freedom (DOFs) is overestimated and using parametric correlation analysis here to derive the p values for cross-validated performance is problematic (Noirhomme et al., 2014; Combrisson et al., 2015). For constructing an empirical distribution of the chance correlation, one can repeatedly run the following two steps 1) shuffle the values of response variable randomly between subjects while keeping everything else exactly the same as that used for predicting the actual values, and then 2) record the (chance-level) correlation coefficient between the shuffled values and their predictions. Afterward, we can compare the true correlation coefficient (i.e., prediction based on the observed values) with the empirical null distribution for deriving the p-values. That is, for example, a null distribution with 1000 chance

correlations is constructed, if the true correlation coefficient exceeds all of the 1000 chance correlations, indicating a statistical significance of p = 0.001 (i.e., right-tailed).

The features (i.e., exploratory variables) I used for brain-based classification of subtypes and prediction of symptom dimensional scores were not the original blood oxygen level-dependent (BOLD) signals obtained from MRI scanning, but the resting-state functional connectivity measurements computed following a series of preprocessing steps. Since the preprocessing procedure for fMRI images was identical in my Ph.D projects, I provided the detailed description here ahead of the two attached papers. Other supporting information and supplementary materials specific to each paper were provided directly after the corresponding papers attached.

3.4 MRI data preprocessing

Preprocessing of resting-state fMRI and T1-weighted structural images was done in Statistical Parametric Mapping software (SPM12; https://www.fil.ion.ucl.ac.uk/spm) and Computational Anatomy Toolbox (CAT12; https://www.neuro.uni-jena.de/cat), respectively. In brief, for the resting-state modality, the first four volumes from all fMRI scans were discarded. Then, the DVARS metric (Power et al., 2012) was employed by calculating the voxel-wise BOLD signal intensity change between one frame (timepoint) and it's backward to detect and remove the patients with excessive movements. This is a critical step before any subsequently quantitative investigations, since excessive head motion will lead to spurious signals that bias the functional connectivity measures (Power et al., 2015). Equation for calculating DVARS was given as follows:

$$DVARS(\Delta I_i) = \sqrt{\langle [\Delta I_i(\vec{x})]^2 \rangle} = \sqrt{\langle I_i(\vec{x}) - I_{i-1}(\vec{x})]^2 \rangle}$$

where $I_i(\vec{x})$ is image BOLD signal intensity at locus $\vec{x}$ on frame *i* and angle brackets denote the spatial average of the voxel-wise signal intensity changes over the whole brain. The DVARS metric was further scaled by dividing by the median brain intensity and then multiplying by 1000 to approximate the magnitude that was reported in Power *et al.* (2012), i.e., 10 units of DVARS refer to 1% BOLD signal change. Afterward, all of the images were slice timing corrected using a newly proposed method of filter shift (Parker et al., 2017). The effectiveness and superiority of this method over the existing interpolation-based methods have been demonstrated (Parker et al., 2017), especially in the case that the subjects have moderate to high head motions. The slice timing corrected images were then head motion corrected in SPM12, and the derived six motion parameters were recorded. Following head motion correction, the images were normalized to MNI152 space by using an EPI template in SPM12 with a 4 x 5 x 4 basis set to alleviate overfitting (Calhoun et al., 2017). The normalized images were resampled to an isotropic voxel size of 2mm. The high-resolution T1-weighted structural images were preprocessed in CAT12 including tissue segmentation and spatial normalization to MNI152 space based on the shoot program (Ashburner and Friston, 2011). The resulting partial volume image for each patient encompasses the segmentations of white matter (WM) and CSF which were used as masks for extracting the global mean WM

and CSF signals. Here a quality control analysis was conducted by using the —check sample homogeneity" module in CAT12 to filter out those subjects with poor segmentation quality in structural images which may bias the estimation of WM and CSF signals. Twenty-four head motion parameters (the 6 head motion parameters of roll, pitch, yaw, translation in three dimensions, their first temporal derivatives, and quadratic term signals), together with the non-neuronal components of the extracted total WM and CSF signals were regressed out from the overall BOLD signals (Varikuti et al., 2017). Finally, band-pass filtering was performed on the data to restrict frequencies between 0.01 and 0.08 Hz.

4. Synopsis of the article

Collectively, the aforementioned aims

Aim 1: To identify a robust, stable, and generalizable factor-structure (i.e., dimensions) of the Positive and Negative Syndrome Scale (PANSS);

Aim 2: To identify psychopathological subtypes expressed along the new axes of psychopathology derived from *aim 1* to realize a hybrid dimensional-categorical conceptualization of schizophrenia symptomatology;

Aim 3: To identify neurobiological divergence between the yielded psychopathological subtypes;

have been addressed by

1) implementing an orthonormal projective non-negative matrix factorization (OPNMF) with a strict evaluation procedure (incl. split-half analyses, bootstrap resampling stability, and 10-fold cross-validation) for model selection to derive the factor-structure that is stable irrespective of data perturbation and generalizable across samples;

2) applying two well-established fuzzy-clustering approaches (fuzzy c-means and Gaussian mixture modeling) to individual patients based on their symptom expressions on the OPNMF-derived stable, and generalizable dimensions of PANSS;

3) performing classification analysis based on regional resting-state functional connectivity (rsFC) patterns using non-linear radial basis function support vector machine. Ten-fold cross-validation was employed to assess the out-of-sample neurobiological classifiability of the identified psychopathological subtypes;

in my first Ph.D paper published in "Biological Psychiatry":

Neurobiological Divergence of the Positive and Negative Schizophrenia Subtypes Identified on a New Factor Structure of Psychopathology Using Non-negative Factorization: An International Machine Learning Study (https://www.biologicalpsychiatryjournal.com/article/S0006-3223(19)31707-X/fulltex).

Aim 4: To link the identified dimensions of psychopathology to intrinsic brain connectivity patterns of functional brain networks;

Aim 5: To investigate whether the identified symptom-predictive networks are associated with the distribution of specific receptor/transporter systems (i.e., molecular architecture);

have been addressed by:

1) conducting network-based predictive modeling using relevance vector machine. That is, individual expressions of the identified symptom dimensions in individual patients were predicted from rsFC within 17 a priori, meta-analytically defined task-activation networks. Besides the application of 10-fold and leave-on-site-out cross-validations, predictive models identified in a multi-site sample were moreover validated in an independent schizophrenia sample.

2) implementing a spatial correlation analysis between the identified symptom-predictive networks and whole-brain density maps of nine receptors and transporters from prior molecular imaging in healthy populations. These receptors and transporters are primarily subserving the dopaminergic, the serotoninergic, and the GABAergic systems.

In my **second** Ph.D paper in "*bioRxiv*" as a preprint:

Connectivity patterns of task-specific brain networks allow individual prediction of cognitive symptom dimension of schizophrenia and link to molecular architecture

(https://www.biorxiv.org/content/10.1101/2020.07.02.185124v1).

5. Paper: Neurobiological Divergence of the Positive and Negative Schizophrenia Subtypes Identified on a New Factor Structure of Psychopathology Using Non-negative Factorization: An International Machine Learning Study

Ji Chen[1,2], Kaustubh R. Patil[1,2], Susanne Weis[1,2], Kang Sim[3,4], Thomas Nickl-Jockschat[5,6], Juan Zhou[7], André Aleman[8], Iris E. Sommer[8,9], Edith J. Liemburg[10], Felix Hoffstaedter[1,2], Ute Habel[11,12], Birgit Derntl[13], Xiaojin Liu[1,2], Lydia Kogler[13], Christina Regenbogen[11,12], Vaibhav A. Diwadkar[14], Jeffrey A. Stanley[14], Valentin Riedl[15], Renaud Jardri[16], Oliver Gruber[17], Aristeidis Sotiras[18], Christos Davatzikos[19,20], Simon B. Eickhoff[1,2,*] and the Pharmacotherapy Monitoring and Outcome Survey (PHAMOUS) investigators

[1]Institute of Neuroscience and Medicine, Brain and Behaviour (INM-7), Research Center Jülich, Jülich, Germany; [2]Institute of Systems Neuroscience, Medical Faculty, Heinrich Heine University Düsseldorf, Düsseldorf, Germany; [3]Department of General Psychiatry, Institute of Mental Health, Singapore; [4]Research Division, Institute of Mental Health, Singapore; [5]Iowa Neuroscience Institute, Carver College of Medicine, University of Iowa, Iowa City, IA, USA; [6]Department of Psychiatry, Carver College of Medicine, University of Iowa, Iowa City, IA, USA; [7]Center for Cognitive Neuroscience, Neuroscience and Behavioral Disorders Program, Duke-National University of Singapore Medical School, Singapore; [8]Department of Neuroscience, University Medical Center Groningen, University of Groningen, Groningen, The Netherlands; [9]BCN Neuroimaging Center, University Medical Center Groningen, University of Groningen, Groningen, The Netherlands; [10]University of Groningen, University Medical Center Groningen, Rob Giel Research center, Groningen, The Netherlands; [11]Department of Psychiatry, Psychotherapy and Psychosomatics, RWTH Aachen University, Germany; [12]JARA-Institute Brain Structure Function Relationship, Research Center Jülich and RWTH Aachen, Jülich, Germany; [13]Department of Psychiatry and Psychotherapy, University of Tübingen, Tübingen, Germany; [14]Department of Psychiatry and Behavioral Neuroscience, Wayne State University, Detroit, MI, USA;[15]Abteilung für diagnostische und interventionelle Neuroradiologie, Klinikum rechts der Isar, Technische Universität München, Germany; [16]Univ Lille, CNRS UMR9193, SCA Lab & CHU Lille, Fontan Hospital, CURE platform, Lille, France; [17]Section for Experimental Psychopathology and Neuroimaging, Department of General Psychiatry, Heidelberg University, Heidelberg, Germany; [18]Department of Radiology and Institute for Informatics, School of Medicine, Washington University in St. Louis, St. Louis, Missouri, USA;[19]Center for Biomedical Image Computing and Analytics, Perelman School of Medicine, University of Pennsylvania, Philadelphia, USA; [20]Department of Radiology, Section of Biomedical Image Analysis, Perelman School of Medicine, University of Pennsylvania, Philadelphia, USA.

Biological Psychiatry (2020): Volume 87; Issue 3. DOI: 10.1016/j.biopsych.2019.08.031.
Impact factor (2019): 12.095; Ranked #2 Psychiatry journal (Google Scholar); Total Citations: 1/155 in Psychiatry.

Own contributions

- Conception and design of experiment
- Reviewing and adapting analysis code
- Statistical data analysis
- Interpretation of results
- Preparing figures
- Writing the paper
- Total contribution 80%

5.1 Main text

Biological Psychiatry

Archival Report

Neurobiological Divergence of the Positive and Negative Schizophrenia Subtypes Identified on a New Factor Structure of Psychopathology Using Non-negative Factorization: An International Machine Learning Study

Ji Chen, Kaustubh R. Patil, Susanne Weis, Kang Sim, Thomas Nickl-Jockschat, Juan Zhou, André Aleman, Iris E. Sommer, Edith J. Liemburg, Felix Hoffstaedter, Ute Habel, Birgit Derntl, Xiaojin Liu, Jona M. Fischer, Lydia Kogler, Christina Regenbogen, Vaibhav A. Diwadkar, Jeffrey A. Stanley, Valentin Riedl, Renaud Jardri, Oliver Gruber, Aristeidis Sotiras, Christos Davatzikos, Simon B. Eickhoff, and the Pharmacotherapy Monitoring and Outcome Survey (PHAMOUS) Investigators

ABSTRACT

BACKGROUND: Disentangling psychopathological heterogeneity in schizophrenia is challenging, and previous results remain inconclusive. We employed advanced machine learning to identify a stable and generalizable factorization of the Positive and Negative Syndrome Scale and used it to identify psychopathological subtypes as well as their neurobiological differentiations.

METHODS: Positive and Negative Syndrome Scale data from the Pharmacotherapy Monitoring and Outcome Survey cohort (1545 patients; 586 followed up after 1.35 ± 0.70 years) were used for learning the factor structure by an orthonormal projective non-negative factorization. An international sample, pooled from 9 medical centers across Europe, the United States, and Asia (490 patients), was used for validation. Patients were clustered into psychopathological subtypes based on the identified factor structure, and the neurobiological divergence between the subtypes was assessed by classification analysis on functional magnetic resonance imaging connectivity patterns.

RESULTS: A 4-factor structure representing negative, positive, affective, and cognitive symptoms was identified as the most stable and generalizable representation of psychopathology. It showed higher internal consistency than the original Positive and Negative Syndrome Scale subscales and previously proposed factor models. Based on this representation, the positive–negative dichotomy was confirmed as the (only) robust psychopathological subtypes, and these subtypes were longitudinally stable in about 80% of the repeatedly assessed patients. Finally, the individual subtype could be predicted with good accuracy from functional connectivity profiles of the ventromedial frontal cortex, temporoparietal junction, and precuneus.

CONCLUSIONS: Machine learning applied to multisite data with cross-validation yielded a factorization generalizable across populations and medical systems. Together with subtyping and the demonstrated ability to predict subtype membership from neuroimaging data, this work further disentangles the heterogeneity in schizophrenia.

Keywords: Brain imaging, Machine learning, Multivariate classification, Non-negative factorization, Schizophrenia, Subtyping

https://doi.org/10.1016/j.biopsych.2019.08.031

Schizophrenia is a heterogeneous disorder with marked interindividual variability of psychopathology, which is related to treatment response and long-term outcomes (1,2). Earlier clinical subtypes (e.g., hebephrenic, paranoid) were eliminated in recent nosological classifications owing to poor diagnostic stability, validity, and utility (3). Considerable efforts have been devoted to better understand and categorize schizophrenia phenomenology by factorizing symptoms into cardinal dimensions or clustering patients into psychopathological subtypes based on scales such as the Positive and Negative Syndrome Scale (PANSS), a well-established assessment of schizophrenia psychopathology (4).

ISSN: 0006-3223

The 3 PANSS subscales (negative, positive, and general psychopathology) are generally suggested to not optimally and adequately capture the latent organization of schizophrenia symptomatology; items within a subscale show modest internal consistency (5), while those across subscales are strongly correlated (6–8). Previous factorizations of the PANSS have been inconsistent, advocating solutions between 4 and 7 factors (6–11). Although a 5-factor structure was most frequently proposed (9–12), it has continuously failed to be confirmed in independent samples (12–15). Interpretations of previous factor models are, furthermore, complicated by lack of sparsity (all items contribute to any factor) (16) and by coexistence of positive and negative weights (17). Finally, most previous studies investigated rather small and geographically restricted samples, raising doubts over generalization to different populations and medical systems because systematic cross-validation to assess stability and generalizability have rarely been performed. Previous work on psychopathological subtyping is likewise inconclusive (18–20), with added concerns related to longitudinal stability and neurobiological differentiability. These aspects are particularly relevant in the emerging context of precision psychiatry and raise the following questions: Do psychopathological subtypes represent stable patient characteristics, and do they relate to divergent neurobiological substrates that are identifiable from brain imaging data? Functional magnetic resonance imaging (fMRI) parameters may serve as an endophenotype, underpinning the symptomatic heterogeneity (21), which has added ample valuable insights into the neural pathophysiology of schizophrenia and its relation to clinical presentations (22,23). However, whether and to what extent the brain functional connectivity (FC) could discriminate psychopathological subtypes remains unknown. A successful classification using endophenotypical characteristics would support distinctiveness of symptomatically derived schizophrenia subtypes expressed along the cardinal axes of psychopathology.

In the current study, we addressed the aforementioned questions as follows: 1) a robust, cross-validated, and interpretable factor structure of schizophrenia psychopathology was identified based on PANSS scores of more than 2000 patients using an unsupervised machine learning approach (orthonormal projective non-negative matrix factorization [OPNMF]) (24–27); 2) core schizophrenia subtypes were derived by applying soft clustering to the identified factor structure, whose longitudinal stability was evaluated in repeatedly assessed patients; and 3) neurobiological differentiation of those subtypes based on resting-state FC (rsFC) patterns was investigated by cross-validated classification analysis, serving as a biological validation of a clinical (multivariate) construct.

METHODS AND MATERIALS

Sample

We used 2 large datasets collectively providing individual-item PANSS scores for 2035 patients with schizophrenia: 1) a subset of 1545 patients (586 followed up after 1.35 ± 0.70 years) with complete individual-item PANSS scores and a diagnosis of schizophrenia (DSM-IV criteria) retrieved from the Pharmacotherapy Monitoring and Outcome Survey (PHAMOUS) database (28,29) (this dataset was recruited from 4 institutions located in The Netherlands and assessed with a uniform protocol); 2) a deliberately heterogeneous sample pooled from 9 centers located in Europe, the United States, and Asia (490 patients) (Table 1 and Supplemental Table S1). This international dataset covers a broad range of clinical states, settings, and medical systems, making it ideal to evaluate the generalization of our factor model to new and diverse populations. Diagnoses in the international sample were established based on the DSM-IV, DSM-IV-TR, or DSM-5 criteria (Supplement). At all sites, data were acquired in accordance with the Declaration of Helsinki and after obtaining informed consent from the patients. Approval for the pooled reanalysis was obtained from the ethics committee of the Heinrich Heine University Düsseldorf.

Factorization of PANSS Using OPNMF

OPNMF (25,27) decomposes given data (PANSS) into 2 non-negative matrices: 1) a basis matrix (dictionary) with factors as columns that can be readily generalized to new data owing to the projective constraint and 2) a factor-loading matrix representing symptomatology of individual patients along these factors. The orthonormality constraint promotes a sparse, and hence interpretable, representation. For choosing the number of factors, a set of sophisticated evaluation strategies was implemented (see Supplement and Supplemental Figures S1 and S2).

We first applied OPNMF to the PANSS scores from the 1545 PHAMOUS patients with the number of factors ranging from 2 to 11. The optimal number of factors was identified by using cross-validation in 10,000 split-half analyses. The PHAMOUS sample was split into two halves, and on each split sample OPNMF was performed to derive the dictionary. The congruency between item-to-factor assignments, based on its largest coefficient, was assessed using the adjusted Rand index (30) and variation of information (31) along with the concordance index (32) between the dictionaries. We also quantified out-of-sample reconstruction error by projecting the data of one split sample onto the dictionary from the other split sample. A lower increase in out-of-sample error compared with within-sample reconstruction error indicates better generalizability. This split-sample analysis was repeated on the international dataset. Additional bootstrap and 10-fold cross-validation analyses were conducted on each of the 2 samples independently.

Most critically, we assessed stability and generalizability between the factorizations of the PHAMOUS sample (good for learning a structure owing to size) and the international sample (good for validation owing to heterogeneity). We performed OPNMF independently on the bootstrapped samples from each dataset. The resulting factorizations were then compared using the approaches described above. That is, for each number of factors, we assessed stability by comparing the dictionaries obtained from factorization of bootstrapped samples (PHAMOUS vs. international). Most important, we also evaluated generalization to new data by measuring the increase in reconstruction error for the international data following projection onto the PHAMOUS dictionary. This cross-sample evaluation was repeated after accounting for between-dataset differences in sample size, age, and illness duration

Table1. Demographic and Clinical Characteristics of the Patients With Schizophrenia

Characteristic	PHAMOUS Sample (*N* = 1545)	International Dataset From Nine Centers (*N* = 490)	International Dataset With Imaging (*N* = 147)	Statistic	*p* Value
Demographic					
Age, years[a]	44.15 (11.42)	33.82 (10.28)	34.89 (11.67)	183.51	<.001
Gender, male/female, *n*	1108/437	333/157	102/45	2.45	.292
Illness duration, years[b]	18.22 (10.54)	9.13 (8.98)	11.37 (10.36)	134.71	<.001
PANSS					
Positive[c]	12.48 (4.91)	14.24 (5.76)	15.36 (5.50)	37	<.001
Negative	14.60 (6.20)	14.67 (7.21)	15.07 (6.06)	0.375	.687
General[d]	26.70 (8.16)	29.10 (11.34)	30.93 (10.97)	23.67	<.001
Symptom severity, total PANSS score[e]	53.78 (16.35)	58.01 (21.87)	61.36 (19.57)	19.48	<.001
P3 item score[f]	2.30 (1.47)	2.66 (1.83)	3.22 (1.91)	28.18	<.001
Medication[g]					
Atypical antipsychotics	NA	167 (34.1%)	110 (74.8%)		
Typical antipsychotics	NA	26 (5.3%)	8 (5.4%)		
Both atypical and typical antipsychotics	NA	16 (3.3%)	9 (6.1%)		
None or unknown	NA	281 (57.3%)	20 (25.9%)		
Current antipsychotic medication[h]	NA	19.64 (14.15)	19.30 (12.57)		

Data are mean (SD) or *n* (%). *p* Values of <.001 indicate a significance of $p < .05$. Except for gender, which was based on χ^2 test, all other statistics were based on 1-way analyses of variance. Of note, because the detailed medication information was missing for several patients in different proportions for those with or without imaging data in the international dataset, statistical comparisons were not conducted.

Post hoc analysis after 1-way analyses of variance showing significant pairwise differences among the 3 datasets are indicated in the footnotes.

NA, not available; PANSS, Positive and Negative Syndrome Scale; PHAMOUS, Pharmacotherapy Monitoring and Outcome Survey; P3 item measures hallucinatory behavior.

[a]PHAMOUS > international sample = international sample with imaging at $p < .05$, Bonferroni corrected.

[b]PHAMOUS > international = international with imaging at $p < .05$, Bonferroni corrected. Information of illness duration was available for 1326 patients in the PHAMOUS sample and 393 patients in the international sample.

[c]PHAMOUS < international sample = international sample with imaging at $p < .05$, Bonferroni corrected.

[d]PHAMOUS < international sample = international sample with imaging at $p < .05$, Bonferroni corrected.

[e]PHAMOUS < international sample = international sample with imaging at $p < .05$, Bonferroni corrected.

[f]PHAMOUS < international sample < international sample with imaging at $p < .05$, Bonferroni corrected.

[g]A total of 211 patients with medication information in the whole international sample. A total of 149 patients also with illness duration information were included in the analysis of variance.

[h]Demonstrated in olanzapine-equivalent dosage (mg/day).

(Supplement). Leave-one-site-out validation was performed on both the PHAMOUS and international samples to check for site bias. We also repeated all analyses after removing outliers or including the repeated PANSS measurements (Supplement). Factorizations of the pooled (PHAMOUS + international) sample, as well as the stability and accuracy of PHAMOUS-generated dictionaries in estimating out-of-sample loadings or item scores, were also assessed (Supplement).

After identifying the optimal PANSS factorization, the international sample was projected onto this PHAMOUS-derived dictionary to obtain factor loadings for subsequent analyses (except for longitudinal analysis because reassessments were available only in the PHAMOUS sample) to avoid double dipping or leakage that would occur if scores were analyzed in the same dataset used to derive the dictionary.

Internal Consistency and Relationship Among Variables

Internal consistency of the optimal OPNMF model, as well as the PANSS subscales (as reference), was assessed using Cronbach's alpha, where higher values indicate more closely related items within a set. Relationships between the OPNMF factor loadings were assessed using linear and partial correlations (controlling for symptom severity, i.e., total PANSS score), including bootstrap stability analyses (Supplement). The OPNMF factor loadings were correlated with the 3 PANSS subscales. Correlations between individual items were also computed. For comparison, we performed an exploratory factor analysis (EFA) on the PHAMOUS sample and a confirmatory factor analysis on the international sample as well as a principal component analysis on both samples (Supplement). Effects of gender, age, illness duration, and symptom severity on the OPNMF factor loadings were analyzed in the international sample (*N* = 393 with complete information). Following a multivariate analysis of variance to assess effects on all the loadings, individual 4-way analyses of variance (ANOVAs) were performed on each loading to identify its association with the demographic and clinical features (corroborated by bootstrap and leave-one-site-out analyses) (Supplement). Current drug dosages of antipsychotic medication, available for 149 patients, were olanzapine-equivalent transformed (33) and included in the 4-way ANOVA models for a supplementary analysis.

Psychopathological Subtypes

After adjusting for age, gender, illness duration, and symptom severity, factor loadings were used as features for clustering patients into psychopathological subtypes. After confirming the data clusterability (34), we applied fuzzy *c*-means clustering (35), which provided cluster membership likelihoods for all patients. The optimal cluster number was determined based on the fuzzy silhouette index (36), the Xie and Beni index (37), and partition entropy (35). Stability was tested by leave-one-site-out replication, subsampling, and bootstrap resampling (Supplement). Given the heterogeneous nature of schizophrenia and the observation of multiple patients with ambiguous memberships, a cutoff over the membership likelihoods was adopted to remove cluster-ambiguous patients. For this, additional evidence from Gaussian mixture modeling (GMM) was considered. Specifically, patients were clustered again using GMM, and the optimal cluster number was determined by Bayesian information criterion (38). After assigning patients to the clusters, we took the intersection of the *c*-means and GMM results. A cutoff was chosen, based on the *c*-means membership likelihoods that well discriminated the patients inside the intersection from those outside, while also retaining a decent sample size for classification. This filtering step is critical because ambiguous patients might obscure otherwise classifiable rsFC patterns for the identified subtypes. Afterward, differences between subtypes regarding factor loadings and demographic and clinical features were ascertained by permutation tests (39). To assess longitudinal stability, the same *c*-means clustering was applied to the repeated assessments of the PHAMOUS sample. The optimal dictionary, identified on the 1545 PHAMOUS patients without repeatedly assessed PANSS scores, was used for projection to yield the factor loadings. After excluding ambiguous cases, patients assigned to the same clusters in both initial and follow-up stages were regarded as longitudinally stable (Supplement). For comparison, the same clustering was also performed on the factor loadings without any covariates or symptom severity adjustment as well as on the PANSS subscales or items both with and without covariates adjustment (Supplement).

Classifying Psychopathological Subtypes From rsFC

Multivariate classification analysis was conducted on patients from the international sample for whom imaging data were available after excluding those with ambiguous subtype assignment, low image quality, or excessive head motion (n = 84) (Supplemental Figure S24). After standard preprocessing (Supplement), regional time series were extracted based on a parcellation scheme with 600 cortical parcels (40) and 36 subcortical parcels (41), adjusted for confounders (42), and were used to compute the functional connectome. We tested each parcel for whether its pattern of rsFC to all other parcels allowed classifying subtype membership in novel subjects. Resulting parcelwise accuracies yielded a whole-brain map indicating the classifiable power of each parcel's connectivity profile. The radial basis function kernel support vector machine classifier, which can deal with the potentially nonlinear relationship between the psychopathological and neural spaces, was employed. A stratified 10-fold cross-validation was implemented to assess the out-of-sample classification performance (Supplemental Figure S25). Effects of age, gender, site, illness duration, symptom severity, and head-motion parameters were adjusted using a linear regression model fitted only in the training sample (43). Significance of the parcelwise accuracy was estimated by permutation tests, followed by false discovery rate correction for multiple comparisons (Supplement). Parcels surviving false discovery rate were functionally characterized (http://brainmap.org/) (44) (Supplement).

RESULTS

Dimensions of Psychopathology

The most robust and generalizable model consisted of 3 factors for the PHAMOUS sample (Figure 1A), which effectively combined the positive and affective symptoms compared with the optimal 4-factor model for the international dataset (Figure 1B). The additional factor in the international dataset may relate to the higher prevalence of psychotic symptoms, particularly auditory hallucinations, compared with the PHAMOUS sample, which contains more long-term patients (Table 1). Consequently, a 4-factor model was identified as the most stable and, importantly, generalizable model of psychopathology in the cross-sample evaluation (Figure 1C). The first factor mainly represents negative symptoms such as blunted affect and apathy (Figure 1D). The second factor represents positive symptoms such as delusions and hallucinations. The third factor comprises symptoms such as depression, anxiety, and tension, reflecting an affective dimension. The fourth factor represents cognitive impairments. Notably, only a few items contributed to multiple dimensions (e.g., active social avoidance contributed to both negative and affective factors).

All findings were fully confirmed by 1) bootstrap and 10-fold cross-validation, 2) removing outliers (18 patients), 3) adding PANSS data from follow-up examination in the PHAMOUS sample, 4) leave-one-site-out validation, 5) accounting for between-dataset differences in sample size, age, and illness duration, 6) pooling the 2 datasets with cross-validation and out-of-sample generalization assessments, and 7) loading or item score predictions across factor solutions, bootstrapped samples, and sites (Supplemental Figures S3–S11).

Internal Consistency and Relationship Among Variables

Items within a factor showed higher and more homogeneous positive correlations (and fewer anticorrelations) for the OPNMF factors than for the PANSS subscales (Figure 2A, B and Supplemental Figure S12). Internal consistency of our OPNMF 4-factor structure (positive: Cronbach's alpha = .75; negative: .92; affective: .85; cognitive: .83) was on average higher than that of the PANSS subscales (positive: .72; negative: .87; general psychopathology: .87), previously reported factor models (ranging from .60 [excited] to .90 [negative]) (7–9,45), and the EFA models derived from the current sample (.49–.91) (Supplemental Table S2). All PHAMOUS-derived 4- to 7-factor EFA models could not be confirmed in the international sample owing to inadequate fit (Supplemental Table S2). Compared with principal component analysis, OPNMF showed

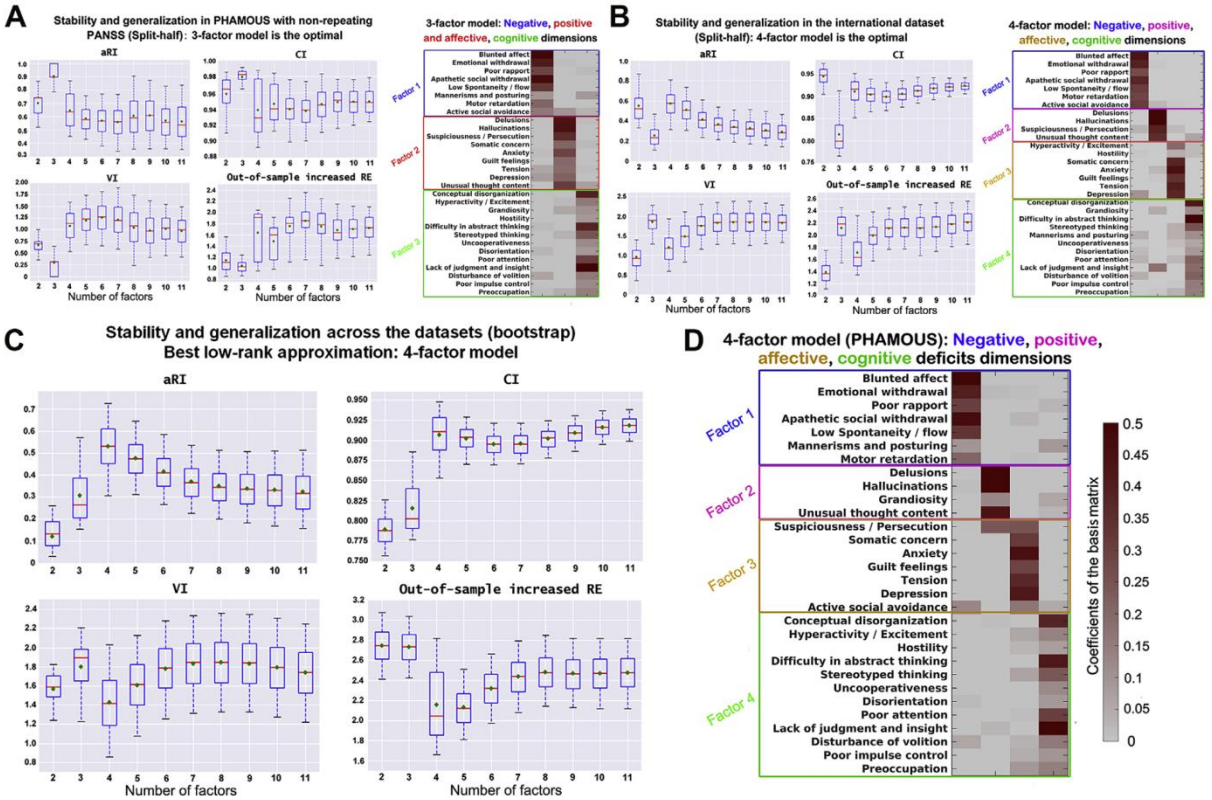

Figure 1. Split-half cross-validation (10,000 repetitions) of stability and generalizability of the factor solutions derived by orthonormal projective non-negative matrix factorization. The 3 indices—adjusted Rand index (aRI), variation of information (VI), and concordance index (CI)—demonstrate the factor stability, while out-of-sample increased reconstruction error (RE) reflects the performance of generalizability. Box plots show stability and generalizability results of the factor solutions. Higher values for aRI and CI (upper row) indicate higher stability. Lower values for VI and out-of-sample increase in RE (bottom row) indicate better stability and generalizability, respectively. For the box plots, the red line depicts the median, the green diamond depicts the mean, and the whiskers represent the 5th and 95th percentiles. For the factor models, the weight of an item in assigning to a specific psychopathological factor (columns of the matrix) is color-coded according to the coefficients by a heat color map from gray (minimum) to dark red (maximum). **(A)** The best factor solution derived from the Pharmacotherapy Monitoring and Outcome Survey (PHAMOUS) data (1545 patients) is shown. According to the 4 aforementioned evaluation indices, a 3-factor model was indicated as the best because both the mean and median values for VI and out-of-sample increase in RE achieve the lowest, while the aRI and CI reach the highest, at that point. **(B)** The best factor solution derived from the international sample (490 patients) is shown. Four factors is the optimal solution because the mean and median values of VI and out-of-sample increase in RE achieve the local minimum, while the aRI reaches maximum and the CI reaches a local maximum. **(C)** The best factor solution identified by the bootstrap comparison of the two datasets (PHAMOUS vs. international) is shown. A 4-factor solution is optimal because the mean and median values of the aRI and CI reach the maximum, while the mean and median values of VI and the median value of out-of-sample increase in RE achieve the minimum. **(D)** The most stable and generalizable 4-factor structure derived from the PHAMOUS sample, serving as the best basis for future studies, is shown. This 4-factor model consists of a negative (factor 1), a positive (factor 2), an affective (factor 3), and a cognitive (factor 4) factor that were named based on the items they contained. PANSS, Positive and Negative Syndrome Scale.

better generalizability (Supplemental Figure S13). The positive and negative factors were highly correlated with the positive and negative PANSS subscales, respectively, both before (r = .92 and r = .97) and after (r = .85 and r = .89) controlling for symptom severity (Supplemental Figure S14). Interestingly, after adjusting for symptom severity, the cognitive factor did not correlate with general psychopathology (r = .02).

Over individual patients, the loadings on our 4 factors were significantly intercorrelated, with negative and positive factors showing the lowest correlation (r = .32 averaged over 10,000 bootstraps) and negative and affective factors showing the highest correlation (r = .70) (Figure 2C). After controlling for symptom severity, positive and negative factors became anticorrelated (r = −.59) (Supplemental Figure S15).

Multivariate analysis of variance revealed a significant influence of symptom severity on the joint factor loadings ($p < .001$). Follow-up 4-way ANOVAs showed that symptom severity had a significant effect on each factor (all ps $< .001$, all βs $> .07$) (Figure 2D). The cognitive factor showed a trend toward a positive relationship with illness duration (p = .081, β = .014) and a significant negative relationship with age (p = .033, β = −.015) (Figure 2D), although both covariates were collinear (r = .65). In contrast, loadings on the negative factor were higher for older individuals (p = .11, β = .016) and lower for those with longer illness duration (p = .18, β = −.015). Gender differences were not observed in any factor. Bootstrap (Figure 2E) and leave-one-site-out analyses corroborated the aforementioned ANOVA findings (Supplement). Adding

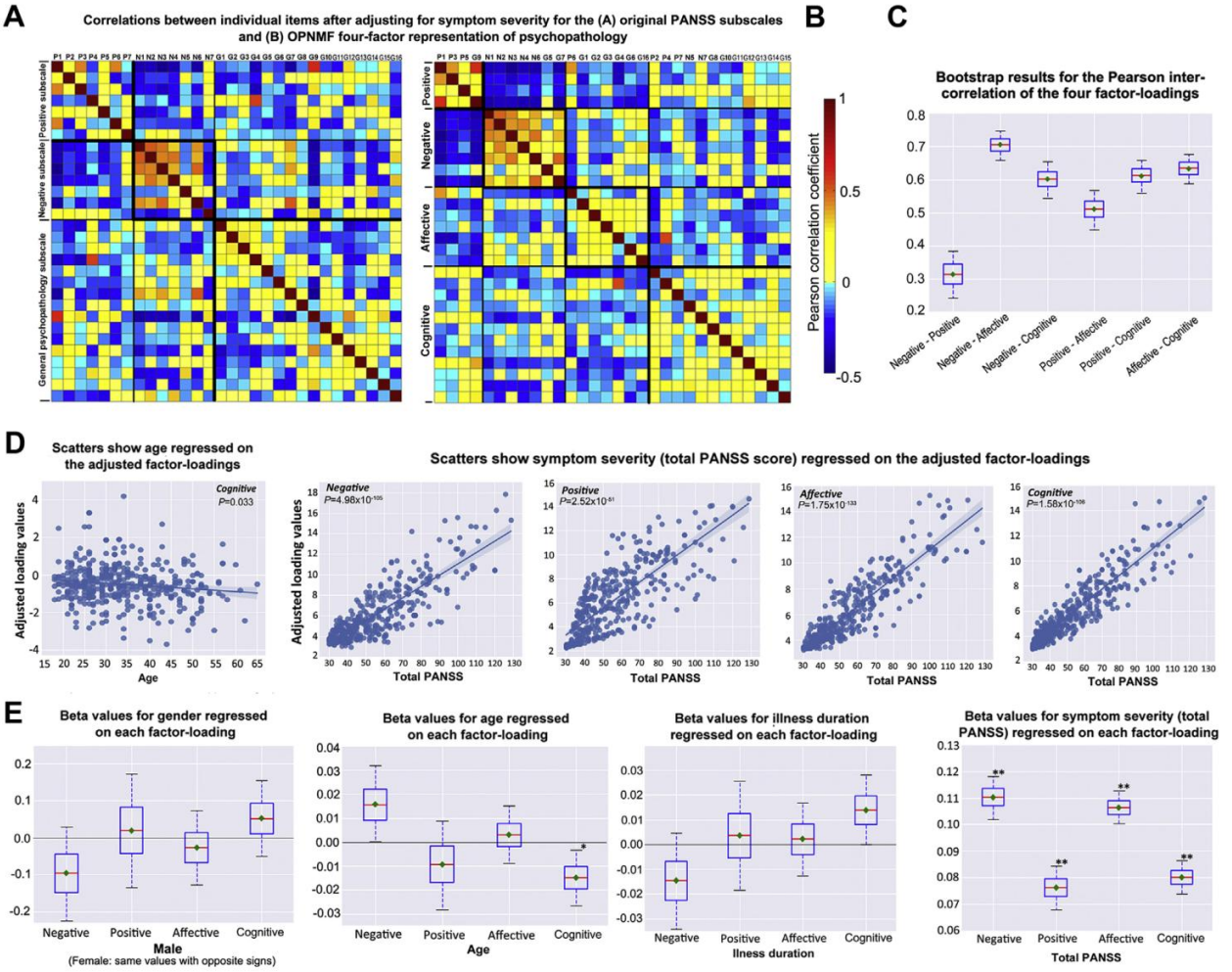

Figure 2. Inter-item correlations, relationship between factors, sociodemographic information, and clinical information. The 4-factor structure, derived from the Pharmacotherapy Monitoring and Outcome Survey sample with initial measure of Positive and Negative Syndrome Scale (PANSS) scores, was adopted as the reference on which the international sample was projected to derive the factor loadings. **(A, B)** Heat maps show interitem correlations for the original PANSS subscales **(A)** and the current orthonormal projective non-negative matrix factorization (OPNMF) 4-factor representation of psychopathology after controlling for symptom severity (total PANSS score) **(B)**. Correlation strength is color-coded (light yellow to red: positive correlations; cyan to blue: negative correlations). **(C)** Box plot shows the bootstrap results (repeated 10,000 times) for the Pearson correlations among the 4-factor loadings. Bootstrap samples were drawn with replacement from the original international sample, and then the correlation analysis was done on them. The red line depicts the median, the green diamond depicts the mean, and the whiskers represent the 5th and 95th percentiles. **(D, E)** Graphs show effects of sociodemographic and clinical features on the 4-factor loadings. **(D).** Scatter plots show 4-way analysis of variance results of the significant negative association between age (adjusted for gender, illness duration, and total PANSS score) and the cognitive loading (p = .033) as well as the significant positive associations between the symptom severity (total PANSS score) and the 4-factor loadings (negative: $p = 4.98 \times 10^{-105}$; positive: $p = 2.52 \times 10^{-51}$; affective: $p = 1.75 \times 10^{-133}$; cognitive: $p = 1.58 \times 10^{-106}$) after adjusting for age, gender, and illness duration. Regression lines are depicted with a 95% confidence interval on the fitted values. **(E)** Bootstrap results for the 4-way analysis of variance are shown. Bootstrap samples were drawn with replacement from the original international sample and then the analyses of variance were done on them. Boxes refer to the beta values. The red line depicts the median, the green diamond depicts the mean, and the whiskers represent the 5th and 95th percentiles. *Median, $p < .05$; **Mean and median, $p < .05$.

olanzapine-equivalent dosage to the 4-way ANOVA did not reveal any significant association with medication.

Psychopathological Subtypes

Fuzzy *c*-means clustering on the adjusted loadings revealed an optimal 2-cluster solution (Figure 3A, B and Supplemental Figures S16 and S17). Although GMM demonstrated an optimal 3-cluster solution, one of the clusters was diffusely distributed in space containing patients from both *c*-means clusters. This GMM cluster was excluded because it would not represent any specific subtype (Figure 3C). Patients inside the *c*-means GMM intersection had higher *c*-means membership likelihoods (roughly > .70) to belong to their own cluster than those outside the intersection ($p < .01$, Wilcoxon rank-sum test) (Figure 3D). We chose the cluster cores using the likelihoods of *c*-means with a cutoff of .70. As a result, 2 core subtypes were defined after filtering out 50 ambiguous patients

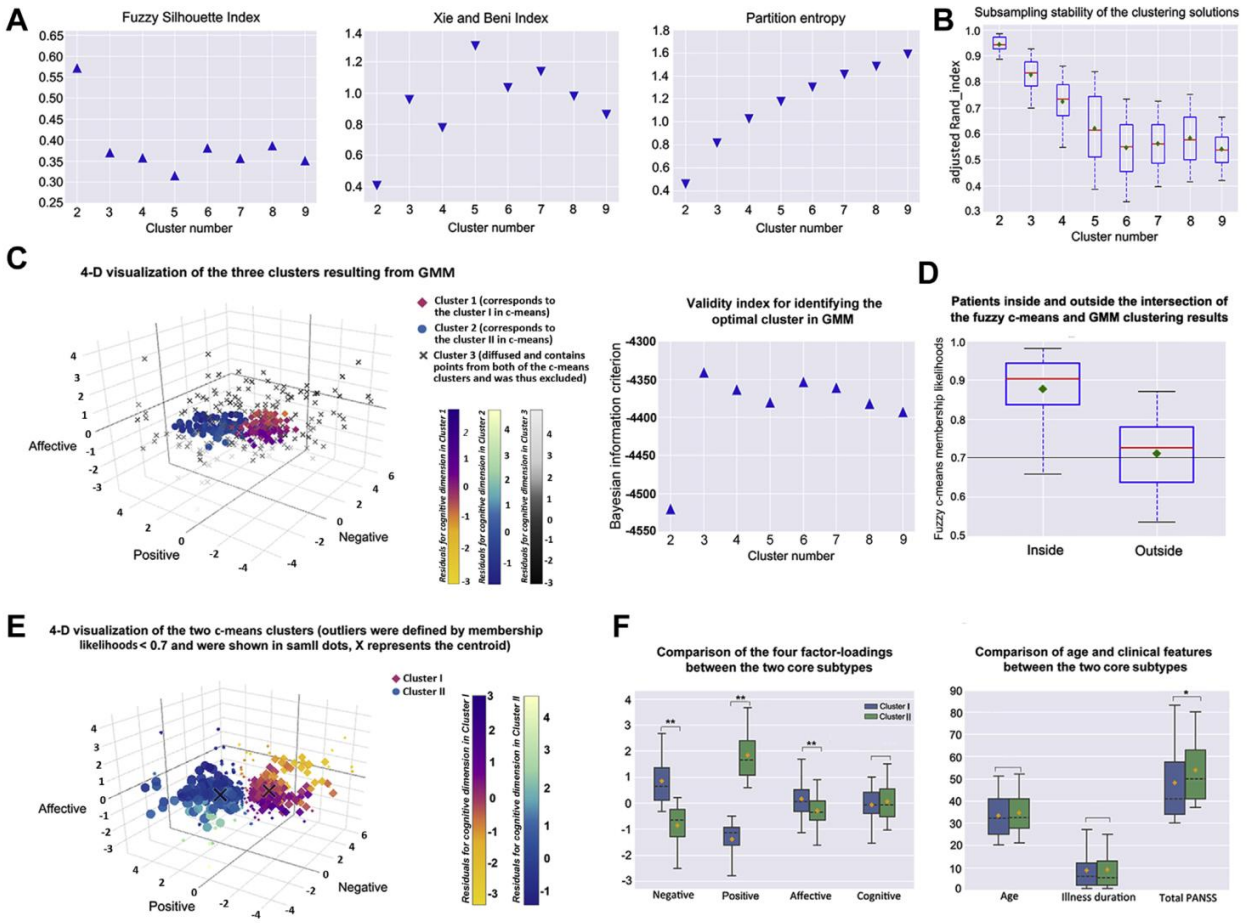

Figure 3. Fuzzy *c*-means clustering results of patient subgroups based on the loadings of the generalizable 4-factor structure. **(A)** The internal validity indices used for determining the optimal cluster number are shown. Higher values of fuzzy silhouette index (in triangle) and lower values of Xie and Beni index and partition entropy (in inverted triangle) indicate a better clustering quality. The maximum for fuzzy silhouette index and the minimums for Xie and Beni index and partition entropy all suggested a 2-cluster solution. Fuzzy silhouette index and Xie and Beni index reflect the compactness and separation of the generated clusters, while partition entropy reflects the fuzziness of the cluster partition, that is, the uncertainty of the patients to be assigned to a certain cluster. **(B)** Box plot shows results of the assessment of clustering stability based on the subsampling technique. The cluster number 2 reaches the highest adjusted Rand index. Adjusted Rand index reflects the convergent assignment of the patient pairs to the clusters between the subsamples and the original sample. **(C)** Four-dimensional visualization of the optimal 3 Gaussian mixture modeling (GMM) clusters determined by the Bayesian information criterion is shown (a higher value indicates a better clustering solution). Magnitude of the cognitive loading was color-coded differently for the 3 clusters (cluster 1 corresponds to the cluster I [i.e., subtype A] in fuzzy *c*-means, yellow to Modena; cluster 2 corresponds to the cluster II [i.e., subtype B] in fuzzy *c*-means, blue to shallow flax; cluster 3 is the excluded diffused cluster that would not present any specific subtype, black to light gray). **(D)** Box plot shows the fuzzy *c*-means membership likelihoods of the patients inside and outside the intersection of the *c*-means and GMM clustering results. The black line indicates a heuristic cutoff of .70. **(E)** A 4-dimensional (4-D) visualization of the optimal fuzzy *c*-means 2-cluster solution is shown. Ambiguous assignments were defined by membership likelihoods $<$ .70, which was selected by interacting with GMM. Those subtype-ambiguous patients are shown in small dots, and X represents the centroid. Magnitude of the cognitive loading is color-coded differently for the two clusters (cluster I, yellow to Modena; cluster II, blue to shallow flax). **(F)** Grouped box plots show the between-subtype (without subtype-ambiguous patients) comparison results of the 4-factor loadings, age, illness duration, and total Positive and Negative Syndrome Scale (PANSS) score. Cluster I is dominated by negative and affective symptoms (i.e., subtype A), and cluster II is significantly prominent in positive symptom expressions (i.e., subtype B). The black dashed line depicts the median, the yellow diamond depicts the mean, and the whiskers represent the 5th and 95th percentiles. $^{*}p < .01$; $^{**}p < .001$.

from each of the 2 *c*-means clusters (Figure 3E). The first subtype showed a psychopathological profile dominated by negative and affective symptomatology (subtype A). The other subtype featured prominent positive symptoms (subtype B; all *p*s $<$ .001 in permutation tests) (Figure 3F and Supplemental Figure S18). Importantly, subtypes did not differ in gender distribution, age, or illness duration (all *p*s $>$ .05), but subtype B showed higher symptom severity (p = .008). The same 2-cluster solution was replicated on the PHAMOUS patients with complete demographic and clinical information (N = 1326; 56% of the 603 ambiguous patients in subtype B when hard-clustered) and on those with repeatedly assessed PANSS scores (n = 527; 45% ambiguous). Nearly 80% of the reassessed patients retained their subtype, with subtype A being more stable (85%) (Supplement). The additional clustering analyses supported our 4-factor model with covariates

adjustment for a clinically meaningful subtyping (Supplemental Figures S19–S23).

Classifying Psychopathological Subtypes From rsFC

The rsFC profile of the parcel located in the right ventromedial prefrontal cortex yielded the highest out-of-sample classification accuracy (70% of patients not used for training were assigned to the correct psychopathological subtypes), followed by parcels in the right temporoparietal junction, bilateral precuneus, and posterior cingulate cortex (Figure 4C). Permutation tests showed that the top 104 classifiable parcels were significant ($p < .05$) against chance (i.e., randomized subtype labels), and 53 parcels survived false discovery rate correction ($q < .05$) (Figure 4B). Of note, parcels are labeled by their microanatomical location with their functional implications (Supplemental Table S4). Classification with additional global mean signal removal or with an rsFC-based subcortical parcellation replacement (7 parcels [46] as a control analysis instead of the finer Brainnetome subcortical parcellation) replicated these results (see Supplement and Supplemental Figure S26).

DISCUSSION

By factorizing the PANSS scores from a large sample using OPNMF and cross-validating the results in a heterogeneous multisite dataset, we revealed a robust, replicable, and generalizable 4-factor structure comprising negative, positive, affective, and cognitive dimensions across populations, settings, and medical systems. Based on this 4-factor structure, 2 core psychopathological subtypes were obtained that showed good longitudinal stability and could be discriminated by regional rsFC patterns, with the right ventromedial prefrontal cortex showing the highest (70%) classification accuracy.

Relationship to Previous Factor Models of PANSS

The 3 PANSS subscales do not reflect the latent structure of this inventory well (5–7). In turn, our model represents a stable, generalizable, and well-interpretable description of schizophrenia psychopathology suited for representing the full range of acute and chronic symptoms. Resonating with this view, a pyramidical model proposed by the PANSS developers comprised 4 components (6). Three of these (negative, positive, and affective dimensions) showed good agreement with our model. The fourth component, however, isolated only excitement, while cognitive disturbances were distributed across all dimensions or discarded. Such a representation is obviously at odds with the importance of cognitive dysfunction and has prompted the proposal of more complex models (7–11), for example, a recent 5-factor model reflecting negative, positive, depressed, excited, and cognitive dimensions (45). However, replicability, external validity, and generalization remain a concern for these models (47). As a striking example, White *et al.* (13) found that none of 20 tested models fit their data adequately, and they put forward a new pentagonal model that later (together with 24 other models) also could not be confirmed (14). In the same study (12), the authors developed an improved 5-factor model using 10-fold cross-validation. However, it still failed to be confirmed, along with 31 other 5-factor models, in a later study involving 2 large Chinese samples (15). In our sample, inadequate fit for EFA models with 4 to 7 factors was also manifested, and the fifth OPNMF factor, compared with the 4 factors, showed the poorest out-of-sample loading predictions (Supplemental Figure S10B). These facts, as a whole, point to a fundamental instability of 5-factor models (9–15,44). Addressing these concerns, the current work not only was based on a large sample for model identification but also, importantly, focused strongly on cross-validated stability and out-of-sample generalization. Critically, the external validation was based on a heterogeneous international sample, and the optimal model suggested a single factor to combine both the cognitive and excited symptoms. This view is corroborated by observations that cognitive and excited symptomatologies are highly correlated (45) and share similar neurobiological substrates (48,49).

Internal Consistency and Relationship Among Variables

Although we identified the optimal representation by its robustness and ability to generalize to new populations, the positive and negative dimensions of our model also showed better internal consistency than the PANSS subscales while differentiating the broad general psychopathology. Moreover, our affective and cognitive factors showed higher internal consistency than those reported in previous factor models (7,8,10,45). Finally, correlations between individual items within OPNMF factors were higher and more homogeneous compared with the PANSS subscales.

Matching previous reports (4,8,45), negative and positive factors from our model were least related before, and showed a strong anticorrelation after, controlling for symptom severity. The inverse age versus illness duration effect on negative symptoms implies that this effect may be more related to age than to illness duration. This is intriguing from the perspective of early aging or degeneration, but it needs to be viewed with caution because age and illness duration are highly correlated. Colinear variables in a single linear regression model make it difficult to disentangle their respective effects on the negative factor as well as on the cognitive factor (50).

Psychopathological Subtypes, Longitudinal Stability, and Neurobiological Differentiability

Our results revealed 2 distinct schizophrenia subtypes featuring predominantly positive and negative symptoms, respectively. The subtypes were longitudinally stable and could be classified from neuroimaging data. Such a positive–negative dichotomy has been widely supported (51,52). Finer distinctions have been proposed but show poor replicability (18–20). The inconsistency of finer subtyping may relate to idiosyncrasies in small samples from a single geographical region and to the lack of explicit analyses of stability and replicability. Moreover, longitudinal stability of our new subtypes was higher than that reported for traditional clinical subtypes or for a positive/negative/mixed topology (53–55). Interestingly, we found subtype A to be particularly stable. Previous studies indicated that both mixed and negative symptom states increase over time, whereas psychotic

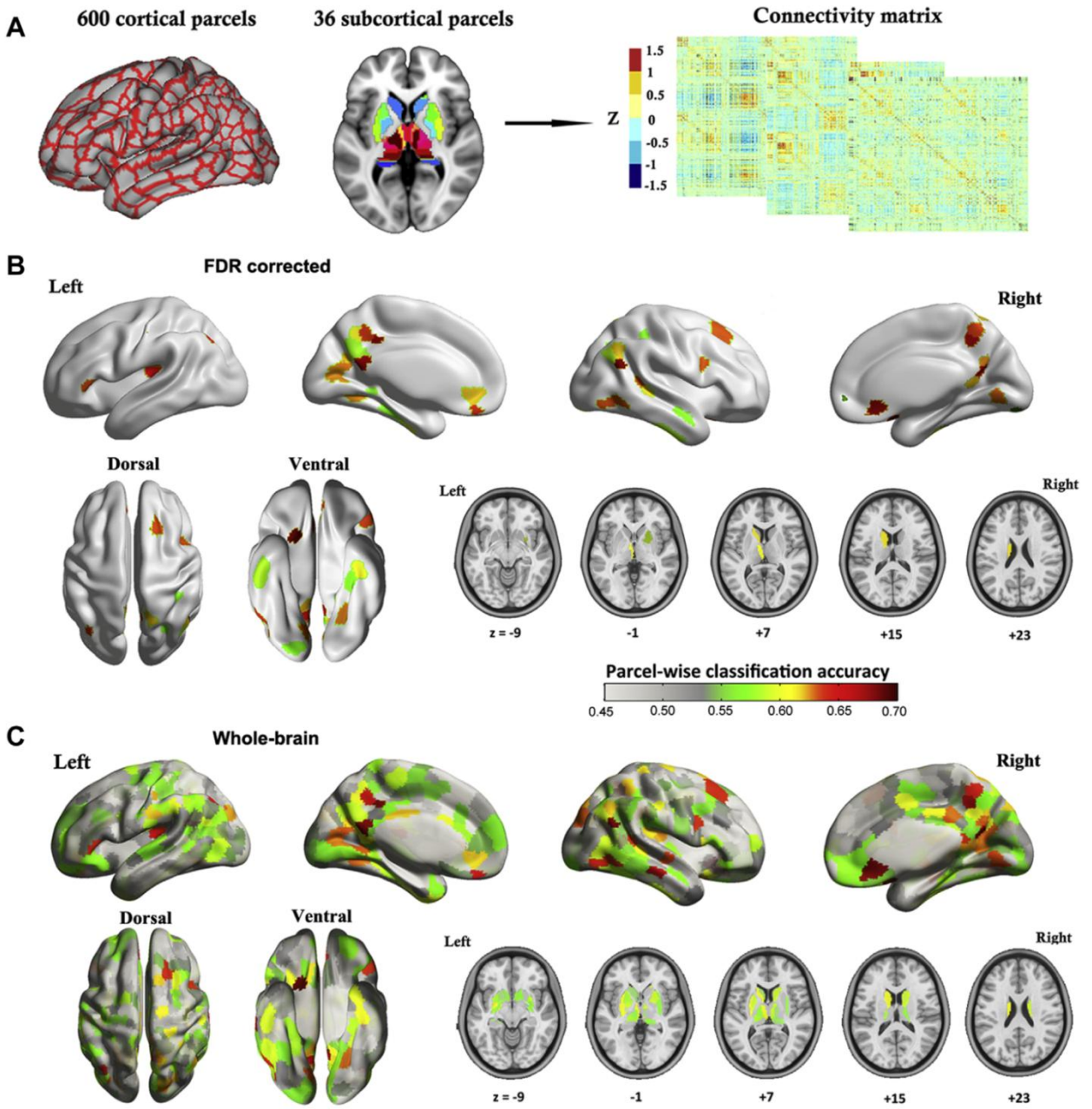

Figure 4. Classifying psychopathological subtypes from resting-state functional connectivity. **(A)** The brain parcellation scheme (600 cortical parcels plus 36 subcortical parcels) and the resting-state functional connectivity matrix that was constructed based on this parcellation system are illustrated. In parcelwise classification analysis, one column of the connectivity matrix was taken to represent the functional connectivity pattern for a single parcel. **(B)** Cortical surface rendering and subcortical axial slices show parcelwise classification results for those parcels that survived false discovery rate (FDR) correction ($q < .05$), demonstrating a neurobiological divergence between the two identified psychopathological subtypes of schizophrenia. **(C)** Cortical surface rendering and subcortical axial slices show parcelwise classification results for the whole brain. The balanced classification accuracy is color-coded from light gray to dark red.

expressions usually diminish outside acute episodes and over time (54,55). Future studies with a longer follow-up duration are desired; the mean of 1.35 years' follow-up assessed in the current study is not a long period in schizophrenia. In addition, the employed soft-clustering method better accommodates ambiguous patients compared with previous hard-clustering methods, and furthermore, patients with ambiguous memberships can be filtered out with appropriate cutoffs to improve the ability of detecting neurobiological distinctions between subtypes. Nonetheless, the cutoff value chosen in the current

study should be noted as heuristic. The cluster-ambiguous patients might represent a transient group lying between the two more differentiated subtypes.

The current top classifiable brain regions all are implicated in schizophrenia pathophysiology and processes relevant to the psychopathological distinction (22,56–60). Previous findings in the literature relating fMRI parameters to differential symptoms exclusively relied on group-level analyses, while our approach bridged an important gap between neurobiological divergence and distinct symptomatic patterns at the individual level. To our knowledge, it is the first study to successfully classify psychopathological subtypes in schizophrenia. Of note, the current classification accuracy was similar to accuracy levels previously reported for classifications of patients with schizophrenia versus healthy participants (61–63). The demonstrated neurobiological differentiability corroborates the currently identified schizophrenia subtypes expressed along the 4 OPNMF dimensions.

Limitations and Considerations

We assessed factor structure, subtypes, and their neurobiological differentiations with a particular emphasis on robustness and generalization. This conservative approach seems necessary given current concerns of nonreplicability in biomedical research, but it might have contributed to the fact that we corroborated the clinically well-established positive–negative distinction rather than identifying more differentiated subtypes. We note, however, that a recent imaging-based clustering also provided evidence for 2 subtypes (64), and we stress that the current analysis of a large heterogeneous sample did not reveal any evidence for a more fine-grained differentiation among the patients. Thus, it remains to be seen whether an additional differentiation between these 2 core subtypes may be robustly revealed by analyzing substantially larger samples or whether previously proposed additional subtypes represent distinctions that could be found in a particular dataset but are not universally present. We also acknowledge that patients were on their regular medication as prescribed by the attending psychiatrists, and thus the current results might be confounded by direct and indirect mediation effects thereof. However, it stands to reason that a multisite study, pooling patients from different psychiatrists with differential medication strategies, will render medication largely as a source of random variation in our data. Such noise would effectively make it harder to identify generalizable psychopathological factors and robust subtypes and, in particular, to train models that work well for out-of-sample classification of subtype membership. Thus, we would argue that the current results should not be driven by medication effects but rather represent general structures of psychopathology and schizophrenia subtypes. In addition, rsfMRI has its own limitations such as variability across scanning sessions and the issue of confounding factors (42,65,66). We focused on rsfMRI because it could temporally better map the likewise state-dependent psychopathology compared with structural MRI.

Using advanced machine learning with cross-sample validation, the current study suggested a stable and generalizable 4-factor model of PANSS. This representation allowed for the definition of a reliable positive–negative subtype differentiation that showed good longitudinal stability and a neurobiological divergence in rsFC. Overall, the current work further disentangled the heterogeneity of schizophrenia, possibly allowing for the design of more specifically targeted treatments.

ACKNOWLEDGMENTS AND DISCLOSURES

This study was supported by the Deutsche Forschungsgemeinschaft (Grant No. EI 816/4-1 [to SBE]), the National Institute of Mental Health (Grant No. R01-MH074457 [to SBE]), the Helmholtz Portfolio Theme "Supercomputing and Modeling for the Human Brain," and the European Union's Horizon 2020 Research and Innovation Programme (Grant Nos. 720270 [HBP SGA1] [to SBE] and 785907 [HBP SGA2] [to SBE]). JC received a Ph.D. fellowship from the Chinese Scholarship Council (Grant No. CSC201609350006). VAD acknowledges support from the National Institutes of Mental Health (Grant No. 1R01 MH111177), and the Cohen Neuroscience Endowment.

We acknowledge Asadur Chowdury (Brain Imaging Research Division, Wayne State University School of Medicine, Detroit, Michigan), who contributed to the early arrangement and communication of the Wayne State dataset. Acknowledgments also go to Laura Waite (Institute of Neuroscience and Medicine, Brain and Behaviour [INM-7], Research Center Jülich, Jülich, Germany) for proofreading.

A Dimensions and Clustering Tool for assessing schizophrenia Symptomatology (DCTS) is available at http://webtools.inm7.de/sczDCTS/.

The authors report no biomedical financial interests or potential conflicts of interest.

ARTICLE INFORMATION

From the Institute of Neuroscience and Medicine, Brain and Behaviour (INM-7) (JC, KRP, SW, FH, XL, JMF, SBE), Research Center Jülich, Jülich; Institute of Systems Neuroscience (JC, KRP, SW, FH, XL, JMF, SBE), Medical Faculty, Heinrich Heine University Düsseldorf, Düsseldorf; Department of Psychiatry, Psychotherapy and Psychosomatics (UH, CR), Rheinisch-Westfälische Technische Hochschule (RWTH) Aachen University, Aachen; Jülich Aachen Research Alliance–Institute Brain Structure Function Relationship (UH, CR), Research Center Jülich, and RWTH Aachen University, Aachen; Department of Psychiatry and Psychotherapy (BD, LK), University of Tübingen, Tübingen; Department of Neuroradiology (VR), Rechts der Isar Hospital, Technical University of Munich, Munich; and Section for Experimental Psychopathology and Neuroimaging (OG), Department of General Psychiatry, Heidelberg University, Heidelberg, Germany; Department of General Psychiatry (KS) and Research Division (KS), Institute of Mental Health, and Center for Cognitive Neuroscience (JZ), Neuroscience and Behavioral Disorders Program, Duke–National University of Singapore Medical School, Singapore; Iowa Neuroscience Institute (TN-J) and Department of Psychiatry (TN-J), Carver College of Medicine, University of Iowa, Iowa City, Iowa; Department of Psychiatry and Behavioral Neuroscience (VAD, JAS), Wayne State University, Detroit, Michigan; Department of Radiology and Institute for Informatics (AS), School of Medicine, Washington University in St. Louis, St. Louis, Missouri; Center for Biomedical Image Computing and Analytics (CD) and Department of Radiology (CD), Section of Biomedical Image Analysis, Perelman School of Medicine, University of Pennsylvania, Philadelphia, Pennsylvania; Department of Neuroscience (AA, IES), BCN Neuroimaging Center (IES), and Rob Giel Research Center (EJL), University of Groningen, University Medical Center Groningen, Groningen, The Netherlands; and University of Lille (RJ), National Centre for Scientific Research, UMR 9193, SCALab and CHU Lille, Fontan Hospital, CURE platform, Lille, France.

PHAMOUS investigators: Agna A. Bartels-Velthuis (University of Groningen, University Medical Center Groningen, University Center for Psychiatry, Rob Giel Research Center; Lentis Psychiatric Institute, Groningen, The Netherlands), Richard Bruggeman (University of Groningen, University Medical Center Groningen, University Center for Psychiatry, Rob Giel Research Center and Faculty of Behavioural and Social Sciences, Department of Clinical Psychology and Developmental Neuropsychology, Groningen, The Netherlands), Stynke Castelein (Lentis Psychiatric Institute; University of Groningen, Faculty of Behavioural and Social Sciences, Department of Clinical Psychology and Experimental Psychopathology,

Groningen, The Netherlands), Frederike Jörg (GGZ Friesland Mental Health Care Organization, Leeuwarden, The Netherlands), Gerdina H.M. Pijnenborg (University of Groningen, Faculty of Behavioural and Social Sciences, Department of Clinical Psychology and Experimental Psychopathology; GGZ Drenthe Mental Health Care Organization, Dennenweg; University of Groningen, University Medical Center Groningen, University Center for Psychiatry, Psychosis Department, Groningen, The Netherlands), Henderikus Knegtering (University of Groningen, University Medical Center Groningen, University Center for Psychiatry, Rob Giel Research Center; Lentis Psychiatric Institute, Groningen, The Netherlands), and Ellen Visser (University of Groningen, University Medical Center Groningen, University Center for Psychiatry, Rob Giel Research Center, Groningen, The Netherlands).

Address correspondence to Kaustubh R. Patil, Ph.D., Institute of Systems Neuroscience, Heinrich Heine University Düsseldorf, 40225 Düsseldorf, Germany, or Institute of Neuroscience and Medicine, Brain and Behaviour (INM-7), Research Center Jülich, 52428 Jülich, Germany; E-mail: k.patil@fz-juelich.de.

Received Mar 16, 2019; revised Jul 22, 2019; accepted Aug 31, 2019.

Supplementary material cited in this article is available online at https://doi.org/10.1016/j.biopsych.2019.08.031.

REFERENCES

1. Lally J, MacCabe JH (2015): Antipsychotic medication in schizophrenia: A review. Br Med Bull 114:169–179.
2. Lang F, Kösters M, Lang S, Becker T, Jäger M (2013): Psychopathological long-term outcome of schizophrenia—A review. Acta Psychiatr Scand 127:173–182.
3. Braff DL, Ryan J, Rissling AJ, Carpenter WT (2013): Lack of use in the literature from the last 20 years supports dropping traditional schizophrenia subtypes from DSM-5 and ICD-11. Schizophr Bull 39:751–753.
4. Kay SR, Fiszbein A, Opler LA (1987): The Positive and Negative Syndrome Scale (PANSS) for schizophrenia. Schizophr Bull 13:261–276.
5. Peralta V, Cuesta MJ (1994): Psychometric properties of the Positive and Negative Syndrome Scale (PANSS) in schizophrenia. Psychiatry Res 53:31–40.
6. Kay SR, Sevy S (1990): Pyramidical model of schizophrenia. Schizophr Bull 16:537–545.
7. Emsley R, Rabinowitz J, Torreman M, RIS-INT-35 Early Psychosis Global Working Group (2003): The factor structure for the Positive and Negative Syndrome Scale (PANSS) in recent-onset psychosis. Schizophr Res 61:47–57.
8. Van den Oord EJ, Rujescu D, Robles JR, Giegling I, Birrell C, Bukszár József, *et al.* (2006): Factor structure and external validity of the PANSS revisited. Schizophr Res 82:213–223.
9. Kim JH, Kim SY, Lee J, Oh KJ, Kim YB, Cho ZH (2012): Evaluation of the factor structure of symptoms in patients with schizophrenia. Psychiatry Res 197:285–289.
10. Levine SZ, RabinowitzJ (2007): Revisiting the 5 dimensions of the Positive and Negative Syndrome Scale. J Clin Psychopharmacol 27:431–436.
11. Wallwork R, Fortgang R, Hashimoto R, Weinberger D, Dickinson D (2012): Searching for a consensus five-factor model of the Positive and Negative Syndrome Scale for schizophrenia. Schizophr Res 137:246–250.
12. van der Gaag M, Hoffman T, Remijsen M, Hijman R, de Haan L, van Meijel B, *et al.* (2006b): The five-factor model of the Positive and Negative Syndrome Scale II: A ten-fold cross-validation of a revised model. Schizophr Res 85:280–287.
13. White L, Harvey PD, Opler L, Lindenmayer J (1997): Empirical assessment of the factorial structure of clinical symptoms in schizophrenia. Psychopathology 30:263–274.
14. van der Gaag M, Cuijpers A, Hoffman T, Remijsen M, Hijman R, de Haan L, *et al.* (2006): The five-factor model of the Positive and Negative Syndrome Scale I: Confirmatory factor analysis fails to confirm 25 published five-factor solutions. Schizophr Res 85:273–279.
15. Jiang J, Sim K, Lee J (2013): Validated five-factor model of Positive and Negative Syndrome Scale for schizophrenia in Chinese population. Schizophr Res 143:38–43.
16. Trninić V, Jelaska I, Štalec J (2013): Appropriateness and limitations of factor analysis methods utilized in psychology and kinesiology: Part II. Fizička Kultura 67:1–17.
17. Devarajan K (2008): Nonnegative matrix factorization: An analytical and interpretive tool in computational biology. PLoS Comput Biol 4: e1000029.
18. Dickinson D, Pratt DN, Giangrande EJ, Grunnagle M, Orel J, Weinberger D, *et al.* (2018): Attacking heterogeneity in schizophrenia by deriving clinical subgroups from widely available symptom data. Schizophr Bull 44:101–113.
19. Dollfus S, Everitt B, Ribeyre JM, Assouly-Besse F, Sharp C, Petit M (1996): Identifying subtypes of schizophrenia by cluster analyses. Schizophr Bull 22:545–555.
20. Helmes E, Landmark J (2003): Subtypes of schizophrenia: A cluster analytic approach. Can J Psychiatry 48:702–708.
21. Gottesman II, Gould TD (2003): The endophenotype concept in psychiatry: Etymology and strategic intentions. Am J Psychiatry 160:636–645.
22. Walton E, Hibar DP, van Erp TGM, Potkin SG, Roiz-Santiañez R, Crespo-Facorro B, *et al.* (2018): Prefrontal cortical thinning links to negative symptoms in schizophrenia via the ENIGMA consortium. Psychol Med 48:82–94.
23. Su TW, Hsu TW, Lin YC, Lin CP (2015): Schizophrenia symptoms and brain network efficiency: A resting-state fMRI study. Psychiatry Res 34:208–218.
24. Varikuti DP, Genon S, Sotiras A, Schwender H, Hoffstaedter F, Patil KR, *et al.* (2018): Evaluation of non-negative matrix factorization of grey matter in age prediction. NeuroImage 173:394–410.
25. Sotiras A, Resnick SM, Davatzikos C (2015): Finding imaging patterns of structural covariance via non-negative matrix factorization. NeuroImage 108:1–16.
26. Sotiras A, Toledo JB, Gur RE, Gur RC, Satterthwaite TD, Davatzikos C (2017): Patterns of coordinated cortical remodeling during adolescence and their associations with functional specialization and evolutionary expansion. Proc Natl Acad Sci U S A 114:3527–3532.
27. Yang Z, Oja E (2010): Linear and nonlinear projective nonnegative matrix factorization. IEEE Trans Neural Netw 21:734–749.
28. Bartels-Velthuis AA, Visser E, Arends J, Pijnenborg GHM, Wunderink L, Jörg F, *et al.* (2018): Towards a comprehensive routine outcome monitoring program for people with psychotic disorders: The Pharmacotherapy Monitoring and Outcome Survey (PHAMOUS). Schizophr Res 197:281–287.
29. Liemburg EJ, Nolte IM, Klein HC, Knegtering H (2018): Relation of inflammatory markers with symptoms of psychotic disorders: A large cohort study. Prog Neuropsychopharmacol Biol Psychiatry 86:89–94.
30. Hubert L, Arabie P (1985): Comparing partitions. J Classif 12:193–218.
31. Meilă M (2007): Comparing clusterings—An information based distance. J Multivar Anal 98:873–895.
32. Raguideau S, Plancade S, Pons N, Leclerc M, Laroche B (2016): Inferring aggregated functional traits from metagenomic data using constrained non-negative matrix factorization: Application to fiber degradation in the human gut microbiota. PLoS Comput Biol 12: e1005252.
33. Gardner DM, Murphy AL, O'Donnell H, Centorrino F, Baldessarini RJ (2010): International consensus study of antipsychotic dosing. Am J Psychiatry 167:686–693.
34. Lawson RG, Jurs PC (1990): New index for clustering tendency and its application to chemical problems. J Chem Inf Comput Sci 30:36–41.
35. Bezdek JC (1981): Objective function clustering. In: Pattern Recognition With Fuzzy Objective Function Algorithms. New York: Springer, 43–93.
36. Campello RJ, Hruschka ER (2006): A fuzzy extension of the silhouette width criterion for cluster analysis. Fuzzy Sets Syst 157:2858–2875.
37. Xie XL, Beni G (1991): A validity measure for fuzzy clustering. IEEE Trans Pattern Anal Mach Intell 13:841–847.

38. Fraley C, Raftery AE (2002): Model-based clustering, discriminant analysis, and density estimation. J Am Stat Assoc 97:611–631.
39. Kaiser J (2007): An exact and a Monte Carlo proposal to the Fisher-Pitman permutation tests for paired replicates and for independent samples. Stata J 7:402–412.
40. Schaefer A, Kong R, Gordon EM, Laumann T, Zuo XN, Holmes A, *et al.* (2017): Local-global parcellation of the human cerebral cortex from intrinsic functional connectivity MRI. Cereb Cortex 28:3095–3114.
41. Fan L, Li H, Zhuo J, Zhang Y, Wang J, Chen L, *et al.* (2016): The human Brainnetome atlas: A new brain atlas based on connectional architecture. Cereb Cortex 26:3508–3526.
42. Varikuti DP, Hoffstaedter F, Genon S, Schwender H, Reid AT, Eickhoff SB (2017): Resting-state test-retest reliability of a priori defined canonical networks over different preprocessing steps. Brain Struct Funct 222:1447–1468.
43. Snoek L, Miletic S, Scholte HS (2019): How to control for confounds in decoding analyses of neuroimaging data. NeuroImage 184:741–760.
44. Genon S, Reid A, Langner R, Amunts K, Eickhoff SB (2018): How to characterize the function of a brain region. Trends Cogn Sci 22:350–364.
45. Rodriguez-Jimenez R, Bagney A, Mezquita L, Martinez-Gras I, Sanchez-Morla E, Mesa N, *et al.* (2013): Cognition and the five-factor model of the Positive and Negative Sndrome Scale in schizophrenia. Schizophr Res 143:77–83.
46. Choi EY, Yeo BTT, Buckner RL (2012): The organization of the human striatum estimated by intrinsic functional connectivity. J Neurophysiol 108:2242–2263.
47. Lehoux C, Gobeil M-H, Lefèbvre A-A, Maziade M, Roy M-A (2009): The five-factor structure of the PANSS: A critical review of its consistency across studies. Clin Schizophr Relat Psychoses 3:103–110.
48. Nishimura Y, Takizawa R, Muroi M, Marumo K, Kinou M, Kasai K (2011): Prefrontal cortex activity during response inhibition associated with excitement symptoms in schizophrenia. Brain Res 1370:194–203.
49. Oh J, Chun J-W, Jo HJ, Kim E, Park H, Lee B, *et al.* (2015): The neural basis of a deficit in abstract thinking in patients with schizophrenia. Psychiatry Res Neuroimaging 234:66–73.
50. Wurm LH, Fisicaro SA (2014): What residualizing predictors in regression analyses does (and what it does not do). J Mem Lang 72:37–48.
51. Kay SR, Singh MM (1989): The positive-negative distinction in drug-free schizophrenic patients: Stability, response to neuroleptics, and prognostic significance. Arch Gen Psychiatry 46:711–718.
52. Andreasen NC, Olsen S (1982): Negative v positive schizophrenia: Definition and validation. Arch Gen Psychiatry 39:789–794.
53. Kendler KS, Gruenberg AM, Tsuang MT (1985): Subtype stability in schizophrenia. Am J Psychiatry 142:827–832.
54. Deister A, Marneros A (1993): Long-term stability of subtypes in schizophrenic disorders: A comparison of four diagnostic systems. Eur Arch Psychiatry Clin Neurosci 242:184–190.
55. Kulhara P, Chandiramani K (1990): Positive and negative subtypes of schizophrenia: A follow-up study from India. Schizophr Res 3:107–116.
56. Schilbach L, Derntl B, Aleman A, Caspers S, Clos M, Diederen KMJ, *et al.* (2016): Differential patterns of dysconnectivity in mirror neuron and mentalizing networks in schizophrenia. Schizophr Bull 42:1135–1148.
57. Vercammen A, Knegtering H, den Boer JA, Liemburg EJ, Aleman A (2010): Auditory hallucinations in schizophrenia are associated with reduced functional connectivity of the temporo-parietal area. Biol Psychiatry 67:912–918.
58. Derntl B, Finkelmeyer A, Eickhoff S, Kellermann T, Falkenberg DI, Schneider F, *et al.* (2010): Multidimensional assessment of empathic abilities: Neural correlates and gender differences. Psychoneuroendocrinology 35:67–82.
59. Nenadic I, Yotter RA, Sauer H, Gaser C (2015): Patterns of cortical thinning in different subgroups of schizophrenia. Br J Psychiatry 206:479–483.
60. Shaffer JJ, Peterson MJ, McMahon MA, Bizzell J, Calhoun V, van Erp TGM, *et al.* (2015): Neural correlates of schizophrenia negative symptoms: Distinct subtypes impact dissociable brain circuits. Mol Neuropsychiatry 1:191–200.
61. Orban P, Dansereau C, Desbois L, Mongeau-Pérusse V, Giguère CE, Nguyen H, *et al.* (2018): Multisite generalizability of schizophrenia diagnosis classification based on functional brain connectivity. Schizophr Res 192:167–171.
62. Mikolas P, Melicher T, Skoch A, Slovakova A, Matejka M, Rydlo J, *et al.* (2016): Diagnostic classification of patients with first-episode schizophrenia spectrum disorders from resting-fMRI. Eur Neuropsychopharmacol 26:S490.
63. Rozycki M, Satterthwaite TD, Koutsouleris N, Erus G, Doshi J, Wolf DH, *et al.* (2017): Multisite machine learning analysis provides a robust structural imaging signature of schizophrenia detectable across diverse patient populations and within individuals. Schizophr Bull 44:1035–1044.
64. Sun H, Lui S, Yao L, Deng W, Xiao Y, Zhang W, *et al.* (2015): Two patterns of white matter abnormalities in medication-naive patients with first-episode schizophrenia revealed by diffusion tensor imaging and cluster analysis. JAMA Psychiatry 72:678–686.
65. Zuo XN, Kelly C, Adelstein JS, Klein DF, Castellanos FX, Milham MP (2010): Reliable intrinsic connectivity networks: Test–retest evaluation using ICA and dual regression approach. NeuroImage 49:2163–2177.
66. Bright MG, Tench CR, Murphy K (2017): Potential pitfalls when denoising resting state fMRI data using nuisance regression. NeuroImage 154:159–168.

5.2 Supporting information

(for complete supplementary methods, tables, and figures please refer to https://www.biologicalpsychiatryjournal.com/cms/10.1016/j.biopsych.2019.08.031/attachment/9bc24329-8974-4452-b65f-d3d634ccc4b1/mmc1.pdf; below I only provided some key aspects for the purpose of an integrative demonstration within the thesis)

5.2.1 Detailed sample information

The Utrecht sample:

Patients with chronic schizophrenia were diagnosed according to the Diagnostic and Statistical Manual of Mental Disorders, Fourth Edition (DSM-IV) criteria (Association AP, 1994) by an independent psychiatrist using the "Comprehensive Assessment of Symptoms and History (CASH)" (Andreasen et al., 1992). This study was approved by the Humans Ethics Committee of the University Medical Center Utrecht with written informed consent obtained from the all participants (Clos et al., 2014).

The Göttingen sample:

Patients were recruited from the Department of Psychiatry and Psychotherapy, University Medical Center Göttingen. They met the diagnostic criteria of schizophrenia according to DSM-IV (Association AP, 1994). Patients who had substance abuse within the last month, cannabis abuse within the last 2 weeks, past or present substance dependency, somatic or mental disorders that would interfere with the protocol, acute suicidal tendency or an inability to give written consent were excluded (Chahine et al., 2017).

The Groningen sample:

Diagnosis of schizophrenia was established based on the DSM-IV criteria (Association AP, 1994), confirmed by a Schedules for Clinical Assessment in Neuropsychiatry (SCAN) interview (Giel and Nienhuis, 1996). Exclusion criteria included a personal or family history of epileptic seizures, a history of significant head trauma or neurological disorder, the presence of intracerebral or pacemaker implants, inner ear prosthesis or other metal prosthetics/implants, severe behavioral disorders, current substance abuse, and pregnancy (Vercammen et al., 2010). The study was approved by the Institutional Review Board of the University Medical Center Groningen.

The Lille sample:

Patients were diagnosed with schizophrenia according to the DSM-IV-TR criteria (Spitzer et al., 2002). All patients routinely presented frequent (more than 10 per day) and resistant hallucinations as evaluated with item P3 of the PANSS. The exclusion criteria included the presence of an Axis-II diagnosis, secondary Axis-I diagnosis, neurological or sensory disorder, and a history of drug abuse, which was based on a clinical interview and urine tests that were administered at admission. The study was approved by the local ethics committee (CPP Nord-Ouest IV, France). Written informed consent from each patient was obtained (Lefebvre et al., 2016).

The Munich sample:

All participants provided informed consent in accordance with the Human Research Committee guidelines of the Klinikum Rechts der Isar, Technische Universität München. Patients with a diagnosis of schizophrenia based on

the Structured Clinical Interview for DSM-IV (SCID-I German version) were recruited from the Department of Psychiatry, Klinikum Rechts der Isar, TU München. Exclusion criteria were current or past neurological or internal systemic disorder, current depressive or manic episode, substance misuse (except for nicotine) and cerebral pathology on MRI (Peters et al., 2017; Sorg et al., 2012).

The Albuquerque sample：

This dataset was collected and shared by the Mind Research Network and the University of New Mexico funded by a National Institute of Health Center of Biomedical Research Excellence (COBRE; http://fcon_1000.projects.nitrc.org/indi/retro/cobre.html). Patients with schizophrenia were diagnosed based on DSM-IV using the Structured Clinical Interview used for DSM-IV axis I disorders (SCID). Informed consent was obtained from participants at the University of New Mexico. All patients were chronic andwith relatively well-treated symptoms by a variety of antipsychotic medications (no medication changes in 1 month).Those patients with a history of neurological disorder, head trauma with loss of consciousness greater than 5 min, mental retardation, active substance dependence or abuse (except for nicotine) within the past year, current use of mood stabilizers, history of dependence on PCP, amphetamines or cocaine, or history of PCP, amphetamine, or cocaine use within the last 12 months were excluded (Mayer et al., 2013).

The Wayne State sample:

Diagnosis of schizophrenia was established according to the DSM-V criteria (Association AP, 2013) using the Structured Clinical Interview used for DSM-V axis I disorders. The Wayne State University Institutional Review Board approved all experimental procedures, and written informed consent was obtained from each patient. All patients were on stable antipsychotic treatments with either first generation, second generation antipsychotics or a combination of both. Exclusion criterion: (i) significant history of, or current medical or neurologic illness requiring systemic treatment; (ii) neurologic disorders, including head injury with loss of consciousness; (iii) Significant drug or alcohol use in the previous month or meeting DSM-V criteria for substance Abuse; (iv) meeting the DSM-V criteria for schizoaffective disorder or any other psychotic disorders other than schizophrenia; (v) co-morbidity for any (major) DSM-V Axis I diagnosis.

The Aachen sample:

Patients were diagnosed with schizophrenia according to the DSM-IV criteria (Association AP, 1994) using the German version of the Structured Clinical Interview for DSM Disorders (SCID) by attending psychiatrists. Any patients with past or current presence of secondary Axis-I diagnosis, neurological or sensory disorder, and a history of drug abuse were excluded. The study was approved by the ethics committee of the Medical Faculty of the RWTH Aachen University with written informed consent obtained (Regenbogen et al., 2015; Schilbach et al., 2016).

The Singapore sample:

Patients were diagnosed with schizophrenia according to the DSM-IV criteria using the Structured Clinical Interview for DSM-IV Axis I disorders-Patient Edition (SCID-P) (First et al., 1994) by the treating psychiatrist. Participants were free from a history of neurological illness or a diagnosis of alcohol or drug misuse in the past three months based on DSM-IV criteria. All patients were on a stable dose of antipsychotic medication for at least 2 weeks, and none had medication withdrawn for the purpose of the study (Collinson et al., 2014).

Table 5.2.1 Demographic and clinical characteristics of the schizophrenia samples for each site

Characteristics	Europe						The USA		Asia	Total
	Aachen	Lille	Göttingen	Groningen	Utrecht	Munich	Albuquerque	Wayne State	Singapore	
Total *N* for OPNMF	89	53	35	28	50	21	48	19	147	490
Age	35.73±9.59	35.09±9.45	32.31±9.83	35.25±11.19	29.98±9.68	34.05±12.27	37.67±13.76	30.53±8.62	32.72±9.10	34.89±11.67
Gender (male/female)	57/32	41/12	28/7	17/11	32/18	10/11	37/11	10/9	101/46	333/157
N with illness duration information for ANOVA and sub-typing	70	40	35	23	11	0	48	19	147	393
Illness duration	8.90± 8.39	12.60± 6.81	7.29±7.72	8.39±7.94	9.00± 7.06	N.A	16.69± 12.47	7.79± 8.29	6.55±7.47	9.13±8.98
PANSS										
P3 item	2.16±1.73	5.13±0.83	4.07±1.71	1.46±1.02	3.60±1.99	2.57±1.81	2.69±1.49	1.95±0.94	1.88±1.25	2.66±1.83
Positive	14.54±5.77	21.32± 4.76	15.82± 5.06	12.03±3.54	16.14±4.43	19.38±6.15	14.50±4.97	11.63±2.16	10.59±3.84	14.24±5.76
Negative	19.38±8.90	21.02±6.08	14.21±4.64	13.57±4.87	16.28±4.99	20.90± 7.75	14.15±4.48	11.63±3.25	9.00±3.03	14.67±7.21
General	34.64±13.68	40.85±10.65	29.11±7.74	27.97±5.86	33.20±7.68	39.95 ±11.09	28.21±8.36	20.79±3.79	20.21±3.70	29.10±11.34
Total	68.56±24.69	83.19±19.06	59.14±14.92	53.57±11.04	65.62±14.32	80.24±21.70	56.85±13.52	44.05±7.55	39.80±8.39	58.01±21.87
N with medication information	29	17	38	24	15	N.A	69	19	N.A	211
Antipsychotic treatment										

FGA	0	3	0	1	5	N.A	8	9	N.A	26
SGA	27	12	29	23	9	N.A	58	9	N.A	167
FGA + SGA	2	2	7	0	1	N.A	3	1	N.A	16
None	0	0	2	0	0	N.A	0	0	N.A	2
OZP-equivalent dosage	20.64±11.03	26.24±21.21	25.06±11.49	14.55±8.31	17.10±12.42	N.A	14.84±10.96	12.47±12.88	N.A	19.64±14.15

Note: Data are mean±SD; N: number of subjects, OPNMF: orthonormal projective nonnegative matrix factorization, FGA: first-generation antipsychotic, SGA: second-generation antipsychotic, PANSS: Positive and negative symptom scale, OZP: Olanzapine, NA, not available.

5.2.2 Model evaluation procedure for OPNMF factorization

To determine the optimal factor model of PANSS as the robust, stable and generalizable low-dimensional representation of schizophrenic symptomatology, a sophisticated evaluation procedure was developed based on three data perturbation methods of split-half, bootstrap, and 10-fold cross-validation. Below I firstly provided a detailed description on the implementation of split-half evaluation.

In summary, in each split-half realization, the set of columns of the original item by patient matrix is randomly split into two independent sets of equal length. Then, OPNMF was performed on the ensuing two-half submatrices and each item was assigned to a certain factor for the submatrices. Three evaluation indices were calculated based on the similarities of item-assignment (adjusted Rand index [aRI], variation of information [VI], Jaccard index [JI]), plus the concordance index (CI) which was calculated based on the whole entries of the basis matrix W (here instead of using the hard-assignment results of the items based on the entries of W, CI was calculated based on the initial values within W) between the two submatrices to demonstrate stability. Generalizability was evaluated by measuring increase in out-of-sample reconstruction error.

Overview

1. Stability:

A. based on hard-assignment of the items to specific factors (as a natural clustering):

Decomposition of the data matrix V results in two matrices, i.e. with the loading matrix W^TV we can cluster on it using cardinal clustering methods to identify the subtypes of schizophrenia patients according to their differential symptomatic expressions; the basis matrix W is exactly the factorization results encoding the latent dimensions of the PANSS. As that conducted in previous literature (Brunet et al., 2004), we assigned the items into k factors based on the largest coefficients. Specifically, item j is placed in factor i if the w_{ij} is the largest entry in column i. Afterward, three evaluation indices of aRI, JI and VI were employed to reflect how similar of the factor-label assignment for each item and item-pair grouping between the two split samples in each split-half realization.

B. based on the initial values of the all entries in the basis matrix W. Since an item can be influenced by multiple dimensions and may have small contributions to other factors (low coefficients loaded on other factors besides the one an item is assigned to), the CI which reflects the concordance of the cosine similarity for each pair of the PANSS items between the factorizations of split-samples was thus employed to account for the items with multiple factor-memberships.

2. Generalizability (indicates how well novel data can be compressed by a given dictionary):

Generalizability is assessed by measuring increase in out-of-sample reconstruction error. The reconstruction error is the absolute differences between the reconstructed matrix and the original data matrix, and then averaged over items (for per subject). The out-of-sample increased reconstruction error refers to how much worse the matrix is reconstructed relative to the original data matrix by the dictionary (basis matrix) obtained from model-unseen sample comparing to the reconstruction error calculated by the matrix recovered from the within-sample dictionary.

Methodological notes for bootstrapping and 10-fold cross-validation based evaluations

In bootstrap and 10-fold cross-validation, we implemented the evaluations in a similar way as that have been done

for the split-half analysis, except for the following highlighted differences:

In bootstrap (within-sample):

The four evaluation indices were calculated based on the comparison of the basis matrix *W* from the bootstrapped sample to the one derived from the original sample; the transfer (out-of-sample increased) reconstruction error was derived as follows: after projecting the left-out sample (patients that were not selected in the bootstraps) onto the dictionary obtained from the bootstrapped sample, we compared the ensuing (out-of-sample) reconstruction error with the within-sample reconstruction error of the left-out data.

In 10-fold:

We created ten partitions of equal length sampling randomly from the original sample, and performed OPNMF on nine of the ten partitions (training set), as well as the held-out one (test set). Then, we calculated the evaluation indices of aRI, JI, VI and CI between the basis matrix from the nine partitions and the one from the test sample. For transfer reconstruction error calculation, we likewise projected the held-out (1/10th) sample onto the dictionary obtained from the other nine partitions (9/10th) and compared the ensuing (out-of-sample) reconstruction error with the within-sample reconstruction error of the test set. The above process was repeated for ten times to ensure that each of the partition has been treated as the held-out (test) sample once. Afterwards, the obtained values were averaged over the ten repeats as the metric for one 10-fold realization. Finally, the above procedures were iterated for 1000 times, i.e. 1000 sets of randomly generated ten partitions.

In between-sample (PHAMOUS vs. international) bootstrap-based comparisons:

In each realization of the between-sample bootstrap-based comparison, we bootstrapped the two datasets independently and performed OPNMF separately on the ensuing bootstrapped samples. The evaluation indices of aRI, JI, VI and CI were calculated between the basis matrices derived from the two bootstrapped samples. To calculate the transfer (out-of-sample increased) reconstruction error, we projected the bootstrapped sample that was drawn from the international data onto the dictionary obtained from the bootstrapped PHAMOUS sample, and then we compared the ensuing (out-of-sample) reconstruction error with the within-sample reconstruction error of the bootstrapped international sample. This reflects how well the PHAMOUS dictionary can decode the international data, indicating the generalization performance of the PAHMOUS derived factor-structure to the heterogeneous, international patient cohorts.

Figure 5.2.2-1 Illustration of OPNMF factorization

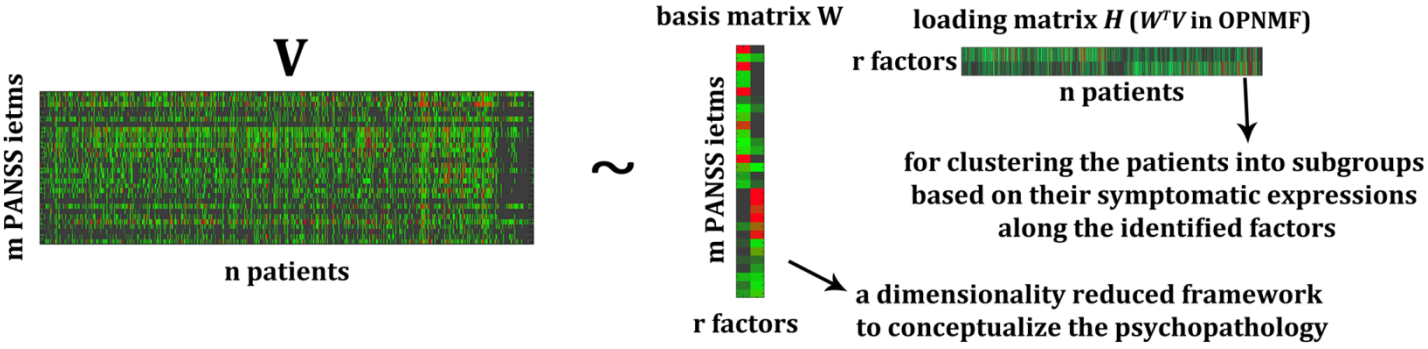

Figure 5.2.2-2 Flow chart for OPNMF model evaluation

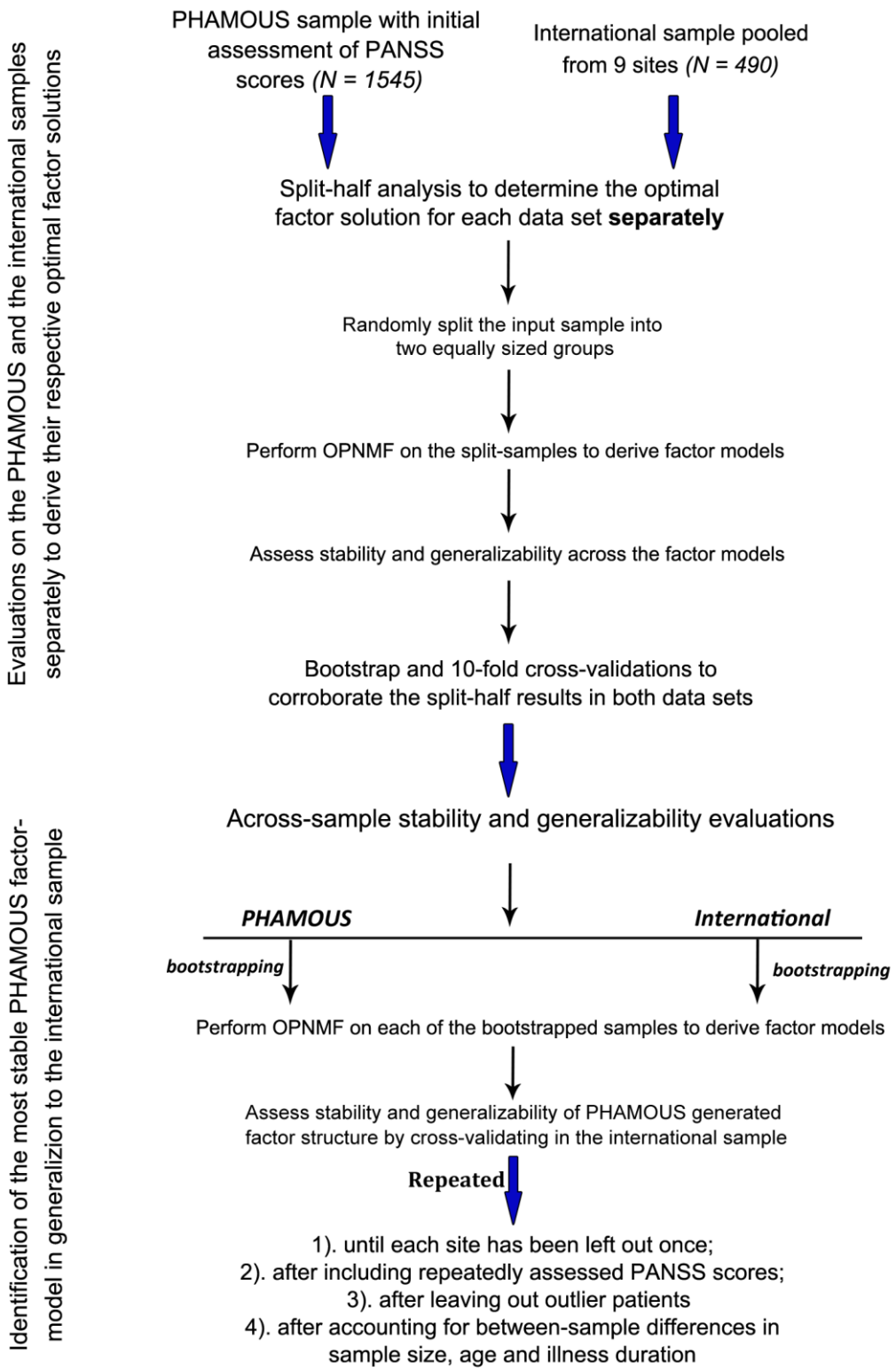

5.2.3 Evaluation of loading and item-score predictions

The stability and accuracy of loading (i.e., dimension score) and item-score predictions were evaluated based on between-sample bootstrap resampling. Basically, we showed the variations of the PHAMOUS dictionary predicted factor-loadings and PANSS item-scores for the international sample over the 5,000 bootstrap realizations, and then aggregated over subjects. In detail, in each bootstrap realization, we computed the factor-loadings for each individual patient in the international sample following the projection of international data onto the PHAMOUS generated dictionaries. Then, the predicted loadings were compared with the loadings that were estimated within the international sample. After multiplying the predicted loadings by the PHAMOUS dictionary, we got the predicted PANSS item-scores for each individual patient in the international sample. Here, the predicted item-scores were compared with the actual ratings. We used two metrics, Pearson correlation coefficient and the normalized root-mean-square-error (nRMSE), to quantify the aforementioned comparisons, denoting the precise patterns of the predicted loadings and the item-scores. Results showed that the best prediction of loadings and item-scores (averaged over the factors and the subjects) was achieved by a model with four factors where the correlation coefficient reaches highest and the nRMSE reaches lowest (Figures 5.2.3-1A, C), providing a solid support for future actionable use of the current OPNMF four-factor model. More specifically, for the four dimension loadings, prediction for the negative loadings was the most stable and accurate (Figure 5.2.3-1B). We also tested the prediction performance for each individual site in the international sample. Basically, the prediction accuracies for both the loadings and the item-scores for each of the nine sites were similar, and local minimums were achieved consistently across sites at a solution with four factors, indicating that the predictions from a four-factor model were stable across sites (Figure 5.2.3-2). In addition, the newly emerged fifth factor in the five-factor model showed the worst out-of-sample prediction accuracy (highest nRMSE and lowest correlation coefficients) with lower stability compared to the other factors in the five-factor model (Figure 5.2.3-1B) and the all factors in the four-factor model (Figure 5.2.3-1B). These results further corroborated that a four-factor model outperforms a model with five factors.

Figure 5.2.3-1 Stability and accuracy of predicting factor-loadings and item-scores for independent sample

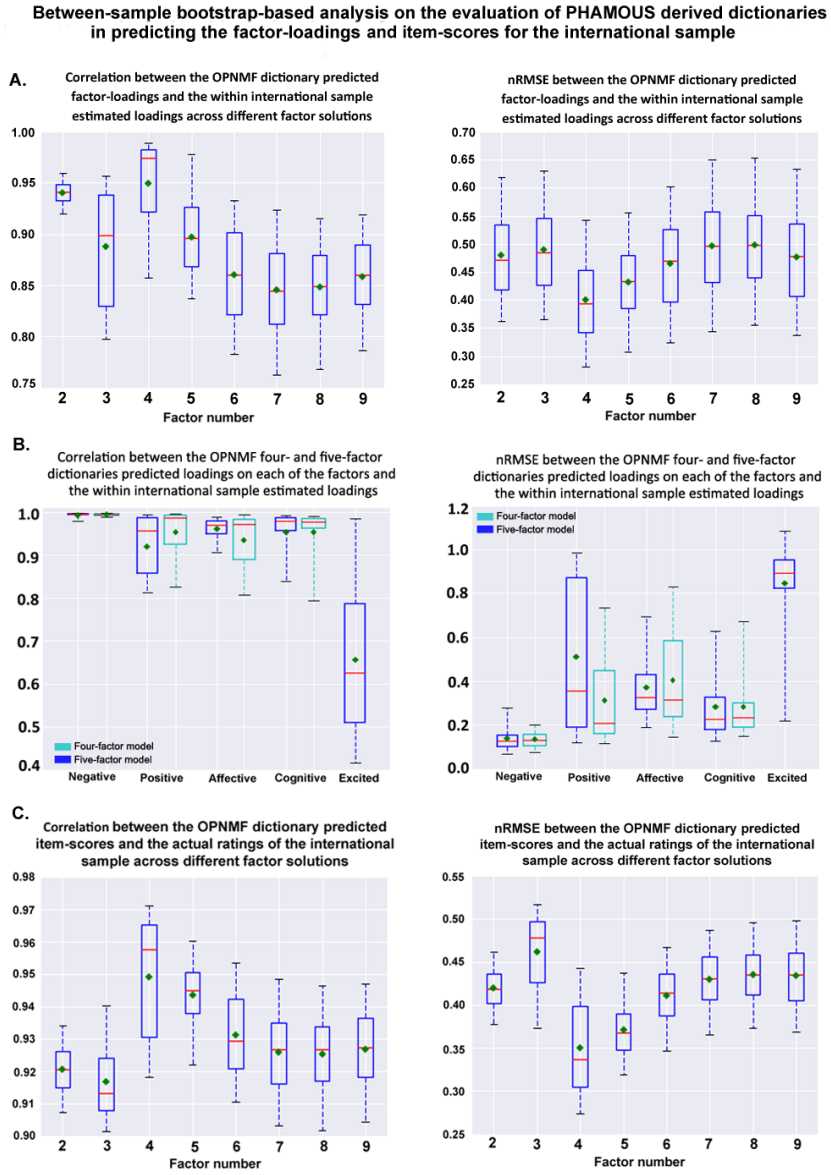

Note: The newly emerged fifth factor in the OPNMF five-factor model represents excited symptoms primarily including poor impulse control and excitement items.

Figure 5.2.3-2 Stability and accuracy of predicting factor-loadings and item-scores for each independent site

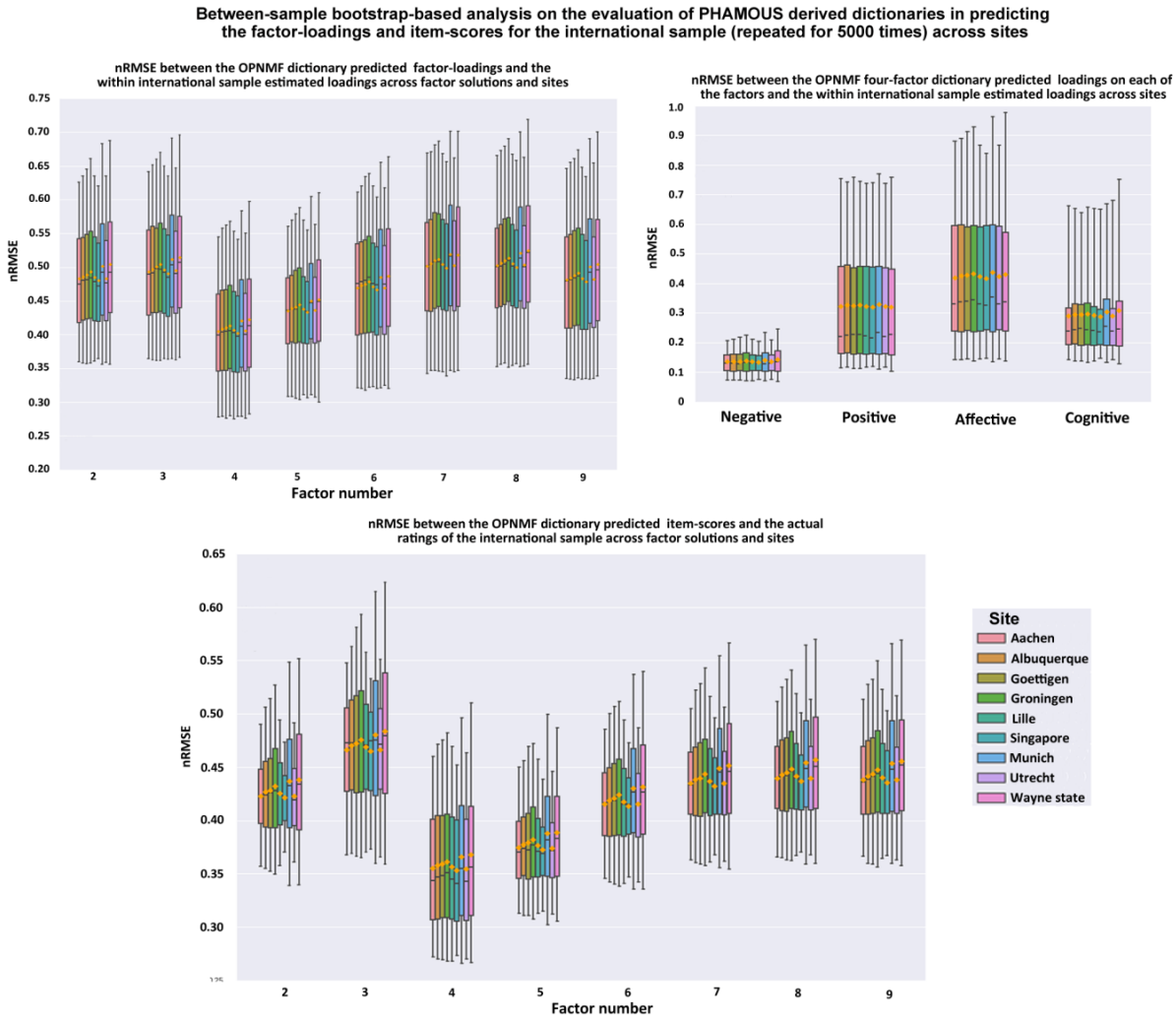

5.2.4 Quantitative comparison of PCA and OPNMF factor models

First, we applied PCA and OPNMF to the PHAMOUS sample (as training set), then we computed the (within-sample) explained variance (EV) for the matrix reconstructed by the basis matrix (i.e., OPNMF dictionary) and the PCA loadings, respectively (Figure 5A). Of note, the higher variance explained by PCA compared to OPNMF is not unexpected as OPNMF applies a lot of regularizations/constraints which will then reduce the final variance that can be explained by the learned factors: 1) *H* and *W* (the learned parameter) must be non-negative; 2) *H* can be replaced by *W'V* (projectable); 3) factors are as orthogonal as possible (*W* becomes sparse). Furthermore, we measured the —loss of EV" metric based on the international sample to indicate the generalization performance. As in the previous evaluations, we performed PCA and OPNMF on the international dataset, and got the within-sample EV for each of the two methods. Then, we tested how much worse (i.e., decreases in EV) when the international data were recovered by the dictionaries/components derived from the PHAMOUS sample. A higher loss of EV indicates worse generalizability of the dictionaries/components (Figure 5B). From these results, obviously that OPNMF is with better generalization performance with lower loss of EV, especially for the four factor model which achieved the local minimum. That is, PCA showed higher within-sample EV, but at the cost of much lower interpretability. In turn, OPNMF showed a slightly lower EV, but it better generalized to new data with lower loss of EV when the trained dictionaries were applied to novel samples. In summary, the good generalization combined with the superior interpretability of a parts-based representation make OPNMF a more appropriate tool for representing latent dimensions of psychopathology than PCA.

Figure 5.2.4 Quantative comparison between OPNMF and PCA

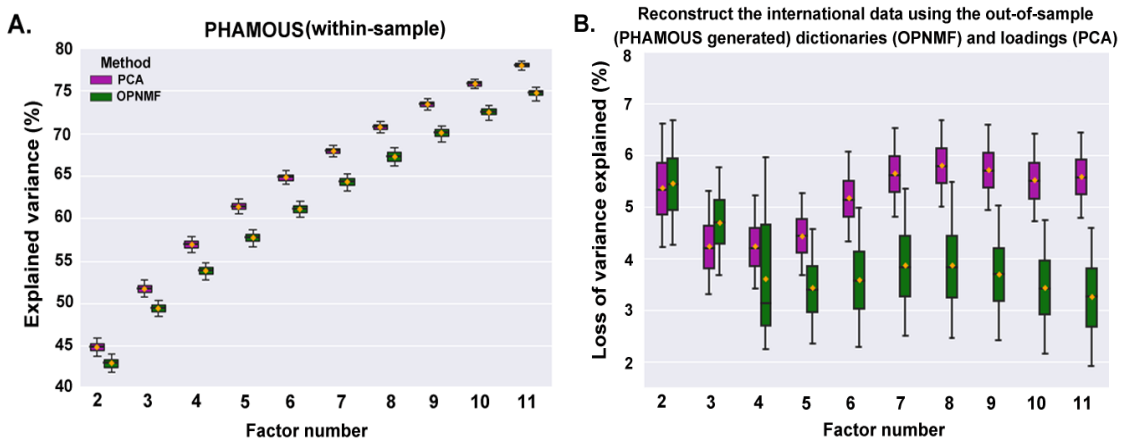

A) Within-sample explained variance (EV) for the matrix reconstructed by OPNMF dictionary and the PCA loadings.
B) A higher loss of EV indicates worse generalizability. OPNMF is with better generalization performance with lower loss of EV, especially for the four factor model which achieved the local minimum.

5.2.5 Exploratory and confirmatory factor analysis

Finally, we conducted exploratory factor analysis (EFA) on the PHAMOUS sample to derive factor-models by setting the factor numbers from four to seven according to previous literature (these factor numbers have been reported in previous PANSS factorial studies) (Kay and Sevy, 1990; Emsley et al., 2003; Van den Oord et al., 2006; van der Gaag et al., 2006b), and then applied confirmatory factor analysis on the international sample to test the goodness of fit of the models that derived from EFA experiments. EFA was done with SPSS version 19.0 (IBM, NY, USA), and the Analysis of Moment Structures (AMOS; version 25) was used for performing CFA. Specifically, in EFA, principal components factor analysis using varimax rotation was conducted. The varimax rotation was chosen to keep consistency with previous factorial studies on PANSS (White et al., 1997; Kim et al., 2012). Following the varimax rotation, items were assigned to factors according to their highest loadings. Internal consistency for each of the factors was quantified by the Cronbach's alpha coefficient (higher values indicate more closely related items within a set) (Cronbach, 1951). Of note, the internal consistency analysis, as well as the below CFA was conducted in the international sample. In all CFA, PANSS items were specified to load on a single factor based on the PHAMOUS-derived EFA models. All factors were allowed to correlate with error covariates set to zero. The robust maximum likelihood method was employed to compute the fit indices, since this method is less likely to be affected by sample size, nonnormality and model size (Bentler, 1985; Chou and Bentler, 1995). In compliance with previous PANSS factorial studies (Kay and Sevy, 1990; Emsley et al., 2003; Van den Oord et al., 2006; van der Gaag et al., 2006b), three indices of the Comparative Fit Index (CFI), the Normed Fit Index (NFI), and the Root Mean Square Errors of Approximation (RMSEA) were adopted to assess the goodness-of-fit. Models assessed by CFA with values of CFI and NFI greater than 0.90 and RMSEA less than 0.08 are indicated to have adequate fit (Kline, 2015; Marsh et al., 2004).

Results showed that the internal consistency coefficients for all of the four factor-models that identified by EFA were variable (ranging from 0.49 to 0.91) with multiple were lower than the least acceptable level of 0.7. All of these factor-models could not to be confirmed in the international sample, i.e., inadequate fit (Table 5.2.5).

Table 5.2.5 Fit indices for EFA models on independent samples

Models	NFI	CFI	RMSEA	Cronbach's alpha
Four-factor	0.712	0.756	0.099	0.59, 0.82, 0.82, 0.91
Five-factor	0.757	0.804	0.089	0.59, 0.79, 0.81, 0.83, 0.91
Six-factor	0.748	0.793	0.092	0.49, 0.59, 0.78, 0.79, 0.81, 0.91
Seven-factor	0.756	0.800	0.091	0.49, 0.59, 0.69, 0.70, 0.78, 0.79, 0.91

Note: NFI: Normed Fit Index, CFI: Comparative Fit Index, RMSEA: the Root Mean Square Errors of Approximation.

5.2.6 Assessment of clustering stability

After the optimal cluster number was determined, leave-one-site-out analysis was performed to validate that the clustering results are not driven by any particular site. Specifically, in each leave-one-site-out experiment, we left out all the patients from one site, and on the remaining sample we re-calculated the residuals after partialling out the effects of age, gender, illness duration and symptom severity from the factor-loadings. Then, the same fuzzy c-means clustering strategy was applied to the obtained residuals followed by the same cluster selection criteria to determine the optimal number of clusters. These processes were repeated until each site had been left out once. Stability of cluster solutions was tested via subsampling and bootstrap resampling evaluation processes, reflecting how stable the partitions hold when the original sample is perturbed. If the structure in the data has been captured well by a partition, this partition should be stable with respect to data perturbation. The evaluation scheme was implemented as follows: the whole dataset is clustered by fuzzy c-means; a set of random subsamples (70% of the whole dataset) and bootstrapped samples are generated and clustered as well. ARI was used to indicate stability, which reflects the similarity between the partition of the reference clustering and the partitions of the subsampled and bootstrapped data, i.e. the consistency of patient-pair assignment between the sub/bootstrapped partitions and the partition derived from the original sample. The best partition in representing the structure of the original sample should have the highest stability (aRI). The idea and the process of testing clustering stability in the present study were similar as that demonstrated in previous literature (Ben-Hur and Guyon, 2003). Also, values of the three employed validity indices were calculated for each subsampled and bootstrapped data, to verify whether the optimal cluster solution holds when the original data were perturbed. Of note, for any new subsampled and bootstrapped data, residuals that used for clustering were re-calculated based on the corresponding covariates of age, gender, illness duration and total PANSS score.

5.2.7 Longitudinal stability analysis of the identified subtypes

Fuzzy c-means clustering with the same parameter settings as the one applied to the international sample was performed on the followed patients in the PHAMOUS sample. 527 patients who have the complete age, gender and illness duration information were involved. The optimal dictionary with four factors, identified on the PHAMOUS 1545 patients without repeatedly assessed PANSS scores, was used for projection to yield the factor-loadings. Effects of age, gender, illness duration and symptom severity (total PANSS score) on the projected loadings were regressed out, and the residuals were used for clustering analysis to identify patient subtypes. The aforementioned three validity indices were employed to ascertain the optimal cluster number, and we found that all the values pointed to a cluster solution equaling to 2 as well. Then, we assessed the longitudinal stability of the identified psychopathological subtypes as follows (i.e., whether a patient preserved his/her subtype over time from the initial recorded PANSS scores to the follow-up psychopathology):

A. Used the optimal four-factor dictionary from the PHAMOS sample (1545 patients with initial PANSS scores) as reference, on which the initially recorded PANSS scores of the 527 follow-up patients were projected to derive the factor-loadings.

B. On the factor-loadings performed 4-way ANOVA analysis and recorded the resulting betas for the four

factor-loadings.

C. Effects of age, gender, illness duration and symptom severity (total PANSS score) on the four factor-loadings were then removed to obtain the residuals. We performed fuzzy c-means on the residuals to partition the patients into 2 clusters and those patients with membership likelihoods lower than 0.7 were excluded. The subtype (cluster label) for each patient and the cluster centers were recorded.

D. Likewise, the four-factor dictionary from the whole PHAMOUS sample was used for deriving the factor-loadings of the repeatedly assessed PANSS scores of the 527 follow-up patients. Of note, we here constructed a regression model using the betas that obtained in B to derive the residuals after removing the effects of age, gender, illness duration and symptom severity on the factor-loadings.

E. Based on the residuals obtained in D, we calculated the squared Euclidean distance between each patient and the two cluster centers defined in C (i.e., based on the initially assessed PANSS scores). Then, each patient was assigned to a specific cluster if its center, comparing to other clusters, has the closest distance to that patient. Afterwards, each patient has a —predicted" cluster label (i.e., psychopathological subtype) according to the follow-up PANSS assessments. In this stage, by comparing the cluster label of each patient based on the repeatedly assessed PANSS scores to the one identified based on the initial assessments derived in C, we have the information about how many patients retained their subtypes longitudinally.

5.2.8 Connectivity matrix construction and classification analysis

Scanning parameters for both the *T1*-weighted structural and resting-state fMRI images were provided in Tables 5.2.8-1&5.2.8-2. The resting-state blood oxygen level-dependent (BOLD) time-series were extracted based on a parcellation system combining Schäfer's 600 cortical parcels (local-global parcellation based on resting-state functional connectivity) (Fan et al., 2016) and 36 subcortical parcels that taken from the brainnetome atlas (Shen et al., 2013). The extracted voxel-wise time-series for each of the 636 parcels were compressed using the first eigenvariate which were then used to calculate pairwise Pearson correlations to form the whole brain connectivity matrix. The correlations were then *Fisher's* z-transformed prior to classification analysis. According to the histograms of the mean DVARS values for the patients (Figure 5.2.8-1), any patient with a DVARS larger than 50 (i.e., 5% BOLD signal change) was treated as an outlier and was removed from the classification analysis. Of note, the threshold of DVARS = 50 is roughly equivalent to a framewise displacement (FD) of 0.5 mm as was demonstrated in Power *et al.* (2012) and the cutoff of FD = 0.5mm has been commonly used in the literature (as reviewed in Power *et al.* [2015]). A supervised support vector machine (SVM) was adopted to approach the classification problem, to classify the psychopathological subtypes for novel patients from the resting-state fMRI features. Parcel-wise classification analysis was conducted using the connectivity profile of each parcel individually. Effects of age, gender, site, illness duration, symptom severity (total PANSS score) and head motion parameter on the connectivity matrix in both the training and the test samples were adjusted using the beta weights obtained from performing linear regression models within only the training samples (Snoek et al., 2019). A nested 10-fold grid-search was implemented among (only) the training data to tune the hyperparameters of C and γ (the kernel parameter) for the radial basis function kernel (Figure 5.2.8-2). Sample imbalance was addressed by setting class weights when training the RBF-SVM models, as well as a stratified 10-fold cross-validation strategy for assessing

the out-of-sample classification performance. The resulting balanced-accuracy for each parcel was averaged over folds and then over 50 replications of the entire procedure to avoid influences of the initial splits.

Figure 5.2.8-1 Histograms for the head motion parameter

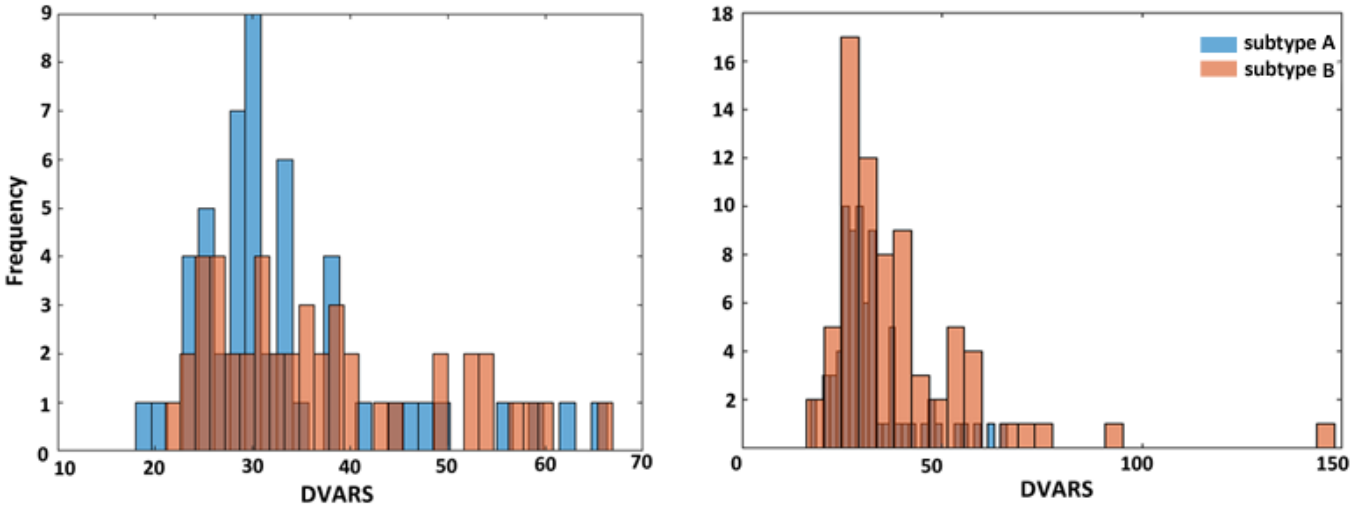

Head motion shown for the patients of core subtypes (left panel), and all patients including those with an ambiguous subtype membership (right panel). Ten DVARS units refer to 1% BOLD signal change.

Figure 5.2.8-2 Schematic for 10-fold cross-validation in classification analysis

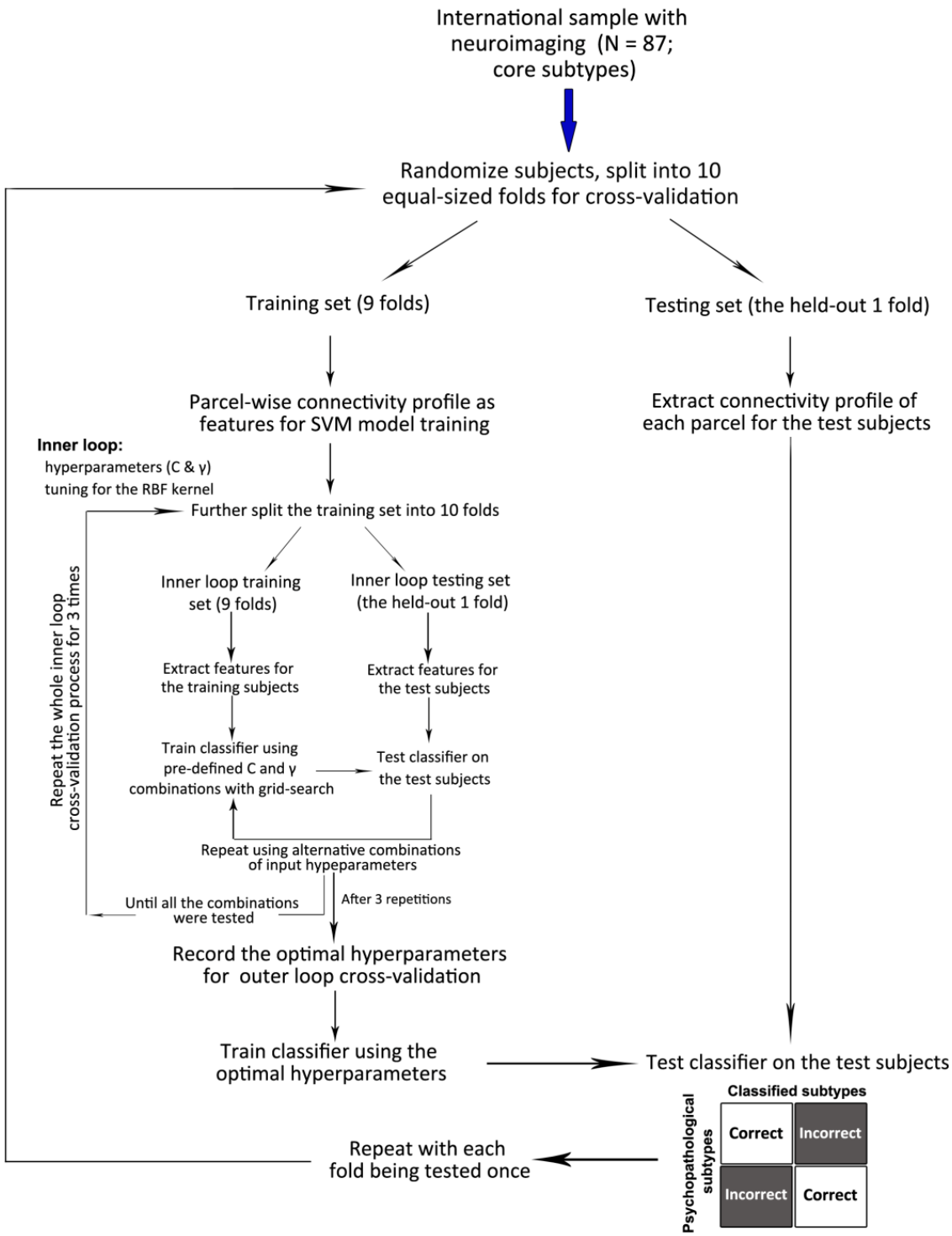

Table 5.2.8-1 Scanning parameters for resting-state BOLD fMRI

Site	Aachen-1	Aachen-2	Groningen	Goettigen	Lille	Albuquerque	Utrecht
Scanner	Siemens TrioTim3T	Siemens TrioTim3T	Philips Achieva3T	Siemens TrioTim 3T	Philips[1] Achieva 3T	Siemens TrioTim 3T	Philips[1] Achieva 3T
TR (ms)	2000	2000	2400	2000	19.25	2000	21.75
TE (ms)	21	28	28	30	9.6	29	32.4
Number of slices	44	34	43	33	45	32	40
Slice-thickness (mm)	3	3.3	3	3	3.22	4	4
Gap (mm)	n.a	3.6	n.a	0.6	n.a	1	n.a
FA (degree)	n.a	77	85	70	9	75	10
Orientation	Axial	Axial	Axial	Axial	Sagittal	Axial	coronal
In-plane resolution (mm^2)	3 x 3	3.6 x 3.6	3.44 x 3.44	3 x 3	n.a	3 x 3	n.a
Voxel size (mm^3)	3 x 3x 3	3.6 x 3.6x 3.3	3.44 x 3.44x 3	3 x 3x 3	3.22 x 3.22 x 3.4	3 x 3x 4	4 x 4 x 4

Note: TR: repetition time, TE: echo time, FA: flip angle; [1]PRESTO-SENSE sequence achieving full brain coverage within 609 ms for the Utrecht site and 1001 ms for the Lille site combining a 3D-PRESTO pulse sequence with parallel imaging in 2 directions (8-channel SENSE head-coil).

Table 5.2.8-2 Scanning parameters for T1-weighted structural MRI

Site	Aachen-1	Aachen-2	Groningen	Goettigen	Lille	Albuquerque	Utrecht
Scanner	Siemens TrioTim3T	Siemens TrioTim3T	Philips Achieva 3T	Siemens TrioTim3T	Philips[1] Achieva 3T	Siemens[2] TrioTim3T	Philips[1] Achieva 3T
TR (ms)	1900	2300	2500	2250	10	2530	9.86
TE (ms)	2	3.03	4.6	3.26	4.6	[1.64, 3.5, 5.36, 7.22, 9.08]	4.6
Number of slices	176	176	160	176	160	176	160
Slice-thickness (mm)	1	1	1	1	1	1	1
FA	n.a	9	30	n.a	n.a	7	n.a
In-plane resolution (mm^2)	0.97 x 0.97	1 x 1	1 x 1	1 x 1	1 x 1	1 x 1	0.875 x 0.875

Note: TR: repetition time, TE: echo time, FA: flip angle; [1]PRESTO-SENSE sequence, [2]a multi-echo MPRAGE (MEMPR) sequence with 5 TEs.

6. Paper: Connectivity patterns of task-specific brain networks allow individual prediction of cognitive symptom dimension of schizophrenia and link to molecular architecture

Ji Chen[1,2,*], Veronika I. Müller[1,2], Juergen Dukart[1,2], Felix Hoffstaedter[1,2], Justin T. Baker[3,4], Avram J. Holmes[5], Deniz Vatansever[6], Thomas Nickl-Jockschat[7], Xiaojin Liu[1,2], Birgit Derntl[8], Lydia Kogler[8], Renaud Jardri[9], Oliver Gruber[10], André Aleman[11], Iris E. Sommer[12], Simon B. Eickhoff[1,2,*], Kaustubh R. Patil[1,2]

[1]Institute of Neuroscience and Medicine, Brain & Behaviour (INM-7), Research Centre Jülich, Jülich, Germany;

[2]Institute of Systems Neuroscience, Medical Faculty, Heinrich Heine University Düsseldorf, Düsseldorf, Germany;

[3]Schizophrenia and Bipolar Disorder Program, McLean Hospital, Belmont, MA 02478;

[4]Department of Psychiatry, Harvard Medical School, Boston, MA 02114;

[5]Department of Psychology, Yale University, New Haven, CT 06520;

[6]Institute of Science and Technology for Brain-Inspired Intelligence, Fudan University, 200433, Shanghai, PR China;

[7]Iowa Neuroscience Institute & Department of Psychiatry, Carver College of Medicine, University of Iowa, Iowa City, IA, USA;

[8]Department of Psychiatry and Psychotherapy, Medical School, University of Tübingen, Germany;

[9]Univ Lille, INSERM U1172, Lille Neuroscience & Cognition Centre, Plasticity & SubjectivitY team & CHU Lille, Fontan Hospital, CURE platform, Lille, France;

[10]Section for Experimental Psychopathology and Neuroimaging, Department of General Psychiatry, Heidelberg University, Germany;

[11]Department of Neuroscience, University of Groningen, University Medical Center Groningen, The Netherlands;

[12]Department of Biomedical Science of Cells and Systems, University of Groningen, University Medical Center Groningen, The Netherlands;

Preprint available at ***bioRxiv***, DOI: https://doi.org/10.1101/2020.07.02.185124, under the CC-BY-NC-ND 4.0 license (http://creativecommons.org/licenses/by-nc-nd/4.0/), anyone can share this material, provided it remains unaltered in any way, this is not done for commercial purposes, and the original authors are credited and cited.
The paper is submitted to journal „*Biological Psychiatry*" for peer review.

Own contributions

Conception and design of experiment
Reviewing and adapting analysis code
Statistical data analysis
Interpretation of results
Preparing figures
Writing the paper
Total contribution 80%

6.1 Main text

Connectivity patterns of task-specific brain networks allow individual prediction of cognitive symptom dimension of schizophrenia and link to molecular architecture

Ji Chen[1,2,*], Veronika I. Müller[1,2], Juergen Dukart[1,2], Felix Hoffstaedter[1,2], Justin T. Baker[3,4], Avram J. Holmes[5], Deniz Vatansever[6], Thomas Nickl-Jockschat[7], Xiaojin Liu[1,2], Birgit Derntl[8], Lydia Kogler[8], Renaud Jardri[9], Oliver Gruber[10], André Aleman[11], Iris E. Sommer[12], Simon B. Eickhoff[1,2,*], Kaustubh R. Patil[1,2]

[1]Institute of Neuroscience and Medicine, Brain & Behaviour (INM-7), Research Centre Jülich, Jülich, Germany;

[2]Institute of Systems Neuroscience, Medical Faculty, Heinrich Heine University Düsseldorf, Düsseldorf, Germany;

[3]Schizophrenia and Bipolar Disorder Program, McLean Hospital, Belmont, MA 02478;

[4]Department of Psychiatry, Harvard Medical School, Boston, MA 02114;

[5]Department of Psychology, Yale University, New Haven, CT 06520;

[6]Institute of Science and Technology for Brain-Inspired Intelligence, Fudan University, 200433, Shanghai, PR China;

[7]Iowa Neuroscience Institute & Department of Psychiatry, Carver College of Medicine, University of Iowa, Iowa City, IA, USA;

[8]Department of Psychiatry and Psychotherapy, Medical School, University of Tübingen, Germany;

[9]Univ Lille, INSERM U1172, Lille Neuroscience & Cognition Centre, Plasticity &SubjectivitY team & CHU Lille, Fontan Hospital, CURE platform, Lille, France;

[10]Section for Experimental Psychopathology and Neuroimaging, Department of General Psychiatry, Heidelberg University, Germany;

[11]Department of Neuroscience, University of Groningen, University Medical Center Groningen, The Netherlands;

[12]Department of Biomedical Science of Cells and Systems, University of Groningen, University Medical Center Groningen, The Netherlands;

***Correspondence should be addressed to:**

Simon B. Eickhoff

Institute of Systems Neuroscience, Heinrich Heine University Düsseldorf, 40225 Düsseldorf, Germany & Institute of Neuroscience and Medicine, Brain and Behaviour (INM-7), Research Center Jülich, 52428 Jülich, Germany. Tel: +49 2461 61 1791; E-mail: S.Eickhoff@fz-juelich.de.

Or

Ji Chen

Institute of Systems Neuroscience, Heinrich Heine University Düsseldorf, 40225 Düsseldorf, Germany & Institute of Neuroscience and Medicine, Brain and Behaviour (INM-7), Research Center Jülich, 52428 Jülich, Germany. Tel: +49 2461 61 85334; E-mail: jichen.allen@hotmail.com.

Abstract

Background: Despite the marked inter-individual variability in the clinical presentation of schizophrenia, it remains unclear the extent to which individual dimensions of psychopathology may be reflected in variability across the collective set of functional brain connections. Here, we address this question using network-based predictive modeling of individual psychopathology along four data-driven symptom dimensions. Follow-up analyses assess the molecular underpinnings of predictive networks by relating them to neurotransmitter-receptor distribution patterns.

Methods: We investigated resting-state fMRI data from 147 schizophrenia patients recruited at seven sites. Individual expression along negative, positive, affective, and cognitive symptom dimensions was predicted using relevance vector machine based on functional connectivity within 17 meta-analytic task-networks following a repeated 10-fold cross-validation and leave-one-site-out analyses. Results were validated in an independent sample. Networks robustly predicting individual symptom dimensions were spatially correlated with density maps of nine receptors/transporters from prior molecular imaging in healthy populations.

Results: Ten-fold and leave-one-site-out analyses revealed five predictive network-symptom associations. Connectivity within theory-of-mind, cognitive reappraisal, and mirror neuron networks predicted negative, positive, and affective symptom dimensions, respectively. Cognitive dimension was predicted by theory-of-mind and socio-affective-default networks. Importantly, these predictions generalized to the independent sample. Intriguingly, these two networks were positively associated with D_1 dopamine receptor and serotonin reuptake transporter densities as well as dopamine-synthesis-capacity.

Conclusions: We revealed a robust association between intrinsic functional connectivity within networks for socio-affective processes and the cognitive dimension of psychopathology. By investigating the molecular architecture, the present work links dopaminergic and serotonergic systems with the functional topography of brain networks underlying cognitive symptoms in schizophrenia.

Introduction

Precise conceptualization of schizophrenia symptoms in terms of their underlying dimensional structure and associated neurobiology remains a challenge (1), as prior work focused on to subscales (positive, negative, and general symptoms) of the Positive and Negative Syndrome Scale (PANSS) (2) has not provided a clear understanding of underlying brain circuitry (3-5). We recently introduced a novel four-dimensional conceptualization of schizophrenia symptomatology which is stable and generalizable across populations and settings (5). As each symptom dimension captures a different clinical facet of schizophrenia (6-8), we would expect these to show differential relationships with functional brain networks. Identification of robust symptom-brain relationships (e.g., connectivity patterns and molecular substrates) is important for the development of reliable biomarkers for targeted treatments of different symptom dimensions. Previous studies proposed that abnormal brain connectivity might be a precipitating factor for schizophrenia symptoms (9,10), questioning region-based analyses but resonating with the dysconnection hypothesis (9-12).

Although resting-state functional MRI (fMRI) reveals broad patterns of impaired brain function that may underlie the pathophysiology of schizophrenia (12-15), the link between targeted symptom dimensions and associated connectivity patterns within distinct functional systems remain largely unknown. Pioneering work has explored symptom-brain associations based on regional activity and intrinsic connectivity networks (ICNs) using univariate group-level correlative approaches, but the results have been largely inconsistent (16-19). The clinical complexity of schizophrenia together with the differences in patient populations, study settings, scanners and scanning protocols across sites may have led to divergent results, posing a major challenge for establishing generalizable network-symptom relationships. Application of multivariable machine-learning and cross-validation strategies to multi-site data and validation of the resulting models on independent datasets is thus needed to derive robust network-symptom associations (20).

It needs to be cautioned, though, that ICNs cannot readily be interpreted relative to cognitive and mental processes due to their unconstrained and task-independent nature (21). In contrast, meta-analytic functional networks are derived from task-activation data, i.e., the identified networks consist of brain areas robustly engaged in specific tasks and therefore mental processes (22,23). Meta-analytic networks thus provide a promising avenue to characterize association between functionally meaningful systems and specific symptom dimensions. Considering these advantages, we here combined multivariable machine-learning and meta-analytically defined networks to explore predictive relationships between network-specific connectivity patterns and individual expressions of different dimensions of psychopathology.

Functional brain systems are known to relate with molecular architecture (24-27). In order to facilitate a link to treatment, we also explored whether robustly symptom-related functional networks would in turn relate to the spatial topography of underlying molecular features. Specifically, connectivity-neurotransmitter coupling has been proposed and observed in healthy populations (28,29). Similarly, network dysconnectivity in schizophrenia has been associated with altered neurotransmission (30,31) with several pathways involving dopaminergic, serotonergic, gamma-aminobutyric acid(GABA)-ergic, and glutamatergic systems reported to be compromised (32-35). Here, it is interesting to note that current anti-psychotic drugs primarily targeting the dopamine system are primarily effective against positive but less so for negative or cognitive symptoms (36,37). Understanding the molecular substrate of specific dimensions of psychopathology may thus provide leads on new treatment strategies.

We therefore assessed a broad range of meta-analytic networks relating to social, affective, executive, memory, language, and sensory-motor functions with respect to their predictive power for individual positive, negative, affective and cognitive symptom-dimensions in schizophrenia. Machine-learning approaches with a stringent validation sequence of 10-fold cross-validation, leave-one-site-out analyses, and generalization to an

independent sample was implemented to identify robust association patterns between the probed networks and the four dimensions of psychopathology (6). Subsequently, whole-brain density maps of nine receptors/transporters from prior in vivo molecular imaging studies were employed to investigate the molecular architecture spatially coupled to the identified predictive networks.

Materials and Methods

Sample

A total of 147 schizophrenia patients from seven centers located in Europe (Aachen [Aachen-1 and Aachen-2], Göttingen, Groningen, Lille, and Utrecht) and the USA (COBRE, Albuquerque, NM) represented the main sample (Table S1; Supplement). These sites differed significantly in illness duration ($p<0.001$)(Table S1). An independent sample with 117 schizophrenia patients (Table S2; Supplement) retrieved from the Bipolar-Schizophrenia Network on Intermediate Phenotypes (B-SNIP) database (38) was used for independent validation of the predictive models. For both samples, diagnosis of schizophrenia was established based on the DSM-IV, the DSM-IV-TR, or the ICD-10 criteria (see Supplement and [6]). These international datasets cover a broad range of clinical states, settings, and medical systems, facilitating identification of robust network-symptom associations. Current drug dosages of antipsychotic medication were olanzapine-equivalent transformed (39). For each site, subjects gave written informed consent and study approval was given by the respective ethics committees/institutional review boards. Additional approval to pool and re-analyze data was provided by the ethics committee of the University of Düsseldorf, Germany.

Calculation of dimensional symptom scores

Severity of psychopathology was assessed using the PANSS (2). The 30 PANSS items were compressed into four (negative, positive, affective, and cognitive) symptom dimensions (Figure S1A) identified in our prior factorization analysis on two large, multi-site schizophrenia samples as stable and well-generalizable across populations, settings, and medical systems (6). The original item-by-subject matrix was projected onto this dimensional-structure of PANSS to yield the dimensional symptom scores for each subject (as implemented in

DCTS: http://webtools.inm7.de/sczDCTS/). Higher scores on a dimension indicate more-severe symptoms (Figure S1B).

Definition of functional brain networks

Seventeen functional networks, which cover a broad range of domains reflecting cognitive, socio-affective, and sensory-motor functions that have been implicated in schizophrenia, were employed (Table S3). These networks were based on coordinate-based meta-analyses (21,22) and represent regions demonstrating convergent activations associated with specific functional domains across many prior task-fMRI studies. They hence provide the best "*a priori*" estimate of the location of specific functional networks and hence here assessed by resting-state fMRI in new subjects. For convenience, we grouped these 17 networks into six broad functional domains (Figure 1&Table S3), though it must be stressed that each network was analyzed separately.

FMRI data preprocessing

All resting-state fMRI scans (Tables S4&S5) were preprocessed using SPM12 (http://www.fil.ion.ucl.ac.uk/spm) (see [6] and Supplement). After excluding subjects with excessive head-motion (40) or poor image quality (details in Supplement), 126 and 100 schizophrenia patients were retained in the main and the B-SNIP validation sample, respectively (Table 1). Head motion differed significantly between the sites in the main sample (p=0.003; one-way ANOVA) and between the main and the B-SNIP samples (p<0.001; two-sample t-test) but did not correlate with the residuals of any symptom dimensions after adjusting for age/gender/site. Still, we adjusted head motion effects in predictive modeling as a conservative approach to rule out (any) possible predictability of symptom dimensions due to movement.

White matter and CSF signals as well as 24 head-motion parameters (41,42) were regressed out from the

overall fMRI time-series (42) but the global mean signals were not removed given ongoing controversies (43,44). The first eigenvariate of the time-series from all the voxels within a 6-mm sphere around each node was extracted (45,46). For each network, the between-node resting-state functional connectivity (rs-FC) was then calculated as Fisher's z-transformed Pearson's correlation between the eigenvariates.

Prediction of symptom dimensions using network rs-FC

Multivariable regression via a relevance vector machine (RVM)(47) was implemented and evaluated using 500x repeated 10-fold cross-validation, individually for each combination of functional network and symptom dimension in the main sample. That is, we assessed the capability of each network's rs-FC to predict each of the four symptom dimensions in held-out patients. Importantly, RVM is a sparse learning method, i.e., only a few of the feature weights learned by RVM are non-zero, lending interpretability as to which features (connections) are predictive. In keeping with the recommended strategy (48), both the symptom dimensional-scores and rs-FC features were adjusted for confounding effects of age, gender, site, and head-motion (DVARS). To avoid data-leakage within cross-validation (49), confound regression models were learned only on the training-set and then applied on both training and test data (50,51). The RVM model was then trained on confound-adjusted training data and applied to the confound-adjusted held-out test data. The folds were stratified to accommodate different sample sizes across sites. Prediction performance was evaluated using *Pearson's* correlation between the (adjusted) scores and their predictions. Significantly predictive associations were further validated for their generalizability across sites using leave-one-site-out cross-validation following the same schematic but training on all sites but one and testing on the left-out site (cf. Supplement). Statistical significance of the cross-validation-based correlations was determined through 1000 permutations by shuffling the symptom dimensional-scores (lowest p=0.001, right-tailed; Supplement) (49,52).

Critically, we validated the associations confirmed as predictive in the leave-one-site-out cross-validation in the independent B-SNIP sample. For this, we trained RVM models on the significantly predictive networks in the entire main sample and then, without further fitting or modification, applied them to held-out B-SNIP data. Robust associations passing this strict three-step validation procedure were then further assessed as described below.

In addition, we performed control analyses by repeating all validation procedures by including illness duration or olanzapine-equivalent dosage as confounds. For comparison, we also predicted the original three PANSS subscales (positive, negative, and general psychopathology) using the same three-step validation procedure.

Identification of reliably predictive connections and subnetworks

The intrinsic feature selection in RVM through its sparse modeling was leveraged to identify reliably predictive connections and the potential subnetworks formed by them. A connection was identified as reliably predictive when it had non-zero weights in: i) at least 80% of the 10-fold cross-validation repetitions, ii) at least six out of the seven (i.e., >80%) leave-one-site-out analyses, and iii) the models trained on the entire main sample for validation in B-SNIP. The cutoff of 80% is suggested as a conservative threshold to select most relevant variables in both real and simulated data (53). To assess the predictive capacity of the subnetworks, RVM models were trained using the rs-FC of the subnetworks on the main sample and tested in B-SNIP.

Spatial correlation with receptor/transporter density estimates

Finally, we evaluated the topographical relationship between network-node location and the distribution of several receptor/transporter systems, assessing if any receptors/transporters were highly-expressed in the identified networks relative to the entire brain. This was tested by comparing the average receptor/transporter density across all nodes within a given network against a null-distribution based on 1000 random network configurations

generated by re-distributing the nodes throughout the grey matter while preserving the between-node distances (±6mm tolerance). Seven dopamine and serotonin receptors (dopaminergic: D_1 and $D_{2/3}$; serotonergic: 5-HT1a, 5-HT1b, and 5-HT2a) and transporters (dopamine transporter and 5-HTT serotonin reuptake transporter), together with F-DOPA (a reflection of presynaptic dopamine-synthesis-capacity) and the GABAergic receptor GABAa were investigated. These three neurotransmitter systems have all been implicated in schizophrenia (32,34,35), while here we tested for more specifically the receptors/transporters. Density estimates for these receptors/transporters were derived from average group maps of healthy volunteers scanned in prior multi-tracer molecular imaging studies (Supplement). For comparability, these maps, in MNI152 space, were all resampled to an isotropic 2mm spatial resolution as in our fMRI data and linearly rescaled to a minimum of 0 and a maximum of 100.

Furthermore, the significantly higher expressed receptors/transporters were entered into a spatial correlation analysis (54,55) calculated as rank correlation between the node importance scores and receptor/transporter densities calculated for these nodes (Figure 4B). The node importance score was calculated by summing the selection frequency of the connections of each node derived from the repeated 10-fold cross-validation. Bootstrap analysis was conducted to ensure robustness. To establish the statistical significance of a spatial correlation against chance, spatial permutation test was employed where the null distribution was estimated based on the correlations between the node importance scores for a given network and the nodal receptor/transporter densities extracted from1000 simulated (random) networks (Supplement).

Results

Network-based prediction of specific symptom dimensions

Predictive modeling with a stringent three-step validation revealed specific networks associated with the four dimensions of psychopathology. In the first step (10-fold cross-validation), the negative, positive, and affective symptom dimensions could be significantly predicted using the rs-FC within the theory-of-mind (ToM), the cognitive emotion regulation (CER), and the mirror neuron networks, respectively, while the cognitive dimension was predicted by three networks, ToM, empathy and eSAD (Figure 2A, B). These six networks-symptom associations (Figure 2B) were then tested in the second validation step, i.e., leave-one-site-out. Except for the empathy-cognitive prediction, all predictive associations were validated by significant correlations between the observed (confound-adjusted) scores for the individual symptom-dimensions and their predictions (Figure 2C).

As the 10-fold cross-validation and leave-one-site-out analyses were both performed in the main sample, they may still be optimistic with respect to the generalization to new patient populations. Therefore we added a third validation step for the five leave-one-site-out validated associations using a completely independent sample. Three of the five leave-one-site-out validated associations (ToM-negative, CER-positive, MNS-affective) were not confirmed in this step. Training RVM models on the entire main sample and testing it in the B-SNIP dataset revealed that the ToM and eSAD networks were significantly predictive of cognitive symptoms (Figure 2D).

In complementary analyses, no significant effects of illness duration or olanzapine-equivalent dosage on the four symptom-dimension scores were found (all $p>0.05$ in the fitted general linear models with additional covariates of age, gender, site, and head motion). Conversely, controlling for illness duration or olanzapine-equivalent dosage did not alter the overall predictive patterns. Highlighting the utility of our four-dimensional conceptualization of schizophrenia symptomatology (6), when considering the traditional three

PANSS subscales, 10-fold cross-validation and leave-one-site-out experiments on the main sample only revealed two predictive patterns: the ToM network predicted the negative subscale, and the eSAD network predicted the general psychopathology subscale (Figure S2A, B). However, these two associations were not generalizable to B-SNIP (Figure S2C).

Reliably predictive connections and the predictiveness of subnetworks

Ten connections within eSAD and eight connections within ToM were identified as consistently relevant for predicting the cognitive symptoms (Figure 3A; Table S6), i.e., were selected in more than 80% of the different cross-validation runs (repeated 10-fold and leave-one-site out) and in the final models trained on the entire main sample for validation in B-SNIP. The ensuing ToM and eSAD subnetworks featured three spatially overlapping nodes located in the ventro-medial prefrontal cortex (vmPFC), left middle temporal gyrus (MTG), and posterior cingulate cortex (PCC)/precuneus and highlighted the vmPFC-PCC/precuneus connection (Figure 3B; Table S7). In turn, connections to subcortical regions including bilateral amygdala/hippocampus and the ventral striatum were specific to the eSAD subnetwork.

A model based on the identified eSAD subnetwork showed almost identical prediction performance for the B-SNIP data compared to the aforementioned one trained on whole eSAD network (Figure 3C, note that subnetwork definition was only based on the main sample, i.e., there is no leakage of information about the B-SNIP data). Interestingly, compared to whole ToM network (Figure 2D), the ToM subnetwork demonstrated an improved performance (Figure 3C) in the prediction of the cognitive dimension in B-SNIP. This confirms the power of sparse modeling in RVM to identify the truly relevant features.

Relationship to molecular architecture

Results showed that eight receptors/transporters (Figure 4A) are highly expressed in both, or in either of the ToM and eSAD networks than in the simulated networks with perturbed spatial configuration of nodes (histograms for within- and between-network distance of nodes shown in Figure S3). Spatial correlation between the node importance (Table S8) and the spatially corresponding density of those significant receptors/transporters revealed a relationship to both the dopaminergic and the serotonergic systems (Figure 4C). Specifically, the nodes of ToM that showed higher importance in predicting the cognitive dimension tracked with higher dopamine-synthesis-capacity (r=0.54, p=0.02). The prediction importance of the nodes within the eSAD network correlated positively with densities of D_1 (r=0.66, p=0.007) and 5-HTT (r=0.53, p=0.046), as well as dopamine-synthesis-capacity (r=0.54, p=0.036). The significance was corroborated by bootstrapped confidence intervals.

Discussion

By employing predictive modeling to multi-site fMRI data with a strict sequence of out-of-sample validation steps (repeated 10-fold, leave-one-site-out, independent dataset), two a priori, meta-analytically defined functional networks, theory-of-mind (ToM) and extended socio-affective default (eSAD), were identified as significantly and robustly predictive of the cognitive symptom dimension. In contrast, prediction using the original PANSS subscales failed to generalize to the independent sample, supporting the notion that these traditional dimensions do not correspond well to underlying neurobiology. Through the implicit feature selection of RVM, reliably predictive connections were identified which constituted subnetworks connecting nodes mainly distributed in the (medial) prefrontal cortex, PCC, temporal regions as well as subcortical structures. Moreover, higher densities of D_1 dopamine receptor and 5-HTT serotonin transporter as well as elevated dopamine-synthesis-capacity were related to the node importance of the ToM and the eSAD networks in the prediction of cognitive symptomatology.

Symptom dimensions were differentially predicted by different functional networks

Schizophrenia is a disorder that is commonly proposed with global or widespread brain deficits (10-12). Our network-based predictive modeling, however, revealed specific networks-psychopathology relationships based on the predictive capacity of specific functional systems for patient-specific symptom severity along four dimensions. Two networks, ToM and eSAD, both predicting the cognitive dimension, passed our strict validation steps. The ToM network subserves social cognition while the eSAD network encompasses regions involved in socio-affective processes. These results provide a firm support for the previous findings indicating that the compromised “social brain” development in schizophrenia relates to higher-level cognitive deficits (56,57). Yet it came as somewhat of a surprise that these two networks did not allow a robust prediction of negative or affective symptoms. However, other socio-affective networks, CER, which relates to the reappraisal process of emotional stimuli (58), and MNS,

which was proposed to represent the emotional aspect of social cognition (18), were predictive of the positive and affective dimensions, respectively, in the main sample. Hence, it stands to reason that different socio-affective networks would capture individual variance of different symptom dimensions of schizophrenia. Of note, these predictions did not generalize to B-SNIP, potentially due to between-sample differences in clinical characteristics but also highlighting that building models that generalize to completely novel cohorts remains a challenge (59). We also noted that the cognitive dimension was not robustly predicted by any of the cognitive networks employed, though the speech production network showed a trend-level prediction in 10-fold cross-validation (r=0.18, p=0.061). Previous work showed that task-based functional connectivity yields better predictions of cognition than the networks at rest (60-62). Following this line of thought, cognitive networks engaged during tasks might likewise be more robustly related with the individual variability in cognitive symptoms than intrinsic connectivity patterns.

Overall, we revealed that the connectivity patterns within the ToM network, even at the level of intrinsic brain activity, are robustly predictive of the cognitive status in individual schizophrenia patients. ToM is the cognitive ability of an individual to infer others' mental states, intentions and believes (63). As these involve complex cognitive processes and considering that the cognitive dimension of schizophrenia psychopathology encompasses symptoms such as "conceptual disorganization", "lack of insight", and "disturbed abstract thinking", it is not unexpected that the ToM network is predictive of the cognitive dimension. Resonating with this finding, ToM deficits, which are prevalent in schizophrenia and a well-established feature and vulnerability marker of this disorder (64), are known to associate with symptoms of disorganization (65). Abnormal neural activation in response to tasks targeting ToM has also been reported in schizophrenia involving temporo-parietal junction as well as prefrontal and temporal regions where the current ToM meta-network is distributed (66,67).

It is interesting to note that the ToM network also predicted negative symptoms in the main sample though this did not generalize to the B-SNIP data. This resonates with the notion that ToM encompasses multiple

components (e.g., affective and cognitive)(68) and an impairment in the sub-processes of ToM may manifest as different consequences. And indeed, the subnetworks of ToM predicting negative and cognitive dimensions, respectively, were largely divergent (Figure 3B, Figure S4).

Intriguingly, cognitive symptoms in schizophrenia were also linked to socio-affective processes via the prediction using the eSAD network. Recent studies consistently linked neural activity patterns in the DMN to cognitive abilities (69,70), and the implication of the DMN-derived eSAD network (71) in cognitive processing is hence unsurprising. Our finding moreover resonates well with a literature suggesting that socio-affective factors impact and modulate cognitive performance like working memory and attention in schizophrenia patients (72-74). The use of seemingly non-cognitive psychosocial methods has been proposed as a potential remediation strategy for cognitive deficits in schizophrenia (72), and indeed successfully applied in practice (74). Consequentially, we would hypothesize that the cognitive dysfunctions in schizophrenia might relate to an impaired integration of self- and other-related affective mental processes. Since the interaction of the DMN with other brain regions and networks is more reflective of schizophrenia symptoms than within-DMN connectivity (18,75,76), it is not surprising that the DMN was not predictive, but the eSAD was which comprises regions going beyond the DMN.

Molecular architecture of the identified networks which robustly predicted cognitive dimension

Cognitive deficits are a lifelong burden for patients with schizophrenia because there are so few effective medications including the mainstay anti-dopaminergic agents (37,77). In line with the notion that dopaminergic dysfunction alone doesn't account for the whole picture of schizophrenia psychopathology (78,79), here we revealed that the networks and nodes predictive of individual cognitive symptom-load are related to both dopaminergic (32) and serotonergic systems (78). These data extend previous region-of-interest analyses (80,81) to a comprehensive topographical level and are supported by findings that cognitive deficits relate to D_1 dopamine

receptor elevation in schizophrenia (80). The extension to a network-level investigation for the molecular architecturethat is related to symptomatology is important, as schizophrenia patients are characterized by dysconnection between distant brain regions and network connectivity-based analyses can nominate mechanisms of action for the development of novel pharmacological treatments (82). In line with involvement of dopamine functioning in cognitive deficits in schizophrenia (32), the cognitive dimension of psychopathology was associated with the dopamine-synthesis-capacity. Increased dopamine-synthesis-capacity in schizophrenia was not only reported in the striatum (32) but also cortical areas including prefrontal cortex (83,84) where multiple nodes within the ToM and the eSAD networks are located.

Moreover, cognitive symptoms were linked to 5-HTT density at network level. 5-HTT plays a critical role in regulating serotonergic concentration and signaling. Serotonergic dysfunction and 5-HTT polymorphism (85) have been involved in schizophrenia pathophysiology (34,78). Previous postmortem and in vivo PET studies have yielded inconsistent results on the alteration of 5-HTT density in schizophrenia (34), while an over-expression of 5-HTT mRNA in the prefrontal and temporal cortex has been demonstrated (86). We here revealed a potential role of 5-HTT in cognitive deficits via the networks involved in socio-affective processes, resonating with the proposed implication of 5-HTT in the affective domain (87,88). While atypical anti-psychotics including olanzapine and risperidone target also the 5-HT_{2a} serotonin receptor (89,90), their effects on 5-HTT seems to be equivocal (91,92). Interestingly, anti-psychotic drugs, pimavanserin and SEP-363856 have just been introduced that preferentially target serotonin and not dopamine receptors (93,94), suggesting increased focus also on serotonergic pathways.

Limitations and Considerations

First, the effect sizes for the correlation between the symptom scores and their predictions were moderate. However, despite the clinical complexity of the population and the heterogeneities in scanners and protocols, the

effect sizes are similar to the previously reported for predicting, e.g., creativity (95), personality (48), and memory performance (96) in healthy subjects (*r*-values mostly around 0.2-0.35). Since olanzapine-equivalent dosage did not correlate with symptom scores or alter the prediction pattern after additionally controlling for the dosage in cross-validation, medication would be largely a source of random variation in our data and hence make our results more conservative. Second, although glutamatergic dysfunction has been increasingly implicated in schizophrenia neurocognitive deficits (79,97), there are no publicly available in vivo maps reflecting aspects of the glutamatergic system. Finally, within-subject (longitudinal) studies assessing symptoms, rs-FC and receptor densities are needed, though acquisition of molecular imaging data in large samples remains difficult.

Based on rs-FC within different meta-analytic task-activation networks covering a broad range of functional domains and predictive modeling with strict validations, intrinsic connectivity patterns of networks implicated in socio-affective processing was revealed to robustly associate with the cognitive dimension of psychopathology. Our investigation of the molecular architecture of the identified predictive networks implied a potential involvement of 5-HTT serotonin transporter, besides the dopaminergic system, in schizophrenia cognitive symptomatology, possibly providing hints into treatments.

.

Acknowledgments: This study was supported by the Deutsche Forschungsgemeinschaft (DFG, EI 816/4-1), the National Institute of Mental Health (R01-MH074457), the Helmholtz Portfolio Theme "Supercomputing and Modeling for the Human Brain", and the European Union's Horizon 2020 Research and Innovation Programme under Grant Agreement No. 720270 (HBP SGA1) and 785907 (HBP SGA2). Ji Chen has received a Ph.D fellowship from the Chinese Scholarship Council.

Disclosures: The authors reported no biomedical financial interests or potential conflicts of interest.

References:

1. Kirkpatrick B, Buchanan RW, Ross DE, Ros, DE, Carpenter WT Jr (2001): A separate disease within the syndrome of schizophrenia. *Arch Gen Psychiatry* 58(2): 165-171.
2. Kay SR, Fiszbein A, Opler LA (1987): The Positive and Negative Syndrome Scale (PANSS) for schizophrenia. *Schizophr Bull* 13: 261–276
3. Lang FU, Walther S, Stegmayer K, Anderson-Schmidt H, Schulze TG, Becker T, Jäger M (2015): Subtyping schizophrenia: A comparison of positive/negative and system-specific approaches. *Compr Psychiatry* 61: 115-121.
4. Pu W, Rolls ET, Guo S, Liu H, Yu Y, Xue Z, *et al.* (2014): Altered functional connectivity links in neuroleptic-naïve and neuroleptic-treated patients with schizophrenia, and their relation to symptoms including volition. *Neuroimage Clin* 6: 463-474.
5. Schilbach L, Derntl B, Aleman A, Caspers S, Clos M, Diederen KMJ, *et al.* (2016): Differential patterns of dysconnectivity in mirror neuron and mentalizing networks in schizophrenia. *Schizophr Bull* 42(5): 1135-1148.
6. Chen J, Patil K R, Weis S, Sim K, Nickl-Jockschat T, Zhou J, *et al.* (2020): Neurobiological Divergence of the Positive and Negative Schizophrenia Subtypes Identified on a New Factor Structure of Psychopathology Using Non-negative Factorization: An International Machine Learning Study. *Biol Psychiatry* 87(3): 282-293
7. Van den Oord EJCG, Rujescu D, Robles J R, Giegling I, Birrell C, Bukszár J, *et al.* (2006): Factor structure and external validity of the PANSS revisited. *Schizophr Res* 82(2-3): 213-223.
8. Marder S R, Galderisi S (2017): The current conceptualization of negative symptoms in schizophrenia. *World Psychiatry*, 16(1): 14-24.
9. Stephan K E, Friston KJ, Frith CD (2009): Dysconnection in schizophrenia: from abnormal synaptic plasticity to failures of self-monitoring. *Schizophr Bull* 35(3): 509-527.
10. Uhlhaas PJ (2013): Dysconnectivity, large-scale networks and neuronal dynamics in schizophrenia. *Curr Opin Neurobiol* 23(2): 283-290.
11. Pettersson-Yeo W, Allen P, Benetti S, McGuire P, Mechelli A (2011): Dysconnectivity in schizophrenia: where are we now? *Neurosci Biobehav Rev* 35(5): 1110-1124.
12. Dong D, Wang Y, Chang X, Luo C, Yao D (2018): Dysfunction of large-scale brain networks in schizophrenia: a meta-analysis of resting-state functional connectivity. *Schizophr Bull* 44(1): 168-181.
13. Baker JT, Holmes AJ, Masters GA, Yeo BTT, Krienen F, Buckner RL, Öngür D (2014): Disruption of cortical association networks in schizophrenia and psychotic bipolar disorder. *JAMA psychiatry* 71(2): 109-118.

14. Baker JT, Dillon DG, Patrick LM, Roffman JL, Brady RO Jr, Pizzagalli DA (2019): Functional connectomics of affective and psychotic pathology. *Proc Natl Acad Sci U S A* 116(18): 9050-9059.

15. Mwansisya T E, Hu A, Li Y, Chen X, Wu G, Huang X (2017): Task and resting-state fMRI studies in first-episode schizophrenia: A systematic review. *Schizophr Res* 189: 9-18.

16. Tregellas JR (2014): Neuroimaging biomarkers for early drug development in schizophrenia. *Biol psychiatry* 76(2): 111-119.

17. Giraldo-Chica M, Woodward ND (2017): Review of thalamocortical resting-state fMRI studies in schizophrenia. *Schizophr Res* 180: 58-63.

18. Hu ML, Zong XF, Mann JJ, Zheng JJ, Liao YH, Li ZC (2017): A review of the functional and anatomical default mode network in schizophrenia. *Neurosci Bull* 33(1): 73-84.

19. Mehta U M, Thirthalli J, Aneelraj D, Jadhav P, Gangadhar BN, Keshavanb MS (2014): Mirror neuron dysfunction in schizophrenia and its functional implications: a systematic review. *Schizophr Res* 160(1-3): 9-19.

20. Shen X, Finn E S, Scheinost D, Rosenberg MD, Chun MM, Papademetris X, Constable RT (2017): Using connectome-based predictive modeling to predict individual behavior from brain connectivity. *Nat Protoc* 12(3): 506-518.

21. Laird A R, Fox P M, Eickhoff S B, Turner JA (2011): Behavioral interpretations of intrinsic connectivity networks. *J Cogn Neurosci* 23(12): 4022-4037.

22. Laird AR, Eickhoff SB, Li K, Robin DA, Glahn DC, Fox PT (2009): Investigating the Functional Heterogeneity of the Default Mode Network Using Coordinate-Based Meta-Analytic Modeling. *J Neurosci* 18, 14496-14505.

23. Eickhoff SB, Bzdok D, Laird AR, Kurth F, Fox PT (2012): Activation likelihood estimation revisited. *Neuroimage* 59, 2349-2361.

24. Zilles K, Bacha-Trams M, Palomero-Gallagher N, Amunts K, Friedericic AD (2015): Common molecular basis of the sentence comprehension network revealed by neurotransmitter receptor fingerprints. *Cortex* 63: 79-89.

25. Zilles K, Palomero-Gallagher N, Grefkes C, Scheperjans F, Boy C, Amunts K, Schleicherb A (2002): Architectonics of the human cerebral cortex and transmitter receptor fingerprints: reconciling functional neuroanatomy and neurochemistry. *Eur Neuropsychopharmacol* 12(6): 587-599.

26. Richiardi J, Altmann A, Milazzo A C, Chang C, Chakravarty MM, Banaschewski T, *et al.* (2015): Correlated gene expression supports synchronous activity in brain networks. *Science* 348(6240): 1241-1244.

27. Anderson K M, Collins M A, Chin R, Ge T, Rosenberg MD, Holmes AJ (2020): Transcriptional and imaging-genetic association of cortical interneurons, brain function, and schizophrenia risk. *Nat Commun* 11(1): 1-15.

28. Stagg C J, Bachtiar V, Amadi U, Gudberg CA, Ilie AS, Sampaio-Baptista C, *et al.* (2014): Local GABA concentration is related to network-level resting functional connectivity. *Elife* 3: e01465.

29. Kringelbach M L, Cruzat J, Cabral J, Knudsen GM, Carhart-Harris R, Whybrow PC, *et al.* (2020): Dynamic coupling of whole-brain neuronal and neurotransmitter systems. *Proc Natl Acad Sci U S A* 117(17): 9566-9576.

30. Landek-Salgado MA, Faust TE, Sawa A (2016): Molecular substrates of schizophrenia: homeostatic signaling to connectivity. *Mol Psychiatry* 21(1): 10-28.

31. Limongi R, Jeon P, Mackinley M, Das T, Dempster K, Théberge J, *et al.* (2020): Glutamate and Dysconnection in the Salience Network: Neurochemical, Effective-connectivity, and Computational Evidence in Schizophrenia. *Biol Psychiatry* In Press, doi: 10.1016/j.biopsych.2020.01.021.

32. Howes OD, Kapur S (2009): The dopamine hypothesis of schizophrenia: version III—the final common pathway. *Schizophr Bull* 35(3): 549-562.

33. Poels E MP, Kegeles LS, Kantrowitz JT, Slifstein M, Javitt DC, Lieberman JA, *et al.* (2014): Imaging glutamate in schizophrenia: review of findings and implications for drug discovery. *Mol Psychiatry* 19(1): 20-29.

34. Selvaraj S, Arnone D, Cappai A, Howes, O (2014): Alterations in the serotonin system in schizophrenia: a systematic review and meta-analysis of postmortem and molecular imaging studies. *Neurosci Biobehav Rev* 45: 233-245.

35. Nakazawa K, Zsiros V, Jiang Z, Nakao K, Kolata S, Zhang S, Belforteb JE (2012): GABAergic interneuron origin of schizophrenia pathophysiology. *Neuropharmacology* 62(3): 1574-1583.

36. Fusar-Poli P, Papanastasiou E, Stahl D, Rocchetti M, Carpenter W, Shergill S, McGuire P (2015): Treatments of negative symptoms in schizophrenia: meta-analysis of 168 randomized placebo-controlled trials. *Schizophr Bull* 41(4): 892-899.

37. Miyamoto S, Duncan GE, Marx CE, Lieberman JA (2005): Treatments for schizophrenia: A critical Review of pharmacology and mechanisms of action of antipsychotic drugs. *Mol Psychiatry* 10: 79–104.

38. Tamminga CA, Ivleva EI, Keshavan MS, Pearlson GD, Clementz BA, Witte B, *et al.* (2013): Clinical phenotypes of psychosis in the Bipolar-Schizophrenia Network on Intermediate Phenotypes (B-SNIP). *Am J Psychiatry* 170(11): 1263-1274.

39. Gardner DM, Murphy AL, O'Donnell H, Centorrino F, Baldessarini RJ (2010): International consensus study of antipsychotic dosing. *Am J Psychiatry* 167: 686–693

40. Power JD, Barnes KA, Snyder AZ, *et al.* (2012): Spurious but systematic correlations in functional connectivity MRI networks arise from subject motion. *Neuroimage* 59(3): 2142-2154.

41. Satterthwaite TD, Elliott MA, Gerraty RT, Ruparel K, Loughead J, Calkins ME, *et al.* (2013): An improved framework for confound regression and filtering for control of motion artifact in the preprocessing of resting-state functional connectivity data. *Neuroimage* 64: 240-256.

42. Varikuti DP, Hoffstaedter F, Genon S, Schwender H, Reid AT, Eickhoff SB (2017): Resting-state test–retest reliability of a priori defined canonical networks over different preprocessing steps. *Brain Struct Funct* 222(3): 1447-1468.

43. Murphy K, Fox MD (2017): Towards a consensus regarding global signal regression for resting state functional connectivity MRI. *Neuroimage* 154: 169-173.

44. Yang GJ, Murray JD, Repovs G, Cole MW, Savic A, Glasser MF, *et al.* (2014): Altered global brain signal in schizophrenia. *Proc Natl Acad Sci U S A* 111(20): 7438-7443.

45. Nostro AD, Müller VI, Varikuti DP, Pläschke RN, Hoffstaedter F, Langner R, *et al.* (2018): Predicting personality from network-based resting-state functional connectivity. *Brain Struct Funct* 223(6): 2699-2719.

46. Pläschke R N, Cieslik E C, Müller VI, Hoffstaedter F, Plachti A, Varikuti DP, *et al.* (2018): On the integrity of functional brain networks in schizophrenia, Parkinson's disease, and advanced age: Evidence from connectivity-based single-subject classification. *Hum Brain Mapp* 39(11): 4633.

47. Tipping ME (2001): Sparse Bayesian learning and the relevance vector machine. *J Mach Learn Res* 1: 211-244.

48. Pervaiz U, Vidaurre D, Woolrich MW, Smith SM (2020): Optimising network modelling methods for fMRI. *NeuroImage* 211, 116604.

49. Dubois J, Galdi P, Paul LK, Adolphs R (2018): A distributed brain network predicts general intelligence from resting-state human neuroimaging data. *Philos Trans R Soc Lond B Biol Sci* 373: 20170284.

50. Snoek L, Miletić S, Scholte HS (2019): How to control for confounds in decoding analyses of neuroimaging data. *NeuroImage* 184: 741-760

51. More S, Eickhoff SB, Julian C, Patil, KR (2020): Confound Removal and Normalization in Practice: A Neuroimaging Based Sex Prediction Case Study. Preprint available at https://juser.fz-juelich.de/record/877721; Accepted in the *European Conference on Machine Learning and Principles and Practice of Knowledge Discovery in Databases* (ECML PKDD; https://ecmlpkdd2020.net/programme/accepted/#ADSTab).

52. Combrisson E, Jerbi K (2015): Exceeding chance level by chance: the caveat of theoretical chance levels in brain signal classification and statistical assessment of decoding accuracy. *J Neurosci Methods* 250: 126-136.

53. Meinshausen N, Bühlmann P (2010): Stability selection. J R Stat Soc Ser B Stat Methodol 72(4): 417-473.

54. Dukart J, Holiga Š, Chatham C, Hawkins P, Forsyth A, McMillan R, *et al.* (2018): Cerebral blood flow predicts differential neurotransmitter activity. *Sci Rep* 8(1): 1-11.

55. Dukart J, Holiga S, Rullmann M, Lanzenberger R, Hawkins PCT, Mehta MA, *et al.* (2020): JuSpace: A tool for spatial correlation analyses of magnetic resonance imaging data with nuclear imaging derived neurotransmitter maps. *bioRxiv* doi: 10.1101/2020.04.17.046300.

56. Addington J, Addington D (1999): Neurocognitive and social functioning in schizophrenia. *Schizophr Bull* 25(1): 173-182.

57. Cohen AS, Forbes CB, Mann MC, Blanchard JJ (2006): Specific cognitive deficits and differential domains of social functioning impairment in schizophrenia. *Schizophr Res* 81(2-3): 227-238.

58. Buhle JT, Silvers JA, Wager TD, Lopez R, Onyemekwu C, Kober H, *et al.* (1991): Cognitive reappraisal of emotion: a meta-analysis of human neuroimaging studies. *Cereb Cortex* 24(11): 2981-2990.

59. Bzdok D, Meyer-Lindenberg A (2018): Machine learning for precision psychiatry: opportunities and challenges. *Biol Psychiatry Cogn Neurosci Neuroimaging* 3: 223-230.

60. Greene AS, Gao S, Scheinost D, Constable RT (2018): Task-induced brain state manipulation improves prediction of individual traits. *Nat Commun* 9(1): 1-13.

61. Gao S, Greene AS, Constable RT, Scheinost D (2019): Combining multiple connectomes improves predictive modeling of phenotypic measures. *Neuroimage* 201: 116038

62. Jiang R, Zuo N, Ford JM, Qi S, Zhi D, Zhuo C, *et al.* (2020): Task-induced brain connectivity promotes the detection of individual differences in brain-behavior relationships. *NeuroImage* 207: 116370.

63. Baron-Cohen S (1995): *Mindblindness: An Essay on Autism and Theory of Mind*. The MIT Press/Bradford: Cambridge, pp 1–7.

64. Bora E, Pantelis C (2013): Theory of mind impairments in first-episode psychosis, individuals at ultra-high risk for psychosis and in first-degree relatives of schizophrenia: systematic review and meta-analysis. *Schizophr Res* 144(1-3): 31-36.

65. Fretland R A, Andersson S, Sundet K, Andreassen OA, Melle I, Vaskinn A (2015): Theory of mind in schizophrenia: error types and associations with symptoms. *Schizophr Res* 162(1-3): 42-46.

66. Benedetti F, Bernasconi A, Bosia M, Cavallaro R, Dallaspezia S, Falini A, *et al.* (2009): Functional and structural brain correlates of theory of mind and empathy deficits in schizophrenia. *Schizophr Res* 114(1-3): 154-160.

67. Das P, Lagopoulos J, Coulston C M, Henderson AF, Malhi GS (2012): Mentalizing impairment in schizophrenia: a functional MRI study. *Schizophr Res* 134(2-3): 158-164.

68. Shamay-Tsoory S G, Shur S, Barcai-Goodman L, Medlovich S, Harari H, Levkovitz Y (2007): Dissociation of cognitive from affective components of theory of mind in schizophrenia. *Psychiatry Res* 149(1-3): 11-23.

69. Vatansever D, Menon D K, Stamatakis EA (2017): Default mode contributions to automated information processing. *Proc Natl Acad Sci U S A* 114(48): 12821-12826.

70. Sormaz M, Murphy C, Wang H, Hymers M, Karapanagiotidis T, Poerio G, *et al.* (2018): Default mode network can support the level of detail in experience during active task states. *Proc Natl Acad Sci U S A* 115(37): 9318-9323.

71. Amft M, Bzdok D, Laird AR, Fox PT, Schilbach L, Eickhoff SB (2015): Definition and characterization of an extended social-affective default network. *Brain Struct Funct* 220(2): 1031-1049.

72. Silverstein SM, Spaulding WD, Menditto AA, Savitz A, Liberman RP, Berten S, Starobin H (2009): Attention shaping: a reward-based learning method to enhance skills training outcomes in schizophrenia. *Schizophr Bull* 35(1): 222-232.

73. Schweizer S, Satpute A B, Atzil S, Field AP, Hitchcock C, Black M, et al. (2019): The impact of affective information on working memory: A pair of meta-analytic reviews of behavioral and neuroimaging evidence. *Psychological Bull* 145(6): 566.

74. Park S, Gibson C, McMichael T (2006): Socioaffective factors modulate working memory in schizophrenia patients. *Neuroscience* 139(1): 373-384.

75. Jardri R, Thomas P, Delmaire C, Delion P, Pins D (2013): The neurodynamic organization of modality-dependent hallucinations. *Cereb Cortex* 23(5): 1108-1117.

76. Whitfield-Gabrieli S, Thermenos H W, Milanovic S, Tsuang MT, Faraone SV, McCarley RW, *et al.* (2009): Hyperactivity and hyperconnectivity of the default network in schizophrenia and in first-degree relatives of persons with schizophrenia. *Proc Natl Acad Sci U S A* 106(4): 1279-1284.

77. Sinkeviciute I, Begemann M, Prikken M, Oranje B, Johnsen E, Lei WU, *et al.* (2018): Efficacy of different types of cognitive enhancers for patients with schizophrenia: a meta-analysis. *NPJ Schizophr* 4(1): 22.

78. Stahl SM (2018): Beyond the dopamine hypothesis of schizophrenia to three neural networks of psychosis: dopamine, serotonin, and glutamate. *CNS Spectr* 23(3): 187-191.

79. Uno Y, Coyle JT (2019): Glutamate hypothesis in schizophrenia. Psychiatry Clin Neurosci 73(5): 204-215.

80. Abi-Dargham A, Mawlawi O, Lombardo I, Gil R, Martinez D, Huang Y, *et al.* (2002): Prefrontal dopamine D1 receptors and working memory in schizophrenia. *J Neurosci* 22:3708–3719

81. Abi-Dargham A, Xu X, Thompson JL, Gil R, Kegeles LS, Urban N, *et al.* (2012): Increased prefrontal cortical D1 receptors in drug naive patients with schizophrenia: a PET study with [11C] NNC112[J]. *J Psychopharmacol* 26(6):

794-805.

82. De Rossi P, Chiapponi C, Spalletta G (2015): Brain functional effects of psychopharmacological treatments in schizophrenia: a network-based functional perspective beyond neurotransmitter systems. *Curr Neuropharmacol* 13(4): 435-444.

83. Lindström L H, Gefvert O, Hagberg G, Lundberg T, Bergström M, Hartvig P, Långström B (1999): Increased dopamine synthesis rate in medial prefrontal cortex and striatum in schizophrenia indicated by L-(β-11C) DOPA and PET. *Biol Psychiatry* 46(5): 681-688.

84. Elkashef AM, Doudet D, Bryant T, Cohen RM, Li SH, Wyatt RJ (2000): 6-(18)F-DOPA PET study in patients with schizophrenia. Positron emission tomography. *Psychiatry Res* 100: 1-11.

85. Malhotra A K, Goldman D, Mazzanti C, Clifton A, Breier A, Pickar D (1998): A functional serotonin transporter (5-HTT) polymorphism is associated with psychosis in neuroleptic-free schizophrenics. *Mol Psychiatry* 3(4): 328-332.

86. Hernandez I, Sokolov BP (1997): Abnormal expression of serotonin transporter mRNA in the frontal and temporal cortex of schizophrenics. *Mol Psychiatry* 2: 57–64.

87. Golimbet VE, Alfimova MV, Shchebatykh TV, Abramova LI, Kaleda VG, Rogaev EI (2004): Serotonin transporter polymorphism and depressive-related symptoms in schizophrenia. *Neuropsychiatr Genet* 126(1): 1-7.

88. Peitl V, Štefanović M, Karlović D (2017): Depressive symptoms in schizophrenia and dopamine and serotonin gene polymorphisms. *Prog Neuro Psychopharmacol Biol Psychiatry* 77: 209-215.

89. Radhakrishnan R, Matuskey D, Nabulsi N, Gaiser E, Gallezot J, Henry S, *et al.* (2020): In vivo 5-HT6 and 5-HT2A receptor availability in antipsychotic treated schizophrenia patients vs. unmedicated healthy humans measured with [11C] GSK215083 PET. *Psychiatry Res Neuroimaging* 295: 111007.

90. Mauri MC, Paletta S, Maffini M, Colasanti A, Dragogna F, Pace CD, Altamura AC (2014): Clinical pharmacology of atypical antipsychotics: an update. *EXCLI J* 13: 1163.

91. Barkan T, Peled A, Modai I, Weizman A, Rehavi M (2006): Characterization of the serotonin transporter in lymphocytes and platelets of schizophrenia patients treated with atypical or typical antipsychotics compared to healthy individuals. *Eur Neuropsychopharmacol* 16(6): 429-436.

92. Lian J, Pan B, Deng C (2016): Early antipsychotic exposure affects serotonin and dopamine receptor binding density differently in selected brain loci of male and female juvenile rats. *Pharmacological Rep* 68(5): 1028-1035.

93. Sahli ZT, Tarazi FI (2018): Pimavanserin: novel pharmacotherapy for Parkinson's disease psychosis. *Expert Opin Drug Discov* 13(1): 103-110.

94. Koblan KS, Kent J, Hopkins SC, Krystal JH, Cheng H, Goldman R, Loebel A (2020): A Non-D2-Receptor-Binding Drug for the Treatment of Schizophrenia. *N Engl J Med* 382(16): 1497-1506.

95. Beaty RE, Rosenberg MD, Benedek M, Chen Q, et al. (2018): Robust prediction of individual creative ability from brain functional connectivity. *Proc Natl Acad Sci U S A* 115: 1087-1092.

96. Persson J, Stening E, Nordin K, Söderlund H (2018): Predicting episodic and spatial memory performance from hippocampal resting-state functional connectivity: Evidence for an anterior-posterior division of function. *Hippocampus* 28: 53-66.

97. Kaminski J, Gleich T, Fukuda Y, Katthagen T, Gallinat J, Heinz A, Schlagenhauf F (2020): Association of cortical glutamate and working memory activation in patients with schizophrenia: A multimodal proton magnetic resonance spectroscopy and functional magnetic resonance imaging study. *Biol Psychiatry* 87(3): 225-233.

Table1. Demographic and clinical characteristics of schizophrenia patients used for predictive analysis

Characteristics	Main sample (N=126, seven sites)	The independent B-SNIP sample for validation (N=100, two sites)	*p*-value
Demographic			
Age (years)	34.19 (11.45)	34.28 (12.31)	0.948
Gender (male/female)	92/34	71/29	0.767
Illness during (years)	10.48 (9.87)	12.35 (11.13)	0.187
PANSS subscales			
Positive	14.86 (5.35)	14.91 (5.72)	0.945
Negative	14.76 (5.85)	15.01 (5.64)	0.743
General	30.25 (10.13)	27.98 (7.46)	0.062
Illness severity (total PANSS)	59.87 (18.11)	57.90 (15.78)	0.390
Scores on the dimensions of PANSS			
Negative	2.76 (2.44)	2.81 (2.23)	0.859
Positive	3.26 (2.36)	3.28 (2.55)	0.954
Affective	3.33 (2.33)	2.69 (1.71)	**0.022**
Cognitive	2.49 (1.92)	2.72 (1.79)	0.357
Medication			
Atypical antipsychotics	97 (75.8%)	71 (71.0%)	
Typical antipsychotics	5 (3.9%)	4 (4.0%)	
Both A & T	7 (5.5%)	13 (13.0%)	
None or unknown	19 (14.8%)	12 (12.0%)	
Current antipsychotic medication[e]	19.23 (11.91)	18.96 (13.47)	

Data are mean (SD), or n (%). *p* Values in bold indicate a significance of $p<0.05$. Except for gender, which was based on chi-square test, other statistics were all based on two-sample t test. Of note, because the detailed medication information was missing for several patients in different proportions for the three datasets, statistical comparisons were not conducted.

PANSS, Positive and Negative Syndrome Scale;

[e]Demonstrated in olanzapine-equivalent dosage (mg/day).

Figures:

Figure 1. Overview of the 17 functional networks derived from prior coordinate-based meta-analytical studies.

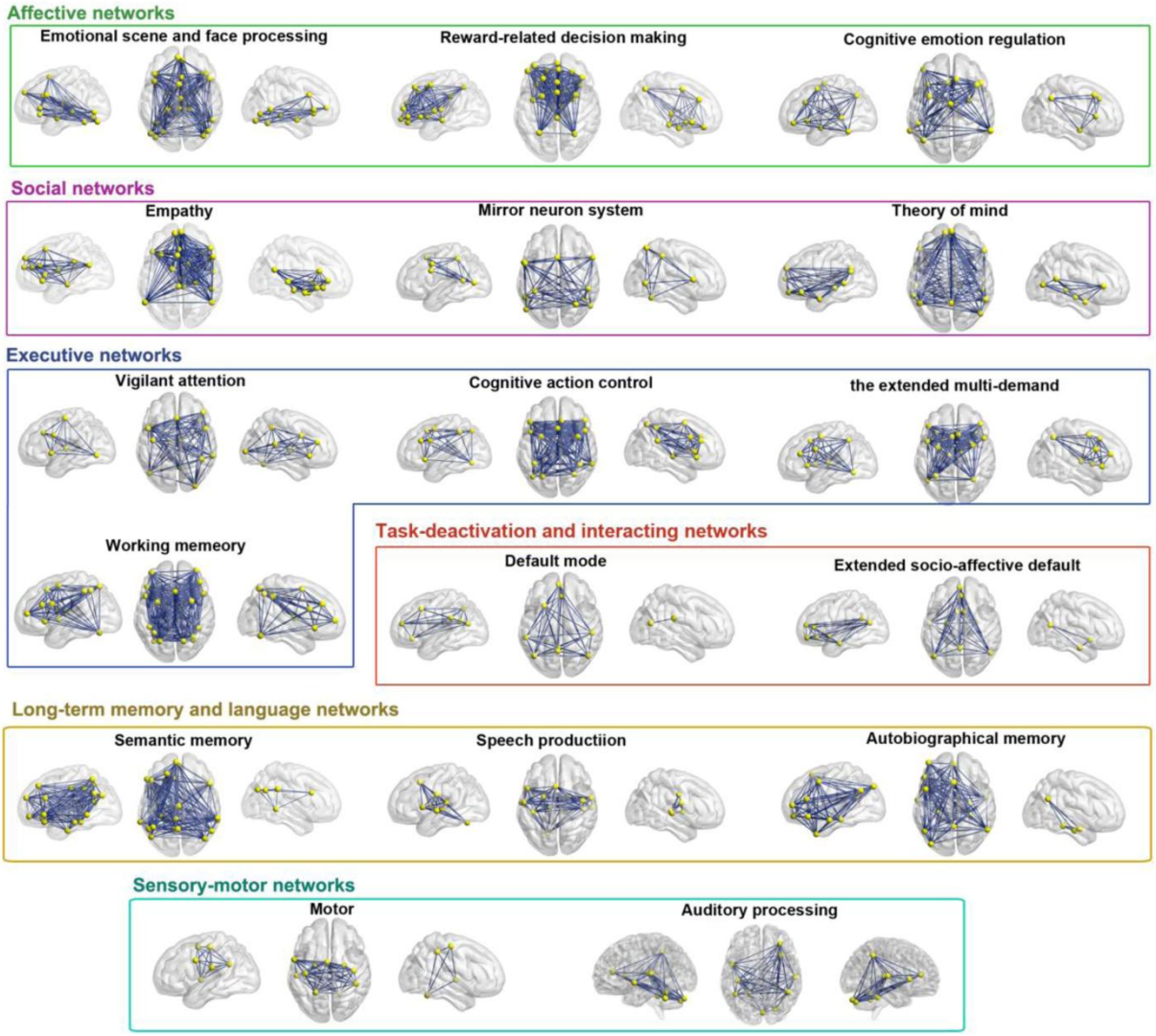

Networks were assigned to six broad domains according to their main functional roles, as implicated in the tasks included in the source publications of these meta-analytical networks, in multiple neuro-cognitive and socio-affective processes. We also note that networks such as the task-deactivation default-mode (DMN) network (22) and the extended socio-affective-default (eSAD) network which is derived from DMN regions (71) can be engaged during multiple processes (69,70). Details can be found in Supplementary Table S3.

Yellow nodes represent the spheres created from the coordinates with 6mm radius and blue lines denote the pair-wise connections between the nodes. Connections within each network were used separately in our predictive modeling to investigate network-specific relationships with individual dimensions of psychopathology.

Figure 2. Multivariable prediction of the four symptom dimensions from within-network resting-state functional connectivity using relevant vector machine.

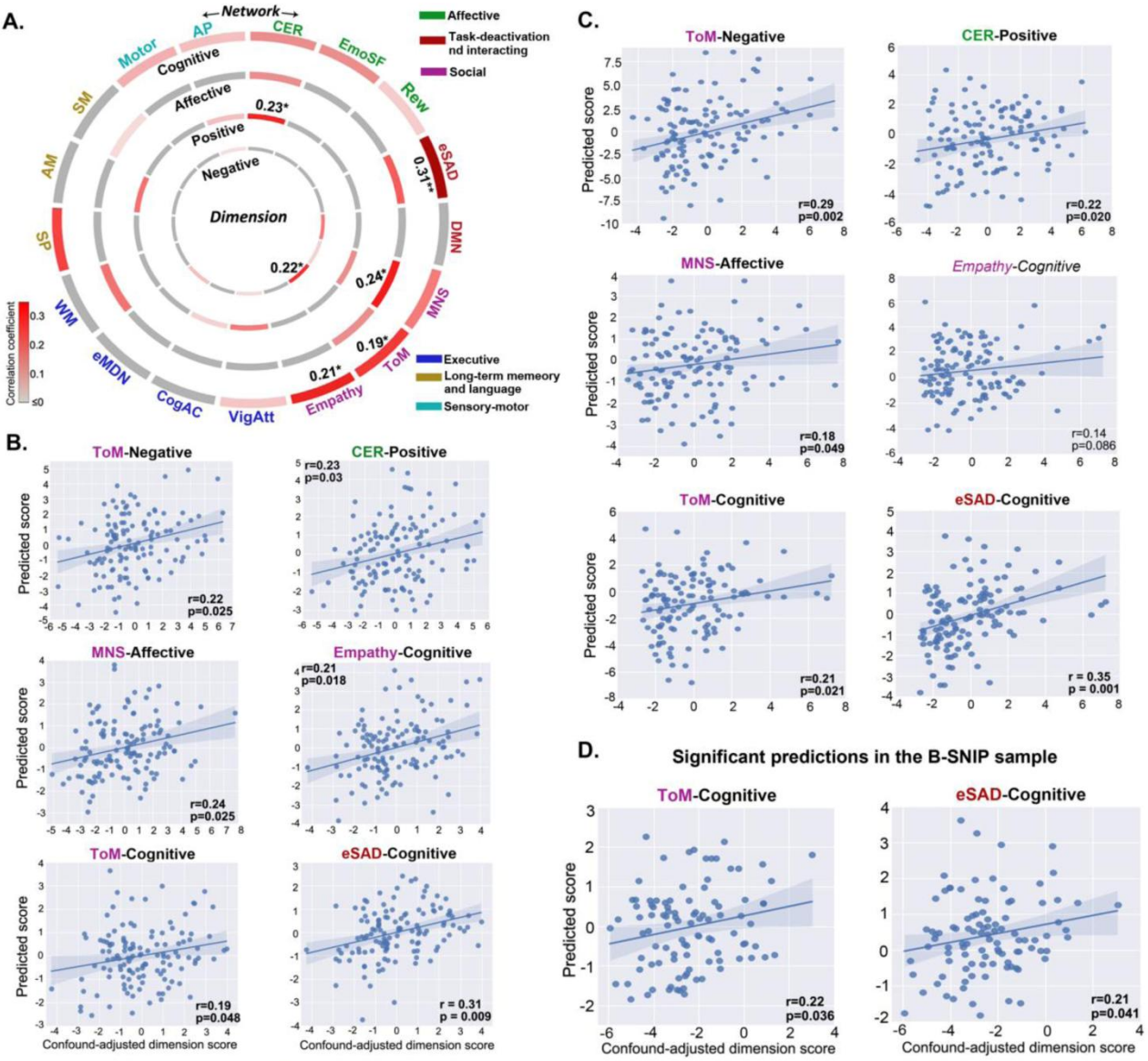

A) Circos plot shows the 500x repeated 10-fold cross-validation results for the main sample. Correlations between the actual (confound-adjusted) dimensional symptom scores and their predictions are color-coded from light grey (0) to dark red (0.35), **p<0.05, **p<0.01.*

B) Scatter plots show the six significant predictions identified by 10-fold cross-validation in main sample.

C) Scatter plots show the leave-one-site-out cross-validation results for the six significant predictions identified by 10-fold cross-validation in main sample. Apart from the prediction of cognitive dimension from the rs-FC within the empathy network, other predictions were all confirmed by leave-one-site-out with significant correlations identified.

D) Scatter plots show the significant predictions in the independent B-SNIP sample. Models trained within the main sample were used for this validation analysis in B-SNIP. Shaded areas represent 95% confidence intervals.

Abbreviations: EmoSF, emotional scene and face processing; Rew, reward-related decision making; CER, cognitive emotion regulation; ToM, theory-of-mind; MNS, minor neuron system; DMN, default mode network; eSAD, extended socio-affective default; VigAtt, vigilant attention; CogAC, cognitive action control; eMDN, the extended multi-demand networks; SM, semantic memory; SP, speech production; WM, working memory; AM, autobiographical memory; APN, auditory processing network.

Figure 3. Reliably predictive connections for the two networks that robustly predicted the cognitive dimension and validation of the formed subnetworks in the independent sample

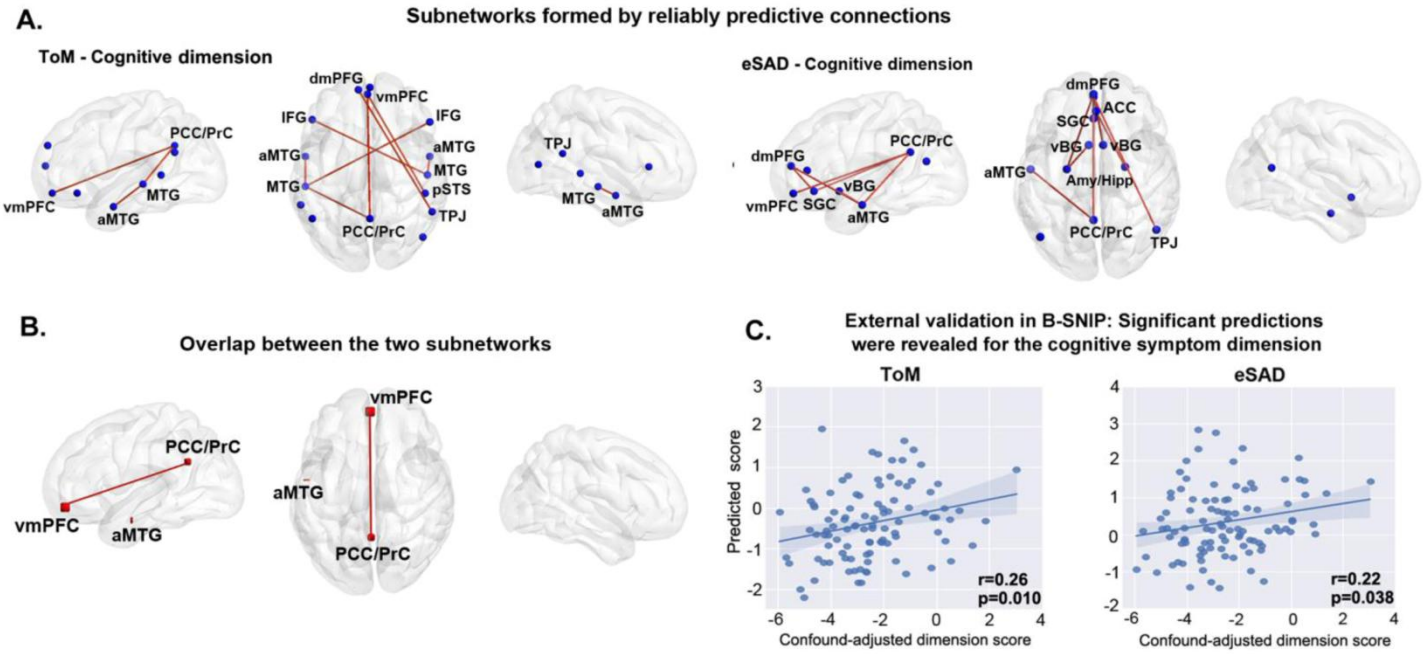

A) Reliably predictive connections selected in more than 80% of the different cross-validation runs (repeated 10-fold and leave-one-site out) and in the final models trained on the entire main sample for validation in B-SNIP.

B) Overlapping between the two subnetworks.

C) Scatter plots show the significant correlations in B-SNIP using the models trained within the main sample.

Abbreviations: ToM, theory-of-mind; eSAD, extended socio-affective default; CER, cognitive emotion regulation, MNS, mirror neuron system. Amy, amygdala; Hipp, hippocampus; vmPFC, ventro-medial prefrontal cortex; dmPFC, dorso-medial prefrontal cortex; mFG, medial frontal cortex; aMTG, anterior middle temporal gyrus, IFG, inferior frontal gyrus; TPJ, temporo-parietal junction, PCC, posterior cingulated cortex, PrC, precuneus; SGC, subgenual cingulate cortex, vBG, ventral basal ganglia; ACC, anterior cingulated cortex.

Figure 4. Significantly highly-expressed receptors and transporters at the nodes of the robustly predictive networks relative to the entire brain, as well as the schematic and results for the spatial correlation analysis with receptor/transporter density maps

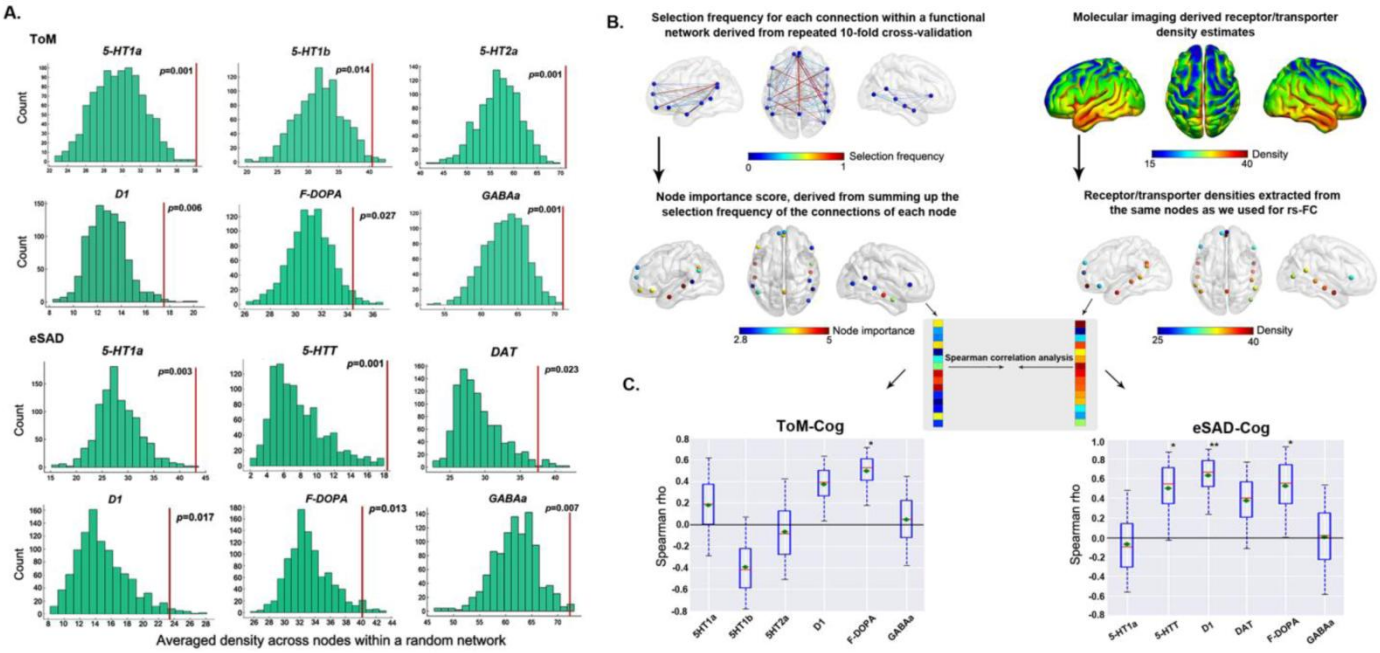

A) Histograms show the null distributions for the receptor/transporter densities of the 1000 simulated (random) networks. Red lines indicate the true averaged receptor/transporter densities across the different nodes within real networks.

B) Procedure for conducting the spatial correlation analysis between network nodes and receptor/transporter density maps.

C) Bootstrapped Spearman correlations (repeated 10,000 times) between the node importance score and the nodal receptor/transporter density estimates for the two identified networks which robustly predicted the cognitive symptom dimension. Bootstrap nodes were drawn with replacement from the real networks, and then the correlation analysis was done on them. Boxes refer to the Spearman rho values. The red line depicts the median, the green diamond depicts the mean, and the whiskers represent the 5th and 95th percentiles. Significant correlations derived from spatial-level permutation tests are marked with an asterisk (*p<0.05, **p<0.01).

Abbreviations: ToM, theory-of-mind; eSAD, extended socio-affective default; Cog, cognitive dimension.

6.2 Supporting information

(for complete supplementary materials and methods please refer to https://www.biorxiv.org/content/10.1101/2020.07.02.185124v1.supplementary-material; below I only provided some key aspects for the purpose of an integrative demonstration within the thesis while avoiding reiteration)

6.2.1 Detailed sample information

Main sample

The main sample used for the discovery of network-symptom associations was the same patient cohorts as that have been employed in the above "*Biological Psychiatry*" paper. Details can be found in "5.2.1 Detailed sample information".

The B-SNIP sample for validation

Subjects with schizophrenia in the independent, validation sample were recruited as part of the Bipolar-Schizophrenia Network on Intermediate Phenotypes (B-SNIP) Consortium study which used identical diagnostic and clinical assessment techniques with similar recruitment approaches at multiple sites (Baltimore, Chicago, Dallas, Detroit, and Hartford). Detailed information on the entire study sample is provided elsewhere (Tamminga et al., 2013). These clinical patients were diagnosed using the Structured Clinical Interview for DSM-IV Axis I Disorders, Patient Edition (SCID-I/P) and were stably medicated outpatients. The study protocol was approved by the institutional review board at each local site and written informed consent was obtained from each of the volunteers. For our current study purpose, only schizophrenia patients with complete PANSS and fMRI data were included. Among the four sites (Baltimore, Dallas, Detroit, and Hartford) data we retrieved, the Dallas site was scanned using a Philips machine such that the details on the order of each slice scanned within a EPI volume were not stored in the *Header* of the resting-state images and was hence excluded, because inaccurate slice timing correction will lead to a biased estimation of resting-state functional connectivity (rs-FC). The Detroit site was also not included due to the small sample size (<10) retained after sample curation and quality control. Resultantly, the dataset (in total 117 schizophrenia patients) pooled from the Hartford site (40 patients) and the Baltimore site (77 patients) was used as an independent validation for our predictive models. The sample size was considered to be sufficient. That is, if the highest effect size of 0.31 (i.e., the correlation r: observed dimensional symptom scores vs. their out-of-sample predictions) which was identified in 10-fold cross-validation within the main sample could be replicated in the validation sample, the minimal sample size for detecting a significant correlation of 0.31 at an α-level of 0.05 (two-tailed) and a power of 80% would be 76 subjects. Our validation sample includes 117 subjects, which still has a power of 70% for detecting a statistical significance at the α-level of 0.05 (one-tailed) even at a lower effect size of 0.2. Therefore, the sample size of 117 was deemed sufficient for validation. Power analysis was performed using the G*Power software (https://www.psychologie.hhu.de/arbeitsgruppen/allgemeine-psychologie-und-arbeitspsychologie/gpower.html) (Faul et al., 2009).

Figure S1. Illustration of the robust four-dimensional representation of psychopathology identified in our prior machine-learning study (A) and the dimensional-scores estimated for the main (B) and the validation (C) samples investigated in the present study

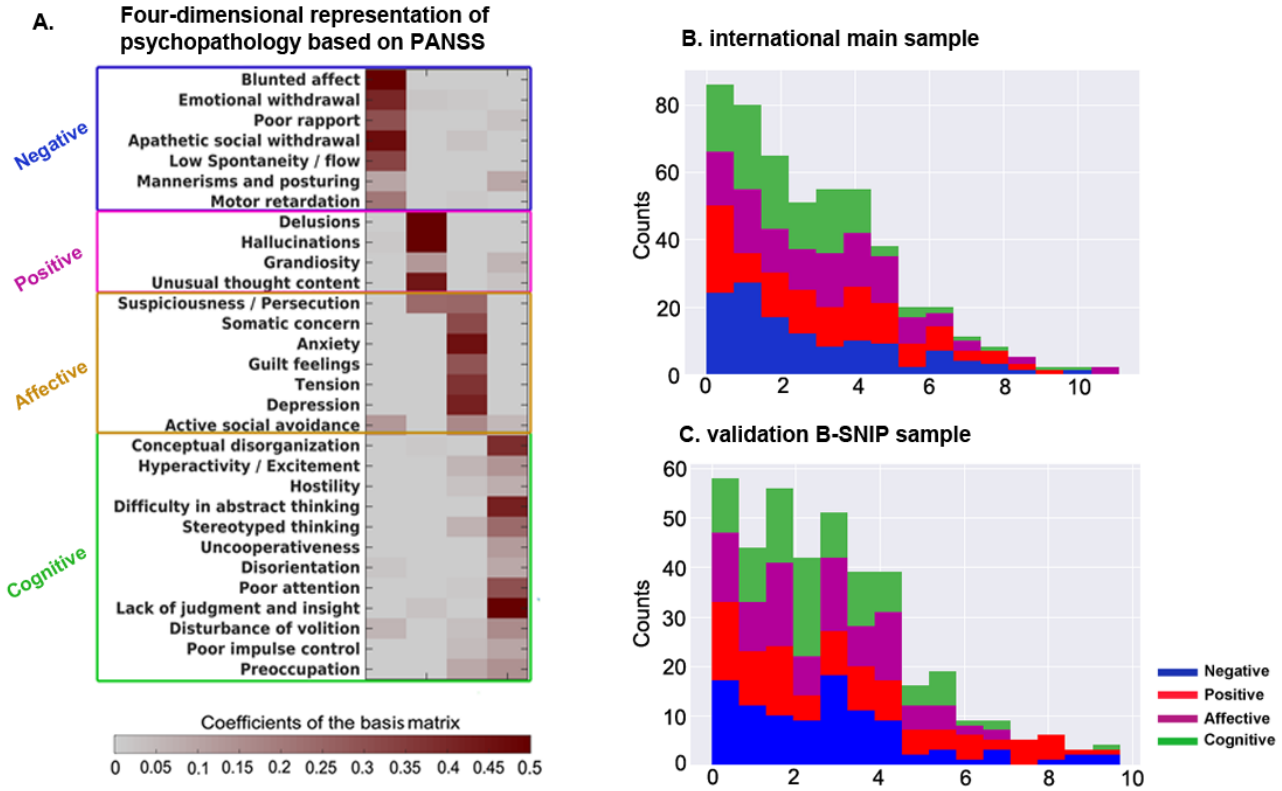

The four dimension model shown in the left panel was adapted from Figure 1 in (Chen et al., 2020) with permission under the CC BY-NC-ND license (http://creativecommons.org/licenses/by-nc-nd/4.0/). The sample used for creating the four dimension model is independent of the main and the validation samples analyzed in the present work. PANSS: Positive and Negative Syndrome Scale.

Table S1. Clinical characteristics of the main, international schizophrenia sample for each site

	Aachen-1	Aachen-2	Albuquerque (COBRE)	Göttingen	Groningen	Utrecht	Lille	Total	*P*-value[1]
N	13	10	47	32	22	10	13	147	
Illness duration	7.93± 8.52	13.11 ±10.93	16.66 ±12.21	7.03 ±7.59	7.64 ±7.23	8.5 ±7.23	12.38±6.06	11.23 ± 10.31	**<0.001**
Gender (Male/Female)	10/3	5/5	36/11	26/6	13/9	5/5	8/5	103/44	0.178
Age	35.07±11.15	34±9.77	37.72±13.9	32.28±9.94	34.05±12.83	33.3±8.69	32.77±8.45	34.77±14.71	0.537
Antipsychotic treatment									
Typical antipsychotics	0	0	4	0	1	1	1	7	
Atypical antipsychotics	13	10	41	26	19	4	10	123	
Both atypical and typical antipsychotics	0	0	2	5	0	0	1	8	
Missing/None	0	0	0	1	2	5	1	9	
olanzapine -equivalent[2]	21.72±10.05	18.92±12.87	14.84 ±10.96	25.06 ± 11.49	14.55 ± 8.31	17.10 ± 12.42	26.24±21.21	18.81 ± 11.60	**0.001**
Scores on the Four Dimensions of PANSS									
Negative	1.78±1.68	5.99±3.94	2.41±2.05	1.93±1.59	2.30±2.20	3.69±2.36	5.59±2.96	2.92±2.53	**<0.001**
Positive	2.99±2.23	4.47±2.97	2.99±2.03	1.61±1.54	4.27±2.32	4.91±1.44	6.45±2.12	3.41±2.44	**<0.001**
Affective	2.65±1.79	6.70±3.29	3.12±2.19	2.76±1.60	3.01±2.11	3.33±1.73	5.12±3.10	3.40±2.38	**<0.001**

Cognitive	1.35±1.26	5.91±2.61	2.12±1.22	2.10±1.35	2.29±1.84	2.69±1.43	5.90±2.30	2.67±2.08	**<0.001**
PANSS subscales									
Positive	15.36±6.70	17.11 ± 5.75	14.53 ± 5.07	11.72 ± 3.52	16.59 ± 5.18	17.2 ± 2.78	22.08±4.70	15.31 ± 5.52	**<0.001**
Negative	11.14±3.90	24.00±8.00	14.08±4.56	12.75±4.22	14.45±4.97	17.50±5.72	22.15±6.07	15.02±6.05	**<0.001**
General	25.29±6.71	49.44±13.09	28.34±8.48	27.56±5.88	29.55±8.56	30.50±8.95	44.15±14.35	30.90±10.98	**<0.001**
Symptom severity (Total score)	51.79±15.44	90.56±22.89	56.98±13.79	52.03±10.36	60.59±16.24	65.20±14.75	88.38±23.86	61.33±19.58	**<0.001**

Note: Data are mean ± SD. N: number of subjects per research site; PANSS, Positive and Negative Symptom Scale; [1]Statistical comparison between sites was conducted using either one-way analysis of variance (ANOVA) or chi-square test where appropriate. [2]Dosage in mg/day.

Table S2. Demographic and clinical characteristics of schizophrenia patients retrieved from the B-SNIP database

Characteristics	Hartford (N=40)	Baltimore (N=77)	*p*-value
Demographic			
Age (years)[a]	30.4 (10.98)	37.25 (12.641)	**0.004**
Gender (male/female)	29/11	56/21	0.979
Illness during (years)[b]	7.62 (7.98)	15.19 (11.77)	**0.001**
PANSS			
Positive[c]	15.03 (5.13)	14.69 (6.19)	0.768
Negative	14.78 (6.69)	15.40 (5.24)	0.578
General[d]	30.68 (8.39)	25.94 (6.12)	0.001
Illness severity (Total PANSS)[e]	60.48 (17.91)	56.03 (13.74)	0.138
Loadings on the dimensions of PANSS			
Negative	2.74 (2.58)	2.85 (2.05)	0.798
Positive	3.27 (2.47)	3.19 (2.58)	0.882
Affective	3.25 (1.70)	2.19 (1.61)	**0.001**
Cognitive	2.89 (1.93)	2.55 (1.65)	0.310

Note: Data are mean (SD). *p*-values in bold indicate a significance of $p < 0.05$. Except for gender, which was based on chi-square test, other statistics were based on two sample t-test.

After estimating subject-wise head movement and assessing T1-image segmentation, 16 patients in the main sample were found to have excessive head-motion and five patients were identified with poor tissue segmentation quality and hence these 21 patients were removed from the subsequent analyses. In the validation B-SNIP sample, one schizophrenia patient was excluded from the Hartford site due to an excessive head-motion, while 16 patients in the Baltimore site were excluded (15 patients had excessive head-motion and one patient was with bad tissue segmentation in the resulting *T1* partial volume image). After filtering out the in total 17 schizophrenia patients in B-SNIP, 39 patients in the Hartford site and 61 patients in the Baltimore site were retained for validation analysis. In the remaining patients, age did not correlate with any of the four symptom dimensions in the main (all *p*-values>0.25; Pearson correlation analysis) and the B-SNIP samples (all *p*-values>0.20). No gender differences were observed for the scores of the four symptom dimensions within the main sample (all *p*-values>0.09). While in the B-SNIP sample, male patients (2.43±1.67) showed significantly lower (p=0.018) affective dimensional-scores than female patients (3.31±1.69). Scores for the other three symptom dimensions did not show any gender differences within the B-SNIP sample. Age and gender were both adjusted in our predictive modeling to avoid (any) possible contributions from them.

6.2.2 Details for the density maps of receptors/transporters from prior molecular imaging studies

As detailed in our prior study (Dukart et al., 2018), the density estimates of gamma-aminobutyric acid (GABAa) and dopamine transporter (DAT) were obtained from flumazenil positron emission tomography (PET) and single photon emission tomography (SPECT), respectively. Here in brief:

DAT

Baseline DAT-SPECT data of 174 healthy elderly volunteers (mean age±SD: 61±11 years, 109 males) were extracted from the Parkinson's Progression Marker Initiative database (PPMI, www.ppmi-info.org/) (Marek et al., 2018). Written informed consent was obtained from all subjects. The study was approved by Institutional Review Boards/Independent Ethics Committees. A mean image was computed from the preprocessed data in MNI space with a Gaussian kernel of 8mm FWHM. DAT density estimates were extracted from this mean image. Of note, previous studies showed that in vivo DAT density in the brain assessed by SPECT declines with age (mostly linear) which is typically up to 10% per decade year for some regions (e.g., caudate and putamen) (roiano et al., 2010; Ishibashi et al., 2009; Shingai et al., 2014). However, that should be less of a concern with respect to our current network-based analysis relying on the relative ratio of regions to each other which is robust to age. This is because the expression of DAT in some specific brain regions e.g., the basal ganglia (and to some little extent the prefrontal cortex) is in very high amounts and hence the relative differences between these DAT-rich areas and other DAT-poverty brain regions (e.g., thalamus) (Shingai et al., 2014) are still fairly large. That is, these observation and relative order of brain regions with respect to each other remains stable throughout a healthy life span. Also, here we used Spearman's rank correlation which assesses monotonic relationships.

GABAa

Dynamic [11C]flumazenil PET scans were acquired from 6 healthy volunteers with full arterial blood sampling for quantitative compartmental modeling (Myers et al., 2012). PET images were reconstructed into 20 frames using filtered back projection. Voxel level spectral analysis (Cunningham and Jones, 1993) with 100 logarithmically distributed orthogonal basis functions between 0.0008 and 1 s-1 was performed to create parametric maps of total distribution volume (VT), with 2.09x2.09x2.42 mm resolution. These individual volumes of distribution maps calculated as the summed integral of the peaks after spectral analysis were used as individual GABAa density estimates and were then normalized to MNI space. This study was approved by a NHS Research Ethics Committee, the Administration of Radioactive Substances Advisory Committee and local NHS Research and Development.

D2/3 (https://datadryad.org/resource/doi:10.5061/dryad.rc073)

The radiotracer [11C]raclopride binding in striatal subregions, the thalamus and the cortex was investigated using the bolus-plus-infusion method and a high resolution PET (Alakurtti et al., 2015). Seven healthy male volunteers underwent two PET [11C]raclopride assessments, with a 5-week retest interval. Spatial resolution in the reconstructed PET images varies in radial and tangential directions from ~2.5 to 3 mm and in axial directions from 2.5 to 3.5 mm in the 10-cm field of view covering the brain. $D_{2/3}$ receptor density was quantified as binding potential using the simplified reference tissue mode tissue compartmental modeling (SRTM) (Lammertsma et al., 1996;

Innis et al., 2007). The cerebellum which is devoid of D2/3 receptors (Hall et al., 1998) was chosen as the reference tissue. For voxel-level model fitting, they used a linearized model using a basis-function approach (Gunn et al., 1997) implemented also in in-house software (http://www.turkupetcentre.net/programs/doc/imgbfbp.html). The absolute variability and intraclass correlation coefficient values demonstrated good test-retest reliability. We accessed to the baseline session and obtained the group average whole-brain map with voxel-wise D2/3 density estimates. The study protocol was approved by the Ethics Committee of the Hospital District of Southwestern Finland. Written consent was obtained from each volunteer.

D1

Thirteen healthy volunteers (7 female, age 33 ± 13 yrs) underwent 90-min emission scans, each after 90-s bolus injection of 486 ± 16 MBq [11C]SCH23390, on two separate days within 2-4 weeks using a PET/MRI system (Kaller et al., 2017). This study was approved by the local ethics committee (registration number 083/11) and the German Federal Office for Radiation Protection (number Z5-22461/2-2012-003). Informed consent was obtained from all participants. Motion correction was performed with Statistical Parametric Mapping (SPM8, Wellcome Department of Cognitive Neurology, London, UK). Individual MRI T1-weighted MPRAGE data sets and the related, already-fused PET data of each subject were spatially reoriented onto a standard brain data set similar to the Talairach space, reconstructing the images to 128×128×64 voxels with dimensions of 1.7×1.7×2.5 mm^3. Parametric images of binding potential (BPND) were generated in PMOD (version 3.5, PMOD Technologies, Zurich, Switzerland) from the PET data by the multi-linear reference tissue model with two parameters (MRTM2) and the cerebellar cortex as the receptor-free reference tissue (Ichise et al. 2003). The BPND maps were used in our present spatial correlation analysis as a reflection of D1 receptor density.

^{18}F-DOPA (https://www.nitrc.org/projects/spmtemplates/):

Participants‘ dopamine synthesis capacity was measured by using [18F]DOPA PET. The map we used for local DSC estimates was the 18F-DOPA template in SPM. Data acquisition and template construction were detailed in the original publication (Gómez et al., 2018) and briefly as follows: Brain PET images were acquired with 18F-DOPA to 12 control subjects (6 males and 6 women aged 55.1 ± 16.6 years) without evidence of nigrostriatal degeneration. PET experiments were performed on a CT scanner Siemens Biograph 16 PET/CT, which provides a 2.0 mm FWHM of the FOV. One hour before the injection of the established dose of 18F-DOPA, 150 mg of carbidopa was administered by oral to block the enzymatic activity of the DOPA decarboxylase. The PET images acquisition started 90 minutes after intravenous injection of the radiotracer using 222 MBq. The emission PET data were acquired for 20 minutes in 3D mode, after a brain CT scan in spiral mode at 120 kVp and 160 mA with the CARE program Dose 4D. The raw data were reconstructed using the OSEM algorithm with 4 iterations, 8 subsets, all-pass filter and a matrix resolution of 128 × 128. All images were transformed from DICOM format to NIfTI using the dcm2nii function in MRIcron (http://www.mccauslandcenter.sc.edu/mricro/mricron/). Then, the baseline PET scans were spatially normalized to a common anatomical space using a T1-weighted structural MRI template as reference in software SPM8 (SPM; Welcome Department of Cognitive Neurology. London, UK). To avoid the intrinsic asymmetries presented in the recruited sample, the left-right hemisphere flipped (i.e., mirrored) images of

the original PET scans for each of the 12 patients were obtained, resulting in total 24 brain PET images for subsequent template construction. Afterward, an intensity normalization procedure was performed on the PET images, which resulted in each voxel has a value between 0 and 1. For a precise alignment to the standardized anatomical space of MNI152 (MNI; http://www.bic.mni.mcgill.ca), the resultant maps were resampled with a bounding box of 90 × 109 × 91 and an isotropic voxel size of 2mm. Finally, the 24 PET images were averaged to form the template, and the value for each voxel in the template was the group mean intensity-normalized value with a Gaussian filter step applied. The authors declared that the procedures conformed to the ethical standards of the responsible human experimentation committee.

Serotonergic receptors and serotonin reuptake transporter

For the serotonergic system, including the three serotonin receptors of 5HT1a, 5HT1b, 5HT2a and serotonin reuptake transporter 5-HTT, the density estimates were derived from a multi-center PET study with different radiotracers (Savli et al., 2012). A total of 95 healthy subjects (mean age= 28.0±6.9 years, range= 18-54, 59% males) were included in this multicenter PET study to map the serotonergic receptors and transporter *in vivo*. All subjects were physically healthy and life-time naïve for psychotropic drugs. All participants gave written informed consent according to the procedures approved by the local Ethics Committees at the Medical University of Vienna, the Medical Faculty of the University of Düsseldorf and the Yale School of Medicine Human Investigation Committee.

For assessing ***5HT1a,*** the [carbonyl-^{11}C]WAY-100635 was used as the radioligand. PET scans were conducted with a GE Advance PET scanner (General Electric Medical Systems, Milwaukee, Wisconsin) with a spatial resolution of 4.36 mm full-width at half maximum (FWHM) at the center of the FOV (35 slices). Details in image acquisition and reconstruction are described elsewhere (Fink et al., 2009).

For ***5HT1b,*** [^{11}C]P943 PET scans were acquired for 120 min on an HRRT PET scanner (207 slices, resolution less than 3 mm full-width at half maximum in 3D acquisition mode). PET image acquisition and image reconstruction were performed as described previously (Gallezot et al., 2010).

For the ***5-HT2a*** receptor, a highly selective radioligand of [^{18}F]altanserin was used. PET measurements were performed in 3D mode on a Siemens ECAT EXACT HR+ scanner (Siemens-CTI, Knoxville, TN, USA; 63 slices; full-width of half maximum 5.8, 5.8, 6.6 mm (x, y, z) at 10 cm from the central axis). Tracer application according to a 2-min bolus plus constant infusion schedule (KBol= 2.1 h), venous blood sampling, metabolite correction of the plasma input function, PET image acquisition and reconstruction were conducted according to the previous publication (Hurlemann et al., 2008.

For *in vivo* quantification of ***5-HTT*** serotonin transporter, [11C]DASB is used as the radioligand which is high affinity and selectivity to 5-HTT. PET scans were obtained from a GE Advance PET scanner (General Electric Medical Systems, Milwaukee, Wisconsin) with a spatial resolution of 4.36 mm full-width at half maximum (FWHM) at the center of the FOV (35 slices).

Apart from the preprocessing of 5-HT2a scans which was performed at the Research Centre Jülich using SPM2 (Hurlemann et al., 2008), the raw PET scans for other receptors and the 5-HTT transporter were preprocessed using SPM8 (http://www.fil.ion.ucl.ac.uk/spm/software/spm8/) and the motion correction was carried

out by co-registration of each frame to the mean of the subjects' motion-free frames. Dynamic PET scans were normalized onto tracer-specific templates in MNI stereotactic space by computing the transformation matrices of individual PETADD (sum over all time frames) and subsequent application to dynamic scans. Ligand-specific templates were created following the approach introduced previously (Meyer et al., 1999) and provided mean values for each voxel. The original PET images were further spatially smoothed with an isotropic 8 mm Gaussian kernel. Finally, the quality of spatially normalized images was visually inspected where necessary.

The binding potential (Innis et al., 2007) was calculated using the kinetic modeling tool PKIN as implemented in PMOD (PMOD Technologies Ltd, Zürich, Switzerland) to denote receptor density. Cerebellum was used as the reference region. For the quantification of [carbonyl-11C] WAY-100635, [11C]P943 and [11C]DASB binding, the —multilinear reference tissue model" (MRTM/MRTM2) was used as described previously (Ichise et al. 2003) to calculate the BP_{ND}, while the [18F]altanserin scans were parameterized on the basis of the cerebellum ($C_{Reference}$) and the plasma activity concentration attributable to parent compound (C_{Plasma}) using the following equation: $BP_P=(C_{ROI}-C_{Reference})/C_{Plasma}$ with radioactivity concentrations averaged from 120 to 180 min p.i. (Pinborg et al., 2003). [18F]altanserin binding potentials were then read out from parameterized maps.

Overall, for comparability, the maps of density estimates obtained from aforementioned multi-tracer molecular imaging studies, in MNI152 space, were linearly rescaled to a minimum of 0 and a maximum of 100 and were resampled to an isotropic 2mm spatial resolution (original resolutions: 1.7-6.6mm) as in our fMRI data. The closest between-node distance within the two robustly predictive networks, theory-of-mind and extended socio-affective default, is 12mm, and thus the nodal density estimates for the investigated receptors/transporters were differentiable in the molecular data.

6.2.3 Assessing statistical significance for spatial correlation analysis

We implemented a spatial permutation testing to assess the statistical significance for the spatial correlation between network nodes and receptor/transporter densities calculated for these nodes. That is, we generated 1000 random networks by re-distributing the nodes throughout the grey matter with the same number of nodes as in real network while preserving the between-node distance (±6mm tolerance). Nodal receptor/transporter densities were extracted from these simulated (random) networks which were then correlated with the node importance scores for the real network. This allowed us to construct a null with 1000 (chance-level) correlations based on a set of randomized topographic configuration of networks. Finally, the true correlation based on the nodal receptor/transporter densities extracted from the real network was compared with the null distribution to derive the significance (lowest p=0.001). If the true correlation obtained from the real network exceeds the 95% percentile of the null, indicating a statistical significance for the true correlation against a (pseudo)-random placement of nodes within the grey matter.

Several metrics were additionally employed to assess the property of the generated random networks, including:

1) between-node distances within each random network;

2) distance between the nodes of random networks;

3) distance between the nodes of the original (real) and the random networks.

Metrics 2) and 3) allowed to check if the random networks are adequately different from each other and from the real network.

As shown in Figure S3, the histograms demonstrated that our simulated random networks well reflected the possible spatial configurations within the grey matter of the entire brain, as these random networks were sufficiently different from, but neither too far or too close to, each other and the two real networks.

Table S3. Meta-analytic functional brain networks, domains and their implications in schizophrenia

	Description of meta-networks			
Domain Network (Abbr.)	**Linked processes**	**Experiments/tasks/contrasts for deriving the networks**	**Number of nodes**	**Source publication**
Affective				
Emotional scene and face processing(EmoSF)	Perception of emotional scenes and faces	Discrimination of emotional faces and scenes from neutral	24	Sabatinelli, (2012)
Reward-related decision making (Rew)	Reward value-based preferences for possible options, selecting and executing actions, and evaluating the outcome	Convergence across reward valence and decision stages	23	Liu *et al.* (2011)
Cognitive emotion regulation (CER)	Reappraisal of emotional stimulus	Reappraise > naturalistic emotional responses	14	Buhle *et al.* (2014)
Social				
Empathy	conscious and isomorphic experience of somebody else's affective state	"feel into" affect-laden social situations > watched or listened passively	22	Bzdok (2012)
Mirror neuron system (MNS)	mental imitation (i.e., "mirroring') of others' nonverbal expression (e.g., actions and behavior)	Action observation ∩ action imitation	11	Caspers *et al.* (2010)
Theory-of-mind (ToM)	the cognitive ability of an individual to 'infer the mental states of others'	ToM > non-social baseline	15	Bzdok *et al.* (2012)
Task-deactivation and interacting				
Extend socio-affective default (eSAD)	A general default mode of socio-affective processing	Regions within the DMN that are consistently found to relate with socio-affective processing[a], together with their intimately coupled regions identified by MACM and ALE	12	Amft *et al.* (2013)
Default mode network (DMN)	Active at rest or during passive rest and mind-wandering that relates to a variety of functions including self-reference, autobiographical	Contrasts that were coded as a Deactivation (e.g., Control - Task) using a Low-Level Control (strictly defined as either resting or fixation conditions) across a wide range of paradigms (i.e., task-independent deactivations)	9	Laird *et al.* (2009)

	information, theory-of-mind and episodic memory.			
Executive				
Vigilant attention (VigAtt)	Maintaining stable and focused attention	Tasks posing only minimal cognitive demands on the selectivity and executive aspects of attention for more than 10s	16	Langner, (2012)
Cognitive action control (CogAC)	Supervisory control for the suppression of a routine action in favor of another, non-routine one	ALE coordinate-based meta-analysis on stroop-task, spatial interference task, stop-signal task and go/no-go tasks	19	Cieslik *et al.* (2011)
Extend multi-demand network (eMDN)	Performance of executive functioning across multiple demands	Using regions of the MDN[b] as seeds for whole-brain resting-state and MACM analyses. The eMDN was then delineated by identifying regions in which the consensus connectivity maps of at least half of the seeds overlapped	17	Camilleri *et al.* (2014)
Working memory (WM)	A limited resource that is distributed flexibly among all items to be maintained in memory	Consistently activated during all WM contrasts/experiments (mainly n-back, Stenberg, DMTS, delayed simple matching)	22	Rottschy, (2012)
Long-term memory and language				
Semantic memory (SM)	The long term storage of personally relevant semantic knowledge, independent of recalling a specific experience	Activated during SM contrasts: experiments mainly comprising paradigms: words vs. pseudo words, semantic vs. phonological task, high vs. low meaningfulness	23	Binder, (2009)
Speech production (SP)	The process by which thoughts are translated into speech, involving the integration of auditory, somatosensory, and motor information	Studies contrasted speech production (including phonemes, syllables, words, sentences or narratives) with a condition in which no speech was produced	13	Adank, (2012)
Autobiographic Memory (AM)	Long-term memory for personal experiences and personal knowledge of an individual's life	Tasks referring to autobiographical recall: episodic recollection of personal events from one‘s own life	23	Spreng, (2008)
Sensory-motor				

Motor	Motor execution	Finger tapping > baseline; excl. regions associated with visually paced finger-tapping tasks	10	Witt *et al.* (2008)
Auditory	Auditory sensory processing	Purely auditory tasks using highly controlled synthesized acoustic stimuli	11	Petacchi *et al.* (2005)

[a]Details on the Identification of DMN regions involved in socio-affective processing can be found at (Schilbach et al., 2012); [b]the MDN network was derived from a conjunction across three neuroimaging meta-analyses on working memory, vigilant attention, and inhibitory control using coordinate-based ALE (Müller et al., 2015). ALE: activation likelihood estimation; MACM: meta-analytic connectivity modeling.

Table S4. Functional MRI scanning parameters for each site in B-SNIP

Site	Scanner Type	Magnetic Field	TR (ms)	TE (ms)	FA (°)	No. Slices	Voxel-size (mm^3)	Orientation	Scan Duration (s)
The validation B-SNIP sample									
Hartford	Siemens Allegra	3.0T	1500	27	70	29	3.4x3.4x5	Axial	315
Baltimore	Siemens Triotim	3.0T	2210	30	70	36	3.4x3.4x3	Axial	309.4

Note: TR: repetition time, TE: echo time, FA: flip angle; [1]PRESTO-SENSE sequence combining a 3D-PRESTO pulse sequence with parallel imaging in 2 directions (8-channel SENSE head-coil) which achieved full brain coverage within 609 ms for the Utrecht site and within 1001 ms for the Lille site.

Table S5. T1-weighted structural MRI scanning parameters for each site in B-SNIP

Site	Scanner Type	Magnetic Field	TR (ms)	TE (ms)	FA (°)	No. Slices	Voxel-size (mm^3)
The validation B-SNIP sample							
Hartford	Siemens Allegra	3.0T	2300	2.91	9	160	1 x 1x1.2
Baltimore	Siemens Triotim	3.0T	2300	2.91	9	160	1 x 1x1.2

Note: TR: repetition time, TE: echo time, FA: flip angle; [1]a multi-echo MPRAGE (MEMPR) sequence with 5 TEs; [2]PRESTO-SENSE sequence.

Table S6. Reliably relevant connections for the ToM and the eSAD networks in the prediction of the cognitive dimension

Network	Connection
ToM	vmPFC<->PCC/PrC; vmPFC<->right pSTS; PCC/PrC<->left MTG; right TPJ<->dmPFC; left MTG<-> left aMTG; left MTG<->right IFG; RMTG<-> left lFG; right MTG<-> right aMTG
eSAD	ACC<-> right Amy; SGC<->PCC/PrC; SGC<->dmPFC; PCC<-> left aMTG; PCC<->vmPFC; dmPFC<->right vBG; dmPFC<-> left Amy; vmPFC<->RTPJ; left vBG<-> left Amy; right Amy<-> left Amy

Abbreviations: ToM, theory-of-mind; eSAD, extended socio-affective default. Amy, amygdala; Hipp, hippocampus; vmPFC, ventro-medial prefrontal cortex; dmPFC, dorso-medial prefrontal cortex; dmPFG, dorso-medial prefrontal cortex; aMTG, anterior middle temporal gyrus, IFG, inferior frontal gyrus; TPJ, temporo-parietal junction, PCC, posterior cingulated cortex, PrC, precuneus; SGC, subgenual cingulate cortex, vBG, ventral basal ganglia; ACC, anterior cingulated cortex.

Table S7. Coordinates and brain locations of the nodes connected by reliably predictive connections within the identified robustly predictive networks

Network	MNI coordinates			Macroanatomy of nodes	Macroanatomy of the connected nodes
	x	y	z		
ToM					
	0	52	-12	vmPFC	PrC; right pSTS
	2	-56	30	PCC/PrC	vmPFC; left MTG
	50	-34	0	pSTS	vmPFC
	56	-50	18	TPJ	dmPFC
	-8	56	30	dmPFC	Right TPJ
	-54	-28	-4	MTG	PrC; left aMTG; right IFG
	52	-18	-12	MTG	left IFG; right aMTG
	54	-2	-20	aMTG	right MTG
	-54	-2	-24	aMTG	left MTG
	-48	30	-12	IFG	right MTG
	54	28	6	IFG	left MTG
eSAD					
	0	38	10	ACC	right Amy/Hipp
	-2	32	-8	SGC	PCC/PrC; dmPFC
	-2	-52	26	PCC/PrC	SGC; left aMTG; vmPFC
	-2	52	14	dmPFC	SGC; right vBG; left Amy/Hipp
	-54	-10	-20	aMTG	PCC/PrC
	-2	50	-10	vmPFC	PCC/PrC; right TPJ
	6	10	-8	vBG	dmPFC
	-6	10	-8	vBG	left Amy/Hipp
	-24	-10	-20	Amy/Hipp	left vBG; dmPFC; right Amy/Hipp
	24	-8	-22	Amy/Hipp	left Amy/Hipp
	50	-60	18	TPJ	vmPFC

Note: Coordinate (x, y, z) of each node is reported in standard space of the Montreal Neurological Institute (MNI) as demonstrated in the source publications of the two identified functional networks. Nodes that were spatially overlapping between the subnetworks of ToM and eSAD are highlighted in red.

Abbreviations: ToM, theory-of-mind; eSAD, extended socio-affective default; Amy, amygdala; Hipp, hippocampus; vmPFC, ventro-medial prefrontal cortex; dmPFC, dorso-medial prefrontal cortex; dmPFG, dorso-medial prefrontal cortex; aMTG, anterior middle temporal gyrus, IFG, inferior frontal gyrus; TPJ, temporo-parietal junction, PCC, posterior cingulated cortex, PrC, precuneus; SGC, subgenual cingulate cortex, vBG, ventral basal ganglia; ACC, anterior cingulated cortex.

Table S8. Node importance for the ToM and the eSAD networks

Network	Node	Importance score
ToM	vmPFC	4.20
	mFG	3.39
	dmPFC	3.33
	PCC/PrC	4.24
	Right TPJ	2.83
	Left TPJ	3.67
	Right aMTG	3.89
	Left aMTG	4.81
	rMTG	4.58
	lMTG	4.87
	Right pSTS	3.11
	lpSTS	2.82
	rIFG	3.07
	lIFG	4.07
	rV5	3.15
eSAD	ACC	3.21
	SGC	4.14
	PCC	4.59
	dmPFC	4.05
	rTPJ	1.96
	lTPJ	2.56
	lvBG	4.40
	rvBG	3.50
	Left aMTG	2.85
	Right Amy	4.27
	Left Amy	3.98
	vmPFC	4.21

Abbreviations: ToM, theory-of-mind; eSAD, extended socio-affective default. Amy, amygdala; Hipp, hippocampus; vmPFC, ventro-medial prefrontal cortex; dmPFC, dorso-medial prefrontal cortex; dmPFG, dorso-medial prefrontal cortex; aMTG, anterior middle temporal gyrus, IFG, inferior frontal gyrus; TPJ, temporo-parietal junction, PCC, posterior cingulated cortex, PrC, precuneus; SGC, subgenual cingulate cortex, vBG, ventral basal ganglia; ACC, anterior cingulated cortex.

Figure S2. Multivariable prediction of the original three PANSS subscales from the resting-state functional connectivity within each of the 17 functional networks using the same validation procedure as we have done for the four symptom dimensions

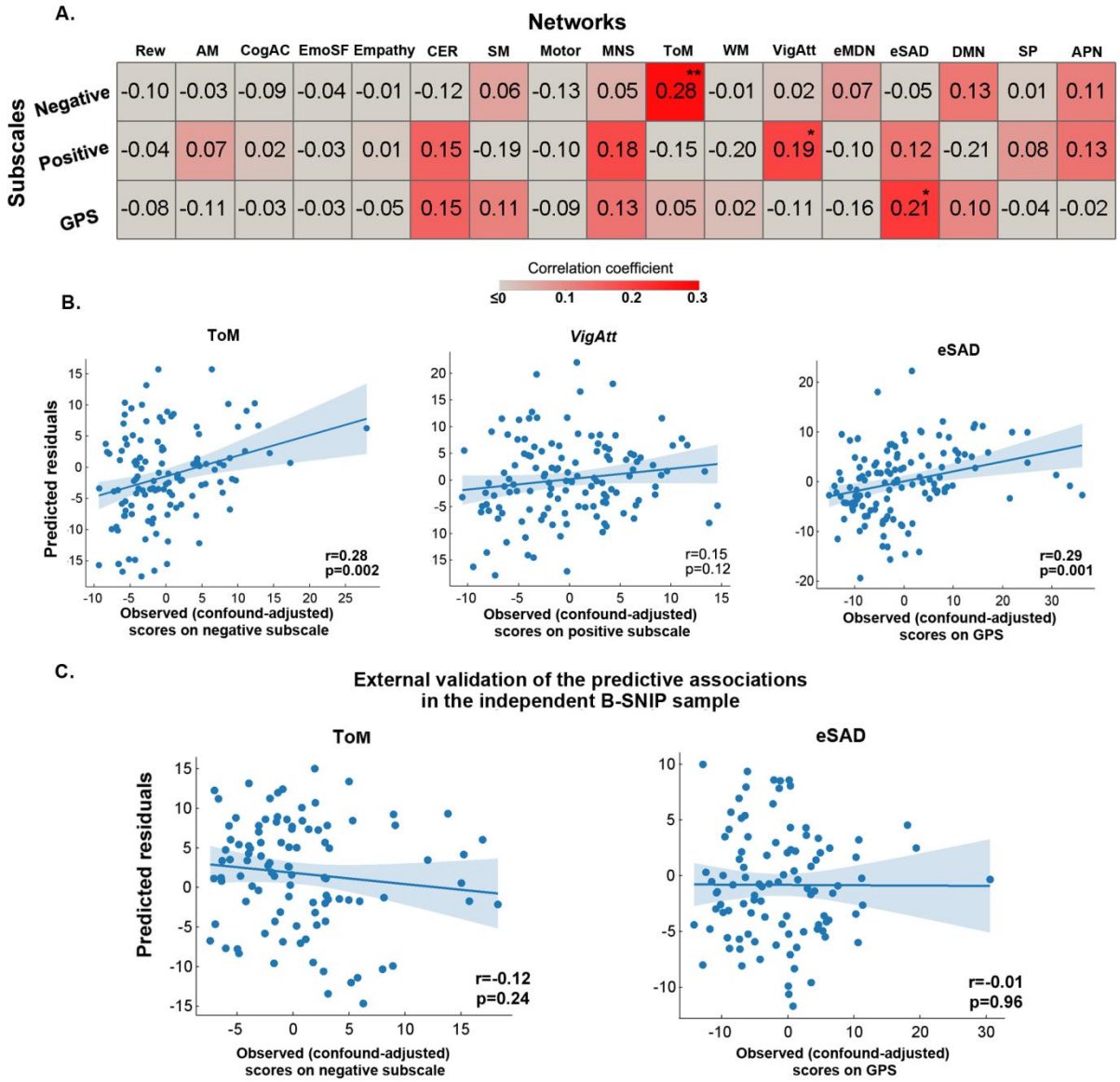

A) Tile plot shows the 10-fold cross-validation results for the main sample in the prediction of the three PANSS subscales. *p<0.05, **p<0.01, identified through 1000 permutation tests.

B) Scatter plots show the leave-one-site-out cross-validation results for the three significant predictions identified in 500x repeated 10-fold cross-validation in the main sample. Except for the prediction of the positive subscale from the rs-FC within the vigilant attention network, other two predictions were both confirmed by leave-one-site-out cross-validation with significant correlations observed.

C) Scatter plot show that neither of the two tested predictive patterns was significant in the B-SNIP sample.

Abbreviations: EmoSF, emotional scene and face processing; Rew, reward-related decision making; CER, cognitive emotion regulation; ToM, theory-of-mind; MNS, minor neuron system; DMN, default mode network; eSAD, extended socio-affective default; VigAtt, vigilant attention; CogAC, cognitive action control; eMDN, the extended multi-demand networks; SM, semantic memory; SP, speech production; WM, working memory; AM, autobiographical memory; APN, auditory processing network. GPS: general psychopathology subscale.

Figure S3. Histograms of the three metrics assessing the property of random networks

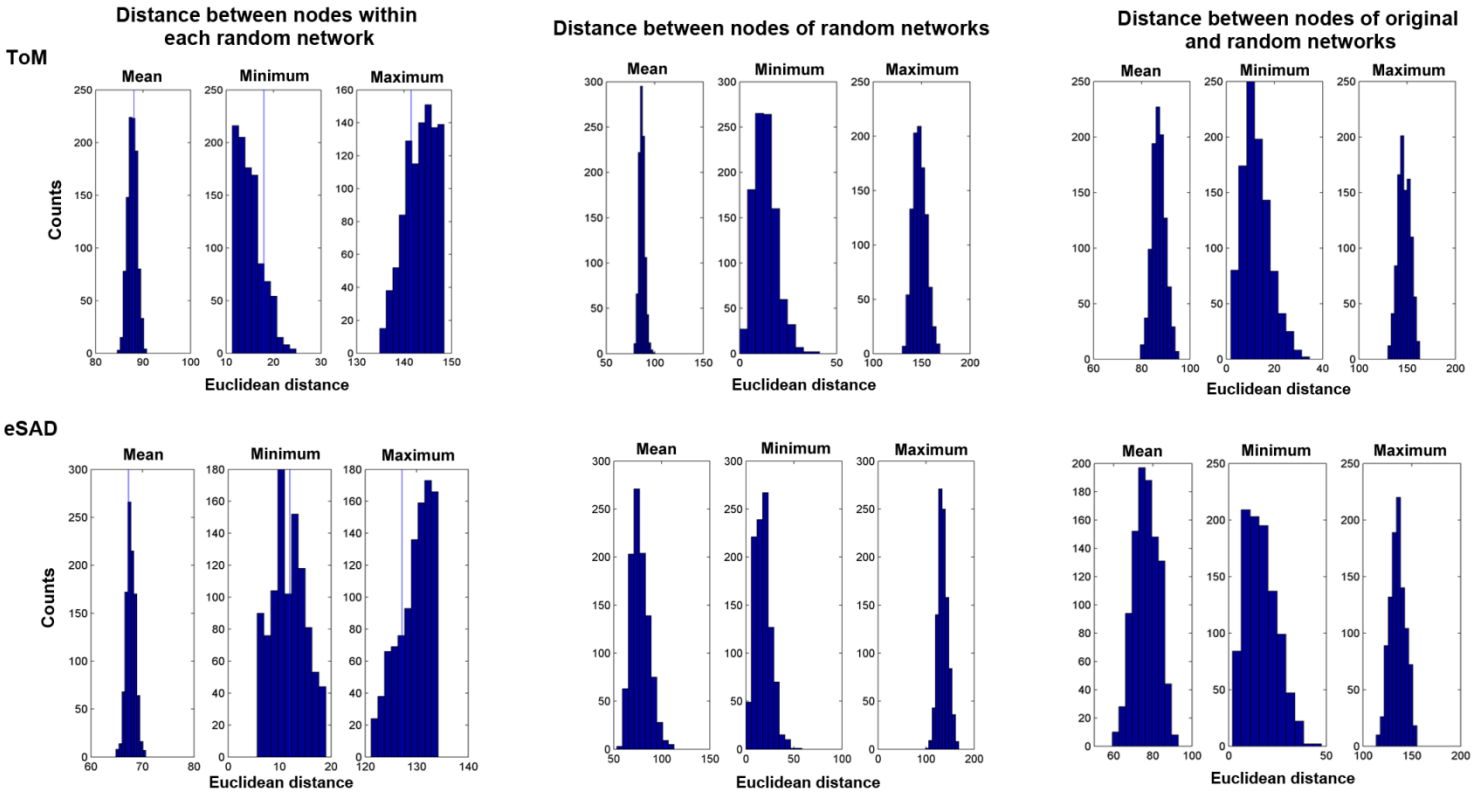

Abbreviations: ToM, theory-of-mind; eSAD, extended socio-affective default

Figure S4. Reliably relevant connections for the ToM network in the prediction of the negative dimension and the two subnetworks within ToM

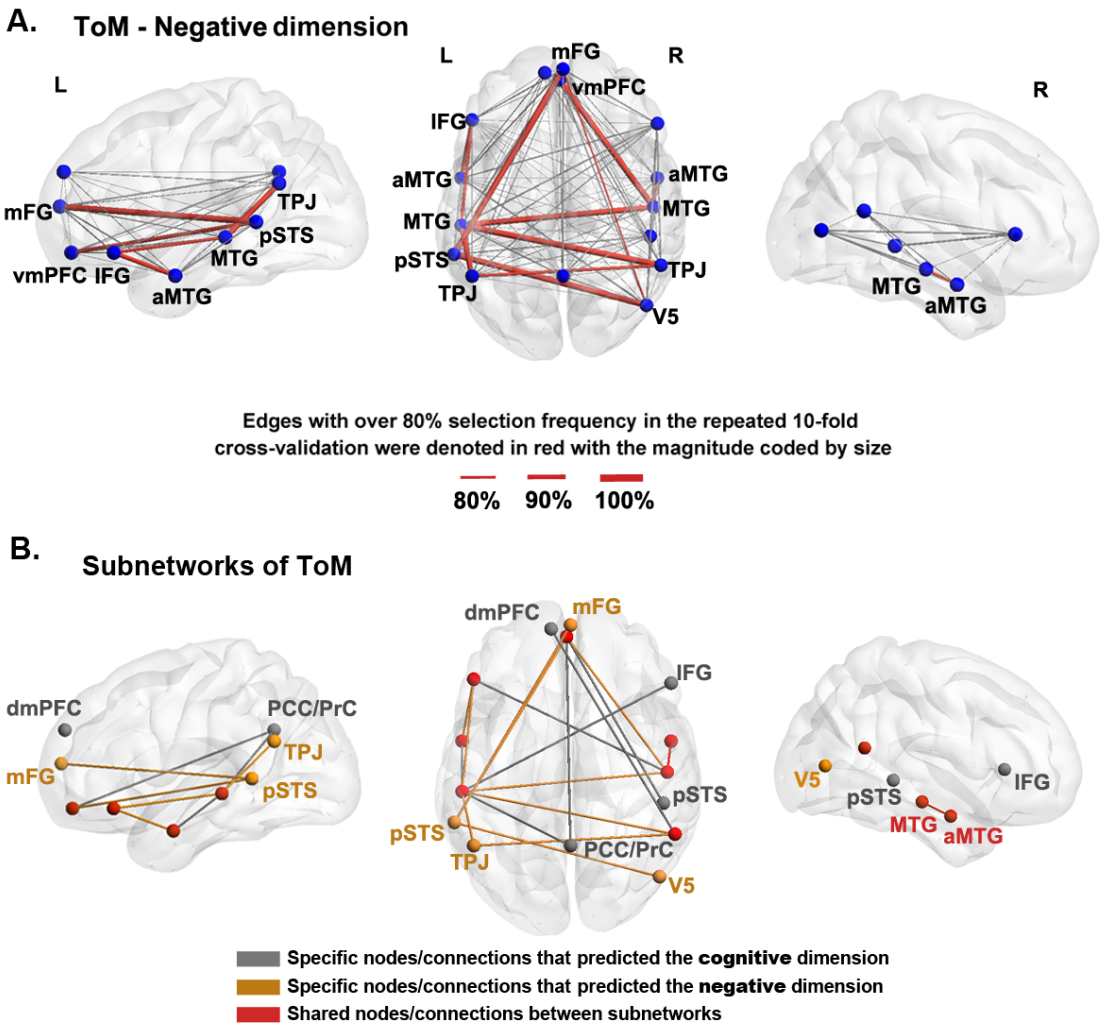

A) Reliably relevant connections selected by 10-fold process on main sample in the prediction of negative dimension. The reliably relevant edges are colored in red and the selection frequency for these edges was coded by line size. Other connections within each of the networks are shown in light grey. These connections were all reliably selected in both the seven leave-one-site-out experiments and the models trained within the entire main sample for validation in B-SNIP.

B) Subnetworks of ToM which predicted the cognitive or the negative dimension of psychopathology. Their shared nodes and connections were shown in red color.

7. Discussion

My Ph.D work provided a novel conceptualization of schizophrenia psychopathology from symptomatology to neurobiology by applying advanced machine-learning approaches and sophisticated cross-validation and out-of-sample generalization assessments to aggregately over 2000 patients recruited from 15 medical centers. A four-dimensional representation of schizophrenia symptomatology comprising negative, positive, affective, and cognitive dimensions was proposed. Along these new axes of psychopathology, two symptomatically well-separated core subtypes representing prominent negative and positive symptomatology of schizophrenia were identified. This positive-negative dichotomy was longitudinally stable and could be moreover discriminated from resting-state functional connectivity (rsFC) profiles of the ventromedial frontal cortex, temporoparietal junction, and precuneus, with a highest classification accuracy of 70%. Moreover, individual expressions of the cognitive symptom dimension were significantly and robustly predicted by rsFC within the theory-of-mind and the extended socio-affective default (eSAD) networks. These two networks are implicated in social and affective processes. Finally, node importance of the identified networks in predicting the cognitive dimension showed a spatial pattern significantly and positively co-varying with D_1 dopamine receptor and serotonin reuptake transporter densities as well as presynaptic dopamine capacity.

7.1 A hybrid dimensional-categorical framework of schizophrenia symptomatology

As discussed in the *"Biological Psychiatry"* paper, our four dimensional-representation of schizophrenia symptomatology showed higher stability, generalizability, and internal consistency than the original three PANSS subscales and previously proposed PCA and EFA models with factor numbers from four to seven. Importantly, the factor-model we identified can be readily applied to new samples that people could project individual PANSS single-item scores onto this four-dimensional structure to obtain dimensional scores for their patient cohorts in future studies. For the convenience of interested researchers, we have set up an online tool (http://webtools.inm7.de/sczDCTS/). With this online tool, users could handily obtain the dimensional scores by simply uploading an excel file with item-wise PANSS scores arranged in a form as instructed on the website. Furthermore, I not only assessed the robustness, stability, and generalizability of the dimensions, but also the stability and robustness of the estimation of dimensional-scores for novel patients.

Probably the most interesting point, that is to compare our four-factor model which represents negative, positive, affective, and cognitive symptom dimensions with the models consisting of five dimensions that have been commonly proposed in previous factorial studies (Kim et al., 2012; Levine et al., 2007; Wallwork et al., 2012; van der Gaag et al., 2006a). Basically, a model with five factors was continuously failed to be confirmed in independent samples (White et al., 1997; van der Gaag et al., 2006a; Lehoux et al., 2009; Jiang et al., 2013). Please refer to the "Discussion" section of the *"Biological Psychiatry"* paper for details. Another interesting point worth mention but has not been detailed in the *"Biological Psychiatry"* paper, is the cross-loadings of some PANSS items displayed in the OPNMF four-factor structure. Although OPNMF generates sparse solutions that the yielded factor structure is almost clustering like, there are still some items loaded on multiple dimensions. For example, the item G16 ("active social avoidance") had almost equally high coefficients on both the negative and the affective

dimensions, while the item G5 (~~"~~mannerisms and posturing") shared the negative and the cognitive dimensions. These observations were in line with previous studies that G16 loaded highest on either of the negative and the affective dimensions and had a secondary loading on another (van der Gaag et a., 2006b). This might owe to the fact that symptoms assessed by item G16 have a complex causation (e.g., lacking of initiative and interest, and/or having negative emotionality). The item G5 has also been assigned to either the cognitive (van der Gaag et al., 2006b) or the negative dimension (White et al., 1997) in literature. Taken together, the cross-loadings of the G16 and the G5 items still presented even when a sparse learning method was used. Hence, our OPNMF four-factor model possibly reflects the causative complexity of schizophrenia symptomatology. Some previous studies have excluded several PANSS items which demonstrated ambiguous or unstable factor-assignment to improve the goodness-of-fit in their final models; however, the excluded items could also reflect specific and important aspects of schizophrenia symptomatology. Removing these items cause the model to fail to capture this part of the variation across individual patients.

I moreover used the new four dimensions of schizophrenia symptomatology to identify subtypes where patients showed a distinct expression pattern of these dimensions. However, previous investigations on schizophrenia symptom dimensions and subtypes were mostly performed in separate studies. Given the consideration that sub-typing, apart from the identification of symptom dimensions, also serves as an important facet capturing the symptomatic heterogeneity within schizophrenia, an integrative investigation of dimensions and subtypes would complement each other to better disentangle the heterogeneity. Also, the identification of reliable schizophrenia subtypes would be largely helpful for the development of more-specifically target treatments on patients with specific symptom profiles. In my Ph.D study, two core subtypes were identified using fuzzy-clustering after filtering out those patients with an ambiguous subtype-membership. The core subtypes should represent the well-defined ends of a spectrum while the ambiguous cases would reflect the intermediate levels of a smooth trend expressed on the continuous dimensional axes. To my best knowledge, there is only one prior attempt to use both categorical and dimensional approaches to characterize the symptoms in schizophrenia (Ahmed et al., 2015).

On the other hand, here I only confirmed the widely-supported positive-negative dichotomy (Kay and Singh 1989; Peralta et al., 1995) as the stable and robust subtypes in schizophrenia. More subtypes have been proposed, but the number and the definition of the yielded subtypes were variable across studies (i.e., poor replicability) (Dollfus et al., 1996; Lykouras et al., 2001; Dickinson et al., 2017; Bartko et al., 1981; Helmes and Landmark, 2003). This might because prior work mostly assessed small and geographically restricted samples using single clustering strategy but lacking an evaluation of stability. The present study, which particularly focused on stability and robustness and used a fairly heterogeneous dataset with respect to patient recruitment criteria (e.g., DSM-IV, DSM-IV-TR, and DSM-5), clinical states of the patients (e.g., in-patients vs. out-patients), study designs, populations, and medical systems, did not support a more fine-grained differentiation among the patients.

7.2 Neurobiological substrates of the new symptom dimensions and subtypes

I furthermore characterized the dimensional-categorical framework of schizophrenia symptomatology from brain intrinsic functional connectivity pattern and molecular architecture. Specifically, classification analysis based on regional rsFC patterns revealed robust neurobiological differentiations of the positive and negative core subtypes of schizophrenia. Network rsFC-based predictive modeling linked the cognitive symptom dimension to socio-affective processing and moreover the dopaminergic and the serotoninergic neurotransmitter systems.

Functional MRI studies targeting neurobiological differences between schizophrenia subgroups are still few. Prior attempts were limited by the utilization of univariate statistical approaches which yielded inconsistent or even contradictory results (Zhang et al., 2014; Meda et al., 2016; Nenadic et al., 2015). Consequently, the question of whether functional brain parameters could serve as a biomarker differentiating patients with distinct symptom profiles remains open. In contrast to previous studies, my Ph.D work serves as the first practice of applying multivariable classification analysis to identify neurobiologically differentiable rsFC patterns for schizophrenia symptomatically distinct subtypes. As assessed through cross-validation, the yielded classifier demonstrated a good performance in differentiating the subtype memberships for novel patients. Moreover, the results revealed that rs-FC profiles of temporo-parietal junction (TPJ), ventro-medial prefrontal cortex (vmPFC), and posterior cingulate cortex (PCC)/precuneus were most classifiable. These top classifiable regions all have been implicated in processes that are related to psychopathological distinction. Here I provided the details which have not been included in the —Biological Psychiatry" paper due to word limits: *i)* the TPJ has been implicated in core positive symptoms of auditory-verbal hallucination (Vercammen et al., 2012; Mondino et al., 2016) and also in the processes of social cognition including theory-of-mind (Döhnel et al., 2012). The later is in itself a negative symptom but could also be related to positive symptoms under hypermentalization (Frith, 2004); *ii)* Structural deficits in vmPFC were only detected in the negative subgroup of schizophrenia but neither the positive nor the disorganized subgroups when compared with healthy subjects (Zhang et al., 2014; Nenadic et al., 2015). Cortical thickness in this region was moreover found to co-vary with negative symptom severity in schizophrenia patients (Walton et al., 2017); *iii)* abnormalities in PCC and precuneus have been closely related with the severity of negative symptoms in schizophrenia (Lee et al., 2011; Shaffer et al., 2015).

Discussions on the relationship between social and affective processes and the predicted cognitive dimension by rsFC within the theory-of-mind and the eSAD networks have been elaborated in the —Discussion" section of my second Ph.D paper. Importantly, the meta-analytically defined task-activation networks employed in the present work comprise regions consistently activated by particular tasks that are functionally convergent in specific processes across a set of task-fMRI studies (Laird et al., 2009, Eickhoff et al., 2012). Predictive modeling based on intrinsic connectivity patterns within these networks is hence able to inform the associated functional processes and systems of the predicted symptom dimensions. Together with the strict validation procedure implemented, a robust link between schizophrenia cognitive dimension and socio-affective processes was revealed, and the networks-symptom association moreover showed a good out-of-sample generalization performance.

One may concern the prediction accuracy reported in the present work, that the effect sizes for the correlation between the observed values and their out-of-sample predictions were moderate. This might because I restricted the feature space to within-network rs-FC in predictive modeling to improve the functional specificity and

interpretability and hence in my Ph.D work I did not rely on the whole-brain connectome as in previous studies (e.g., Lei et al., 2019; Huang et al., 2018; Orban et al., 2017). Although whole-brain connectome may include more features that are predictive of symptoms than single networks, the feature/sample ratio will become very high when using the whole-brain connectome as features leading to curse of dimensionality which affects all standard machine learning algorithms (Friedman, Hastie and Tibshirani 2017). Therefore, the inclusion of more features needs larger samples; while it is necessary to perform a careful feature reduction in the case of limited samples, the restriction to network-connectivity as we implemented here should have effectively addressed the issue of high feature/sample ratio. Intriguingly, despite the clinical complexity of schizophrenia patient cohorts across sites and the differences in scanners and MRI scanning protocols, the effect size we revealed is similar to those reported for predicting, e.g., creativity (Beaty et al., 2018), personality (Nostro et al., 2018), and memory performance (Persson et al, 2018), from resting-state data in healthy subjects (*r*-values mostly around 0.2-0.35). Similar concerns may rise with regard to the top accuracy of 70% in classifying the two core subtypes. However, we would demonstrate this accuracy as fairly desirable, that previous image-based classification experiments in discriminating schizophrenia patients from healthy controls using multi-site samples reported percent accuracies mostly in 70s / low 80s (Mikolas et al., 2016; Rozycki et al., 2017; Orban et al., 2017; Mikolas et al., 2017; Yan et al., 2017).

Cognitive deficits are a core feature of schizophrenia, which occur in the prodrome and present throughout the illness (reviewed in Cannon et al., 2015). However, including the mainstay antidopaminergic agents, few pharmacological treatments could effectively ameliorate the cognitive symptoms in schizophrenia, (Miyamoto et al., 2005; Arnsten et al., 2017). According to the previously proposed neuroconnectivity-neurotransmission coupling rationale (Stagg et al., 2014; Kringelbach et al., 2020), I came up with the idea that the identification of connectivity patterns within specific functional networks that are robustly associated with schizophrenia symptomatology may in turn allow to uncover the distribution of specific receptor/transporter systems (i.e., molecular architecture) that are related to the identified networks. Besides the commonly proposed D_1 dopaminergic hypofunctioning in the involvement of schizophrenia cognitive symptomatology (McClure et al., 2010; Arnsten et al., 2017; Howes and Kapur, 2009), our results revealed that the spatial distribution of 5-HTT serotonin transporter was correlated with the eSAD network and the node importance of the eSAD network in predicting the cognitive dimension was moreover co-varying positively with the 5-HTT density. The extension of previous regional findings in molecular imaging studies (e.g., Abi-Dargham et al., 2002; Okubo et al., 1997; Ngan et al., 2000) to the current network-level analysis of receptor/transporter systems is important, as network dysconnection has been proposed as an important pathophysiological component that underlies schizophrenia symptomatology (Pettersson-Yeo et al., 2011; Uhlhaas, 2013; Dong et al., 2018) and network-based analyses are moreover suggested to be helpful for understanding the mechanisms of action of anti-psychotic drugs (De Rossi et al., 2015).

Overall, the present work provided an integrative receptor-connectivity-symptom link in schizophrenia, starting from factorization of the PANSS. Apart from the yielded new insights into the involvement of socio-affective processes, as well as the dopaminergic and the serotoninergic neurotransmitter systems in the cognitive dimension of schizophrenia, the analyses performed on the brain data in turn added validity to the usefulness of my novel, four-dimensional presentation of psychopathology.

8. Considerations and future directions

First, medication effects on brain data have long been a topic of discussion in schizophrenia studies. This is because most patients, when recruited for specific research aims, have been medicated or are still on pharmacological treatments with different kinds of anti-psychotics. Current atypical anti-psychotics act upon anti-psychotic effects by regulating mainly the dopaminergic and also the serotoninergic systems (Mauri et al., 2014). Regulated neurotransmission would lead to alterations in neural activation and functional connectivity (Landek-Salgado et al., 2016; Limongi et al., 2020). Anti-psychotics have also been shown to alter regional grey matter volumes (Scherk and Falkai, 2006; Emsley et al., 2017), especially in the striatum (Deng et al., 2009; Ebdrup et al., 2011). Consequently, medication effects may confound the observed neurobiological correlates of schizophrenia symptomatology. However, pharmacological treatments including types of anti-psychotic drugs and dosage can vary markedly among individual patients owing to different psychiatrists and medical centers. Different anti-psychotic drugs likewise vary in specific mechanisms of action as well as targeted receptor subunits (Mauri et al., 2014; Radhakrishnan et al., 2020). Therefore, it stands to reason that pooling schizophrenia patient cohorts from international sites will render medication largely as a source of random variation in our data. Indeed, there were no significant correlations observed between individual expressions of the four symptom dimensions and olanzapine-equivalent dosage. Also, the symptom-network correlative patterns were unchanged after additionally adjusting for olanzapine-equivalent dosage in predictive modeling, which confirmed that the possible medication effects are not systematic. Although cross-validation procedures could mitigate the effects caused by random variation on the assessment of symptom-network relationships, such random noise would have made our results more conservative. Future studies with drug-naïve first-episode schizophrenia patients would be ideal to elucidate the neural pathological mechanism of symptoms, completely free from medication effects and with improved statistical power. However, in practice, it remains difficult to recruit multi-center drug-naïve schizophrenia patients with a decent sample size.

Second, the symptom-connectivity-receptor link revealed in the present work does not imply causality. This is because the brain imaging data we recruited were cross-sectional. Future studies with patients longitudinally assessed both phenotypic and neurobiological data would be largely helpful for clarifying the causal relationship between them.

Third, the presently revealed molecular architecture of the networks whose intrinsic connectivity robustly predicted the cognitive symptomatology could allow future neurochemical and molecular biology researchers to specifically focus on the underlying mechanisms of the D_1 dopamine receptor group and the serotonin reuptake transporter in animals with schizophrenia-like cognitive deficits modeled via manipulating copy number variants (reviewed in Forsingdal et al., 2018). There are multiple techniques available for an assessment of receptors in animal models. For example, reverse transcription-polymerase chain reaction and western-blotting can be used to quantify receptor-related mRNA and protein expressions, respectively. Patch-clamp recording and *invivo* electrophysiology are both powerful techniques for examining the electroneurographic signals mediated by receptors and transmitters. Moreover, specific antagonists and agonists can be administered to investigate how the affected receptors possibly mediate alterations in neurotransmission. This is particularly interesting, as an

investigation of the potential interactions among dopaminergic, serotonergic, and glutamatergic systems is critical since they are not functioning alone. The multi-facet symptom expressions in schizophrenia are likewise unlikely to result from deficits in only one of the many neurotransmitter systems (Coyle and Balu, 2018; Uno and Coyle, 2019). Although the glutamatergic hypofunction has been increasingly implicated in schizophrenia neurocognitive deficits (Dempster et al., 2015; Uno and Coyle, 2019; Kaminski et al., 2020), there are no publicly available *in-vivo* measured density maps for glutamate or glutamate receptors (e.g., Nmethyl-D-aspartate [NMDA]). Future studies with patients assessed both the glutamine and the NMDA receptor densities as well as functional connectivity are desired to specifically investigate the involvement of glutamatergic transmission in schizophrenia cognitive symptomatology. Also, future neurochemical and molecular studies to specifically investigate 5-HTT signaling with pharmacological interventions to regulate 5-HTT functioning for probing its relationship with schizophrenia cognitive symptoms are required to verify the link as we implied here.

Forth, the classification and prediction analyses performed in the present work were all relying on functional connectivity measurements since functional brain parameters would temporally better align with the likewise state-dependent symptomatology. Notwithstanding, the features used for multivariable machine-learning could also be structural brain metrics (e.g., grey matter volume, cortical thickness, and structural covariance) and diffusion MRI derived measures. Combining metrics from multi-modal fMRI in future studies may prospectively improve the accuracies in classification and prediction experiments. More importantly, multi-modal fMRI studies would allow for an investigation of the potential structural-functional coupling basis for specific dimensions of psychopathology in schizophrenia.

9. Acknowledgements

First I would like to extend my greatest gratitude to the Faculty of Mathematics and Natural Sciences, Heinrich-Heine-Universität Düsseldorf for admitting me to pursue the Ph.D degree in the field of psychology and Prof. Christian Bellebaum my advisor there, the China Scholarship Council (CSC) who granted me the four-year Ph.D fellowship, as well as the Institute of Neuroscience and Medicine (INM-7), Research Center Jülich for providing facilities, equipments, and computational resources to support my Ph.D researches, and the director of INM-7 Prof. Simon B. Eickhoff who offered me the Ph.D position in computational psychiatry and acted as my Ph.D supervisor.

During the four-year Ph.D time, Prof Eickhoff always showed his patience in guiding me on scientific researches including but not limited to knowledge in programming, clinical psychiatry, neuroscience, neuroimaging, statistics and machine-learning techniques and kept encouraging me when I encountered difficulties and obstacles. What is more impressed me, was his guidance and advice in my personal development for achieving a productive scientific career. Furthermore, Prof. Eickhoff always tried to cultivate my ability to be independent and put me in contact with international collaborations which offered me opportunities to directly discuss projects and scientific questions with professors and senior researches since the early time of my Ph.D. Prof. Eickhoff is my highly respected mentor, reliable guide, and valuable fortune in my life.

INM-7 is an excellent multi-disciplinary institute with a friendly atmosphere that people from different backgrounds closely work together and exchange ideas and thoughts in scientific questions. Dr. Kaustubh R. Patil co-supervised my Ph.D projects since the second year of my Ph.D and I appreciated for his technical supports in machine-learning and his guidance in the interpretation of the results from machine-learning algorithms. Thomas Nickl-Jockschat in Aachen (now in University of Iowa) also co-supervised me a project in clinical psychiatry where he guided me particularly on the clinical aspects of psychosis and the results interpretation of the developed machine-learning models. Acknowledgements also go to other colleagues in INM-7. Sincere thanks to Veronika Müller and Edna Cieslik for their supports and important inputs in cognitive neuroscience, clinical psychiatry, and meta-analysis; to Robert for his kindly help not only in science but also during the time when I troubled with renting an apartment in Jülich; to Felix Hoffstaedter for his support in image data preprocessing and quality control analysis; to Jürgen Dukart for introducing me into the spatial correlation analysis with receptors in the combination with fMRI data; to Xiaojin Liu for all his help in my daily life in Jülich as one of my best friends in Germany; to Debo Dong and Jianxiao Wu for the happy moments we stay together and for the excellent discussions on brain-behavior relationships and multivariate analyses in clinical data; to Julia Camilleri for her assistance in functional characterization analysis; to Susanne Weis for the great pipeline in parcel-wise functional connectivity based classification modeling; to Jona M. Fischer for setting up the online tool for factorization; to Alexander Waite and the whole ‐Data and Platforms" team for taking care of the servers and the infrastructures, to Laura Waite for proof read the manuscript as well as the application and arrangement for open source data; to all other people who had helped me and provided supports in my Ph.D time including Sarah Genon, Shahrzad Kharabian, Laura Muzzarelli, Sofie Valk, Stephan Wolf, Niels Reuter, Shammi More, Lya Paas, Anna Plachti, and Ting-Yat Wong (I might have not enumerated everyone who is working at INM-7 but I will definitely keep everyone's kindness in my mind); and finally to our secretaries Julia Mans and Anna Geiger, and our scientific coordinator Claudia Voigt in

HHU for their help in administrative stuffs.

My Ph.D projects are multi-site studies with data recruited from many medical centers, and I‘d like to express my gratitude to all of our external collaborators who spent time and efforts in data collection and kindly shared the data that made the current work possible. I am also very much appreciated for their insightful and constructive comments and suggestions on my projects and manuscripts. Names are listed with no particular order: Kang Sim and Juan Zhou (Singapore); André Aleman, Iris E. Sommer, Edith J. Liemburg (Netherland); Valentin Riedl, Ute Habel, Birgit Derntl, Lydia Kogler, Christina Regenbogen, Oliver Gruber (Germany); Renaud Jardri (France); Deniz Vatansever (China); Thomas Nickl-Jockschat, Vaibhav A. Diwadkar, Jeffrey A. Stanley, Aristeidis Sotira, and Christos Davatzikos (the USA); and the Pharmacotherapy Monitoring and Outcome Survey (PHAMOUS) Investigators in the Netherland: Agna A. Bartels-Velthuis, Richard Bruggeman, Stynke Castelein, Frederike Jörg, Gerdina H.M. Pijnenborg, Henderikus Knegtering, and Ellen Visser. Gratitude definitely is also expressed to each of the subjects who spent their time and energy in participating this study and their cooperation. I am also thanks a lot for the potential reviewers who will spend time and efforts in reviewing my Ph.D thesis.

In the end, I would like to highlight some funding sources that supported my projects: the Deutsche Forschungsgemeinschaft (DFG, EI 816/4-1 to S.B.E.), the National Institute of Mental Health (R01-MH074457 to S.B.E.), the Helmholtz Portfolio Theme "Supercomputing and Modeling for the Human Brain", the European Union‘s Horizon 2020 Research and Innovation Programme under Grant Agreement No. 720270 (HBP SGA1) and 785907 (HBP SGA2).

10. References

Abi-Dargham, A., Gil, R., Krystal, J., Baldwin, R.M., Seibyl, J.P., Bowers, M., van Dyck, C.H., Charney, D.S., Innis, R.B., Laruelle, M. (1998) Increased striatal dopamine transmission in schizophrenia: confirmation in a second cohort. American Journal of Psychiatry, 155:761-767.

Abi-Dargham, A., Mawlawi, O., Lombardo, I., Gil, R., Martinez, D., Huang, Y., Hwang, D.-R., Keilp, J., Kochan, L., Van Heertum, R. (2002) Prefrontal dopamine D1 receptors and working memory in schizophrenia. Journal of Neuroscience, 22:3708-3719.

Abi-Dargham, A., Rodenhiser, J., Printz, D., Zea-Ponce, Y., Gil, R., Kegeles, L.S., Weiss, R., Cooper, T.B., Mann, J.J., Van Heertum, R.L. (2000) Increased baseline occupancy of D2 receptors by dopamine in schizophrenia. Proceedings of the National Academy of Sciences, 97:8104-8109.

Abram, S.V., Wisner, K.M., Fox, J.M., Barch, D.M., Wang, L., Csernansky, J.G., MacDonald III, A.W., Smith, M.J. (2017) Fronto-temporal connectivity predicts cognitive empathy deficits and experiential negative symptoms in schizophrenia. Human Brain Mapping, 38:1111-1124.

Adank, P. (2012) The neural bases of difficult speech comprehension and speech production: Two Activation Likelihood Estimation (ALE) meta-analyses. Brain and language, 122:42-54.

Adolphs, R., Tranel, D., Damasio, H., Damasio, A. (1994) Impaired recognition of emotion in facial expressions following bilateral damage to the human amygdala. Nature, 372:669-672.

Ahmed, A.O., Strauss, G.P., Buchanan, R.W., Kirkpatrick, B., Carpenter, W.T. (2015) Are negative symptoms dimensional or categorical? Detection and validation of deficit schizophrenia with taxometric and latent variable mixture models. Schizophrenia bulletin, 41:879-891.

Ahmed, A.O., Strauss, G.P., Buchanan, R.W., Kirkpatrick, B., Carpenter, W.T. (2018) Schizophrenia heterogeneity revisited: Clinical, cognitive, and psychosocial correlates of statistically-derived negative symptoms subgroups. Journal of psychiatric research, 97:8-15.

Alakurtti, K., Johansson, J.J., Joutsa, J., Laine, M., Bäckman, L., Nyberg, L., Rinne, J.O. (2015) Long-term test–retest reliability of striatal and extrastriatal dopamine D2/3 receptor binding: study with [11C] raclopride and high-resolution PET. Journal of Cerebral Blood Flow & Metabolism, 35:1199-1205.

Amft, M., Bzdok, D., Laird, A.R., Fox, P.T., Schilbach, L., Eickhoff, S.B. (2015) Definition and characterization of an extended social-affective default network. Brain Structure and Function, 220:1031-1049.

Amrhein, V., Greenland, S., McShane, B. (2019) Scientists rise up against statistical significance. Nature Publishing Group.

Anderson, K.M., Collins, M.A., Chin, R., Ge, T., Rosenberg, M.D., Holmes, A.J. (2020) Transcriptional and imaging-genetic association of cortical interneurons, brain function, and schizophrenia risk. Nature Communications, 11:1-15.

Andreasen, N.C. (1984) Scale for the assessment of positive symptoms (SAPS). University of Iowa Iowa City.

Andreasen, N.C. (1989) The Scale for the Assessment of Negative Symptoms (SANS): conceptual and theoretical foundations. The British journal of psychiatry, 155:49-52.

Andreasen, N.C., Flaum, M., Arndt, S. (1992) The Comprehensive Assessment of Symptoms and History (CASH): an instrument for assessing diagnosis and psychopathology. Archives of general psychiatry, 49:615-623.

Arnsten, A.F., Girgis, R.R., Gray, D.L., Mailman, R.B. (2017) Novel dopamine therapeutics for cognitive deficits in schizophrenia. Biological psychiatry, 81:67-77.

Ashburner, J., Friston, K.J. (2011) Diffeomorphic registration using geodesic shooting and Gauss–Newton optimisation. NeuroImage, 55:954-967.

Association, A.P. (2013) Diagnostic and statistical manual of mental disorders (DSM-5®). American Psychiatric Pub.

Avants, B.B., Libon, D.J., Rascovsky, K., Boller, A., McMillan, C.T., Massimo, L., Coslett, H.B., Chatterjee, A., Gross, R.G., Grossman, M. (2014) Sparse canonical correlation analysis relates network-level atrophy to multivariate cognitive measures in a neurodegenerative population. Neuroimage, 84:698-711.

Azorin, J.M., Belzeaux, R., Adida, M. (2014) Negative symptoms in schizophrenia: Where we have been and where we are heading. CNS neuroscience & therapeutics, 20:801-808.

Banerjee, A., Wang, H.-Y., Borgmann-Winter, K.E., MacDonald, M.L., Kaprielian, H., Stucky, A., Kvasic, J., Egbujo, C., Ray, R., Talbot, K. (2015) Src kinase as a mediator of convergent molecular abnormalities leading to NMDAR hypoactivity in schizophrenia. Molecular psychiatry, 20:1091-1100.

Barch, D.M., Sheffield, J.M. (2017) Cognitive control in schizophrenia: Psychological and neural mechanisms.

Barkan, T., Peled, A., Modai, I., Weizman, A., Rehavi, M. (2006) Characterization of the serotonin transporter in lymphocytes and platelets of schizophrenia patients treated with atypical or typical antipsychotics compared to healthy individuals. European neuropsychopharmacology, 16:429-436.

Bartko, J.J., Carpenter, W.T., Strauss, J.S. (1981) Statistical basis for exploring schizophrenia. The American journal of psychiatry.

Beaty, R.E., Kenett, Y.N., Christensen, A.P., Rosenberg, M.D., Benedek, M., Chen, Q., Fink, A., Qiu, J., Kwapil, T.R., Kane, M.J. (2018) Robust prediction of individual creative ability from brain functional connectivity. Proceedings of the National Academy of Sciences, 115:1087-1092.

Ben-Hur, A., Guyon, I. (2003) Detecting stable clusters using principal component analysis. Functional genomics: Springer. p 159-182.

Benedetti, F., Bernasconi, A., Bosia, M., Cavallaro, R., Dallaspezia, S., Falini, A., Poletti, S., Radaelli, D., Riccaboni, R., Scotti, G. (2009) Functional and structural brain correlates of theory of mind and empathy deficits in schizophrenia. Schizophrenia research, 114:154-160.

Benoit, A., Bodnar, M., Malla, A., Joober, R., Lepage, M. (2012) The structural neural substrates of persistent negative symptoms in first-episode of non-affective psychosis: a voxel-based morphometry study. Frontiers in psychiatry, 3:42.

Bentler, P.M. (1985) Efficient estimation via linearization in structural models. Multivariate analysis:9-42.

Berman, R.A., Gotts, S.J., McAdams, H.M., Greenstein, D., Lalonde, F., Clasen, L., Watsky, R.E., Shora, L., Ordonez, A.E., Raznahan, A. (2016) Disrupted sensorimotor and social–cognitive networks underlie symptoms in childhood-onset schizophrenia. Brain, 139:276-291.

Bernard, J.A., Dean, D.J., Kent, J.S., Orr, J.M., Pelletier-Baldelli, A., Lunsford-Avery, J.R., Gupta, T., Mittal, V.A. (2014) Cerebellar networks in individuals at ultra high-risk of psychosis: Impact on postural sway and symptom severity. Human brain mapping, 35:4064-4078.

Bezdek, J.C. (1981) Objective function clustering. Pattern recognition with fuzzy objective function algorithms: Springer. p 43-93.

Binder, J.R., Desai, R.H., Graves, W.W., Conant, L.L. (2009) Where is the semantic system? A critical review and meta-analysis of 120 functional neuroimaging studies. Cerebral cortex, 19:2767-2796.

Blanke, O., Arzy, S. (2005) The out-of-body experience: disturbed self-processing at the temporo-parietal junction. The Neuroscientist, 11:16-24.

Bonfils, K.A., Lysaker, P.H., Minor, K.S., Salyers, M.P. (2016) Affective empathy in schizophrenia: a meta-analysis. Schizophrenia research, 175:109-117.

Bora, E., Pantelis, C. (2013) Theory of mind impairments in first-episode psychosis, individuals at ultra-high risk for

psychosis and in first-degree relatives of schizophrenia: systematic review and meta-analysis. Schizophrenia research, 144:31-36.

Borgan, F., O'Daly, O., Veronese, M., Marques, T.R., Laurikainen, H., Hietala, J., Howes, O. (2019) The neural and molecular basis of working memory function in psychosis: a multimodal PET-fMRI study. Molecular Psychiatry:1-11.

Bourne, J.A. (2001) SCH 23390: the first selective dopamine D1-like receptor antagonist. CNS drug reviews, 7:399-414.

Boutsidis, C., Gallopoulos, E. (2008) SVD based initialization: A head start for nonnegative matrix factorization. Pattern recognition, 41:1350-1362.

Braff, D.L., Ryan, J., Rissling, A.J., Carpenter, W.T. (2013) Lack of use in the literature from the last 20 years supports dropping traditional schizophrenia subtypes from DSM-5 and ICD-11. Schizophrenia bulletin, 39:751-753.

Braver, T.S., Barch, D.M., Cohen, J.D. (1999) Cognition and control in schizophrenia: a computational model of dopamine and prefrontal function. Biological psychiatry, 46:312-328.

Breier, A., Su, T.-P., Saunders, R., Carson, R., Kolachana, B., De Bartolomeis, A., Weinberger, D., Weisenfeld, N., Malhotra, A., Eckelman, W. (1997) Schizophrenia is associated with elevated amphetamine-induced synaptic dopamine concentrations: evidence from a novel positron emission tomography method. Proceedings of the National Academy of Sciences, 94:2569-2574.

Brunet, J.-P., Tamayo, P., Golub, T.R., Mesirov, J.P. (2004) Metagenes and molecular pattern discovery using matrix factorization. Proceedings of the national academy of sciences, 101:4164-4169.

Buhle, J.T., Silvers, J.A., Wager, T.D., Lopez, R., Onyemekwu, C., Kober, H., Weber, J., Ochsner, K.N. (2014) Cognitive reappraisal of emotion: a meta-analysis of human neuroimaging studies. Cerebral cortex, 24:2981-2990.

Bzdok, D., Schilbach, L., Vogeley, K., Schneider, K., Laird, A.R., Langner, R., Eickhoff, S.B. (2012) Parsing the neural correlates of moral cognition: ALE meta-analysis on morality, theory of mind, and empathy. Brain Structure and Function, 217:783-796.

Calhoun, V.D., Wager, T.D., Krishnan, A., Rosch, K.S., Seymour, K.E., Nebel, M.B., Mostofsky, S.H., Nyalakanai, P., Kiehl, K. (2017) The impact of T1 versus EPI spatial normalization templates for fMRI data analyses. Human brain mapping, 38:5331-5342.

Camilleri, J., Müller, V.I., Fox, P., Laird, A.R., Hoffstaedter, F., Kalenscher, T., Eickhoff, S.B. (2018) Definition and characterization of an extended multiple-demand network. NeuroImage, 165:138-147.

Campello, R.J., Hruschka, E.R. (2006) A fuzzy extension of the silhouette width criterion for cluster analysis. Fuzzy Sets and Systems, 157:2858-2875.

Cannon, T.D. (2015) How schizophrenia develops: cognitive and brain mechanisms underlying onset of psychosis. Trends in cognitive sciences, 19:744-756.

Cao, H., Bertolino, A., Walter, H., Schneider, M., Schäfer, A., Taurisano, P., Blasi, G., Haddad, L., Grimm, O., Otto, K. (2016) Altered functional subnetwork during emotional face processing: a potential intermediate phenotype for schizophrenia. JAMA psychiatry, 73:598-605.

Carpenter, W., Buchanan, R. (1989) Domains of psychopathology relevant to the study of etiology and treatment of schizophrenia. Schizophrenia: Scientific Progress:13-22.

Carpenter, W.T., Heinrichs, D.W., Wagman, A.M. (1988) Deficit and nondeficit forms of schizophrenia: the concept. The American journal of psychiatry.

Caspers, S., Zilles, K., Laird, A.R., Eickhoff, S.B. (2010) ALE meta-analysis of action observation and imitation in

the human brain. Neuroimage, 50:1148-1167.

Catts, V.S., Lai, Y.L., Weickert, C.S., Weickert, T.W., Catts, S.V. (2016) A quantitative review of the postmortem evidence for decreased cortical N-methyl-d-aspartate receptor expression levels in schizophrenia: How can we link molecular abnormalities to mismatch negativity deficits? Biological psychology, 116:57-67.

Chahine, G., Richter, A., Wolter, S., Goya-Maldonado, R., Gruber, O. (2017) Disruptions in the left frontoparietal network underlie resting state endophenotypic markers in schizophrenia. Human Brain Mapping, 38:1741-1750.

Chen, J., Patil, K.R., Weis, S., et al. (2020) Neurobiological Divergence of the Positive and Negative Schizophrenia Subtypes Identified on a New Factor Structure of Psychopathology Using Non-negative Factorization: An International Machine Learning Study. Biological psychiatry, 87(3):282-293.

Chen, X., Duan, M., Xie, Q., Lai, Y., Dong, L., Cao, W., Yao, D., Luo, C. (2015) Functional disconnection between the visual cortex and the sensorimotor cortex suggests a potential mechanism for self-disorder in schizophrenia. Schizophrenia Research, 166:151-157.

Chou, C.-P., Bentler, P.M. (1995) Estimates and tests in structural equation modeling.

Cichocki, Ł., Cechnicki, A., Polczyk, R. (2012) Consistency of symptomatic dimensions of schizophrenia over 20 years. Psychiatry research, 200:115-119.

Cieslik, E.C., Mueller, V.I., Eickhoff, C.R., Langner, R., Eickhoff, S.B. (2015) Three key regions for supervisory attentional control: evidence from neuroimaging meta-analyses. Neuroscience & biobehavioral reviews, 48:22-34.

Clos, M., Diederen, K.M., Meijering, A.L., Sommer, I.E., Eickhoff, S.B. (2014) Aberrant connectivity of areas for decoding degraded speech in patients with auditory verbal hallucinations. Brain Structure and Function, 219:581-594.

Cohen, A.S., Brown, L.A., Minor, K.S. (2010) The psychiatric symptomatology of deficit schizophrenia: a meta-analysis. Schizophrenia research, 118:122-127.

Collins, A.G., Brown, J.K., Gold, J.M., Waltz, J.A., Frank, M.J. (2014) Working memory contributions to reinforcement learning impairments in schizophrenia. Journal of Neuroscience, 34:13747-13756.

Collinson, S.L., Gan, S.C., San Woon, P., Kuswanto, C., Sum, M.Y., Yang, G.L., Lui, J.M., Sitoh, Y.Y., Nowinski, W.L., Sim, K. (2014) Corpus callosum morphology in first-episode and chronic schizophrenia: combined magnetic resonance and diffusion tensor imaging study of Chinese Singaporean patients. The British Journal of Psychiatry, 204:55-60.

Combrisson, E., Jerbi, K. (2015) Exceeding chance level by chance: The caveat of theoretical chance levels in brain signal classification and statistical assessment of decoding accuracy. Journal of neuroscience methods, 250:126-136.

Coyle, J.T., Balu, D.T. (2018) The role of serine racemase in the pathophysiology of brain disorders. Advances in Pharmacology: Elsevier. p 35-56.

COYLE, J.T., TSAI, G., GOFF, D. (2003) Converging evidence of NMDA receptor hypofunction in the pathophysiology of schizophrenia. Annals of the New York Academy of Sciences, 1003:318-327.

Cronbach, L.J. (1951) Coefficient alpha and the internal structure of tests. psychometrika, 16:297-334.

Cuervo-Lombard, C., Lemogne, C., Gierski, F., Bera-Potelle, C., Tran, E., Portefaix, C., Kaladjian, A., Pierot, L., Limosin, F. (2012) Neural basis of autobiographical memory retrieval in schizophrenia. The British Journal of Psychiatry, 201:473-480.

Cunningham, V.J., Jones, T. (1993) Spectral analysis of dynamic PET studies. Journal of Cerebral Blood Flow & Metabolism, 13:15-23.

Döhnel, K., Schuwerk, T., Meinhardt, J., Sodian, B., Hajak, G., Sommer, M. (2012) Functional activity of the right temporo-parietal junction and of the medial prefrontal cortex associated with true and false belief reasoning. Neuroimage, 60:1652-1661.

Das, P., Lagopoulos, J., Coulston, C.M., Henderson, A.F., Malhi, G.S. (2012) Mentalizing impairment in schizophrenia: a functional MRI study. Schizophrenia research, 134:158-164.

Daubechies, I., Roussos, E., Takerkart, S., Benharrosh, M., Golden, C., D'ardenne, K., Richter, W., Cohen, J.D., Haxby, J. (2009) Independent component analysis for brain fMRI does not select for independence. Proceedings of the National Academy of Sciences, 106:10415-10422.

De Rossi, P., Chiapponi, C., Spalletta, G. (2015) Brain functional effects of psychopharmacological treatments in schizophrenia: a network-based functional perspective beyond neurotransmitter systems. Current neuropharmacology, 13:435-444.

Dempster, K., Norman, R., Théberge, J., Densmore, M., Schaefer, B., Williamson, P. (2015) Glutamatergic metabolite correlations with neuropsychological tests in first episode schizophrenia. Psychiatry Research: Neuroimaging, 233:180-185.

Deng, M.Y., McAlonan, G.M., Cheung, C., Chiu, C.P., Law, C.W., Cheung, V., Sham, P.C., Chen, E.Y., Chua, S.E. (2009) A naturalistic study of grey matter volume increase after early treatment in anti-psychotic naive, newly diagnosed schizophrenia. Psychopharmacology, 206:437-446.

Derntl, B., Finkelmeyer, A., Eickhoff, S., Kellermann, T., Falkenberg, D.I., Schneider, F., Habel, U. (2010) Multidimensional assessment of empathic abilities: neural correlates and gender differences. Psychoneuroendocrinology, 35:67-82.

Devarajan, K. (2008) Nonnegative matrix factorization: an analytical and interpretive tool in computational biology. PLoS Comput Biol, 4:e1000029.

Diagnostic, A. (1994) statistical manual of mental disorders. 4th edn American Psychiatric Association. Washington, DC.

Dickinson, D., Pratt, D.N., Giangrande, E.J., Grunnagle, M., Orel, J., Weinberger, D.R., Callicott, J.H., Berman, K.F. (2018) Attacking heterogeneity in schizophrenia by deriving clinical subgroups from widely available symptom data. Schizophrenia bulletin, 44:101-113.

Dollfus, S., Everitt, B., Ribeyre, J.M., Assouly-Besse, F., Sharp, C., Petit, M. (1996) Identifying subtypes of schizophrenia by cluster analyses. Schizophrenia Bulletin, 22:545-555.

Dong, D., Wang, Y., Chang, X., Luo, C., Yao, D. (2018) Dysfunction of large-scale brain networks in schizophrenia: a meta-analysis of resting-state functional connectivity. Schizophrenia bulletin, 44:168-181.

Du, X., Choa, F.-S., Chiappelli, J., Wisner, K.M., Wittenberg, G., Adhikari, B., Bruce, H., Rowland, L.M., Kochunov, P., Hong, L.E. (2019) Aberrant middle prefrontal-motor cortex connectivity mediates motor inhibitory biomarker in schizophrenia. Biological psychiatry, 85:49-59.

Du, Y., Pearlson, G.D., Yu, Q., He, H., Lin, D., Sui, J., Wu, L., Calhoun, V.D. (2016) Interaction among subsystems within default mode network diminished in schizophrenia patients: a dynamic connectivity approach. Schizophrenia research, 170:55-65.

Dukart, J., Holiga, Š., Chatham, C., Hawkins, P., Forsyth, A., McMillan, R., Myers, J., Lingford-Hughes, A.R., Nutt, D.J., Merlo-Pich, E. (2018) Cerebral blood flow predicts differential neurotransmitter activity. Scientific reports, 8:1-11.

Ebdrup, B.H., Skimminge, A., Rasmussen, H., Aggernaes, B., Oranje, B., Lublin, H., Baaré, W., Glenthøj, B. (2011) Progressive striatal and hippocampal volume loss in initially antipsychotic-naive, first-episode schizophrenia patients treated with quetiapine: relationship to dose and symptoms. International Journal of

Neuropsychopharmacology, 14:69-82.

Ebisch, S.J., Gallese, V., Salone, A., Martinotti, G., Di Iorio, G., Mantini, D., Perrucci, M.G., Romani, G.L., Di Giannantonio, M., Northoff, G. (2018) Disrupted relationship between ―resting state" connectivity and task-evoked activity during social perception in schizophrenia. Schizophrenia research, 193:370-376.

Edwards, J., Pattison, P.E., Jackson, H.J., Wales, R.J. (2001) Facial affect and affective prosody recognition in first-episode schizophrenia. Schizophrenia research, 48:235-253.

Eggers, A.E. (2013) A serotonin hypothesis of schizophrenia. Medical hypotheses, 80:791-794.

Eickhoff, S.B., Bzdok, D., Laird, A.R., Kurth, F., Fox, P.T. (2012) Activation likelihood estimation meta-analysis revisited. Neuroimage, 59:2349-2361.

Emsley, R., Asmal, L., Du Plessis, S., Chiliza, B., Phahladira, L., Kilian, S. (2017) Brain volume changes over the first year of treatment in schizophrenia: relationships to antipsychotic treatment. Psychological medicine, 47:2187.

Emsley, R., Rabinowitz, J., Torreman, M., Group, R.-I.-E.P.G.W. (2003) The factor structure for the Positive and Negative Syndrome Scale (PANSS) in recent-onset psychosis. Schizophrenia research, 61:47-57.

Erritzoe, D., Rasmussen, H., Kristiansen, K.T., Frokjaer, V.G., Haugbol, S., Pinborg, L., Baaré, W., Svarer, C., Madsen, J., Lublin, H. (2008) Cortical and subcortical 5-HT 2A receptor binding in neuroleptic-naive first-episode schizophrenic patients. Neuropsychopharmacology, 33:2435-2441.

Eryilmaz, H., Tanner, A.S., Ho, N.F., Nitenson, A.Z., Silverstein, N.J., Petruzzi, L.J., Goff, D.C., Manoach, D.S., Roffman, J.L. (2016) Disrupted working memory circuitry in schizophrenia: disentangling fMRI markers of core pathology vs other aspects of impaired performance. Neuropsychopharmacology, 41:2411-2420.

Eyler, L.T., Olsen, R.K., Jeste, D.V., Brown, G.G. (2004) Abnormal brain response of chronic schizophrenia patients despite normal performance during a visual vigilance task. Psychiatry Research: Neuroimaging, 130:245-257.

Fan, L., Li, H., Zhuo, J., Zhang, Y., Wang, J., Chen, L., Yang, Z., Chu, C., Xie, S., Laird, A.R. (2016) The human brainnetome atlas: a new brain atlas based on connectional architecture. Cerebral cortex, 26:3508-3526.

Faul, F., Erdfelder, E., Buchner, A., Lang, A.-G. (2009) Statistical power analyses using G* Power 3.1: Tests for correlation and regression analyses. Behavior research methods, 41:1149-1160.

Fink, M., Wadsak, W., Savli, M., Stein, P., Moser, U., Hahn, A., Mien, L.-K., Kletter, K., Mitterhauser, M., Kasper, S. (2009) Lateralization of the serotonin-1A receptor distribution in language areas revealed by PET. Neuroimage, 45:598-605.

First, M.B., Spitzer, R.L., Gibbon, M., Williams, J.B. (1995) Structured clinical interview for DSM-IV axis I disorders, patient version (SCID-P), version 2. New York: NewYork State Psychiatric Institute Biometrics Research.

Fischer, B.A., Keller, W.R., Arango, C., Pearlson, G.D., McMahon, R.P., Meyer, W.A., Francis, A., Kirkpatrick, B., Carpenter, W.T., Buchanan, R.W. (2012) Cortical structural abnormalities in deficit versus nondeficit schizophrenia. Schizophrenia research, 136:51-54.

Force, R.B., Venables, N.C., Sponheim, S.R. (2008) An auditory processing abnormality specific to liability for schizophrenia. Schizophrenia research, 103:298-310.

Forsingdal, A., Jørgensen, T.N., Olsen, L., Werge, T., Didriksen, M., Nielsen, J. (2019) Can animal models of copy number variants that predispose to schizophrenia elucidate underlying biology? Biological psychiatry, 85:13-24.

Fraley, C., Raftery, A.E. (2002) Model-based clustering, discriminant analysis, and density estimation. Journal of the American statistical Association, 97:611-631.

Fretland, R.A., Andersson, S., Sundet, K., Andreassen, O.A., Melle, I., Vaskinn, A. (2015) Theory of mind in

schizophrenia: error types and associations with symptoms. Schizophrenia research, 162:42-46.

Friedman, J., Hastie, T., Tibshirani, R. (2001) The elements of statistical learning. Springer series in statistics New York.

Frith, C.D. (2004) Schizophrenia and theory of mind. Psychological medicine, 34:385-389.

Fusar-Poli, P., Papanastasiou, E., Stahl, D., Rocchetti, M., Carpenter, W., Shergill, S., McGuire, P. (2015) Treatments of negative symptoms in schizophrenia: meta-analysis of 168 randomized placebo-controlled trials. Schizophrenia bulletin, 41:892-899.

Gómez, F.J.G., Huertas, I., Ramírez, J.A.L., Solís, D.G. (2018) Elaboración de una plantilla de SPM para la normalización de imágenes de PET con 18F-DOPA. Imagen Diagnóstica, 9:23-25.

Galderisi, S., Maj, M., Mucci, A., Cassano, G.B., Invernizzi, G., Rossi, A., Vita, A., Dell'Osso, L., Daneluzzo, E., Pini, S. (2002) Historical, psychopathological, neurological, and neuropsychological aspects of deficit schizophrenia: a multicenter study. American Journal of Psychiatry, 159:983-990.

Gallezot, J.-D., Nabulsi, N., Neumeister, A., Planeta-Wilson, B., Williams, W.A., Singhal, T., Kim, S., Maguire, R.P., McCarthy, T., Frost, J.J. (2010) Kinetic modeling of the serotonin 5-HT1B receptor radioligand [11C] P943 in humans. Journal of Cerebral Blood Flow & Metabolism, 30:196-210.

Garrity, A.G., Pearlson, G.D., McKiernan, K., Lloyd, D., Kiehl, K.A., Calhoun, V.D. (2007) Aberrant "default mode" functional connectivity in schizophrenia. American journal of psychiatry, 164:450-457.

Ghosh, S., Mujumdar, P.P. (2008) Statistical downscaling of GCM simulations to streamflow using relevance vector machine. Advances in water resources, 31:132-146.

Giel, R., Nienhuis, F. (1996) SCAN-2.1: Schedules for clinical assessment in neuropsychiatry. Geneve/Groningen: WHO.

Giraldo-Chica, M., Rogers, B.P., Damon, S.M., Landman, B.A., Woodward, N.D. (2018) Prefrontal-thalamic anatomical connectivity and executive cognitive function in schizophrenia. Biological psychiatry, 83:509-517.

Giraldo-Chica, M., Woodward, N.D. (2017) Review of thalamocortical resting-state fMRI studies in schizophrenia. Schizophrenia research, 180:58-63.

Girgis, R.R., Phillips, M.R., Li, X., Li, K., Jiang, H., Wu, C., Duan, N., Niu, Y., Lieberman, J.A. (2011) Clozapine v. chlorpromazine in treatment-naive, first-episode schizophrenia: 9-year outcomes of a randomised clinical trial. The British Journal of Psychiatry, 199:281-288.

Gold, J.M., Strauss, G.P., Waltz, J.A., Robinson, B.M., Brown, J.K., Frank, M.J. (2013) Negative symptoms of schizophrenia are associated with abnormal effort-cost computations. Biological psychiatry, 74:130-136.

Gold, J.M., Waltz, J.A., Prentice, K.J., Morris, S.E., Heerey, E.A. (2008) Reward processing in schizophrenia: a deficit in the representation of value. Schizophrenia bulletin, 34:835-847.

Gottesman, I.I., Gould, T.D. (2003) The endophenotype concept in psychiatry: etymology and strategic intentions. American journal of psychiatry, 160:636-645.

Graff-Guerrero, A., Mizrahi, R., Agid, O., Marcon, H., Barsoum, P., Rusjan, P., Wilson, A.A., Zipursky, R., Kapur, S. (2009) The dopamine D 2 receptors in high-affinity state and D 3 receptors in schizophrenia: a clinical [11 C]-(+)-PHNO PET study. Neuropsychopharmacology, 34:1078-1086.

Gray, L., Van Den Buuse, M., Scarr, E., Dean, B., Hannan, A.J. (2009) Clozapine reverses schizophrenia-related behaviours in the metabotropic glutamate receptor 5 knockout mouse: association with N-methyl-D-aspartic acid receptor up-regulation. International Journal of Neuropsychopharmacology, 12:45-60.

Gunn, R.N., Lammertsma, A.A., Hume, S.P., Cunningham, V.J. (1997) Parametric imaging of ligand-receptor binding in PET using a simplified reference region model. Neuroimage, 6:279-287.

Guo, N., Hwang, D.-R., Lo, E.-S., Huang, Y.-Y., Laruelle, M., Abi-Dargham, A. (2003) Dopamine depletion and in

vivo binding of PET D 1 receptor radioligands: implications for imaging studies in schizophrenia. Neuropsychopharmacology, 28:1703-1711.

Gur, R.E., McGrath, C., Chan, R.M., Schroeder, L., Turner, T., Turetsky, B.I., Kohler, C., Alsop, D., Maldjian, J., Ragland, J.D. (2002) An fMRI study of facial emotion processing in patients with schizophrenia. American Journal of Psychiatry, 159:1992-1999.

Hall, H., Köhler, C., Gawell, L., Farde, L., Sedvall, G. (1988) Raclopride, a new selective ligand for the dopamine-D2 receptors. Progress in neuro-psychopharmacology & biological psychiatry, 12:559.

Helmes, E., Landmark, J. (2003) Subtypes of schizophrenia: a cluster analytic approach. The Canadian Journal of Psychiatry, 48:702-708.

Hendler, T., Raz, G., Shimrit, S., Jacob, Y., Lin, T., Roseman, L., Wahid, W.M., Kremer, I., Kupchik, M., Kotler, M. (2018) Social affective context reveals altered network dynamics in schizophrenia patients. Translational psychiatry, 8:1-12.

Hernandez, I., Sokolov, B. (1997) Abnormal expression of serotonin transporter mRNA in the frontal and temporal cortex of schizophrenics. Molecular psychiatry, 2:57-64.

Herold, C.J., Lässer, M.M., Schmid, L.A., Seidl, U., Kong, L., Fellhauer, I., Thomann, P.A., Essig, M., Schröder, J. (2013) Hippocampal volume reduction and autobiographical memory deficits in chronic schizophrenia. Psychiatry Research: Neuroimaging, 211:189-194.

Herold, C.J., Lässer, M.M., Schmid, L.A., Seidl, U., Kong, L., Fellhauer, I., Thomann, P.A., Essig, M., Schröder, J. (2015) Neuropsychology, autobiographical memory, and hippocampal volume in ―younger" and ―older" patients with chronic schizophrenia. Frontiers in psychiatry, 6:53.

Hofree, M., Shen, J.P., Carter, H., Gross, A., Ideker, T. (2013) Network-based stratification of tumor mutations. Nature methods, 10:1108-1115.

Horan, W.P., Pineda, J.A., Wynn, J.K., Iacoboni, M., Green, M.F. (2014) Some markers of mirroring appear intact in schizophrenia: evidence from mu suppression. Cognitive, Affective, & Behavioral Neuroscience, 14:1049-1060.

Howes, O.D., Kapur, S. (2009) The dopamine hypothesis of schizophrenia: version III—the final common pathway. Schizophrenia bulletin, 35:549-562.

Hoyer, D., Hannon, J.P., Martin, G.R. (2002) Molecular, pharmacological and functional diversity of 5-HT receptors. Pharmacology Biochemistry and Behavior, 71:533-554.

Hsu, C.-W., Chang, C.-C., Lin, C.-J. (2003) A practical guide to support vector classification. Taipei.

Hu, M.-L., Zong, X.-F., Mann, J.J., Zheng, J.-J., Liao, Y.-H., Li, Z.-C., He, Y., Chen, X.-G., Tang, J.-S. (2017) A review of the functional and anatomical default mode network in schizophrenia. Neuroscience bulletin, 33:73-84.

Huang, P., Cui, L.-B., Li, X., Lu, Z.-L., Zhu, X., Xi, Y., Wang, H., Li, B., Hou, F., Miao, D. (2018) Identifying first-episode drug naïve patients with schizophrenia with or without auditory verbal hallucinations using whole-brain functional connectivity: A pattern analysis study. NeuroImage: Clinical, 19:351-359.

Hurlemann, R., Matusch, A., Kuhn, K.-U., Berning, J., Elmenhorst, D., Winz, O., Kolsch, H., Zilles, K., Wagner, M., Maier, W. (2008) 5-HT 2A receptor density is decreased in the at-risk mental state. Psychopharmacology, 195:579-590.

Ichise, M., Liow, J.-S., Lu, J.-Q., Takano, A., Model, K., Toyama, H., Suhara, T., Suzuki, K., Innis, R.B., Carson, R.E. (2003) Linearized reference tissue parametric imaging methods: application to [11C] DASB positron emission tomography studies of the serotonin transporter in human brain. Journal of Cerebral Blood Flow & Metabolism, 23:1096-1112.

Innis, R.B., Cunningham, V.J., Delforge, J., Fujita, M., Gjedde, A., Gunn, R.N., Holden, J., Houle, S., Huang, S.-C., Ichise, M. (2007) Consensus nomenclature for in vivo imaging of reversibly binding radioligands. Journal of Cerebral Blood Flow & Metabolism, 27:1533-1539.

Insel, T., Cuthbert, B., Garvey, M., Heinssen, R., Pine, D.S., Quinn, K., Sanislow, C., Wang, P. (2010) Research domain criteria (RDoC): toward a new classification framework for research on mental disorders. Am Psychiatric Assoc.

Ishibashi, K., Ishii, K., Oda, K., Kawasaki, K., Mizusawa, H., Ishiwata, K. (2009) Regional analysis of age-related decline in dopamine transporters and dopamine D2-like receptors in human striatum. Synapse, 63:282-290.

Jamadar, S., O'Neil, K.M., Pearlson, G.D., Ansari, M., Gill, A., Jagannathan, K., Assaf, M. (2013a) Impairment in semantic retrieval is associated with symptoms in schizophrenia but not bipolar disorder. Biological psychiatry, 73:555-564.

Jamadar, S.D., Pearlson, G.D., O'Neil, K.M., Assaf, M. (2013b) Semantic association fMRI impairments represent a potential schizophrenia biomarker. Schizophrenia research, 145:20-26.

Javitt, D. (1987) Negative schizophrenic symptomatology and the PCP (phencyclidine) model of schizophrenia. The Hillside journal of clinical psychiatry, 9:12.

Javitt, D., Duncan, L., Balla, A., Sershen, H. (2005) Inhibition of system A-mediated glycine transport in cortical synaptosomes by therapeutic concentrations of clozapine: implications for mechanisms of action. Molecular psychiatry, 10:275-287.

Javitt, D.C., Zukin, S.R. (1991) Recent advances in the phencyclidine model of schizophrenia. The American journal of psychiatry.

Jia, W., Zhu, H., Ni, Y., Su, J., Xu, R., Jia, H., Wan, X. (2020) Disruptions of frontoparietal control network and default mode network linking the metacognitive deficits with clinical symptoms in schizophrenia. Human Brain Mapping, 41:1445-1458.

Jiang, J., Sim, K., Lee, J. (2013) Validated five-factor model of positive and negative syndrome scale for schizophrenia in Chinese population. Schizophrenia research, 143:38-43.

Kaiser, R., Tremblay, P., Schmider, J., Henneken, M., Dettling, M., Müller-Oerlinghausen, B., Uebelhack, R., Roots, I., Brockmöller, J. (2001) Serotonin transporter polymorphisms: no association with response to antipsychotic treatment, but associations with the schizoparanoid and residual subtypes of schizophrenia. Molecular psychiatry, 6:179-185.

Kaller, S., Rullmann, M., Patt, M., Becker, G.-A., Luthardt, J., Girbardt, J., Meyer, P.M., Werner, P., Barthel, H., Bresch, A. (2017) Test–retest measurements of dopamine D 1-type receptors using simultaneous PET/MRI imaging. European journal of nuclear medicine and molecular imaging, 44:1025-1032.

Kaminski, J., Gleich, T., Fukuda, Y., Katthagen, T., Gallinat, J., Heinz, A., Schlagenhauf, F. (2020) Association of cortical glutamate and working memory activation in patients with schizophrenia: A multimodal proton magnetic resonance spectroscopy and functional magnetic resonance imaging study. Biological Psychiatry, 87:225-233.

Kanahara, N., Sekine, Y., Haraguchi, T., Uchida, Y., Hashimoto, K., Shimizu, E., Iyo, M. (2013) Orbitofrontal cortex abnormality and deficit schizophrenia. Schizophrenia research, 143:246-252.

Kay, S.R., Sevy, S. (1990) Pyramidical model of schizophrenia. Schizophrenia bulletin, 16:537-545.

Kay, S.R., Singh, M.M. (1989) The positive-negative distinction in drug-free schizophrenic patients: Stability, response to neuroleptics, and prognostic significance. Archives of General Psychiatry, 46:711-718.

Kegeles, L.S., Slifstein, M., Xu, X., Urban, N., Thompson, J.L., Moadel, T., Harkavy-Friedman, J.M., Gil, R., Laruelle, M., Abi-Dargham, A. (2010) Striatal and extrastriatal dopamine D2/D3 receptors in schizophrenia

evaluated with [18F] fallypride positron emission tomography. Biological psychiatry, 68:634-641.

Kestler, L., Walker, E., Vega, E. (2001) Dopamine receptors in the brains of schizophrenia patients: a meta-analysis of the findings. Behavioural pharmacology, 12:355-371.

Kim, D.I., Mathalon, D., Ford, J., Mannell, M., Turner, J., Brown, G., Belger, A., Gollub, R., Lauriello, J., Wible, C. (2009) Auditory oddball deficits in schizophrenia: an independent component analysis of the fMRI multisite function BIRN study. Schizophrenia bulletin, 35:67-81.

Kim, J.-H., Kim, S.-Y., Lee, J., Oh, K.-J., Kim, Y.-B., Cho, Z.-H. (2012) Evaluation of the factor structure of symptoms in patients with schizophrenia. Psychiatry research, 197:285-289.

Kim, J.-H., Son, Y.-D., Kim, J.-H., Choi, E.-J., Lee, S.-Y., Lee, J.E., Cho, Z.-H., Kim, Y.-B. (2015) Serotonin transporter availability in thalamic subregions in schizophrenia: A study using 7.0-T MRI with [11C] DASB high-resolution PET. Psychiatry Research: Neuroimaging, 231:50-57.

Kim, J., Mouw, K.W., Polak, P., Braunstein, L.Z., Kamburov, A., Tiao, G., Kwiatkowski, D.J., Rosenberg, J.E., Van Allen, E.M., D D'Andrea, A. (2016a) Somatic ERCC2 mutations are associated with a distinct genomic signature in urothelial tumors. Nature genetics, 48:600-606.

Kim, M.-s., Kang, B.-N., Lim, J.Y. (2016b) Decision-making deficits in patients with chronic schizophrenia: Iowa Gambling Task and Prospect Valence Learning model. Neuropsychiatric disease and treatment, 12:1019.

Kirkpatrick, B., Buchanan, R.W., Ross, D.E., Carpenter, W.T. (2001) A separate disease within the syndrome of schizophrenia. Archives of general psychiatry, 58:165-171.

Kirkpatrick, B., Fenton, W.S., Carpenter, W.T., Marder, S.R. (2006) The NIMH-MATRICS consensus statement on negative symptoms. Schizophrenia bulletin, 32:214-219.

Kirkpatrick, B., Galderisi, S. (2008) Deficit schizophrenia: an update. World Psychiatry, 7:143.

Kline, R.B. (2015) Principles and practice of structural equation modeling. Guilford publications.

Kraemer, H.C. (2019) Is it time to ban the P value? Jama Psychiatry, 76:1219-1220.

Kringelbach, M.L., Cruzat, J., Cabral, J., Knudsen, G.M., Carhart-Harris, R., Whybrow, P.C., Logothetis, N.K., Deco, G. (2020) Dynamic coupling of whole-brain neuronal and neurotransmitter systems. Proceedings of the National Academy of Sciences, 117:9566-9576.

Krystal, J.H., Karper, L.P., Seibyl, J.P., Freeman, G.K., Delaney, R., Bremner, J.D., Heninger, G.R., Bowers, M.B., Charney, D.S. (1994) Subanesthetic effects of the noncompetitive NMDA antagonist, ketamine, in humans: psychotomimetic, perceptual, cognitive, and neuroendocrine responses. Archives of general psychiatry, 51:199-214.

Kubicki, M., McCarley, R.W., Nestor, P.G., Huh, T., Kikinis, R., Shenton, M.E., Wible, C.G. (2003) An fMRI study of semantic processing in men with schizophrenia. Neuroimage, 20:1923-1933.

Laird, A.R., Eickhoff, S.B., Li, K., Robin, D.A., Glahn, D.C., Fox, P.T. (2009) Investigating the functional heterogeneity of the default mode network using coordinate-based meta-analytic modeling. Journal of Neuroscience, 29:14496-14505.

Lammertsma, A.A., Hume, S.P. (1996) Simplified reference tissue model for PET receptor studies. Neuroimage, 4:153-158.

Landek-Salgado, M.A., Faust, T.E., Sawa, A. (2016) Molecular substrates of schizophrenia: homeostatic signaling to connectivity. Molecular psychiatry, 21:10-28.

Langdon, R., Ward, P.B., Coltheart, M. (2010) Reasoning anomalies associated with delusions in schizophrenia. Schizophrenia bulletin, 36:321-330.

Langner, R., Eickhoff, S.B. (2013) Sustaining attention to simple tasks: a meta-analytic review of the neural mechanisms of vigilant attention. Psychological bulletin, 139:870.

Laruelle, M. (1998) Imaging dopamine transmission in schizophrenia: a review and meta-analysis. The Quarterly Journal of Nuclear Medicine and Molecular Imaging, 42:211.

Laruelle, M., Abi-Dargham, A. (1999) Dopamine as the wind of the psychotic fire: new evidence from brain imaging studies. Journal of Psychopharmacology, 13:358-371.

Laruelle, M., Abi-Dargham, A., Casanova, M.F., Toti, R., Weinberger, D.R., Kleinman, J.E. (1993) Selective abnormalities of prefrontal serotonergic receptors in schizophrenia: a postmortem study. Archives of general psychiatry, 50:810-818.

Laruelle, M., Abi-Dargham, A., Van Dyck, C.H., Gil, R., D'Souza, C.D., Erdos, J., McCance, E., Rosenblatt, W., Fingado, C., Zoghbi, S.S. (1996) Single photon emission computerized tomography imaging of amphetamine-induced dopamine release in drug-free schizophrenic subjects. Proceedings of the National Academy of Sciences, 93:9235-9240.

Lee, D.D., Seung, H.S. (Algorithms for non-negative matrix factorization). In; 2001. p 556-562.

Lee, J., Park, S. (2005) Working memory impairments in schizophrenia: a meta-analysis. Journal of abnormal psychology, 114:599.

Lee, J.S., Park, H.-J., Chun, J.W., Seok, J.-H., Park, I.-H., Park, B., Kim, J.-J. (2011) Neuroanatomical correlates of trait anhedonia in patients with schizophrenia: a voxel-based morphometric study. Neuroscience letters, 489:110-114.

Lefebvre, S., Demeulemeester, M., Leroy, A., Delmaire, C., Lopes, R., Pins, D., Thomas, P., Jardri, R. (2016) Network dynamics during the different stages of hallucinations in schizophrenia. Human brain mapping, 37:2571-2586.

Lehoux, C., Gobeil, M.-H., Lefèbvre, A.-A., Maziade, M., Roy, M.-A. (2009) The five-factor structure of the PANSS: a critical review of its consistency across studies. Clinical schizophrenia & related psychoses, 3:103-110.

Lei, D., Pinaya, W.H., van Amelsvoort, T., Marcelis, M., Donohoe, G., Mothersill, D.O., Corvin, A., Gill, M., Vieira, S., Huang, X. (2019) Detecting schizophrenia at the level of the individual: relative diagnostic value of whole-brain images, connectome-wide functional connectivity and graph-based metrics. Psychological Medicine:1-10.

Lenzenweger, M.F., Dworkin, R.H., Wethington, E. (1991) Examining the underlying structure of schizophrenic phenomenology: Evidence for a three-process model. Schizophrenia Bulletin, 17:515-524.

Levine, S.Z., Rabinowitz, J. (2007) Revisiting the 5 dimensions of the Positive and Negative Syndrome Scale. Journal of clinical psychopharmacology, 27:431-436.

Levine, S.Z., Rabinowitz, J., Ascher-Svanum, H., Faries, D.E., Lawson, A.H. (2011) Extent of attaining and maintaining symptom remission by antipsychotic medication in the treatment of chronic schizophrenia: evidence from the CATIE study. Schizophrenia research, 133:42-46.

Lewis, R., Kapur, S., Jones, C., DaSilva, J., Brown, G.M., Wilson, A.A., Houle, S., Zipursky, R.B. (1999) Serotonin 5-HT2 receptors in schizophrenia: a PET study using [18F] setoperone in neuroleptic-naive patients and normal subjects. American Journal of Psychiatry, 156:72-78.

Lian, J., Pan, B., Deng, C. (2016) Early antipsychotic exposure affects serotonin and dopamine receptor binding density differently in selected brain loci of male and female juvenile rats. Pharmacological Reports, 68:1028-1035.

Lieberman, J.A., Tollefson, G.D., Charles, C., Zipursky, R., Sharma, T., Kahn, R.S., Keefe, R.S., Green, A.I., Gur, R.E., McEvoy, J. (2005) Antipsychotic drug effects on brain morphology in first-episode psychosis. Archives of general psychiatry, 62:361-370.

Limongi, R., Jeon, P., Mackinley, M., Das, T., Dempster, K., Théberge, J., Bartha, R., Wong, D., Palaniyappan, L. (2020) Glutamate and Dysconnection in the salience network: Neurochemical, effective-connectivity, and

computational evidence in schizophrenia. Biological Psychiatry.

Liu, X., Hairston, J., Schrier, M., Fan, J. (2011) Common and distinct networks underlying reward valence and processing stages: a meta-analysis of functional neuroimaging studies. Neuroscience & Biobehavioral Reviews, 35:1219-1236.

Lykouras, L., Oulis, P., Daskalopoulou, E., Psarros, K., Christodoulou, G.N. (2001) Clinical subtypes of schizophrenic disorders: a cluster analytic study. Psychopathology, 34:23-28.

Müller, V.I., Langner, R., Cieslik, E.C., Rottschy, C., Eickhoff, S.B. (2015) Interindividual differences in cognitive flexibility: influence of gray matter volume, functional connectivity and trait impulsivity. Brain Structure and function, 220:2401-2414.

Malhotra, A., Goldman, D., Mazzanti, C., Clifton, A., Breier, A., Pickar, D. (1998) A functional serotonin transporter (5-HTT) polymorphism is associated with psychosis in neuroleptic-free schizophrenics. Molecular Psychiatry, 3:328-332.

Manoach, D.S., Gollub, R.L., Benson, E.S., Searl, M.M., Goff, D.C., Halpern, E., Saper, C.B., Rauch, S.L. (2000) Schizophrenic subjects show aberrant fMRI activation of dorsolateral prefrontal cortex and basal ganglia during working memory performance. Biological psychiatry, 48:99-109.

Marder, S.R., Galderisi, S. (2017) The current conceptualization of negative symptoms in schizophrenia. World Psychiatry, 16:14-24.

Marek, K., Chowdhury, S., Siderowf, A., Lasch, S., Coffey, C.S., Caspell-Garcia, C., Simuni, T., Jennings, D., Tanner, C.M., Trojanowski, J.Q. (2018) The Parkinson's progression markers initiative (PPMI)–establishing a PD biomarker cohort. Annals of clinical and translational neurology, 5:1460-1477.

Marsh, H.W., Hau, K.-T., Wen, Z. (2004) In search of golden rules: Comment on hypothesis-testing approaches to setting cutoff values for fit indexes and dangers in overgeneralizing Hu and Bentler's (1999) findings. Structural equation modeling, 11:320-341.

Marsman, A., van den Heuvel, M.P., Klomp, D.W., Kahn, R.S., Luijten, P.R., Hulshoff Pol, H.E. (2013) Glutamate in schizophrenia: a focused review and meta-analysis of 1H-MRS studies. Schizophrenia bulletin, 39:120-129.

Marvel, C.L., Turner, B.M., O'Leary, D.S., Johnson, H.J., Pierson, R.K., Ponto, L.L.B., Andreasen, N.C. (2007) The neural correlates of implicit sequence learning in schizophrenia. Neuropsychology, 21:761.

Massey, S.H., Stern, D., Alden, E.C., Petersen, J.E., Cobia, D.J., Wang, L., Csernansky, J.G., Smith, M.J. (2017) Cortical thickness of neural substrates supporting cognitive empathy in individuals with schizophrenia. Schizophrenia research, 179:119-124.

Matosin, N., Newell, K.A. (2013) Metabotropic glutamate receptor 5 in the pathology and treatment of schizophrenia. Neuroscience & Biobehavioral Reviews, 37:256-268.

Matsumoto, I., Inoue, Y., Iwazaki, T., Pavey, G., Dean, B. (2005) 5-HT2A and muscarinic receptors in schizophrenia: a postmortem study. Neuroscience letters, 379:164-168.

Mauri, M., Paletta, S., Maffini, M., Colasanti, A., Dragogna, F., Di Pace, C., Altamura, A. (2014) Clinical pharmacology of atypical antipsychotics: an update. EXCLI journal, 13:1163.

Mayer, A.R., Ruhl, D., Merideth, F., Ling, J., Hanlon, F.M., Bustillo, J., Cañive, J. (2013) Functional imaging of the hemodynamic sensory gating response in schizophrenia. Human brain mapping, 34:2302-2312.

McClure, M.M., Harvey, P.D., Goodman, M., Triebwasser, J., New, A., Koenigsberg, H.W., Sprung, L.J., Flory, J.D., Siever, L.J. (2010) Pergolide treatment of cognitive deficits associated with schizotypal personality disorder: continued evidence of the importance of the dopamine system in the schizophrenia spectrum. Neuropsychopharmacology, 35:1356-1362.

McGuire, P., Quested, D., Spence, S., Murray, R., Frith, C., Liddle, P. (1998) Pathophysiology of positive thought

disorder in schizophrenia. The British Journal of Psychiatry, 173:231-235.

Meador-Woodruff, J.H., Haroutunian, V., Powchik, P., Davidson, M., Davis, K.L., Watson, S.J. (1997) Dopamine receptor transcript expression in striatum and prefrontal and occipital cortex: focal abnormalities in orbitofrontal cortex in schizophrenia. Archives of general psychiatry, 54:1089-1095.

Meda, S.A., Clementz, B.A., Sweeney, J.A., Keshavan, M.S., Tamminga, C.A., Ivleva, E.I., Pearlson, G.D. (2016) Examining functional resting-state connectivity in psychosis and its subgroups in the bipolar-schizophrenia network on intermediate phenotypes cohort. Biological Psychiatry: Cognitive Neuroscience and Neuroimaging, 1:488-497.

Mehta, U.M., Basavaraju, R., Thirthalli, J. (2014a) Mirror neuron activity and symptom severity in drug-naïve mania–a transcranial magnetic stimulation study. Brain Stimulation: Basic, Translational, and Clinical Research in Neuromodulation, 7:757-759.

Mehta, U.M., Thirthalli, J., Aneelraj, D., Jadhav, P., Gangadhar, B.N., Keshavan, M.S. (2014b) Mirror neuron dysfunction in schizophrenia and its functional implications: a systematic review. Schizophrenia research, 160:9-19.

Melke, J., Westberg, L., Nilsson, S., Landén, M., Soderstrom, H., Baghaei, F., Rosmond, R., Holm, G., Björntorp, P., Nilsson, L.-G. (2003) A polymorphism in the serotonin receptor 3A (HTR3A) gene and its association with harm avoidance in women. Archives of general psychiatry, 60:1017-1023.

Merritt, K., Egerton, A., Kempton, M.J., Taylor, M.J., McGuire, P.K. (2016) Nature of glutamate alterations in schizophrenia: a meta-analysis of proton magnetic resonance spectroscopy studies. JAMA psychiatry, 73:665-674.

Meyer, J.H., Gunn, R.N., Myers, R., Grasby, P.M. (1999) Assessment of spatial normalization of PET ligand images using ligand-specific templates. Neuroimage, 9:545-553.

Mikolas, P., Hlinka, J., Pitra, Z., Skoch, A., Frodl, T., Spaniel, F., Hajek, T. (2017) Classification of first-episode schizophrenia spectrum disorders and controls from whole brain white matter fractional anisotropy using machine learning. European Psychiatry, 41:S191-S191.

Mikolas, P., Melicher, T., Skoch, A., Slovakova, A., Matejka, M., Rydlo, J., Spaniel, F., Hajek, T. (2016) Diagnostic classification of patients with first-episode schizophrenia spectrum disorders from resting-fMRI. European Neuropsychopharmacology, 2:S490.

Minzenberg, M.J., Laird, A.R., Thelen, S., Carter, C.S., Glahn, D.C. (2009) Meta-analysis of 41 functional neuroimaging studies of executive function in schizophrenia. Archives of general psychiatry, 66:811-822.

Minzenberg, M.J., Lesh, T.A., Niendam, T.A., Yoon, J.H., Rhoades, R.N., Carter, C.S. (2014) Frontal cortex control dysfunction related to long-term suicide risk in recent-onset schizophrenia. Schizophrenia research, 157:19-25.

Mita, T., Hanada, S., Nishino, N., Kuno, T., Nakai, H., Yamadori, T., Mizoi, Y., Tanaka, C. (1986) Decreased serotonin S2 and increased dopamine D2 receptors in chronic schizophrenics. Biological Psychiatry, 21:1407-1414.

Mitelman, S.A., Buchsbaum, M.S., Christian, B.T., Merrill, B.M., Buchsbaum, B.R., Mukherjee, J., Lehrer, D.S. (2019) Positive association between cerebral grey matter metabolism and dopamine D2/D3 receptor availability in healthy and schizophrenia subjects: an 18F-fluorodeoxyglucose and 18F-fallypride positron emission tomography study. The World Journal of Biological Psychiatry:1-15.

Miyamoto, S., Duncan, G., Marx, C., Lieberman, J. (2005) Treatments for schizophrenia: a critical review of pharmacology and mechanisms of action of antipsychotic drugs. Molecular psychiatry, 10:79-104.

Mondino, M., Jardri, R., Suaud-Chagny, M.-F., Saoud, M., Poulet, E., Brunelin, J. (2016) Effects of fronto-temporal

transcranial direct current stimulation on auditory verbal hallucinations and resting-state functional connectivity of the left temporo-parietal junction in patients with schizophrenia. Schizophrenia bulletin, 42:318-326.

Mothersill, O., Tangney, N., Morris, D.W., McCarthy, H., Frodl, T., Gill, M., Corvin, A., Donohoe, G. (2017) Further evidence of alerted default network connectivity and association with theory of mind ability in schizophrenia. Schizophrenia research, 184:52-58.

Mucci, A., Galderisi, S., Kirkpatrick, B., Bucci, P., Volpe, U., Merlotti, E., Centanaro, F., Catapano, F., Maj, M. (2007) Double dissociation of N1 and P3 abnormalities in deficit and nondeficit schizophrenia. Schizophrenia research, 92:252-261.

Mwansisya, T.E., Hu, A., Li, Y., Chen, X., Wu, G., Huang, X., Lv, D., Li, Z., Liu, C., Xue, Z. (2017) Task and resting-state fMRI studies in first-episode schizophrenia: A systematic review. Schizophrenia research, 189:9-18.

Myers, J.F., Rosso, L., Watson, B.J., Wilson, S.J., Kalk, N.J., Clementi, N., Brooks, D.J., Nutt, D.J., Turkheimer, F.E., Lingford-Hughes, A.R. (2012) Characterisation of the contribution of the GABA-benzodiazepine α1 receptor subtype to [11C] Ro15-4513 PET images. Journal of Cerebral Blood Flow & Metabolism, 32:731-744.

Nagels, A., Cabanis, M., Oppel, A., Kirner-Veselinovic, A., Schales, C., Kircher, T. (2018) S-ketamine-induced NMDA receptor blockade during natural speech production and its implications for formal thought disorder in schizophrenia: a pharmaco-fMRI study. Neuropsychopharmacology, 43:1324-1333.

Nenadic, I., Yotter, R.A., Sauer, H., Gaser, C. (2015) Patterns of cortical thinning in different subgroups of schizophrenia. The British Journal of Psychiatry, 206:479-483.

Ngan, E.T., Yatham, L.N., Ruth, T.J., Liddle, P.F. (2000) Decreased serotonin 2A receptor densities in neuroleptic-naive patients with schizophrenia: a PET study using [18F] setoperone. American Journal of Psychiatry, 157:1016-1018.

Nishimura, Y., Takizawa, R., Muroi, M., Marumo, K., Kinou, M., Kasai, K. (2011) Prefrontal cortex activity during response inhibition associated with excitement symptoms in schizophrenia. Brain research, 1370:194-203.

Noirhomme, Q., Lesenfants, D., Gomez, F., Soddu, A., Schrouff, J., Garraux, G., Luxen, A., Phillips, C., Laureys, S. (2014) Biased binomial assessment of cross-validated estimation of classification accuracies illustrated in diagnosis predictions. NeuroImage: Clinical, 4:687-694.

Nostro, A.D., Müller, V.I., Varikuti, D.P., Pläschke, R.N., Hoffstaedter, F., Langner, R., Patil, K.R., Eickhoff, S.B. (2018) Predicting personality from network-based resting-state functional connectivity. Brain Structure and Function, 223:2699-2719.

O'Gráda, C., Barry, S., McGlade, N., Behan, C., Haq, F., Hayden, J., O'Donoghue, T., Peel, R., Morris, D.W., O'Callaghan, E. (2009) Does the ability to sustain attention underlie symptom severity in schizophrenia? Schizophrenia research, 107:319-323.

Oh, J., Chun, J.-W., Jo, H.J., Kim, E., Park, H.-J., Lee, B., Kim, J.-J. (2015) The neural basis of a deficit in abstract thinking in patients with schizophrenia. Psychiatry Research: Neuroimaging, 234:66-73.

Okubo, Y., Suhara, T., Suzuki, K., Kobayashi, K., Inoue, O., Terasaki, O., Someya, Y., Sassa, T., Sudo, Y., Matsushima, E. (1997) Decreased prefrontal dopamine D1 receptors in schizophrenia revealed by PET. Nature, 385:634-636.

Okubo, Y., Suhara, T., Suzuki, K., Kobayashi, K., Inoue, O., Terasaki, O., Someya, Y., Sassa, T., Sudo, Y., Matsushima, E. (2000) Serotonin 5-HT2 receptors in schizophrenic patients studied by positron emission tomography. Life sciences, 66:2455-2464.

Orban, P., Dansereau, C., Desbois, L., Mongeau-Pérusse, V., Giguère, C.-É., Nguyen, H., Mendrek, A., Stip, E., Bellec, P. (2018) Multisite generalizability of schizophrenia diagnosis classification based on functional brain

connectivity. Schizophrenia research, 192:167-171.

Ozkan, I., Turksen, I. (2007) Upper and lower values for the level of fuzziness in FCM. Fuzzy Logic: Springer. p 99-112.

Park, S., Gibson, C., McMichael, T. (2006) Socioaffective factors modulate working memory in schizophrenia patients. Neuroscience, 139:373-384.

Parker, D., Liu, X., Razlighi, Q.R. (2017) Optimal slice timing correction and its interaction with fMRI parameters and artifacts. Medical image analysis, 35:434-445.

Peralta, V., Cuesta, M., De Leon, J. (1995) Positive and negative symptoms/syndromes in schizophrenia: reliability and validity of different diagnostic systems. Psychological Medicine, 25:43-50.

Peralta, V., Cuesta, M.J. (1994) Psychometric properties of the positive and negative syndrome scale (PANSS) in schizophrenia. Psychiatry research, 53:31-40.

Perez, V.B., Woods, S.W., Roach, B.J., Ford, J.M., McGlashan, T.H., Srihari, V.H., Mathalon, D.H. (2014) Automatic auditory processing deficits in schizophrenia and clinical high-risk patients: forecasting psychosis risk with mismatch negativity. Biological psychiatry, 75:459-469.

Persson, J., Stening, E., Nordin, K., Söderlund, H. (2018) Predicting episodic and spatial memory performance from hippocampal resting-state functional connectivity: Evidence for an anterior–posterior division of function. Hippocampus, 28:53-66.

Petacchi, A., Laird, A.R., Fox, P.T., Bower, J.M. (2005) Cerebellum and auditory function: An ALE meta-analysis of functional neuroimaging studies. Human brain mapping, 25:118-128.

Peters, H., Riedl, V., Manoliu, A., Scherr, M., Schwerthöffer, D., Zimmer, C., Förstl, H., Bäuml, J., Sorg, C., Koch, K. (2017) Changes in extra-striatal functional connectivity in patients with schizophrenia in a psychotic episode. The British Journal of Psychiatry, 210:75-82.

Pettersson-Yeo, W., Allen, P., Benetti, S., McGuire, P., Mechelli, A. (2011) Dysconnectivity in schizophrenia: where are we now? Neuroscience & Biobehavioral Reviews, 35:1110-1124.

Phillips, M.L., Williams, L., Senior, C., Bullmore, E.T., Brammer, M.J., Andrew, C., Williams, S.C., David, A.S. (1999) A differential neural response to threatening and non-threatening negative facial expressions in paranoid and non-paranoid schizophrenics. Psychiatry Research: Neuroimaging, 92:11-31.

Piantadosi, P.T., Khayambashi, S., Schluter, M.G., Kutarna, A., Floresco, S.B. (2016) Perturbations in reward-related decision-making induced by reduced prefrontal cortical GABA transmission: Relevance for psychiatric disorders. Neuropharmacology, 101:279-290.

Pilowsky, L., Bressan, R., Stone, J., Erlandsson, K., Mulligan, R., Krystal, J., Ell, P. (2006) First in vivo evidence of an NMDA receptor deficit in medication-free schizophrenic patients. Molecular psychiatry, 11:118-119.

Pinborg, L.H., Adams, K.H., Svarer, C., Holm, S., Hasselbalch, S.G., Haugbøl, S., Madsen, J., Knudsen, G.M. (2003) Quantification of 5-HT2A receptors in the human brain using [18F] altanserin-PET and the bolus/infusion approach. Journal of Cerebral Blood Flow & Metabolism, 23:985-996.

Poels, E., Kegeles, L., Kantrowitz, J., Slifstein, M., Javitt, D., Lieberman, J., Abi-Dargham, A., Girgis, R. (2014) Imaging glutamate in schizophrenia: review of findings and implications for drug discovery. Molecular psychiatry, 19:20-29.

Pol, H.E.H., Schnack, H.G., Mandl, R.C., Cahn, W., Collins, D.L., Evans, A.C., Kahn, R.S. (2004) Focal white matter density changes in schizophrenia: reduced inter-hemispheric connectivity. Neuroimage, 21:27-35.

Pomarol-Clotet, E., Salvador, R., Sarro, S., Gomar, J., Vila, F., Martinez, A., Guerrero, A., Ortiz-Gil, J., Sans-Sansa, B., Capdevila, A. (2008) Failure to deactivate in the prefrontal cortex in schizophrenia: dysfunction of the default mode network? Psychological medicine, 38:1185.

Postmes, L., Sno, H., Goedhart, S., Van Der Stel, J., Heering, H., De Haan, L. (2014) Schizophrenia as a self-disorder due to perceptual incoherence. Schizophrenia research, 152:41-50.

Power, J.D., Barnes, K.A., Snyder, A.Z., Schlaggar, B.L., Petersen, S.E. (2012) Spurious but systematic correlations in functional connectivity MRI networks arise from subject motion. Neuroimage, 59:2142-2154.

Power, J.D., Schlaggar, B.L., Petersen, S.E. (2015) Recent progress and outstanding issues in motion correction in resting state fMRI. Neuroimage, 105:536-551.

Pralong, D., Tomaskovic-Crook, E., Opeskin, K., Copolov, D., Dean, B. (2000) Serotonin2A receptors are reduced in the planum temporale from subjects with schizophrenia. Schizophrenia research, 44:35-45.

Pridmore, S., Brüne, M., Ahmadi, J., Dale, J. (2008) Echopraxia in schizophrenia: possible mechanisms. Australian & New Zealand Journal of Psychiatry, 42:565-571.

Rüsch, N., van Elst, L.T., Valerius, G., Büchert, M., Thiel, T., Ebert, D., Hennig, J., Olbrich, H.-M. (2008) Neurochemical and structural correlates of executive dysfunction in schizophrenia. Schizophrenia research, 99:155-163.

Radhakrishnan, R., Matuskey, D., Nabulsi, N., Gaiser, E., Gallezot, J.-D., Henry, S., Planeta, B., Lin, S.-f., Ropchan, J., Huang, Y. (2020) In vivo 5-HT6 and 5-HT2A receptor availability in antipsychotic treated schizophrenia patients vs. unmedicated healthy humans measured with [11C] GSK215083 PET. Psychiatry Research: Neuroimaging, 295:111007.

Ragland, J.D., Moelter, S., Bhati, M., Valdez, J., Kohler, C., Siegel, S., Gur, R., Gur, R. (2008) Effect of retrieval effort and switching demand on fMRI activation during semantic word generation in schizophrenia. Schizophrenia research, 99:312-323.

Ramsey, N.F., Koning, H., Welles, P., Cahn, W., Van Der Linden, J., Kahn, R. (2002) Excessive recruitment of neural systems subserving logical reasoning in schizophrenia. Brain, 125:1793-1807.

Regenbogen, C., Kellermann, T., Seubert, J., Schneider, D.A., Gur, R.E., Derntl, B., Schneider, F., Habel, U. (2015) Neural responses to dynamic multimodal stimuli and pathology-specific impairments of social cognition in schizophrenia and depression. The British Journal of Psychiatry, 206:198-205.

Reuter, B., Jäger, M., Bottlender, R., Kathmann, N. (2007) Impaired action control in schizophrenia: the role of volitional saccade initiation. Neuropsychologia, 45:1840-1848.

Richiardi, J., Altmann, A., Milazzo, A.-C., Chang, C., Chakravarty, M.M., Banaschewski, T., Barker, G.J., Bokde, A.L., Bromberg, U., Büchel, C. (2015) Correlated gene expression supports synchronous activity in brain networks. Science, 348:1241-1244.

Rodriguez-Jimenez, R., Bagney, A., Mezquita, L., Martinez-Gras, I., Sanchez-Morla, E.-M., Mesa, N., Ibañez, M.-I., Diez-Martin, J., Jimenez-Arriero, M.-A., Lobo, A. (2013) Cognition and the five-factor model of the positive and negative syndrome scale in schizophrenia. Schizophrenia Research, 143:77-83.

Rosenheck, R., Leslie, D., Keefe, R., McEvoy, J., Swartz, M., Perkins, D., Stroup, S., Hsiao, J.K., Lieberman, J., Group, C.S.I. (2006) Barriers to employment for people with schizophrenia. American Journal of Psychiatry, 163:411-417.

Rossell, S.L., Francis, P.S., Galletly, C., Harris, A., Siskind, D., Berk, M., Bozaoglu, K., Dark, F., Dean, O., Liu, D. (2016) N-acetylcysteine (NAC) in schizophrenia resistant to clozapine: a double blind randomised placebo controlled trial targeting negative symptoms. BMC psychiatry, 16:1-9.

Rottschy, C., Langner, R., Dogan, I., Reetz, K., Laird, A.R., Schulz, J.B., Fox, P.T., Eickhoff, S.B. (2012) Modelling neural correlates of working memory: a coordinate-based meta-analysis. Neuroimage, 60:830-846.

Rozycki, M., Satterthwaite, T.D., Koutsouleris, N., Erus, G., Doshi, J., Wolf, D.H., Fan, Y., Gur, R.E., Gur, R.C., Meisenzahl, E.M. (2018) Multisite machine learning analysis provides a robust structural imaging signature of

schizophrenia detectable across diverse patient populations and within individuals. Schizophrenia bulletin, 44:1035-1044.

Rubia, K., Russell, T., Bullmore, E.T., Soni, W., Brammer, M.J., Simmons, A., Taylor, E., Andrew, C., Giampietro, V., Sharma, T. (2001) An fMRI study of reduced left prefrontal activation in schizophrenia during normal inhibitory function. Schizophrenia research, 52:47-55.

Sabatinelli, D., Fortune, E.E., Li, Q., Siddiqui, A., Krafft, C., Oliver, W.T., Beck, S., Jeffries, J. (2011) Emotional perception: meta-analyses of face and natural scene processing. Neuroimage, 54:2524-2533.

Sadanandam, A., Lyssiotis, C.A., Homicsko, K., Collisson, E.A., Gibb, W.J., Wullschleger, S., Ostos, L.C.G., Lannon, W.A., Grotzinger, C., Del Rio, M. (2013) A colorectal cancer classification system that associates cellular phenotype and responses to therapy. Nature medicine, 19:619-625.

Savli, M., Bauer, A., Mitterhauser, M., Ding, Y.-S., Hahn, A., Kroll, T., Neumeister, A., Haeusler, D., Ungersboeck, J., Henry, S. (2012) Normative database of the serotonergic system in healthy subjects using multi-tracer PET. Neuroimage, 63:447-459.

Scherk, H., Falkai, P. (2006) Effects of antipsychotics on brain structure. Current opinion in psychiatry, 19:145-150.

Schilbach, L., Bzdok, D., Timmermans, B., Fox, P.T., Laird, A.R., Vogeley, K., Eickhoff, S.B. (2012) Introspective minds: using ALE meta-analyses to study commonalities in the neural correlates of emotional processing, social & unconstrained cognition. PloS one, 7:e30920.

Schilbach, L., Derntl, B., Aleman, A., Caspers, S., Clos, M., Diederen, K.M., Gruber, O., Kogler, L., Liemburg, E.J., Sommer, I.E. (2016) Differential patterns of dysconnectivity in mirror neuron and mentalizing networks in schizophrenia. Schizophrenia bulletin, 42:1135-1148.

Schlösser, R., Gesierich, T., Kaufmann, B., Vucurevic, G., Hunsche, S., Gawehn, J., Stoeter, P. (2003) Altered effective connectivity during working memory performance in schizophrenia: a study with fMRI and structural equation modeling. Neuroimage, 19:751-763.

Schmack, K., de Castro, A.G.-C., Rothkirch, M., Sekutowicz, M., Rössler, H., Haynes, J.-D., Heinz, A., Petrovic, P., Sterzer, P. (2013) Delusions and the role of beliefs in perceptual inference. Journal of Neuroscience, 33:13701-13712.

Schneider, F., Habel, U., Reske, M., Kellermann, T., Stöcker, T., Shah, N.J., Zilles, K., Braus, D.F., Schmitt, A., Schlösser, R. (2007) Neural correlates of working memory dysfunction in first-episode schizophrenia patients: an fMRI multi-center study. Schizophrenia research, 89:198-210.

Schobel, S.A., Chaudhury, N.H., Khan, U.A., Paniagua, B., Styner, M.A., Asllani, I., Inbar, B.P., Corcoran, C.M., Lieberman, J.A., Moore, H. (2013) Imaging patients with psychosis and a mouse model establishes a spreading pattern of hippocampal dysfunction and implicates glutamate as a driver. Neuron, 78:81-93.

Schwieler, L., Linderholm, K.R., Nilsson-Todd, L.K., Erhardt, S., Engberg, G. (2008) Clozapine interacts with the glycine site of the NMDA receptor: electrophysiological studies of dopamine neurons in the rat ventral tegmental area. Life sciences, 83:170-175.

Scrucca, L., Fop, M., Murphy, T.B., Raftery, A.E. (2016) mclust 5: clustering, classification and density estimation using Gaussian finite mixture models. The R journal, 8:289.

Selvaraj, S., Arnone, D., Cappai, A., Howes, O. (2014) Alterations in the serotonin system in schizophrenia: a systematic review and meta-analysis of postmortem and molecular imaging studies. Neuroscience & Biobehavioral Reviews, 45:233-245.

Sepehrmanesh, Z., Heidary, M., Akasheh, N., Akbari, H., Heidary, M. (2018) Therapeutic effect of adjunctive N-acetyl cysteine (NAC) on symptoms of chronic schizophrenia: a double-blind, randomized clinical trial. Progress in Neuro-Psychopharmacology and Biological Psychiatry, 82:289-296.

Shaffer, J.J., Peterson, M.J., McMahon, M.A., Bizzell, J., Calhoun, V., van Erp, T.G., Ford, J.M., Lauriello, J., Lim, K.O., Manoach, D.S. (2015) Neural correlates of schizophrenia negative symptoms: distinct subtypes impact dissociable brain circuits. Molecular neuropsychiatry, 1:191-200.

Shamay-Tsoory, S.G., Shur, S., Barcai-Goodman, L., Medlovich, S., Harari, H., Levkovitz, Y. (2007) Dissociation of cognitive from affective components of theory of mind in schizophrenia. Psychiatry research, 149:11-23.

Shen, X., Tokoglu, F., Papademetris, X., Constable, R.T. (2013) Groupwise whole-brain parcellation from resting-state fMRI data for network node identification. Neuroimage, 82:403-415.

Shim, M., Kim, D.-W., Lee, S.-H., Im, C.-H. (2014) Disruptions in small-world cortical functional connectivity network during an auditory oddball paradigm task in patients with schizophrenia. Schizophrenia research, 156:197-203.

Shin, K.S., Kim, J.S., Kang, D.-H., Koh, Y., Choi, J.-S., O'Donnell, B.F., Chung, C.K., Kwon, J.S. (2009) Pre-attentive auditory processing in ultra-high-risk for schizophrenia with magnetoencephalography. Biological psychiatry, 65:1071-1078.

Shingai, Y., Tateno, A., Arakawa, R., Sakayori, T., Kim, W., Suzuki, H., Okubo, Y. (2014) Age-related decline in dopamine transporter in human brain using PET with a new radioligand [18 F] FE-PE2I. Annals of nuclear medicine, 28:220-226.

Silverstein, B.H., Bressler, S.L., Diwadkar, V.A. (2016) Inferring the dysconnection syndrome in schizophrenia: Interpretational considerations on methods for the network analyses of fMRI data. Frontiers in psychiatry, 7:132.

Singh, S., Modi, S., Goyal, S., Kaur, P., Singh, N., Bhatia, T., Deshpande, S.N., Khushu, S. (2015) Functional and structural abnormalities associated with empathy in patients with schizophrenia: An fMRI and VBM study. Journal of biosciences, 40:355-364.

Snoek, L., Miletić, S., Scholte, H.S. (2019) How to control for confounds in decoding analyses of neuroimaging data. NeuroImage, 184:741-760.

Soentpiet, R. (1999) Advances in kernel methods: support vector learning. MIT press.

Sorg, C., Manoliu, A., Neufang, S., Myers, N., Peters, H., Schwerthöffer, D., Scherr, M., Mühlau, M., Zimmer, C., Drzezga, A. (2013) Increased intrinsic brain activity in the striatum reflects symptom dimensions in schizophrenia. Schizophrenia bulletin, 39:387-395.

Sotiras, A., Resnick, S.M., Davatzikos, C. (2015) Finding imaging patterns of structural covariance via non-negative matrix factorization. Neuroimage, 108:1-16.

Sotiras, A., Toledo, J.B., Gur, R.E., Gur, R.C., Satterthwaite, T.D., Davatzikos, C. (2017) Patterns of coordinated cortical remodeling during adolescence and their associations with functional specialization and evolutionary expansion. Proceedings of the National Academy of Sciences, 114:3527-3532.

Spitzer, R.L., Gibbon, M.E., Skodol, A.E., Williams, J.B., First, M.B. (2002) DSM-IV-TR casebook: A learning companion to the diagnostic and statistical manual of mental disorders, text rev. American Psychiatric Publishing, Inc.

Spreng, R.N., Mar, R.A., Kim, A.S. (2009) The common neural basis of autobiographical memory, prospection, navigation, theory of mind, and the default mode: a quantitative meta-analysis. Journal of cognitive neuroscience, 21:489-510.

Stagg, C.J., Bachtiar, V., Amadi, U., Gudberg, C.A., Ilie, A.S., Sampaio-Baptista, C., O‘Shea, J., Woolrich, M., Smith, S.M., Filippini, N. (2014) Local GABA concentration is related to network-level resting functional connectivity. Elife, 3:e01465.

Stahl, S.M. (2018) Beyond the dopamine hypothesis of schizophrenia to three neural networks of psychosis:

dopamine, serotonin, and glutamate. CNS spectrums, 23:187-191.

Strauss, G.P., Kappenman, E.S., Culbreth, A.J., Catalano, L.T., Ossenfort, K.L., Lee, B.G., Gold, J.M. (2015) Emotion regulation abnormalities in schizophrenia: Directed attention strategies fail to decrease the neurophysiological response to unpleasant stimuli. Journal of abnormal psychology, 124:288.

Suhara, T., Okubo, Y., Yasuno, F., Sudo, Y., Inoue, M., Ichimiya, T., Nakashima, Y., Nakayama, K., Tanada, S., Suzuki, K. (2002) Decreased dopamine D2 receptor binding in the anterior cingulate cortex in schizophrenia. Archives of general psychiatry, 59:25-30.

Sullivan, S.K., Strauss, G.P. (2017) Electrophysiological evidence for detrimental impact of a reappraisal emotion regulation strategy on subsequent cognitive control in schizophrenia. Journal of abnormal psychology, 126:679.

Sweet, R.A., Bergen, S.E., Sun, Z., Marcsisin, M.J., Sampson, A.R., Lewis, D.A. (2007) Anatomical evidence of impaired feedforward auditory processing in schizophrenia. Biological Psychiatry, 61:854-864.

T T J, K., Liddle, P.F., Brammer, M.J., WILLIAMS, S.C.R., Murray, R.M., McGuire, P.K. (2002) Reversed lateralization of temporal activation during speech production in thought disordered patients with schizophrenia. Psychological medicine, 32:439.

Tamminga, C.A., Ivleva, E.I., Keshavan, M.S., Pearlson, G.D., Clementz, B.A., Witte, B., Morris, D.W., Bishop, J., Thaker, G.K., Sweeney, J.A. (2013) Clinical phenotypes of psychosis in the Bipolar-Schizophrenia Network on Intermediate Phenotypes (B-SNIP). American Journal of psychiatry, 170:1263-1274.

Tandon, R., Gaebel, W., Barch, D.M., Bustillo, J., Gur, R.E., Heckers, S., Malaspina, D., Owen, M.J., Schultz, S., Tsuang, M. (2013) Definition and description of schizophrenia in the DSM-5. Schizophrenia research, 150:3-10.

Thomas, E.H., Bozaoglu, K., Rossell, S.L., Gurvich, C. (2017) The influence of the glutamatergic system on cognition in schizophrenia: a systematic review. Neuroscience & Biobehavioral Reviews, 77:369-387.

Tikàsz, A., Dumais, A., Lipp, O., Stip, E., Lalonde, P., Laurelli, M., Lungu, O., Potvin, S. (2019) Reward-related decision-making in schizophrenia: A multimodal neuroimaging study. Psychiatry Research: Neuroimaging, 286:45-52.

Tipping, M.E. (2001) Sparse Bayesian learning and the relevance vector machine. Journal of machine learning research, 1:211-244.

Tregellas, J.R. (2014) Neuroimaging biomarkers for early drug development in schizophrenia. Biological psychiatry, 76:111-119.

Trichard, C., Paillère-Martinot, M.-L., Attar-Levy, D., Blin, J., Feline, A., Martinot, J.-L. (1998) No serotonin 5-HT2A receptor density abnormality in the cortex of schizophrenic patients studied with PET. Schizophrenia research, 31:13-17.

Trninić, V., Jelaska, I., Štalec, J. (2013) Appropriateness and limitations of factor analysis methods utilized in psychology and kinesiology: Part II. Fizička kultura, 67:1-17.

Troiano, A.R., Schulzer, M., Fuente-Fernandez, R.d.L., Mak, E., Mckenzie, J., Sossi, V., Mccormick, S., Ruth, T.J., Stoessl, A.J. (2010) Dopamine transporter PET in normal aging: dopamine transporter decline and its possible role in preservation of motor function. Synapse, 64:146-151.

Uhlhaas, P.J. (2013) Dysconnectivity, large-scale networks and neuronal dynamics in schizophrenia. Current opinion in neurobiology, 23:283-290.

Uno, Y., Coyle, J.T. (2019) Glutamate hypothesis in schizophrenia. Psychiatry and clinical neurosciences, 73:204-215.

Van den Oord, E.J., Rujescu, D., Robles, J.R., Giegling, I., Birrell, C., Bukszár, J., Murrelle, L., Möller, H.-J.,

Middleton, L., Muglia, P. (2006) Factor structure and external validity of the PANSS revisited. Schizophrenia research, 82:213-223.

van der Gaag, M., Hoffman, T., Remijsen, M., Hijman, R., de Haan, L., van Meijel, B., van Harten, P.N., Valmaggia, L., De Hert, M., Cuijpers, A. (2006) The five-factor model of the Positive and Negative Syndrome Scale II: a ten-fold cross-validation of a revised model. Schizophrenia research, 85:280-287.

Varikuti, D.P., Hoffstaedter, F., Genon, S., Schwender, H., Reid, A.T., Eickhoff, S.B. (2017) Resting-state test–retest reliability of a priori defined canonical networks over different preprocessing steps. Brain Structure and Function, 222:1447-1468.

Veerman, S., Schulte, P., Begemann, M., Engelsbel, F., De Haan, L. (2014) Clozapine augmented with glutamate modulators in refractory schizophrenia: a review and metaanalysis. Pharmacopsychiatry, 47:185-194.

Vercammen, A., Knegtering, H., den Boer, J.A., Liemburg, E.J., Aleman, A. (2010) Auditory hallucinations in schizophrenia are associated with reduced functional connectivity of the temporo-parietal area. Biological psychiatry, 67:912-918.

Verhoeff, N.P.L., Meyer, J.H., Kecojevic, A., Hussey, D., Lewis, R., Tauscher, J., Zipursky, R.B., Kapur, S. (2000) A voxel-by-voxel analysis of [18F] setoperone PET data shows no substantial serotonin 5-HT2A receptor changes in schizophrenia. Psychiatry Research: Neuroimaging, 99:123-135.

Vyas, N.S., Buchsbaum, M.S., Lehrer, D.S., Merrill, B.M., DeCastro, A., Doninger, N.A., Christian, B.T., Mukherjee, J. (2018) D2/D3 dopamine receptor binding with [F-18] fallypride correlates of executive function in medication-naïve patients with schizophrenia. Schizophrenia research, 192:442-456.

Wallwork, R., Fortgang, R., Hashimoto, R., Weinberger, D., Dickinson, D. (2012) Searching for a consensus five-factor model of the Positive and Negative Syndrome Scale for schizophrenia. Schizophrenia research, 137:246-250.

Walther, S., Stegmayer, K., Federspiel, A., Bohlhalter, S., Wiest, R., Viher, P.V. (2017) Aberrant hyperconnectivity in the motor system at rest is linked to motor abnormalities in schizophrenia spectrum disorders. Schizophrenia bulletin, 43:982-992.

Walton, E., Hibar, D.P., Van Erp, T.G., Potkin, S.G., Roiz-Santianez, R., Crespo-Facorro, B., Suarez-Pinilla, P., van Haren, N.E., De Zwarte, S., Kahn, R.S. (2018) Prefrontal cortical thinning links to negative symptoms in schizophrenia via the ENIGMA consortium. Psychological medicine, 48:82-94.

Wang, G., Hu, C., Jiang, T., Luo, J., Hu, J., Ling, S., Liu, M., Xing, G. (2010) Overexpression of serotonin receptor and transporter mRNA in blood leukocytes of antipsychotic-free and antipsychotic-naive schizophrenic patients: gender differences. Schizophrenia research, 121:160-171.

Weickert, T.W., Goldberg, T.E., Gold, J.M., Bigelow, L.B., Egan, M.F., Weinberger, D.R. (2000) Cognitive impairments in patients with schizophrenia displaying preserved and compromised intellect. Archives of general psychiatry, 57:907-913.

Wende, K.C., Nagels, A., Stratmann, M., Chatterjee, A., Kircher, T., Straube, B. (2015) Neural basis of altered physical and social causality judgements in schizophrenia. Schizophrenia research, 161:244-251.

White, L., Harvey, P.D., Opler, L., Lindenmayer, J. (1997) Empirical assessment of the factorial structure of clinical symptoms in schizophrenia. Psychopathology, 30:263-274.

Willner, P. (1997) The dopamine hypothesis of schizophrenia: current status, future prospects. International Clinical Psychopharmacology.

Witt, S.T., Laird, A.R., Meyerand, M.E. (2008) Functional neuroimaging correlates of finger-tapping task variations: an ALE meta-analysis. Neuroimage, 42:343-356.

Wolf, D.H., Turetsky, B.I., Loughead, J., Elliott, M.A., Pratiwadi, R., Gur, R.E., Gur, R.C. (2008) Auditory oddball

fMRI in schizophrenia: association of negative symptoms with regional hypoactivation to novel distractors. Brain imaging and behavior, 2:132-145.

Xie, X.L., Beni, G. (1991) A validity measure for fuzzy clustering. IEEE Transactions on pattern analysis and machine intelligence, 13:841-847.

Yan, W., Plis, S., Calhoun, V.D., Liu, S., Jiang, R., Jiang, T.-Z., Sui, J. (Discriminating schizophrenia from normal controls using resting state functional network connectivity: A deep neural network and layer-wise relevance propagation method). In; 2017. IEEE. p 1-6.

Yang, Z., Oja, E. (2010) Linear and nonlinear projective nonnegative matrix factorization. IEEE Transactions on Neural Networks, 21:734-749.

Zakzanis, K.K., Hansen, K.T. (1998) Dopamine D2 densities and the schizophrenic brain. Schizophrenia research, 32:201-206.

Zavitsanou, K., Ward, P.B., Huang, X.-F. (2002) Selective alterations in ionotropic glutamate receptors in the anterior cingulate cortex in schizophrenia. Neuropsychopharmacology, 27:826-833.

Zhang, T., Koutsouleris, N., Meisenzahl, E., Davatzikos, C. (2015) Heterogeneity of structural brain changes in subtypes of schizophrenia revealed using magnetic resonance imaging pattern analysis. Schizophrenia bulletin, 41:74-84.

Zheng, Y.-T., Neo, S.-Y., Chua, T.-S., Tian, Q. (Probabilistic optimized ranking for multimedia semantic concept detection via RVM). In; 2008. p 161-168.

Zhou, C., Tang, X., Wang, X., Zhang, X., Zhang, X., Yu, M. (2019) Altered patterns of the fractional amplitude of low-frequency fluctuation and functional connectivity between deficit and non-deficit schizophrenia. Frontiers in Psychiatry, 10:680.

Zilles, K., Bacha-Trams, M., Palomero-Gallagher, N., Amunts, K., Friederici, A.D. (2015) Common molecular basis of the sentence comprehension network revealed by neurotransmitter receptor fingerprints. Cortex, 63:79-89.

Zilles, K., Palomero-Gallagher, N., Grefkes, C., Scheperjans, F., Boy, C., Amunts, K., Schleicher, A. (2002) Architectonics of the human cerebral cortex and transmitter receptor fingerprints: reconciling functional neuroanatomy and neurochemistry. European Neuropsychopharmacology, 12:587-599.

11. Publication list

1. **Chen J**, Patil K R, Weis S, et al. Neurobiological Divergence of the Positive and Negative Schizophrenia Subtypes Identified on a New Factor Structure of Psychopathology Using Non-negative Factorization: An International Machine Learning Study. *Biological psychiatry*, 2020, 87(3): 282-293.
2. **Chen J***, Yan Y, Yuan F, et al. Brain grey matter volume reduction and anxiety-like behavior in lipopolysaccharide-induced chronic pulmonary inflammation rats: A structural MRI study with histological validation. *Brain, behavior, and immunity*, 2019, 76: 182-197.
3. **Chen J**, Zhang J, Liu X, et al. Abnormal subcortical nuclei shapes in patients with type 2 diabetes mellitus. *European radiology* 2017; 27(10): 4247-4256.
4. **Chen J**, Lin I-T, Zhang H, et al. Reduced cortical thickness, surface area in patients with chronic obstructive pulmonary disease: a surface-based morphometry and neuropsychological study. *Brain imaging and behavior* 2016; 10(2): 464-476.
5. **Chen J**, Zhang J, et al. Increased intra-regional synchronized neural activity in adult brain after prolonged adaptation to high-altitude hypoxia: A resting-state fMRI study. *High altitude medicine&biology* 2016; 17(1):16-24.
6. **Chen J**, Zhang J, et al. Long-term acclimatization to high-altitude hypoxia modifies interhemispheric functional and structural connectivity in the adult brain. *Brain and behavior* 2016; 6(9): e00512.
7. **Chen J***, Mueller VI, Dukart J, et al. Connectivity patterns of task-specific brain networks allow individual prediction of cognitive symptom dimension of schizophrenia and link to molecular architecture. Preprint available at *bioRxiv*; 2020; *doi: https://doi.org/10.1101/2020.07.02.185124*.
8. Liu X, Eickhoff SB, Hoffstaedter F, Genon S, Caspers S, Reetz K, Dogan I, Eickhoff CR, **Chen J**, et al. Joint multimodal parcellation of the human striatum: functions and clinical relevance. *Neuroscience Bulletin* 2020; Accepted.
9. Li C, Wang F, Jiang X, **Chen J**, et al. Classification of schizophrenia spectrum disorder using machine learning and functional connectivity: reconsidering the clinical application. Preprint available at *medRxiv*, 2020; *doi: https://doi.org/10.1101/2020.05.30.20118026*
10. Dong D, Guell X, Genon S, Wang Y, **Chen J,** et al. Linking cerebellar functional gradients to transdiagnostic behavioral dimensions of psychopathology. Preprint available at *bioRxiv*, 2020; *doi: https://doi.org/10.1101/2020.06.15.153254*.
11. Li H, Lin Y, **Chen J**, et al. Abnormal regional homogeneity and functional connectivity in adjustment disorder of new recruits: a resting-state fMRI study. *Japanese journal of radiology* 2017; 35(4): 151-160.
12. Zhang J, **Chen J**, Fan C, et al. Alteration of Spontaneous Brain Activity After Hypoxia–Reoxygenation: A Resting-State fMRI Study. *High altitude medicine&biology* 2017; 18(1): 20-26.
13. Zhang J, **Chen J**, Yu Q, et al. Alteration of spontaneous brain activity in COPD patients. *International Journal of Chronic Obstructive Pulmonary Disease* 2016; 11(1): 1713-1719.
14. Song M, Chen J-H, **Chen J**, Lin I-T. Comparisons between the 35 mm Quadrature Surface Resonator at 300 K and the 40 mm High-Temperature Surface Resonator at 77 K in a 3T MRI imager. *PLoS One* 2015; 10(3):

e0118892.

15. Zhang J, Zhang H, **Chen J**, et al. Structural Modulation of Brain Development by Oxygen: Evidence on Adolescents Migrating from High Altitude to Sea Level Environment. *PLoS One* 2013; 8(7): e67803.
16. Zhang J, Zhang H, Li J, **Chen J**, et al. Adaptive modulation of adult brain gray and white matter to high altitude: structural MRI studies. *PLoS One* 2013; 8(7): e68621.